Moraxella catarrhalis and rhinovirus infection and co-infection of healthy and chronic obstructive pulmonary disease ciliated respiratory epithelium

Simona Asenova Velkova

Department of Infection, Immunity, Inflammation and Research Teaching

Respiratory, Critical Care and Anaesthesia section

UCL Great Ormond Street Institute of Child Health

Institute for Global Health

London, WC1N 1EH

A thesis submission for the degree of Doctor of Philosophy

UCL 2020

Statement of Work

I, Simona Asenova Velkova confirm that the work presented in this thesis is original and my own. In places where work from other sources is presented, I confirm that this has been indicated in the thesis.

Abstract

This research project investigated the effects of rhinovirus and *Moraxella catarrhalis* (*M. catarrhalis*) infection of the ciliated respiratory epithelium given the clinical infections caused by both pathogens in healthy individuals. However, as both rhinovirus and *M. catarrhalis* infection are known to exacerbate disease in a number of chronic respiratory diseases we were keen to determine if the underlying cellular response was different in such conditions. We chose to investigate chronic obstructive pulmonary disease (COPD) to allow comparison with results from healthy individuals. COPD is a progressive pulmonary disease characterised by chronic airway inflammation, emphysema, airway remodelling and chronic bronchitis. Exacerbations in COPD are primarily caused by bacterial and viral infections.

As most studies looking at viral and bacterial infection of cells have focused on cell lines or basal cells we wanted to determine if differentiation to a ciliated phenotype, mimicking the host more closely affected response to infection. Primary healthy and COPD nasal tissue, differentiated at air-liquid interface allowed us to assess the initial interaction of *M. catarrhalis* and rhinovirus with the ciliated epithelium *in vitro*. Host-pathogen interactions were explored utilising high speed video, confocal and electron microscopy, western blotting, flow cytometry and immune-based assays.

It was found that *M. catarrhalis* binds rapidly to the cilia of beating ciliated cells, altering ciliary function and invading epithelial cells, particularly COPD epithelial cells, initiating a cascade of signalling events involving the epidermal growth factor receptor and phosphoinositide-3 kinase pathway, leading to induction of pro-inflammatory cytokines. It was also demonstrated that rhinovirus targets ciliated cells in primary cultures, causing their shedding from the epithelial layer via apoptosis. This resulted in depletion of ciliated cells and a severely disrupted airway epithelium.

Investigation of the mechanisms associated with bacterial-viral co-infections showed that rhinovirus pre-infection followed by a subsequent *M. catarrhalis* infection further decreased ciliary function of epithelial cultures and increased the release of pro-inflammatory mediators. Additionally, it was found that initial viral infection can potentially cause later dissemination of pathogens in the respiratory tract through triggered detachment of ciliated cells which appeared to have bound *M. catarrhalis*. Detached cells and reduction in ciliary function are likely to exacerbate airways obstruction.

Impact statement

M. catarrhalis has been long and largely considered as a commensal that can colonise the respiratory airways without causing a disease. In the past two decades however, *M. catarrhalis* has emerged as a pathogenic organism reported to cause otitis media, sinusitis, bacteraemia and also exacerbations in COPD patients. Limited information is available on how *M. catarrhalis* interacts with the airway epithelium to initiate a disease. Rhinovirus is a pathogen that causes common colds in children and adults, and more seriously also drives exacerbations in COPD patients. Bacterial-viral co-infections in COPD patients are linked to severe exacerbations, contributing to a severe lung function impairment, prolonged hospitalisation and subsequent hospital readmissions. However, detailed information on how bacterial-viral co-infections trigger acute exacerbations, and what their effect on the airway epithelium is currently unknown, additionally, studies looking at *M. catarrhalis* and rhinovirus co-infections are missing. Thus, the focus of the current project was to investigate in more detail the cellular and molecular mechanisms associated with pathogen infections of the respiratory epithelium. Moreover, the use of primary tissue from healthy volunteers and COPD patients enabled the more accurate representation of real *in vivo* infections.

This project studied bacterial - viral interactions using ciliated airway epithelium and revealed previously unrecognised detrimental effects of the pathogens on the respiratory epithelium, including rapid reduction of ciliary movement and significant reduction of ciliation. This may ultimately severely impair essential mucociliary clearance of pathogens. This project brings novel insight into on how bacterial and viral pathogens singly and in combination affect the human airway epithelium. This may provide clues for future therapeutic intervention to prevent serious problematic events which occur during exacerbations.

In the scientific context of these observations, the current study found that bacterial and viral infections may contribute to the structural changes of the airways in COPD patients. This is based on the findings that *M. catarrhalis* triggered epidermal growth factor (EGFR) activation, previously shown to change the fate of basal cell type towards mucus producing cells, and that rhinovirus can severely impair the ciliogenesis of the respiratory epithelium, suggesting that both pathogens can alter the structure and defensive function of the airway epithelium. Importantly, this study discovered a novel compound (PI4KIIIβ inhibitor -GSK2998533) which could be of

therapeutic benefit in the prevention of rhinovirus infection, and would be advantageous for COPD patients but also the general population, as good antiviral compounds are scarce. This study demonstrated that rhinovirus and *M. catarrhalis in vitro* infections are associated with the clinical outcomes of COPD patients reported during exacerbations. It also showed the importance of understanding the underlying cellular mechanisms associated with respiratory symptoms seen in hospitals.

Acknowledgements

First and foremost, I would like to thank my supervisor Professor Chris O'Callaghan for the guidance and help throughout my entire PhD. His enthusiasm and mentoring have been invaluable for my graduate experience. I would like to say thank you for the continuous support and patience during the challenges I encountered in the last few years, and for your advice that has been vital to become the scientist I am today. I would like to thank my secondary supervisors Dr Claire Smith and Professor Rosalind Smyth for the encouragement and helpful advice for my research.

A very special thank you to Dr Primrose Freestone from the Department of Infection, Immunity and Inflammation at The University of Leicester for her priceless support, brilliant comments and suggestions for my research work. Most importantly, she has shown me inexplicable kindness and understanding far beyond that of a supervisor throughout my time as a PhD student. Special thank you to Anna Straatman-Iwanowska and Natalie Allcock for their help with the electron microscopy studies.

My thanks to Dr Rick Williamson, Dr Soren Beinke, Dr Edith Hessel, Dr David Michalovich, Dr Ken Grace, Dr Gareth Wayne, Dr Augustin Armour from the Refractory Respiratory and Inflammation discovery unit at GlaxoSmithKline, Stevenage for their expertise, suggestions and technical support during this entire project. Special thanks to Dr Tanja Hoegg who helped with the statistics part in my research project.

I would like to express my gratitude to my colleagues from the Great Ormond Street Institute of Child Health who have been invaluable part of my PhD and wouldn't have been able to complete my research without their support. I would particularly like to thank Ms Dani Lee who has dedicated a lot of time in the lab to teach me techniques and her invaluable assistance with the primary tissue work. I want to specifically thank Dr Daniela Cardinale for her technical support in the laboratory and also her advice and guidance throughout this research project. I am also thankful to Dr Alina Petris for her assistance and support during the years and her readiness to always help. Thank you Dani, Daniela and Alina you have contributed immensely to my personal and professional time at UCL. I would also like to thank Angela Dwornik and Hemlata Varsani who have been of incredible support in the course of this research project.

I want to extend my thanks to the members of the Smyth's group for their assistance during my PhD work. I would additionally like to thank Dr Dale Moulding for his help

with the microscopy techniques developed during my PhD and Dr Ayad Eddaoudi for his help with the flow cytometry techniques.

Finally, many thanks to my partner, family and friends, who despite not understanding much of what I do, have provided moral support and constant encouragement throughout this whole experience.

The time and care you have all devoted made it possible for me to complete my PhD project.

Thesis outline

The introduction chapter of this thesis presents background information on the respiratory ciliated epithelium in healthy and COPD subjects, the development of a COPD disease and its pathogenesis, it also involves information on the pathogens studied and their significance for the development of COPD exacerbations; important signalling mechanism involved in the defence mechanisms of the respiratory epithelium are shortly presented along with the most commonly found in COPD patients inflammatory mediators.

The methodology chapter of this thesis outlines how primary tissue was collected from different subjects and how it was differentiated at air-liquid interface to become of mucociliary phenotype; basic techniques such as high speed video microscopy, confocal live imaging, western blotting, flow cytometry and immuno-based assays are also explained.

The first results chapter investigates the interaction of *M. catarrhalis* with the ciliated airway epithelium *in vitro* and presents the major findings from this part of the project. The second chapter presents single rhinovirus infection and its effects on the ciliated airway epithelium. The third results chapter describes the early effects of rhinovirus and *M. catarrhalis* co-infection of the ciliated epithelium.

The results chapters are followed by a general discussion of the current study and the implications associated with the respiratory epithelium together with future work directions.

Table of Contents

List of Figures

List of Tables

Abbreviations

ALI	air-liquid interface
AF	apical fluid
ATP	adenosine triphosphate
BAB	blood agar base
BAL	bronchoalveolar lavage samples
BHI	brain heart infusion
CA	ciliary activity
CARD	caspase recruitment domain- containing protein
CBA	ciliary beat amplitude
CBF	ciliary beat frequency
CC10	club cell 10-kDa protein
CCR2	chemokine receptor
CCSP	club cell secretory protein
CDHR3	cadherin-related-family-member 3 receptor
CEACAM3	carcinoembryonic antigen related cell adhesion molecule 3
CFU	colony forming unit
CLRs	C-type lectin receptors
COPD	Chronic Obstructive Pulmonary Disease
CXCL	CXC-chemokine ligand
DAI	DNA-dependent activator of IFN-regulatory factors
DNA	deoxyribonucleic acid

DTT	Dithiothreitol
EGFR	epidermal growth factor receptor
ENA-78	epithelial neutrophil activating peptide
ER	endoplasmic reticulum
FEV1	forced expiratory volume in 1 second
FOXA3	forkhead box A3
FOXJ1	forkhead boxJ1
FVC	forced vital capacity
GM-CSF	granulocyte macrophage colony stimulating factor
GRO-α	growth-related gene-α
GPR9	G-protein coupled receptor 9
GMP	guanosine monophosphate
GTPases	guanosine triphosphate hydrolase enzymes
H_2O_2	hydrogen peroxide
ICAM-1	Intracellular adhesion molecule -1
IFI16	Interferon-gamma-inducible protein 16
IFN	Interferon
Ig	Immunoglobulin
IL	interleukin
IP-10	Interferon-gamma inducible protein-10
IRAK2	IL-1 receptor associated kinase 2
ISG	interferon stimulated genes
I-TAC	interferon inducible T-cell alpha chemoattractant

JAG1	jagged-1
JAKs	janus kinases
KRT5	cytokeratin 5
KRT8	cytokeratin 8
KRT14	cytokeratin 14
LDLR	low density lipoprotein receptor
LOS	lipooligosaccharide
Lbp	lactoferrin binding protein
LPS	lipopolysaccharides
MARCKS	myristoylated alanine-rich C-kinase substrate
MAPK	mitogen activated protein kinase
MAVs	mitochondrial antiviral signalling
McaP	*Moraxella catarrhalis* adherence protein
MCP1	monocyte chemotactic protein 1
M. catarrhalis	*Moraxella catarrhalis*
MDA-5	melanoma differentiation-associated gene 5
MID/Hag	immunoglobulin D binding protein/hemagglutinin
MIG	Monokine induced by interferon gamma
MIP3α	Macrophage inflammatory protein 3 alpha
Mha proteins	*M. catarrhalis* filamentous Hag proteins
MMP	matrix metalloproteinases
MPO	myeloperoxidase
MUC5AC	mucin 5AC

MUC5B	mucin 5B
Mx	Myxovirus resistance
NDRs	NOD-like receptors
NF-kB	nuclear factor kappa-light chain-enhancer of activated B cells
NK cells	natural killer cells
NO	nitric oxide
NOS	nitric oxide synthase
NTHI	non-typeable *Haemophilus influenzae*
OAS	2'-5'-oligoadenylate synthase
OD	optical density
OMVs	outer membrane vesicles
OMP	outer membrane protein
PAF	platelet activating factor
P. aeruginosa	*Pseudomonas aeruginosa*
PBS	phosphate buffered saline
PEG	polyethylene glycol
Pell1	Pellino 1 receptor
PI3K	phosphoinositide– 3 kinase
PKG	cyclic GMP-dependent protein kinase
PKC	protein kinase C
PKR	protein kinase R
RANTES	regulated on activation, normal T cell expressed and secreted
RIG-1	retinoic acid inducible gene 1

RFX	regulatory factor X
RNA	ribonucleic acid
ROS	reactive oxygen species
RV	rhinovirus
SEM	standard error of mean
SCGB1A1	secretoglobin family 1A member 1
SLPI	secretory leukocyte protease inhibitor
Sp1	specificity protein 1
S. pneumoniae	*Streptococcus pneumoniae*
SO_2	sulfur dioxide
SPDEF	sterile alpha motif pointed domain–containing E-twenty-six transformation specific transcription factor
SP	surfactant protein-A
Syk	spleen tyrosine kinase
Tbp	transferrin binding proteins
TBS	Tris Buffered Saline
Tc1	Type 1 cytotoxic
TEER	transepithelial electrical resistance
TEM	Transmission Electron Microscopy
TFP	Type IV pili
TGF-β	transforming growth factor-β
Th1/2	T helper lymphocyte type 1/2
TIR	Toll/Interluikin-1 receptor

TNF-α	tumour necrosis factor- alpha
TNFR2	Tumor Necrosis Factor receptor 2
TLR	toll like receptor
TRP63	transformation-related protein 63
Usp	ubiquitous surface proteins
VCAM-1	Vascular adhesion molecule – 1
Viperin	virus inhibitory protein, endoplasmic reticulum associated IFN inducible
VP	viral proteins
VPg	virion protein genome linked
ZO-1	zona occludens-1

Chapter 1. Introduction

1.1 The human airway epithelium

The human airway is a network of inter-connected tubes that allow airflow in and out of the lungs (Lee et al., 2009). The airways can be divided into two zones - conducting and respiratory (Soleas et al., 2011). The conducting airways involve the nasal cavities, pharynx, larynx and the trachea. The trachea divides into two major bronchi which then subdivide into smaller bronchioles. The conducting airways' primary function is to concentrate bulk air flow during breathing (Soleas et al., 2011). It is also the site of the airways where airflow obstruction occurs in diseases such as asthma and COPD. The respiratory zone involves the terminal bronchioles branching into alveolar ducts and sacs. Its main function is to promote gas exchange efficiently during breathing (Lee et al., 2009).

Trophic units of the lungs carry out specific functions and have specialised epithelium lined with different cell types (Crystal et al., 2008; Lynch and Engelhardt 2014). The human airway is mostly covered by a pseudostratified epithelium with 10^{10} epithelial cells in a total surface area of 2471 cm^2 from the trachea to the bronchioles. Nasal and bronchial epithelial cells have been shown similar in size, shape, growth rate, ciliary activity (ciliary beat frequency of nasal cells 10.8 ± 0.7Hz and 11.8 ± 2.3Hz of bronchial cells) and expression of cellular adhesion receptors such as CD44, intracellular adhesion molecule 1 (ICAM-1) and integrin $\alpha v\beta 5$ (Devalia et al., 1990, McDougall et al., 2008). Cytokine release has been found greater in nasal airway cells than in bronchial. In response to interleukin-1 β (IL-1β) and tumour necrosis factor-α (TNF-α) stimulation, however, the magnitude of cytokine release has been found similar between the upper and lower airways (McDougall et al., 2008). Different from the dermal and intestinal epithelia, the airway epithelium is not fast renewing unless damaged (Tilley et al., 2015).

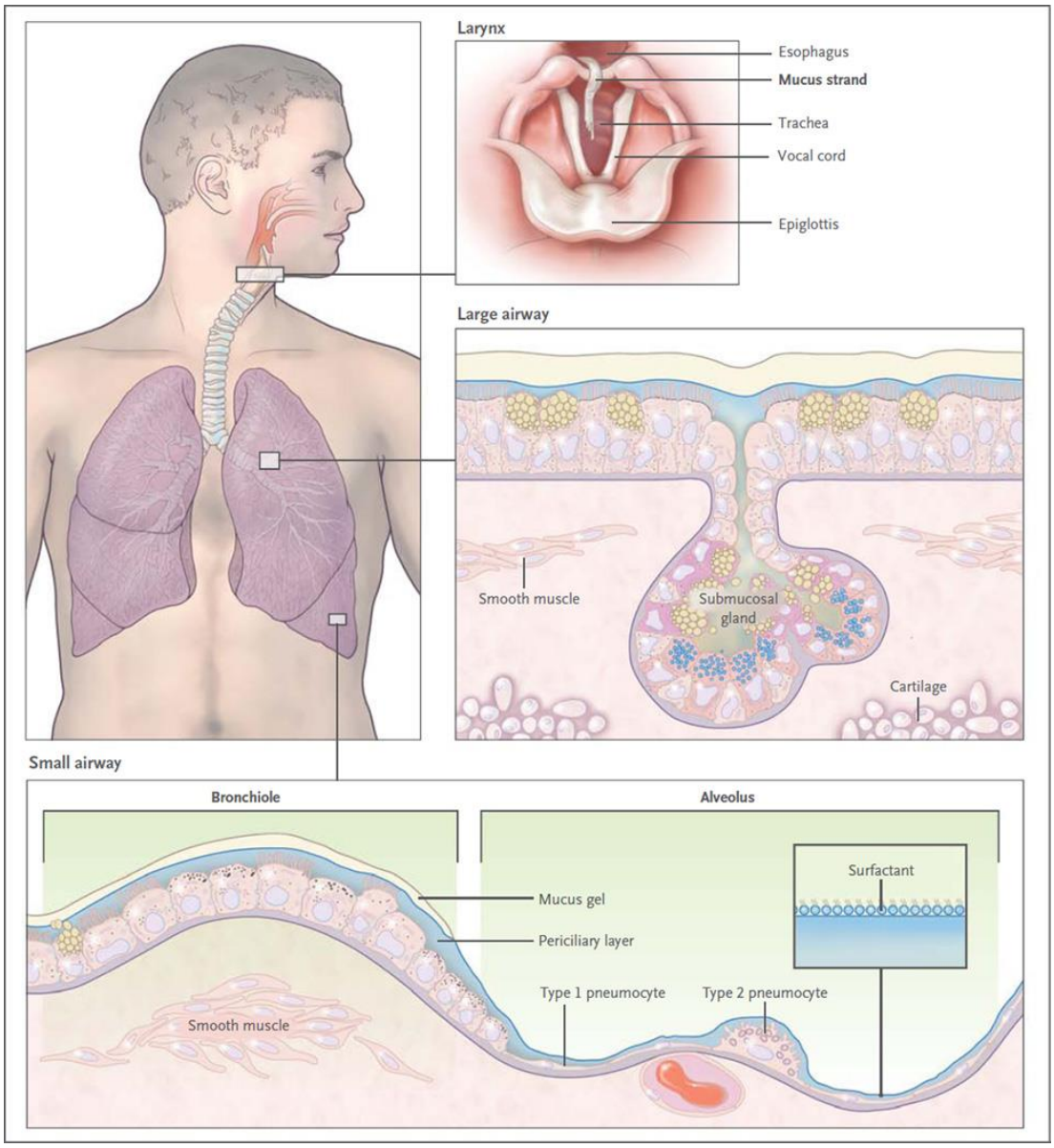

Figure 1-1: The human airways.

Air inhaled through the nose travels through the trachea and reaches the left and right bronchi (large airways), air passes through the bronchi which branch into smaller bronchioles (small airways) and finally air passes into the very thin alveoli allowing gas exchange between the alveoli and the surrounding capillary network. The large airways are lined by a pseudostratified epithelium, covered by a mucous layer formed of mucins secreted from secretory cells and glands. The small airways are lined by more cuboidal epithelial cells, which are covered by a thin mucous layer and a periciliary layer (Adapted from Fahy and Dickey 2010).

1.1.1 Types of cells in the human airways

The entire human airways are lined up with a continuous layer of epithelial cells which change in distribution, type and abundance depending on the region of the airways they are located (Ganesan et al., 2013; Tilley et al., 2015). Four major types of cells cover the human airways – ciliated, undifferentiated columnar, secretory and basal cells (Rackley and Stripp 2012; Tilley et al., 2015). The upper airways are covered with ciliated and mucus producing goblet cells so as to trap inhaled particles and pathogens (Ganesan et al., 2013; Tilley et al., 2015; Vieira Braga et al., 2019). Submucosal glands located in the proximal airways and the cartilaginous bronchioles also produce a significant proportion of mucus. Basal cells are present in relatively lower numbers in the upper airways than in the lower airways, where ciliated cells become the predominant cell type together with club cells (Vieira Braga et al., 2019). Other cell types in the conducting airways are chemosensory cells, important for fluid secretion, and neuroendocrine cells with a pyramidal shape, that extend from the basal lamina and possess microvilli (Ganesan et al., 2013). At the terminal bronchioles the airway epithelium merges with the alveolar epithelium, covered by alveolar type I and type II cells (Rackley and Stripp 2012).

1.1.1.1 Basal cells

Basal cells are abundant in the larger airways and attached to the basement membranes via hemodesmoses ($\alpha 6\beta 4$ integrins associated with laminin 5 to assemble cell – extracellular matrix connections) (Michelson et al., 2000), providing a base for ciliated and goblet cells to adhere to the basal lamina. Thus, basal cells are in contact with the basement membrane, the columnar epithelial layer above them and the mesenchymal cells *e.g.* fibroblasts and immune cells below them (Evans et al., 2001; Rock et al., 2011). Basal cells' most important function is self-renew and produce other undifferentiated cells which can later become ciliated or secretory in a ratio of 10 ciliated to 1 secretory cell (Crystal, 2014). Basal cells act as progenitors and respond to senescence and injury in the lungs. In addition, they can also regulate neurogenic inflammation, inflammatory response, oxidative tissue defence and trans-epithelial water movement (Evans et al., 2001). Interestingly, basal cells secrete a variety of growth factors *e.g.* vascular endothelial factors, transforming growth factors, fibroblasts growth factors, platelet-derived growth factors and also express receptors for epidermal growth factor, transforming growth factor tumour necrosis factor, histamine, IL-1, serotonin, thus can influence and respond to surrounding cells (Crystal, 2014).

Basal cells have a high nuclear to cytoplasmic ratio, small amounts of organelles and scattered microvilli. They express high levels of transformation-related protein 63 (TRP63), cytokeratin 5 (KRT5) and cytokeratin 14 (KRT14), which are highly upregulated during lung damage and tissue renewal (Hogg et al., 2004; Rock et al., 2011). Basal cells ability to differentiate into secretory and ciliated cell types has been shown in multiple studies. Firstly, human isolated basal cells have been demonstrated to turn into ciliated and secretory cells in xenographs (Engelhardt et al., 1995). Later work showed epithelial cells isolated from human airways, positive for TRP63 and KRT5, were able to differentiate at air-liquid interface, where the basal site of cells is exposed to media and the apical site to air (Hackett et al., 2008). More recently, for research purposes several studies have used basal cells isolated from nasal turbinate or bronchial brushings to restore multi-layered and well differentiated epithelium at air-liquid interface *in vitro* (Hirst et al., 2010; Smith et al., 2014; Jing et al., 2019).

As basal cells act as stem cells, modifications in their genomes or constant external agents like cigarette smoke can affect individual's predisposition to respiratory disorders (Rock et al., 2011). Therefore, airway basal cells have also a role into development and progression of airway diseases such as COPD. The active proliferation of basal cells can also lead to basal hyperplasia whereas the inappropriate cell fate may induce goblet hyperplasia or squamous metaplasia or dysplasia, all of which define pathological airway remodelling. Similarly, basal cells inability to proliferate and increased differentiation can lead to basal cell hypoplasia (Rock et al., 2011).

1.1.1.2 Undifferentiated columnar epithelial cells

The airway epithelium is slowly self-renewing, unless an injury occurs. In a murine model of injury/repair by inhaled sulphur dioxide (SO_2), it has been established that peak of proliferation occurs at 24h, whereas stratification at around 36h (Rock et al., 2011). At this time basal cells, goblet cells and ciliated markers are absent. A population of undifferentiated supra-basal cells which express cytokeratin 8 (KRT8) has been therefore recognised as early progenitors in the airway epithelium (Rock et al., 2011). When basal cells proliferate into different types by creating clonal patches, they expand into an intermediate type of cells which, depending on the influence of microenvironment stimuli turn into a ciliated or secretory cell (Crystal, 2014).

The fate of epithelial cells is dictated by the expression of different transcription factors (Crystal, 2014; Tilley et al., 2015). Basal cells derived progenitors differentiate into ciliated cells when forkhead boxJ1 (FOXJ1) transcription factor is activated with the

contribution of multicillin, cyclin O and regulatory factor X (RFX) transcription factors or into mucus producing cells when the transcription factors sterile alpha motif pointed domain–containing E-twenty-six transformation specific transcription factor (SPDEF) and forkhead box A3 (FOXA3) are activated. Differentiation into a secretory lineage is governed by Notch signalling pathways (Crystal 2014; Tilley et al., 2015) and is discussed below.

1.1.1.3 Secretory cells

Overproduction of mucus is a common feature of respiratory diseases, directly associated with increased number of mucus producing cells (Crystal et al., 2008). The large airways are lined by a ciliated pseudostratified epithelium where goblet cells and submucosal glands secrete mucus. The proximal area of the small, distal airways (bronchioles) is lined by a ciliated columnar pseudostratified epithelium, which becomes more cuboidal in the distal airways, where club (clara) cells replace goblet (mucous secreting) cells (Livraghi and Randell 2007; Turner et al., 2011; Wong et al., 2009). The small airways is a crucial zone for lung diseases such as COPD (Crystal et al., 2008).

Recently, Notch signalling has become of interest in the process of epithelial differentiation. There are four Notch receptors present on airway bronchial epithelial cells Notch1-4 and in accordance to which of them is overexpressed, the differentiation of basal cells is skewed to either secretory or ciliated cell type (Jing et al., 2019; Rock et al., 2011). Receptors Notch 1 and 3 overexpression is associated with secretory cell differentiation but not ciliated. Additionally, there are five notch ligands, of which jagged-1 (JAG1) has been shown to regulate cell type differentiation (Gomi et al., 2016; Jing et al., 2019). For instance, human primary basal cells and immortalised basal cells grown at ALI, enriched in JAG1, promote secretory cell differentiation with increased expression of secretory cell markers *e.g.* mucin 5AC (MUC5AC) and secretoglobin family 1A member 1 (SCGB1A1) and stimulate secretory cell differentiation into neighbouring basal cells (Gomi et al., 2016).

1.1.1.3.1 Goblet cells

Basal cells differentiate into goblet cells which appear as the principal secretory cell in the cartilaginous airways (Turner et al., 2011). They secrete high molecular weight glycoproteins known as mucins (Rogers, 2003; Turner et al., 2011). To date, 17 human mucins have been identified, of which MUC5AC and MUC5B are the most abundant in airway secretions from healthy, COPD and asthmatic patients. Mucus

secretion is associated with mucin granules moving towards the apical membrane and opening of the granules to secrete mucins on to the airway surface (Rogers, 2003, Turner et al., 2011; Hiemstra et al., 2015). The process is mediated by the interaction of mucin secretagogues with cell surface receptors to activate protein kinase C (PKC) and cyclic guanosine monophosphate (GMP) -dependent protein kinase (PKG) that further phosphorylate myristoylated alanine-rich C-kinase substrate (MARCKS) which then modulates the movement of granules to the apical membrane (Rogers, 2003).

Goblet cell numbers increase in response to external stimuli such as cigarette smoke, toxic gases, inflammatory mediators and bacterial infections (Rogers, 2003, Schamberger et al., 2015). Mucin overproduction is associated with higher numbers of goblet cells, but T helper 2 (Th2) cytokines such as IL-4, IL-9, IL-13 can additionally stimulate increased secretion of mucins and induce goblet cell hyperplasia. The role of these stimuli has been demonstrated *in vitro,* by Atherton and colleagues (Atherton et al., 2003), who used differentiated bronchial epithelial cells, where goblet cells metaplasia was induced by IL-4 and IL-13 via mitogen activated protein kinase (MAPK) and phosphoinositide-3 kinase (PI3K).

Amongst the various stimulators of mucin hypersecretion EGFR signalling cascade can also stimulate MUC5AC synthesis through MAPK, influenced by Th2 cytokines, cigarette smoke, neutrophils and oxidative stress (Rogers, 2003; Crystal et al., 2008, Turner et al., 2011). For instance, reactive oxygen species (ROS) and activated neutrophils can activate EGFR and mucin synthesis in NCI-H292 epithelial cells via MAPK phosphorylation, which can be inhibited by tyrosine EGFR and mitogen activated protein kinase kinase blockers (Takeyama et al., 2000). Similarly, ROS exposure induces goblet cell hyperplasia, high MUC5AC gene and protein expression in differentiated normal human bronchial cells by phosphorylation of EGFR and MAPK (Casalino-Matsuda et al., 2006). In NCI-H292 airway epithelial cells and in whole animals such as rats, cigarette smoke induces mucus hyper-production through EGFR activation that can be attenuated by a platelet derived growth factor receptor kinase inhibitor (Takeyama et al., 2000).

Although secretion of mucins that form a mucus layer is protective against inhaled pathogens and particles, increased mucus secretion can also facilitate for the pathology of lung diseases *e.g.* COPD (Turner et al., 2011).

1.1.1.3.2 Club cells

Club cells contain cytoplasmic granules and are a secretory cell type found in the terminal bronchioles (Boers et al., 1999). Club cells are highly metabolic and can self-renew and proliferate into other cell types (Rogers, 2003; Wong et al., 2009). Club cells represent approximately 22% of the surface epithelium in the respiratory bronchioles (Boers et al., 1999).

Club cells produce club cell secretory protein (CCSP) also known as club cell 10-kDa protein (CC10), or secretoglobin family 1A member 1 (SCGB1A1). This is one of the most prevalent secretory proteins in the airway surface fluid that has biochemical and biological functions such as airway surface fluid maintenance, anti-tumorigenic properties, repair and regeneration capacity (Shijubo et al., 1999; Wong et al., 2009). CCSP has been found to inhibit phospholipase A and C and prostaglandin 2 involved in arachidonic acid inflammatory cascade associated with stimulation of pro-inflammatory lipid mediators. It is thought, therefore, that CCSP can control anti-inflammatory reactions and help maintain anti-inflammatory activity in the human airways (Shijubo et al., 1999; Wong et al., 2009). CCSP anti-inflammatory properties have been confirmed in CCSP knockout mice that were found to be more susceptible to oxidative stress and lung injury associated with increased production of pro-inflammatory cytokines (Wong et al., 2009). Club cells also express P450 enzymes that serve to detoxify and metabolise toxins helping to reduce the damaging effects of inhaled substances (Wong et al., 2009).

Decreased numbers of club cells have been reported in asthmatics compared to non-smokers, in co-occurrence with increased number of T- cells and mast cells (Shijubo et al., 1997). Additionally, lower levels of CCSP have been detected in smokers and bronchoalveolar lavage (BAL) fluid from patients with lung diseases such as asthma and COPD (Shijubo et al., 1997; Pilette et al., 2001). Decreased levels of serum CCSP in COPD patients has been correlated with the accelerated decrease of lung function in these patients over a period of 9 years (Park et al., 2013). Altogether these findings confirm CCSP important anti-inflammatory role in the airways of healthy subjects and patients with chronic lung diseases and suggest it has a vital role for the progression of lung diseases (Park et al., 2013).

1.1.1.4 Ciliated cells

Ciliated cells are the most abundant cell type of the airway epithelium. They comprise 50% of the conducting airways epithelial cells and are differentiated from basal cells

(Ganesan et al., 2013). They have a columnar shape and are anchored to the basement membrane of the epithelial surface. Cilia are protruding from the apical membrane of differentiated cells and are orientated in the luminal surface. At the apical surface ciliated cells also have microvilli which help for fluid and electrolytes movement (Tilley et al., 2015). Adjacent ciliated cells are connected via tight junctions which enable the passage of ions across the epithelium (discussed below in section 1.1.2.1). At the basolateral site, ciliated cells are attached to the basal cells and respectively to the airway basal membrane via desmosomes. The main function of ciliated cells is to transport mucus with the cohesive beating of cilia, to support the mucociliary escalator activity to remove inhaled particles, toxic gases and other external materials (Crystal, 2014; Tilley et al., 2015). Recently, it has been suggested ciliated cells are capable of dedifferentiating into squamous, cuboidal or columnar cells following lung injury to promote repair of the epithelium (Park et al., 2006) or to dedifferentiate into goblet cells upon persistent activation of EGFR and therefore induce goblet cell hyperplasia (Tyner et al., 2006).

1.1.1.4.1 Cilia

Cilia are classified as motile and non-motile based on their structural characteristics (Tilley et al., 2015). The airway cilia are motile and thus their ultrastructure will be discussed in more detail below.

Each motile cilium has a diameter of 200 to 300nm and a length of 6 μm to 7 μm (Tilley et al., 2015). A cilium is attached to the apical site of a cell by a plasma membrane microtubule core called the axoneme (Choksi et al., 2014). The axoneme is constructed from 9 radially organised microtubule doublets and 1 singlet microtubule in the centre (Figure 1-2). Doublets are linked to the central pair by radial spoke heads (Gudis et al., 2012). The central microtubules are connected by paired bridges while outer microtubule doublets interact with adjacent pairs by inner and outer dynein arms and nexins. Each doublet has α and β tubules which comprise of α and β tubulin dimers (Gudis et al., 2012). Phosphorylation of outer dynein arms controls the frequency of cilia beating while phosphorylation of inner dynein arms controls the wave pattern of cilia beating (Gudis et al., 2012). Radial spoke heads limit the sliding of microtubules during the ciliary stroke and thus allow bending of the axoneme. Normal motile cilia synchronise bending with cilia of neighbouring cells and create uniform motion which allows mucus clearance (Gudis et al., 2012).

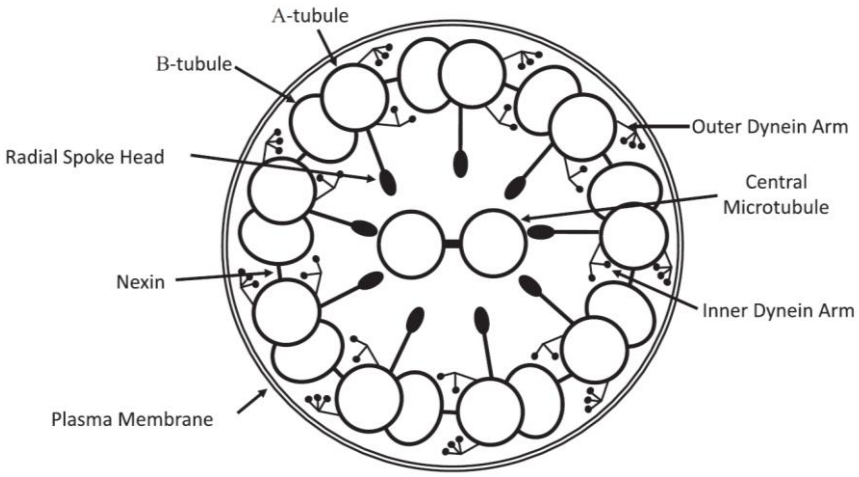

Figure 1-2: Ultrastructure of motile cilia axoneme.

The plasma membrane derived axoneme has 9 + 2 classical organisation of microtubule pairs. Doublets interact via nexins, inner and outer dynein arms. The central pair is linked to outer microtubules by radial spoke heads (Adapted from Gudis et al., 2012).

In healthy human airways cilia beat at 12-15 beats per second (Hz) and propel mucus in a proximal direction at 4-20 mm/min (Tilley et al., 2015). Cilia have a powerful forward stroke followed by a reverse (recovery) stroke. At the forward stoke cilia are fully extended, their distal tips touch the outer mucus layer and conduct directional force. At the reverse stroke cilia sweep back to their original starting position with minimal sideways deviation, passing below the mucus layer (Chilvers and O'Callaghan 2000). A number of factors may influence ciliary beat frequency (CBF) and uniform mucus transport. Increased pH, temperature, calcium levels, cyclic AMP, nitric oxide concentration, mechanical stress and cytokines such as TNFα, IL-1β can upregulate CBF, while decreased pH, temperature and increased hydrogen peroxidase levels can downregulate CBF (Gudis et al., 2012). Impaired ciliary function has been implicated in a number of diseases (O'Callaghan et al., 2007; Thomas et al., 2010). The best known is Primary Ciliary Dyskinesia where underlying ciliary defects result in cilia that are either static or that beat in a uniformly dyskinetic pattern (Bukowy et al., 2011).

1.1.2 Properties of the airway epithelium

The human airway has an important barrier function helping to protect it from the external environment that it is in constant contact with. The epithelium affords protection against infectious agents and noxious particles, and other pollutants. It maintains tissue homeostasis without inducing inflammation (De Rose et al., 2018). The main components contributing to the protective barrier of the airway epithelia are apical junction complexes such as tight junctions and gap junctions, antimicrobial peptides and the mucociliary escalator (Vareille et al., 2011; Ganesan et al., 2013).

1.1.2.1 Apical junction complexes

Integrity of the polarised epithelial layer is maintained by apical junctions such as tight and adherens junctions, GAP junctions and desmosomes, found on the apicolateral border of airway cells (De Rose et al., 2018). The most important are tight junctions - zona occludens proteins (ZO), occludin, claudin and junctional adherence molecules. Tight junctions consist of interacting proteins which maintain the cell barrier impermeable and at the same time allow transport of ions and macromolecules through the epithelial layer (Vareille et al., 2011). Tight junctions are multiprotein structures which keep airway epithelial cells together and at the same time separate the apical and basolateral membranes (Tilley et al., 2015). Tight junction integrity can be measured by transepithelial electrical resistance (TEER). In healthy ciliated cultures TEER values range from 700-1000 Ω/cm^2 (Shaykhiev et al., 2011).

Gap junctions are small channels between epithelial cells that allow diffusion of metabolites and second messengers to adjacent cells. Desmosomes provide mechanical strength as they form strong adhesive bonds with neighbouring cells (Vareille et al., 2011). Adherens junctions are situated below tight junctions and include E-cadherin and α and β catenins, which modulate cell-cell adhesion in a calcium depended manner (Ganesan et al., 2013). The extracellular domain of an E-cadherin binds to another E-cadherin of an adjacent cell (De Rose et al., 2018; Ganesan et al., 2013). The α-catenin protein links E-cadherin through β-catenin to the actin cytoskeleton, however dissociation of E-cadherin from β-catenin results in its translocation to the nucleus where Wnt/β-catenin signalling promotes cell proliferation but not differentiation (Drees et al., 2005; Ganesan et al., 2013). Additionally, apical junctions can alter cell growth and differentiation when E-cadherin dissociates from its catenin complex causing redistribution of EGFR that later can be apically activated by EGF stimuli to cause cell proliferation (Ganesan et al., 2013).

1.1.2.2 Antimicrobial products

Airway epithelial cells secrete different antimicrobial peptides (lactoferrin, defensins, cathelicidin), protease inhibitors (secretory leukoprotease inhibitor –SLPI, elafin, alpha-1-antitrypsin, enzymes (lysozymes) and oxidants (nitric oxide and peroxidase) that act against inhaled pathogens (Ganesan et al., 2013; De Rose et al., 2018, Vareille et al., 2011). Proteases inhibitors can reduce the effects of pathogen secreted proteases and recruited immune cells proteases, helping to maintain the balance between proteases and anti-proteases to help prevent lung inflammation and to maintain tissue homeostasis (Ganesan et al., 2013). Enzymes such as lysozymes can also degrade the peptidoglycan layer of gram positive and gram negative bacteria, though only in the presence of the iron binding protein lactoferrin which damages the bacterial outer membrane (De Rose et al., 2018).

Lactoferrin is an antimicrobial iron bound glycoprotein that can be antibacterial by chelating iron which is essential for bacterial respiration or antiviral by stopping binding of the virus to the host cell or binding to the actual viral particle (De Rose et al., 2018). Human defensins are subclassified into α and β defensins. Human β defensins 1-4 are the most prevalent antimicrobial peptides in the lungs and are protective against fungi, bacteria and viruses. Defensins can permeabilise the membranes of pathogens, inhibit bacterial protein synthesis and bind to membrane glycoproteins to mediate an antiviral function (Ganz, 2003). Defensins can also be immunomodulatory as they can attract immune cells such as T cells, dendritic cells and monocytes by binding to chemotactic receptors *e.g.* CCR6 (Ganz, 2003). Cathelicidin is from a different antimicrobial peptide class and the only one identified to date is named LL-37, which has the ability to bind lipopolysaccharides and inhibit their activity (Ganesan et al., 2013).

Airway epithelial cells can synthesise nitric oxide (NO) by synthases NOS1, NOS2, NOS3 (Schairer et al., 2012). At low concentrations, NO signals to induce growth and activation of immune cells and at high concentrations, NO can bind to deoxyribonucleic acid (DNA), proteins and lipids, inactivating and killing viruses and bacteria. More specifically, when NO reacts with oxygen or superoxide free radicals this leads to the production of intermediate reactive nitrogen species which induce oxidative and nitrosative damage by changes in DNA, enzyme activity and induction of lipid peroxidation (Schairer et al., 2012).

1.1.2.2.1 Mucociliary escalator

The respiratory epithelium is persistently exposed to inhaled infective agents and airborne particles which can damage the airway lining (Hackett et al., 2008; Ganesan et al., 2013; De Rose et al., 2018). It is protected by a 10μm thick layer of airway surface liquid made of watery periciliary fluid and a mucus layer above it (Holgate et al., 2009; Boucher, 2019). The initial defence mechanism of the respiratory epithelium is the mucus which traps infectious pathogens and particles while the beating of cilia clears them from the airways (Soleas et al., 2011). This process is called mucociliary clearance.

Mucus is comprised of 97% water, 1% sodium chloride, 1% different antioxidants, antimicrobial and immunomodulatory molecules (lysozymes, defensins, IgA, cytokines) and 1% mucin glycoproteins (Gudis et al., 2012; Munkholm and Mortensen 2014). As discussed earlier (section 1.1.1.3.1), the major mucin types detected in sputum are MUC5AC and MUC5B, secreted by goblet cells and submucosal glands (Vareille et al., 2011). MUC5AC and MUC5B secretion is also regulated by the transcription factors nuclear factor kappa-light chain-enhancer of activated B cells (NF-kb) and specificity protein 1 (Sp1) (Vareille et al., 2011). Mucus has to be at correct viscosity and elasticity to maintain mucociliary clearance (Rogers, 2007). Viscosity is a fluid feature which allows mucus to trap and retain inhaled particles. Elasticity is a solid characteristic important for efficient mucus transport (Fahy and Dickey 2010).

The airway surface liquid depth and hydration is maintained through ion channels through the secretion of chloride ions and the absorption of sodium ions (De Rose et al., 2018). In addition, airway surface hydration is maintained by mechanosensory properties of cilia, detecting the mucus layer concentration (percentage of volume consisting of non-volatile solids), and the release of ATP by cilia into the airway surface layer (Boucher, 2019). A well hydrated mucus layer allows for mucus transport. However, in muco-obstructive diseases the fluid absorption is altered, leading to increased mucus concentration (dehydrated mucus), reduced mucociliary transport or static mucus (Boucher, 2019). For example, in cystic fibrosis. The periciliary fluid surrounds and lubricates cilia. Its low viscosity allows for rapid ciliary beating and thus for mucus movement and clearance. Button and colleagues (Button et al., 2012) have suggested a new periciliary fluid composition in which the periciliary fluid layer is full of mucins and mucopolysaccharides closely tethered to the cilia, termed as a ‘gel-on-brush model’. The resultant mesh prevents mucus from

penetrating into the periciliary space and explains why the mucus and the periciliary layers do not mix up (Button et al., 2012). Immunohistochemistry studies of fixed human airways samples identified that the membrane tethered macromolecules in the periciliary fluid are mucin 1 and 4 (MUC1 and MUC 4). The density of MUC1 and MUC4 is sufficient to form a protective ‘mesh’, which prevents particles bigger than 40nm to penetrate into the periciliary fluid and at the same time maintains airway surface hydration (Button et al., 2012).

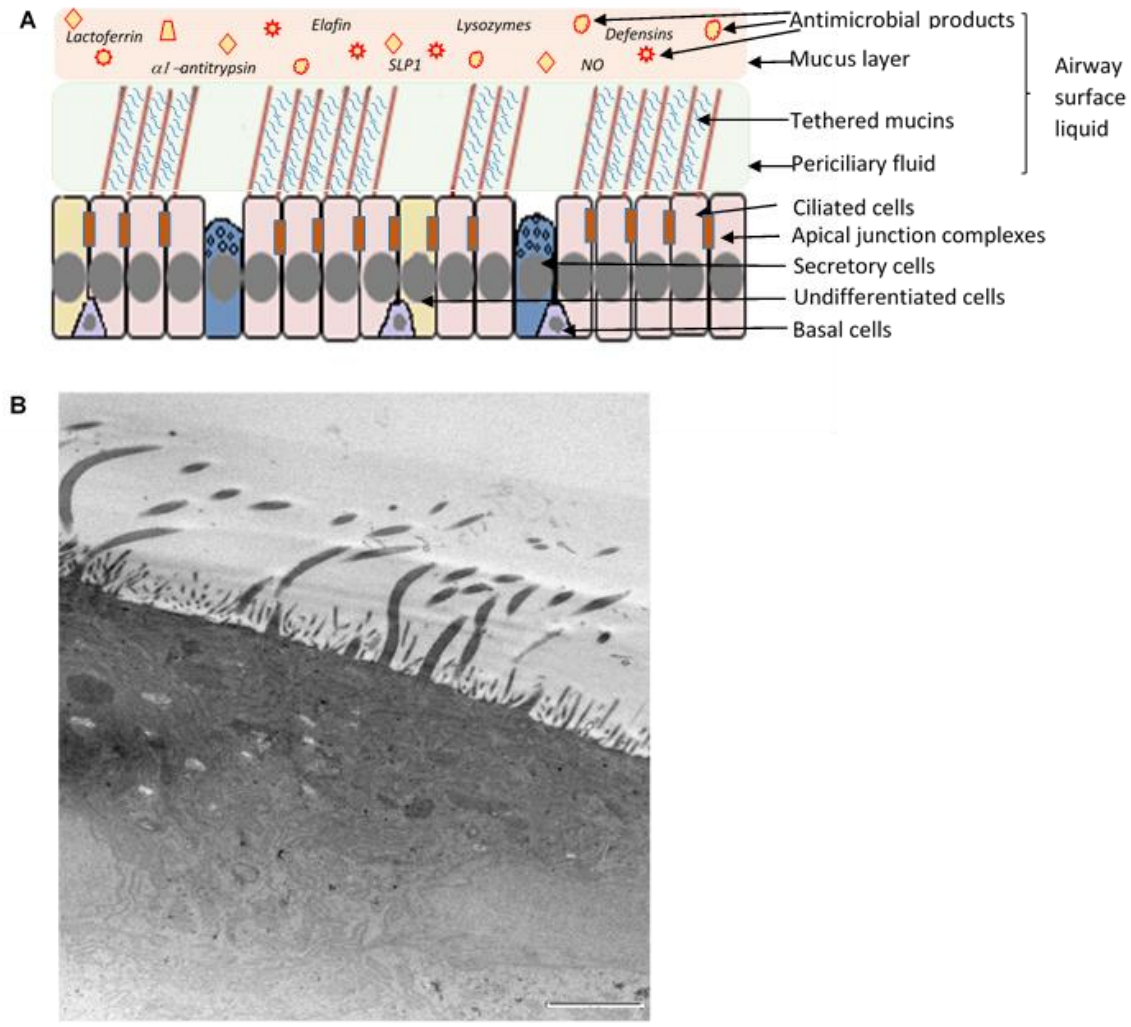

Figure 1-3: Schematic representation of the respiratory tract (*original figure*).
A) Four different types of cells cover the respiratory tract – ciliated, secretory, undifferentiated columnar and basal cells, interconnected by apical junction complexes which allow paracellular passage of macromolecules and ions. Ciliated cells play a vital role for mucociliary clearance with the help of the highly coordinated beating of cilia. The periciliary fluid layer is composed of tethered mucins that prevent mixture with the mucus layer situated above it. Antimicrobial peptides are present in the airway surface liquid to fight inhaled pathogens. B) Transmission Electron Microscopy (TEM) image of the human healthy ciliated epithelium, scale bar=2μM

1.2 Chronic Obstructive Pulmonary Disease

1.2.1 Epidemiology

COPD is characterised by progressive limitation of airflow in the lungs and is associated with chronic inflammatory responsiveness in the airways (Global Initiative for chronic lung diseases- GOLD 2018). It is the fourth leading cause of death in the world, and estimated to become the third leading cause of death by 2030 (World Health Organisation 2016). In the UK, approximately 3 million people suffer from COPD and the disease accounts for 25% of all lung associated deaths (British Thoracic Society, accessed Feb 2019). Globally, 3 million people die from COPD each year, and this number is expected to rise to 4.5 million by 2030. COPD has a great healthcare burden accounting for 38.6 billion euros a year of the budget for respiratory diseases in the European Union.

The most characteristic symptoms of COPD are dyspnea and persistent cough with sputum production, due to excess production of mucus and mucociliary dysfunction. Additionally, COPD patients can suffer from wheezes and tightness of the chest and in some severe cases from fatigue, weight loss and anorexia (GOLD 2018).

The GOLD spirometry grading system of COPD is defined by the level of airflow obstruction. The spirometry criterion, post a bronchodilator drug aims to minimise variability and uses the ratio of forced expiratory volume in 1 second (FEV_1) to forced vital capacity (FVC), which below 0.7 indicates the presence of an obstructive disease (GOLD 2018). COPD is classified into 4 severity stages according to predicted percentage (%) of FEV_1 in patients with FEV_1/ FVC ratio < 0.70 (GOLD 2018) (Table 1-1).

Table 1-1: COPD classification based on percentage of predicted FEV_1 post a bronchodilator.

In patients with FEV_1/ FVC ratio < 0.70		
Grade	Group	Description
GOLD 1	Mild	$FEV_1 \geq 80\%$ predicted
GOLD 2	Moderate	$50\% \leq FEV_1 < 80\%$ predicted
GOLD 3	Severe	$30\% \leq FEV_1 < 50\%$ predicted
GOLD 4	Very severe	$FEV_1 < 30\%$ predicted

Several environmental and genetic factors play an important role for the development of COPD (GOLD 2018). These factors are summarised in Table 1-2. Of which, the biggest contributor to COPD is significant exposure to noxious gases and particles such as cigarette smoke. Yet, only 20% of all smokers develop COPD (GOLD 2018). Smoking disturbs the normal gas exchange in the lungs, thus affecting the biological function and structure of the airway epithelium (Harvey et al., 2007). Smoking has been linked to upregulation of antioxidant genes (Hackett et al., 2003; Pierrou et al., 2007) and genes involved in innate immune responses in airway epithelial cells from bronchial brushings (Harvey et al., 2007). Additionally, smoking contributes to shortened cilia length of bronchial ciliated cells that would also cause reduced mucociliary clearance (Leopold et al., 2009). Of interest, smoking has been shown to induce gene expression changes in the respiratory tracts of healthy individuals which were found to overlap in the upper and lower airways, supporting the hypothesis that smoking causes an airway wide response (Zhang et al., 2010). In a different study by Takkila smoking has been shown to change inflammation, epithelial cell stress response, proliferation and cell fate in nasal epithelium of healthy subjects (Tekkila et al., 2017). Epidemiological studies reveal that non-smokers can also develop chronic

inflammation in the lungs, however these patients experience fewer and milder symptoms as well as having a lower risk of developing a cardiovascular disease or lung cancer (GOLD 2018).

Table 1-2: Factors influencing the development of COPD.

Factor	Type	Role	Source
Severe hereditary alpha-1 antitrypsin deficiency	Genetic host factor	Inhibitor of serine proteases	Hogg and Timens 2009; Martinez et al., 2018
Sex and age	Host factor	Women are more prone to tobacco induced changes	GOLD 2018; Martinez et al., 2018
Lung growth and development	Host factor	Reduced lung function during childhood	Martinez et al., 2018
Asthma	Host factor	Irreversible airflow limitation, airway hyper responsiveness	GOLD 2018
Chronic bronchitis	Host factor	Declined lung function	GOLD 2018; Martinez et al., 2018
Infections e.g. HIV and tuberculosis	Environmental factor	Accelerate onset of smoking-induced emphysema	Sethi, 2010
Exposure to tobacco, dust, chemical agents, fumes, indoor and outdoor pollution	Environmental factor	Declines lung function	Martinez et al., 2018; Hiemstra et al., 2015; Sethi, 2010

1.2.2 Treatment

Current treatment of COPD has only partial effect on disease manifest (GOLD 2018). It aims to decrease symptoms, severity and frequency of exacerbations and improve overall health status, however no evidence suggests it helps improving long term decline of lung function (GOLD 2018). Treatment options include:

Bronchodilators - Short acting and long acting bronchodilators such as Salbutamol and Fenoterol, aim to improve FEV_1 and airflow obstruction in patients with COPD, usually prescribed on a regular basis. COPD patients are given short-acting bronchodilators to decrease severity of symptoms, while a combination of short and long acting bronchodilators has been shown to be superior in improving FEV_1 and exacerbations frequency (GOLD 2018).

Corticosteroids – both oral and inhaled corticosteroids such as prednisolone and fluticasone are often prescribed with the aim to reduce inflammation in the lungs. However, these medications do not a have marked effect on FEV_1 in stable COPD patients and can be linked to adverse effects (GOLD 2018, NICE 2018). A combination of long acting bronchodilators with inhaled corticosteroids such as Salmeterol/ Fluticasone is tolerated well in patients with moderate to severe COPD (GOLD 2018). The combination can be effective in reducing breathlessness and frequency of exacerbations. Patients may also benefit from a triple combination of inhaled corticosteroids/ long acting muscarinic antagonist/ long acting β2-agonist as it may improve lung function, symptoms, exacerbation risk and overall health status (GOLD 2018).

Antibiotics – the prophylactic use of antibiotics does not help in reducing the number of exacerbations in patients with COPD (GOLD 2018). However, the more frequent use of some antibiotics *e.g.* azithromycin and erythromycin has been beneficial in reducing the risk of exacerbations when taken for one year, however no associated benefits are observed beyond that period (GOLD 2018).

1.2.3 Pathogenesis, inflammation and pathophysiology

Remodelling of the airways and persistent inflammation are common characteristics of COPD (Shaykhiev and Crystal 2014). The airway epithelium is a main site of molecular and pathological alteration. In COPD, the epithelium is thicker with basal and goblet cell hyperplasia (Shaykhiev and Crystal 2014). Mucus is excessively produced and has been shown to occupy the airway lumen and to be cleared inappropriately compared to normal subjects (Barnes, 2017). Emphysema can also

occur with damaged air-sacs, reduced alveolar attachment to the small airways and loss of elasticity, making the lungs incapable to remain open during expiration (GOLD 2018, Shaykhiev and Crystal 2014). Differentiation of ciliated cells and length of cilia are reduced in COPD patients (Shaykhiev and Crystal 2014). Club cells are replaced by mucous secreting cells that is thought to contribute to mucus build up in the small airways and the terminal bronchioles (Shaykhiev and Crystal 2014). At this site of the airways mucus is thought to be difficult to clear by coughing (Jeffery, 2000). Tight junction integrity is also impaired and permeability of the epithelium is increased, as reflected by a decrease in the TEER. This is also thought to increase the susceptibility to airway infections in COPD patients (Hiemstra et al., 2015). The changed phenotype of the respiratory epithelium therefore contributes to both airflow obstruction and lowered defence mechanisms (Shaykhiev and Crystal 2014).

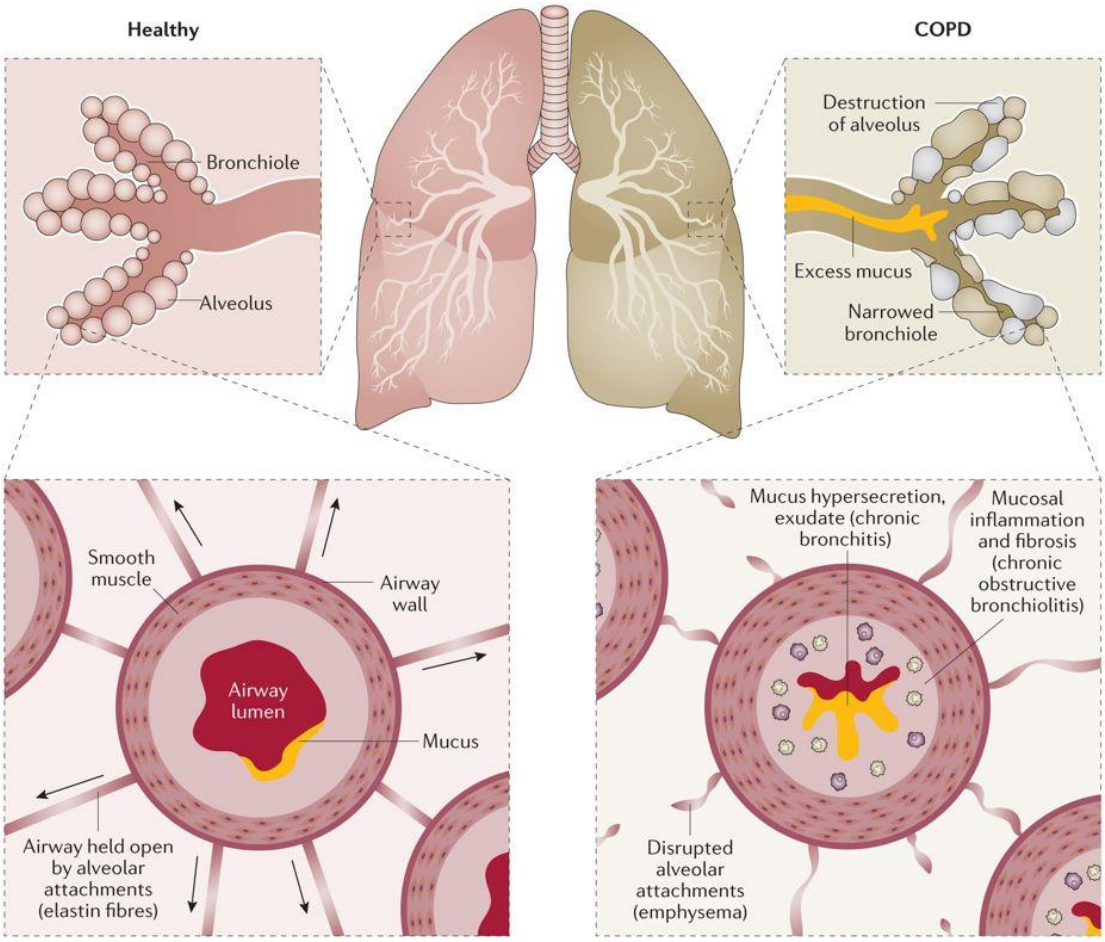

Figure 1-4: Structural characteristics of the healthy and COPD airways.
The bronchioles (small airways) in healthy airways are open because of elastic alveolar wall attachments. The bronchioles in COPD airways are obstructed due to narrowed thickened bronchiolar periphery wall as a result of inflammation and disrupted alveolar attachments caused by mucus hypersecretion and fibrosis (Adapted from Barnes et al., 2015).

The altered permeability of the COPD epithelium and its capability to secrete cytokines and growth factors modulate inflammation (Hiemstra et al., 2015). Cytokines are extracellular signalling molecules, some of which are overexpressed in COPD. Elevated levels of pro-inflammatory cytokines such as interleukins IL-1β, IL-6, IL-8/ CXCL8, TNFα, monocyte chemotactic protein 1 (MCP1)/ CCL2, growth-related gene-α (GRO-α)/ CXCL1 (discussed in more detail in section 1.5.2) have been seen in COPD sputum samples and further elevated during exacerbations, promoting inflammation (Barnes, 2016; Chung, 2001; Hogg and Timens 2009). Cigarette smoke

can modulate innate and adaptive immune responses in the lungs, contributing to the pathogenesis of COPD (Hogg and Timens 2009). Further, inflammatory cells that contribute to a heightened state of inflammation such as neutrophils, lymphocytes, eosinophils and macrophages have been detected in COPD bronchial biopsy specimens (Jeffery, 2000; Barnes et al., 2016). It has been reported that upper airway inflammation is also associated with exacerbation presentation in COPD (Hurst et al., 2006a; Hurst et al., 2006b; Vachier et al., 2004). High levels of T lymphocytes, neutrophils and macrophages are common in the nasal, upper airways of COPD patients (Vachier et al., 2004). The inflammatory cells concentrations in the Vachier study were similar in the nose and in the bronchi, with squamous cell metaplasia being the most common structural change observed in the two airway compartments (Vachier et al., 2004). Hurst has described the relationship between upper and lower airway inflammation at exacerbation using nasal washes, sputum and serum samples from 41 COPD patients (Hurst et al., 2006a). A positive correlation between nasal washes and serum has been found for the inflammatory markers IL-6, IL-8/ CXCL8 and myeloperoxidase (MPO). The degree of upper airway inflammation was similar to that in the lower airways as indicated by similar MPO concentrations in the two airway compartments (Hurst et al., 2006a). In addition, nasal airway obstruction and nasal symptoms reflect pulmonary airway obstruction in COPD (Hurst et al., 2006b). Similarities between upper and lower airways have been confirmed by gene expression profiling of nasal and bronchial brushes from 31 COPD patients. The expression of genes related to O-glycan biosynthesis, glycosphingolipid synthesis, DNA replication, RNA degradation and tight junctions was in common and overlapped in the two locations (Boudewijn et al., 2017).

1.2.3.1 Inflammatory cells

1.2.3.1.1 Macrophages

Macrophages are derived from circulating monocytes and are involved in tissue repair processes and phagocytosis (Morales-Nebreda et al., 2015). Fixed stained lung tissue from COPD patients at different GOLD stages, have shown inflammatory response is reflected by the number of accumulated leukocytes, macrophages and lymphocyte cells *e.g.* $CD4^+$, $CD8^+$ and B cells, organised in lymphoid follicles, while severity of inflammatory response is regulated mainly by $CD8^+$ and B cells (Hogg et al., 2004). Two classes of macrophages are designated according to the type of immune response they elicit (Shaykhiev and Crystal 2013). Polarised M1

macrophages are activated by lipopolysaccharides (LPS) and yield pro-inflammatory cytokines, whereas polarised M2 macrophages are activated by IL-4 and IL-13 and function in repair processes to produce anti-inflammatory cytokines (Gordon and Tylor 2005, Gordon and Martinez 2010). Increased chemoattractants *e.g.* CCL2 and CXC-chemokine ligand 1 (CXCL1) in the airways are linked to increased numbers of macrophages in the airways (Traves et al., 2004). In turn, activated macrophages secrete more IL-1β, IL-6, TNF-α, GRO-α/ CXCL1, IL-8/ CXCL8, MCP1/ CCL2, monokine induced by interferon gamma (MIG or CXCL9), Interferon-gamma inducible protein-10 (IP-10 or CXCL10) and CXCL11 (CXC chemokine ligand 11)/ I-TAC (interferon inducible T-cell alpha chemoattractant) which attract $CD8^+$ cytotoxic Tc1 cells and $CD4^+$ T helper cells (Shaykhiev et al., 2009). Additionally, there is clinical evidence suggesting COPD patients exhibit M2 polarised macrophages, induced by cigarette smoke (Shaykhiev et al., 2009). Increased expression of the M2 marker on alveolar macrophages has been linked to COPD pathogenesis (Kaku et al., 2014). Macrophages in COPD patients release more ROS and matrix metalloproteinases (MMP)-2, 9, 12 compared to healthy and non-smoking individuals (Culpitt et al., 2005, Grumelli et al., 2004; Barnes, 2017).

1.2.3.1.2 Eosinophils

Eosinophils are generated in the bone marrow and play an important role in growth factors secretion (e.g. transforming growth factor-β - TGF-β) that are vital for tissue remodelling. An important mediator for the secretion and survival of eosinophils in the airways is IL-5, secreted by T-helper 2 (Th2) lymphocytes (Bafadhel et al., 2009). Their migration to the lungs is dependent on the chemoattractants – RANTES/ CCL5, MCP3/ CCL7, eotaxin-1/ CCL11, MCP-4/ CCL13 (Tashkin and Wechsler 2018). Increased numbers of eosinophils have been associated with an increased risk of exacerbations, and significantly higher numbers of tissue eosinophils have been detected in COPD subjects with exacerbations, compared to patients with stable state COPD and healthy individuals (Chung, 2001; Saha and Brightling 2006; Vedel-Krogh et al., 2016). When present within the lungs, eosinophils secrete pro-inflammatory cytokines and growth factors, thus inducing inflammation (Tashkin and Wechsler 2018). COPD patients who exhibit eosinophilic inflammation are more likely to respond to corticosteroid therapy (Bafadhel et al., 2009). This may allow a specific group of COPD patients to be treated with corticosteroid therapy to reduce exacerbation rate and lung function decline (Bafadhel et al., 2009).

1.2.3.1.3 Neutrophils

High numbers of neutrophils are often detected in sputum and bronchoalveolar lavage (BAL) samples from COPD patients (Hogg et al., 2004). Neutrophils have the primary function to destroy pathogenic microorganism via the internal generation of ROS and proteases such as neutrophil elastase and cathepsins (Hoenderdos and Condliffe 2013). Neutrophils are the most common inflammatory cell found in the bronchial walls of COPD patients. They are attracted to the lungs by chemoattractants such as GRO-α/ CXCL1, ENA-78 (epithelial derived neutrophil attractant) / CXCL5, IL-8/ CXCL8 derived from epithelial cells, macrophages and T cells (Hoenderdos and Condliffe 2013, Barnes, 2017). Prolonged and persistent infections in COPD lead to accumulation of activated neutrophils which release myeloperoxidase (MPO), serine proteases *e.g.* neutrophil elastase, cathepsin G, MMP-1/2, MMP-9. The close proximity of proteases, secreted by neutrophils, to extracellular matrix components *e.g.* collagen and fibronectin can result in their degradation (Hoenderdos and Condliffe 2013). Furthermore, neutrophils in COPD have reduced chemotactic accuracy and are defective in clearing pathogens (Sapey et al., 2011). Degranulation of neutrophils has been detected in COPD and associated with secretion of bioactive lipids that damage tissues (Hoenderdos and Condliffe 2013). In addition to damaging the lungs in COPD, neutrophils are associated with mucus hypersecretion. Neutrophil elastase induces mucus hypersecretion through activation of epidermal growth factor receptors, which helps to explain the link between neutrophilic inflammation and mucous plugs in COPD patients (Barnes, 2017).

1.2.3.1.4 Lymphocytes

Lymphocytes are white blood cells which originate from the bone marrow, include natural killer (NK) cells, T and B cells. They are associated with adaptive immune responses and are located in different parts of the body to fight infections (Gasteiger and Rudensky 2014). Adaptive responses in the lungs are associated with dendritic cells which carry antigens from the lungs to the lymph nodes (Curtis, 2005). In turn, antigen presentation on dendritic cells activates naïve CD4 T cells (T helper cells) to stimulate polarised type I or II (Th1 and Th2) immune response (Curtis, 2005). In COPD patients, the number of CD4+ and CD8+ and B cells is increased (Hogg et al., 2004; Grumelli et al., 2004). There is increasing evidence to suggest the infiltration of CD8+ cells from central and peripheral airways is correlated to the severity of airflow obstruction in COPD (Di Stefano et al., 2002; Saetta et al., 1998). Furthermore, the prevalence of CD8+ T lymphocytes in COPD shifts the ratio of CD4/CD8 cells towards

CD8+ T cells which leads to a more cytotoxic response (Barnes, 2017). CD8+ T lymphocytes are known to help to resolve infections but recurrent infections in COPD may lead to their excessive recruitment (Di Stefano et al., 2002; Barnes, 2017). Both CD4+ and CD8+ cells express the chemokine receptors CCR5 and CXCR3 and secrete IL-2 and IFN-γ that are associated with a Th1 response. In turn, the availability of CXCR3 upregulates IP-10/ CXCL10 and MIG/ CXCL9 in COPD patients with emphysema (Grumelli et al., 2004; Hogg et al., 2004). Further, IP-10/ CXCL10 and MIG/ CXCL9, also associated with Th1 responses, trigger a high expression of MMP-12 in macrophages derived from the lungs, which in turn causes tissue destruction (Hogg et al., 2004). These findings strongly suggest T lymphocytes are associated with the progression of COPD and remodelling of the airways in these patients (Barnes, 2017).

In summary, the infiltration of accumulated inflammatory cells in the lungs, together with repair processes, lead to damage and remodelling of the COPD airways (Hogg et al., 2004; Shaykhiev et al., 2009; Shaykhiev and Crystal 2013).

1.2.3.2 Oxidative stress

Oxidative stress is an important factor in the pathogenesis of COPD (GOLD 2018, Kirkham and Barnes 2013). Markers of oxidative stress such as hydrogen peroxide (H_2O_2) and 8-isoprostane are often increased in the exhaled breath condensate, sputum and systemic circulation in COPD patients (GOLD 2018). ROS *e.g.* peroxides, superoxide and hydroxyl radicals could originate from external sources (*e.g.* cigarette smoke or noxious particles) or endogenous sources (*e.g.* inflammatory cells or epithelium). ROS can induce oxidative stress and impair antioxidant defences leading to oxidant/ antioxidant imbalance (Kirkham and Barnes 2013). The biological reaction of ROS with proteins, lipids, DNA and RNA can cause damage to the cells followed by necrosis (Kirkham and Barnes 2013). A few natural antioxidants, which function to neutralise mitochondria derived ROS, such as glutathione, ascorbic acid, α-tocopherol have been found reduced in COPD (Kirkham and Barnes 2013). Moreover, TGF-β which is increased in COPD, inhibits catalase and superoxide dismutase 2, both important scavengers of ROS in the lungs (Kirkham and Barnes 2013). Oxidative stress can also amplify inflammation as it can activate redox sensitive transcription factors such as NF-kB and thus a range of cytokines and chemokines (Barnes, 2014).

1.2.3.3 Systemic inflammation

As well as heightened inflammation, systemic inflammation is a feature in more severe cases of COPD, measured by circulating inflammatory markers. Systemic airway inflammation accounts for increased levels of C-reactive protein, leukocytes, fibrinogen, IL-6, IL-8/ CXCL8 and TNF-α (Barnes, 2014). Systemic inflammation contributes to structural alterations in the airways of patients with COPD (Barnes and Celli 2009). These include narrowed small airways, damaged lung parenchyma and loss of alveolar sac attachment (GOLD 2018). Systemic inflammation also leads to declined lung function, which escalates during exacerbations (Barnes and Celli 2009).

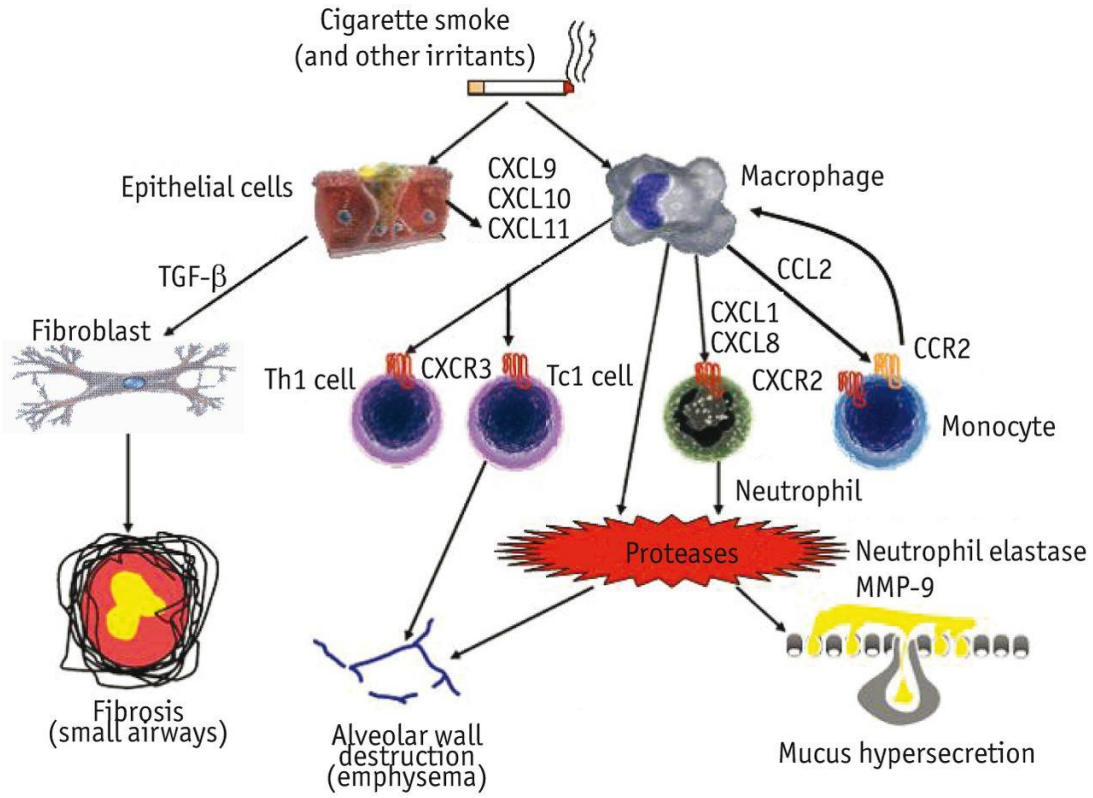

Figure 1-5: Inflammatory and immune cells in the COPD airways.

Inhaled particles or cigarette smoke initiate the production of CCL2 chemokine ligand 2/ MCP-1 from epithelial cells and macrophages which acts on CCR2 (chemokine receptor 2) to stimulate monocytes, CXCL1 (CXC chemokine ligand 1)/ GRO-α and CXCL8 (CXC chemokine ligand 8)/ IL-8 to stimulate neutrophils and monocytes (which later become macrophages). Cigarette smoke initiates also the production of CXCL9 (CXC chemokine ligand 9)/ MIG, CXCL10 (CXC ligand 10)/ IP-10, CXCL11 (CXC chemokine ligand 11)/ I-TAC (interferon inducible T-cell alpha chemoattractant). The chemokines work on CXCR3/ GPR9 (G-protein coupled receptor 9) to induce T helper 1 (Th1) and Type 1 cytotoxic (Tc1) cells and together with macrophages and epithelial cells proteases cause elastin degradation and emphysema. Neutrophil elastase stimulates the mucus production whilst transforming growth factor β (TGF-β) released from epithelial cells causes fibrosis in the small airways through the stimulation of fibroblasts (Adapted from Barnes et al., 2011).

1.2.4 Exacerbations

Exacerbations are the long term hallmark of COPD which are characterised by the worsening of clinical symptoms and a decline in lung function *e.g.* increased cough, sputum, wheezing and dyspnea (GOLD 2018). Acute exacerbations of COPD are a major burden on the European health care system because they account for increased hospitalisation and increased mortality risk (GOLD 2018). Exacerbations in COPD patients are most commonly triggered by respiratory bacterial and viral infections which may amplify inflammatory response and are associated with further decline of FEV_1 in COPD subjects (Hogg and Timens 2009). Other aetiological factors for exacerbations include the presence of comorbidities such as cardiovascular disease. The impact of exacerbations may continue for several weeks until the patient returns to a stable state (GOLD 2018).

1.2.4.1 Frequency of exacerbations

Not all COPD subjects suffer from the same frequency of exacerbations (Donaldson et al., 2002). Patients who experience more than 3 exacerbations a year are considered as frequent exacerbators (Donaldson et al., 2002). More frequent exacerbations are linked to poorer quality of life and morbidity (GOLD 2018). They also manifest with greater airway inflammation and declined lung function (Barnes, 2014). The predisposition to exacerbations is currently unknown, nevertheless the best predictor remains previous exacerbations within the year (GOLD 2018).

The exacerbation rate of COPD patients ranges between 1-7 exacerbations/ 2 year period (Seemungal et al., 2009). The more frequent the exacerbations are, the greater the risk of mortality (Donaldson et al., 2002; Seemungal et al., 2009). As discussed earlier (section 1.2.2) pharmacologic agents such as corticosteroids and antibiotics may improve COPD patient health status and decrease the severity and frequency of exacerbations (Seemungal et al., 2009). To date, one of the largest longitudinal studies which was termed ECLIPSE (Evaluation of COPD Longitudinally to Identify Predictive Surrogate Endpoints) recruited 2138 COPD patients, and evaluated the occurrence of exacerbations over a period of 3 years. It was reported that frequency of past exacerbations is associated with severity of the present disease. More precisely, 22% of patients classified as GOLD stage 2, 33% with stage 3 and 47% with stage 4, presented with the most frequent exacerbations (Hurst et al., 2010). Overall, if patients presented frequent exacerbations in year 1 and 2 of the study, this

trend also continued in year 3 with the most important determinant of exacerbation likelihood being the previous history of exacerbations (Hurst et al., 2010).

1.2.4.2 Bacterial infections

The lungs of COPD patients are colonised with bacteria, most often from the genera of *Streptococcus, Prevotella, Fusobacteria, Haemophilus,* and *Veilloinella* whose presence within COPD patients has been related to consistently high levels of inflammatory immune markers (Beasley et al., 2012; Wang et al., 2016). Bacterial infections have an adverse effect on COPD patients' health status as they also trigger exacerbations (Hiemstra, 2013). More importantly, up to one half of all acute exacerbations in COPD patients are associated with bacterial infections (Sethi, 2004; Murphy et al., 2005). Conventional methods such as the sputum culture method have identified non-typeable *Haemophilus influenzae* (NTHI), *M. catarrhalis* and *Streptococcus pneumoniae* (*S. pneumoniae*) are the most common pathogens isolated during exacerbations while *Pseudomonas aeruginosa* (*P. aeruginosa*) is isolated mainly in severe cases (Sethi, 2004, Murphy et al., 2005). Interestingly, Erkan and colleagues detected atypical bacteria such as *Chlamydophila pneumoniae* and *Mycoplasma pneumoniae* in the sputum of 46 out of 75 COPD subjects during acute exacerbations (Erkan et al, 2008).

Next generation sequencing and polymerase chain reaction (PCR) methods have increased the accuracy of detection and advanced the characterisation of the bacterial communities in the lungs of COPD patients (Shimizu et al., 2015; Wang et al., 2016). For instance, identification of gram negative bacteria during exacerbations has been linked to extended hospitalisation (Shimizu et al., 2015) Garcha (Garcha et al., 2012) confirmed very high levels of *Haemophilus influenzae* (*H. influenzae*) and *M. catarrhalis* in the sputum of COPD patients. *H. influenzae* was found the most prevalent at both stable state (21.6%) and exacerbation state (26%) while *M. catarrhalis* was found to be more predominant during exacerbations (17%) compared to stable state (7%). These results corresponded with a longitudinal study carried out by Wang and colleagues which included 476 sputum samples collected from 87 COPD subjects (Wang et al., 2016). Wang showed the diversity of the COPD lung microbiome shifts during exacerbations with *M. catarrhalis* having a leading prevalence followed by *H. influenzae* (Wang et al., 2016). Interestingly, the bacterial load of *M. catarrhalis* correlated positively with sputum neutrophils and macrophages (Wang et al., 2016). In addition, treatment with corticosteroids was associated with lower numbers of *Streptococcus* species and higher of *Haemophilus* and *Moraxella*

(Wang et al., 2016). Furthermore, a recent large longitudinal study profiled the microbiome of 716 sputum samples from 281 COPD subjects, and showed that microbial dysbiosis is frequent during exacerbations, and is associated with decreased FEV_1 and FVC, in concert with eosinophilic inflammation (Wang et al., 2018). These studies point towards the important role of bacterial infections during COPD exacerbations (Shimizu et al., 2015; Garcha et al., 2012; Wang et al., 2016; Wang et al., 2018).

1.2.4.3 Viral infections

Studies have also confirmed detection of respiratory viruses during COPD exacerbations (52%) compared to stable state COPD cases (15%) (Hewitt et al., 2016; Rohde et al., 2003). Importantly, it is estimated that half of COPD exacerbations are associated with respiratory viral infections and more specifically with rhinovirus, influenza virus and respiratory syncytial virus (Seemungal et al., 2001; Papi et al., 2006; Perotin et al., 2013; Shaykhiev and Crystal 2013). Other types of viruses *e.g.* parainfluenza virus, coronavirus, adenovirus and meta-pneumovirus are also detected in COPD patients during exacerbations (Seemungal et al., 2001; Rohde et al, 2003; Dimopoulos et al., 2012; Perotin et al., 2013). Interestingly, patients with a higher rate of exacerbations have more symptomatic colds (Hurst et al., 2005). Patients with acute exacerbations caused by a virus, have been shown to have high levels of serum IL-6 and plasma fibrinogen and decreased FEV_1 (Seemungal et al., 2001; Wedzicha et al., 2000; Rohde et al., 2008), emphasising the link between induced inflammation and airflow obstruction. Viral induced exacerbations are accompanied by cold symptoms, dyspnea and longer period of recovery (Seemungal et al., 2001; Seemungal et al., 2000). In addition to that, virus-induced exacerbations are more frequent and severe in the winter months when hospitalisation of COPD patients is greatest (Donaldson and Wedzicha 2006).

Amongst all viruses, rhinovirus is the most prevalent virus detected during COPD exacerbations (Seemungal et al., 2001; Papi et al., 2006; Perotin et al., 2013). In a study by George and colleagues rhinovirus load measured in 77 COPD patients was significantly higher during exacerbations compared with the stable state of the disease (George et al., 2014). Rhinovirus is present at higher levels in COPD patients with marked cold symptoms and sore throat compared to rhinovirus negative exacerbations with no upper airway symptoms (Seemungal et al., 2000; Wilkinson et al., 2006; George et al., 2014). The presence of rhinovirus during COPD exacerbations is associated with greater nasal discharge and sputum production

(Seemungal et al., 2000). Further, rhinovirus is positively correlated with exacerbation frequency (George et al., 2014). The relationship between respiratory exacerbations and rhinovirus has been confirmed in an experimental rhinovirus infection of COPD patients (Mallia et al., 2011). In the COPD subjects, rhinovirus induced lower respiratory symptoms. Elevated levels of IL-6, IL-8/ CXCL8 and C-reactive protein (CRP) together with decreased interferon β (IFN-β) were detected in the sputum of 13 COPD patients. In addition, high neutrophil influx and neutrophil elastase were also detected in the sputum of COPD patients (Mallia et al., 2011). Further, lymphocytes numbers were significantly higher in BAL samples from COPD patients compared to healthy controls, implicating viruses as causative agents of airway inflammation in COPD exacerbations (Mallia et al., 2011).

1.2.4.4 Viral and bacterial co-infections

Despite the big role of single bacterial or viral infections in the aetiology of COPD exacerbations, viral and bacterial co-infections are associated with significant morbidity (Papi et al., 2006; Wilkinson et al., 2006). COPD patients with viral and bacterial co-infections are often hospitalised for longer periods and have worse lung function indicators and more severe symptoms compared to single bacterial or viral infections (Papi et al., 2006; Wilkinson et al., 2006). In addition, sputum eosinophilia, high bacterial load and higher IL-6 levels have also been reported in patients with co-infections, suggesting that viruses and bacteria interactions might contribute to the severity of exacerbations (Papi et al., 2006; Wilkinson et al., 2006).

Co-infections are detected in 19% - 27% of all COPD exacerbations according to epidemiological studies and rhinovirus has been found the most prevalent during co-infections (Papi et al., 2006; Perotin et al., 2013; Hutchinson et al., 2007). In contrast to previous studies (Papi et al., 2006; Wilkinson et al., 2006), a more recent paper by Perotin and colleagues (Perotin et al., 2013) failed to find a causal link between co-infections and severity of COPD exacerbations or an increased risk of exacerbation reoccurrence within 3 to 6 months. In a longitudinal study by Hutchinson and co-workers, 36% of exacerbations with a virus detected at the beginning of an exacerbation, also became positive for a bacterial infection 7 days later (*e.g. S. pneumoniae*, *H. Influenzae*, *P. aeruginosa*) (Hutchinson et al., 2007). This finding has been confirmed in an experimental rhinovirus infection, where 60% of COPD patients infected with rhinovirus subsequently developed a secondary bacterial infection (Mallia et al., 2011). In this study, the peak of airflow obstruction and airway inflammation was found to overlap with the peak of rhinovirus replication at day 5, but

symptoms associated with the infection persisted until day 15 and 21 when the bacterial load peaked and viral load decreased. This study suggests secondary bacterial infections may prolong the length of respiratory exacerbations. Secondary bacterial infections have also been associated with elevated levels of neutrophil elastase and reduced antimicrobial SLPI and elafin peptides (Mallia et al., 2012). In another experimental rhinovirus infection in COPD patients, George and colleagues have shown that during an exacerbation when the viral load was high, sputum samples were negative for bacteria (George et al., 2014). Fourteen days later, 73% of sputum samples were positive for bacteria. Together these findings strongly suggest that infection by rhinovirus may have a direct link to a subsequent bacterial infection. However, the detection of co-infections in COPD patients is also dependent on the number of samples taken during an exacerbation, thus multiple sampling during exacerbations may be more beneficial in accurately determining the aetiology of exacerbations (George et al., 2014).

1.3 *Moraxella Catarrhalis*

1.3.1 Clinical importance and characteristics

Moraxella Catarrhalis (*M. catarrhalis* or *Branhamella Catarrhalis)* is a human restricted gram-negative non capsulated bacterium. Originally *M. catarrhalis* was identified as a commensal because of its capability to colonise human airways without causing disease (Karalus et al., 2000). *M. catarrhalis* nasopharynx colonisation is common in children, 66% of infants are colonised with *M. catarrhalis* at least once in the first year of life, with active turnover of strains (Goldstein et al., 2009; Faden et al., 1994). The rate of colonisation is also high during the second year life with 77% of children being colonised at least once with *M. catarrhalis* (Faden et al., 1994). The colonisation percentage declines down to 5.4% in adults and rises again to 23% in elderly (Vaneechoutte et al., 1990).

Over the last 20 years, the bacterium has been recognised not only as a coloniser but a pathogen causing upper and lower respiratory tract infections as well as ear and chest infections (Verduin et al., 2002; Abdillahi et al., 2015; Blakeway et al., 2017). In children, the bacterium is a leading cause of otitis media just after *S. pneumoniae* and NTHI (Blakeway et al., 2017). In addition in young children, it can cause respiratory diseases leading to severe infections such as septicaemia, bacteraemia and meningitis (Peng et al., 2005). *M. catarrhalis* is often isolated from COPD patients during exacerbations, and accounts for 10-15% of all pulmonary exacerbations (Murphy et al., 2005; Sethi and Murphy 2008).

M. catarrhalis is an emerging pathogen and the need for greater understanding of the molecular pathogenesis of *M. catarrhalis* is essential. Antibiotic resistance to some strains has increased from 30% to 96% in the past decade as *M. catarrhalis* strains can secrete the periplasmic lipoprotein β-lactamase -BRO that can hydrolyse the β-lactam ring of β-lactam antibiotics such as penicillin (Verduin et al., 2002). Currently, there is no vaccine against this pathogen, however *M. catarrhalis* outer membrane proteins may be good vaccine candidates. Studies towards developing novel vaccines are also focused on reactive antibodies that target the bacterial surface proteins (Yang et al., 2011; Pettigrew et al., 2017; Augustyniak et al., 2018). In this context, the use of pneumococcal vaccines has decreased otitis media incidence caused by pneumococcus by 20% but has resulted in increased cases of prevalent *M. catarrhalis* and NTHI isolates (Blakeway et al., 2017).

1.3.2 Structure

M. catarrhalis is non capsulated and its outer membrane is composed of phospholipids, lipooligosaccharides, integral outer membrane proteins and lipoproteins (de Vries et al., 2009). *M. catarrhalis* adhesion to host cells is mediated by surface macromolecules which serve as virulence factors to bind mucosal surfaces *e.g.* cell receptors and extracellular matrix (de Vries et al., 2009; Su et al., 2012). These macromolecules include ubiquitous surface proteins A, immunoglobulin D binding protein/hemagglutinin (MID/Hag), *M. catarrhalis* adherence protein (McaP), *M. catarrhalis* filamentous Hag proteins (Mha proteins), lipooligosaccharide (LOS) and will be discussed in more detail below (de Vries et al., 2009).

1.3.2.1 Outer membrane proteins important for adhesion

Ubiquitous surface proteins A (UspAs) - are oligometric coiled-coil adhesins important for host cell attachment (de Vries et al., 2009). They consist of an N-terminal peptide, N-terminal domain region which are responsible for protein's biological function, and a C-terminal which is involved in pore formation that allows translocation of the protein across the bacterial outer membrane. The C-terminal is linked to the N-domain region via a coiled-coil stalk region (de Vries et al., 2009). *M. catarrhalis* UspAs proteins can be divided into three groups: UspA1, UspA2 and UspA2H. They all project from the bacterial cell membrane and their N-region is thought to mediate binding as it protrudes beyond the outer membrane. UspAs proteins are similar in homology in the stalk and C-terminal regions but differ in the N-terminal regions (de Vries et al., 2009). The adhesion properties of the UspA proteins are dependent on differences of poly (G) residues expression in their homopolymeric (G) tract which

may occur during DNA replication (de Vries et al., 2009) Recently, it has been suggested lower growth temperature (such as 26^{o}C) can induce higher expression of UspA1 and therefore result in persistent nasopharynx survival (which is typically much cooler than the core body temperature) (Heiniger et al., 2005). UspA proteins have also a binding domain for carcinoembryonic antigen related cell adhesion molecule (CEACAM) receptors which mediates binding to host epithelium.

MID/Hag protein – is also an oligometric coiled-coil adhesin and shares the structure of the UspA proteins (de Vries et al., 2009). Sequence homology of MID proteins amongst different strains is highly conserved with some regions being identical at 97% (de Vries et al., 2009). MID protein's function is to initiate non-immune binding to soluble IgD (Immunoglobulin D) and to stimulate IgD positive B lymphocytes. MID adhesion properties have been confirmed by depletion of MID expression, reducing overall bacteria-host cell attachment rates by 50-93% in Chang (conjunctival) and NCIH292 (lung) epithelial cells (Bullard et al., 2007). MID expression in *M. catarrhalis* is dependent on translational phase variation and G residue expression, as evidenced that multiple subculture of strains with initially highly expressed *mid*, leads to lower *mid* expression (de Vries et al., 2009).

McaP – is another important autotransporter protein with a 12-β-barrel translocator domain and an N-terminal domain (de Vries et al., 2009). McaP is important for adhesion and lipolytic activity. Its sequence homology is highly preserved amongst strains with almost 100% identity (de Vries et al., 2009). It has been shown mutant strains with knockout *mcap* have reduced adherence to epithelial cells, however the protein's exact role in pathogenesis is still unclear (de Vries et al., 2009).

OMP CD – is another protein involved in bacterial adhesion (de Vries et al., 2009). It contains a β-barrel domain and a C-terminal functional domain. It is heat modifiable, yet highly conserved porin-like protein in the outer membrane of *M. catarrhalis* (de Vries et al., 2009).

Mha Proteins – MhaC, MhaB1 and MhaB2 are outer membrane proteins that function as two partner secretion locus, a highly conserved system in gram negative bacteria involved in the secretion of virulence proteins (de Vries et al., 2009). MhaC is thought to form a porin like channel structure on the outer membrane of *M. catarrhalis* and is thought to be involved in facilitating MhaB1 and MhaB2 movement across the membrane (Balder et al., 2007). In addition, MhaB1 and MhaB2 expression is highly dependent on *mhaC* distribution on the bacterial membrane (de Vries et al., 2009). A

study with knockout of Mha genes has confirmed the Mha protein role in *M. catarrhalis* adhesion to host epithelial cells (Balder et al., 2007).

TFP proteins – these are filamentous protein polymers that form pili on the surface of a variety of bacterial pathogens. They are important for bacterial adhesion, motility, biofilm formation and competence for natural DNA transformation (de Vries et al., 2009; Luke et al., 2007). Loss of TFP results in decreased virulence of the *M. catarrhalis* bacterium. For instance, type IV pili has been identified to be important for *M. catarrhalis* attachment to eukaryotic epithelial cells and chinchilla nasopharynx colonisation and persistence on mucosal surfaces (Luke et al., 2007).

LOS – are highly expressed glycolipids on the surface of *M. catarrhalis,* and consist of a lipooligosaccharide core and lipid A. Despite the fact that the lipid A structures are similar amongst other bacteria from the *Haemophilus, Neisseria* and *Bordatella* genera, the LOS of *M. catarrhalis* is thought to be different as it lacks O-antigen polysaccharide chain (de Vries et al., 2009). LOS is important for bacterial adherence to host cells, host cell invasion and resistance to serum killing (de Vries et al., 2009; Blakeway et al., 2017) Three major serotypes of *M. catarrhalis* LOS have been identified– serotype A, B and C have been identified by polyclonal antisera, with serotypes A and B being the predominant in clinical isolates. Furthermore, serotype B LOS strains have been found more frequently in the airways of adults compared to children (Blakeway et al., 2017).

1.3.2.2 *M. catarrhalis* nutrient acquisition proteins

Efficient nutrient acquisition is important for *M. catarrhalis* colonisation of the nasopharynx in children and adults and its persistence within its host. *M. catarrhalis* requires specific environmental factors to grow on mucosal surfaces, and is unable to grow in anaerobic conditions, even though *M. catarrhalis* possesses nitrate reductase, nitrite reductase and nitric oxidase reductase, all important in anaerobic metabolism (Wang et al., 2009). *M. catarrhalis* cannot utilise exogenous carbohydrates as it lacks the enzymes to transport and process these, which indicates *M. catarrhalis* cannot synthesise acid from glucose, it doesn't have a glycolytic pathway or a sugar transport system (de Vries et al., 2009; Wang et al., 2011). However, *M. catarrhalis* possesses all the enzymes for aerobic sugar metabolism, as it can produce acetate, lactate, fatty acids and arginine through the citric acid cycle, glyoxylate cycle, electron transport and ATP synthase systems in order to grow (de Vries et al., 2009; Wang et al., 2011). In addition, *M. catarrhalis* is able to utilise free and complexed host iron, a metal that is essential for many bacteriological processes through iron binding proteins

expressed on the bacterial membrane. In humans, iron is found in haemoglobin, lactoferrin (carrier of iron in mucosal surfaces) and transferrin (carrier of iron in serum) (Ratledge and Dover 2000). However, lactoferrin and transferrin sequester iron as a preventative mechanism against bacterial colonisation (de Vries et al., 2009).

CopB – is an iron acquisition protein found in the outer membrane of *M. catarrhalis*, which is important also for serum resistance (de Vries et al., 2009; Blakeway et al., 2017). It is thought most isolates of *M. catarrhalis* from children and adults possess the gene for *copB*. In iron depleted conditions, *copB* expression has been found to be increased, suggesting that *M. catarrhalis* express iron-capture proteins (Campagnari et al., 1994).

Lbp and Tbp – lactoferrin binding proteins A and B and transferrin binding proteins have been identified to be functionally and genetically similar in bacteria (Ratledge and Dover, 2000). These are necessary for bacteria to acquire iron from the host. Campagnari and his colleagues (Campagnari et al., 1994) have determined that in iron restricted media, *M. catarrhalis* is able to utilise iron from human lactoferrin and transferrin to grow. In agreement with this finding, the process occurs without siderophore production, it has been therefore postulated that *M. catarrhalis* expresses specific proteins to bind transferrin and lactoferrin. However, the *Moraxella* lactoferrin and transferrin binding proteins are thought to be minimally expressed in iron rich conditions and highly expressed upon iron restriction, an environment similar to that within a human host (Du et al., 1998).

1.3.3 Pathogenesis of *M. catarrhalis*

Virulence features and pathogenicity of bacteria are associated with the bacterial ability to escape host defence mechanisms. Virulence refers to bacterial binding to a host and its colonisation, host invasion, replication in the *in vivo* host environment, interference with host defence mechanisms and ultimate host damage (Verduin et al., 2002). *M. catarrhalis* virulence has not been completely elucidated however recent research has focused on the role of molecular adherence to host cells, host cell invasion and biofilm formation as important aspects of *M. catarrhalis* disease pathogenesis (De Vries et al., 2009).

1.3.3.1 Adherence to host epithelium

M. catarrhalis attaches to epithelial respiratory cells and the host cell extracellular matrix via its adhesion proteins (Section 1.3.2.1). The best recognised *M. catarrhalis* outer membrane proteins responsible for epithelial adherence are UspA1, UspA2 and

MID/Hag. UspA1 and UspA2 have been shown to mediate *M. catarrhalis* binding *in vitro* to Chang conjunctival epithelial cells, Hep-2 epithelial cells and A549 type II alveolar cells (Lafontaine et al., 2000; Holm et al., 2003; Hill et al., 2012). *M. catarrhalis* can also bind to CEACAM1 expressed on epithelial cells in the human oropharynx and lower respiratory tract (Conners et al., 2008; De Vries et al., 2009). *M. catarrhalis* immunoglobulin D binding protein has been associated with adherence to human A549 lung cells *in vitro* (Holm et al., 2003). More recently, this protein has also been described to specifically target cilia of normal human bronchial differentiated cultures *in vitro* (Balder et al., 2009). Interestingly, MID/Hag gene expression is not seen following colonisation in COPD patients (Murphy et al., 2019).

Other outer membrane proteins implicated in *M. catarrhalis* binding to epithelial cells are McaP which facilitates *M. catarrhalis* adherence to Chang and A549 epithelial cells (Timpe et al., 2003) and OMP CD which facilitates adherence to A549 epithelial cells (Holm et al., 2004). Mha outer membrane proteins – MhaB1, MhaB2 and MhaC have also been demonstrated to be involved in adherence to epithelial cells. Various knockout mutations in *Mha* genes showed different degree of decreased bacterial adherence to Chang, Hep2 and 16HBE14o$^-$ cells but no effect on attachment to NCIH292 or A549 cells (Balder et al., 2007). The Balder et al study elaborated on the importance of the two partner secretion system (TFS) in *M. catarrhalis* adherence to epithelial cells. Similar to the above studies, LOS has also been found to initiate *M. catarrhalis* binding to human epithelia as mutants lacking the gene showed significant decrease of adherence to Chang, Hela and A549 epithelial cell lines (Peng et al., 2005). In addition, LOS deletion mutants exhibited decreased *M. catarrhalis* attachment to mouse lungs, suggesting LOS is an essential virulence factor in the pathogenesis of *M. catarrhalis* infections (Peng et al., 2005).

In a study by De Vries and his colleagues (De Vries et al., 2013), *M. catarrhalis* exhibited binding to pharynx epithelial Detroit 562 cells and alveolar A549 cells via proteins encoded by *aroA, lgt1, ecnAB, tmB* genes involved in cell envelope, LOS biosynthesis, DNA repair, cellular processes and energy metabolism. Upon adherence, the *M catarrhalis* transcriptional profile changed. Expression of 34 genes was upregulated and 16 genes were downregulated predominantly from classes associated with metabolism, transport and binding e.g. acyl-CoA dehydrogenase, ABC transporter genes. Interestingly none of the so far known genes associated with adhesion *e.g.* UspaA1, MID/Hag, OmcP or McaP were found to be differentially changed upon adherence to host cells (De Vries et al., 2013).

M. catarrhalis binding to the host cell cartilage oligomeric matrix protein (COMP), an extracellular matrix protein found in cartilage and involved in the regulation of complement activity (De Vries et al., 2013), via UspaA2 helps *M. catarrhalis* to evade the host immune system. The binding enables the blockade of complement killing of *M. catarrhalis*, the inhibition of neutrophil phagocytosis of *M. catarrhalis* as well as reduced killing by human lung epithelial cells (De Vries et al., 2013).

1.3.3.2 Invasion of human host epithelial cells

Bacterial invasion of human host epithelia is crucial for pathogen survival and escape from immunoglobulins and immune cell- driven phagocytosis in the lungs (Slevogt et al., 2007). Bacterial entry can be triggered via receptor mediated interaction with the host cell membrane which mediates a 'zippering' process during which a vacuole engulfs the bacterium and relatively few changes are induced to the host cytoskeleton. Alternatively, the bacterium can directly interact with the cell machinery in a 'triggering' process that regulates cytoskeleton machinery via injection of effector proteins directly into the host cytoplasm, causing actin polymerisation and formation of macropinocytotic pockets and membrane ruffling (Cossart and Sansonetti 2004).

The *M. catarrhalis* capacity to invade human bronchial epithelial cell lines such as BEAS-2B cells, A549 alveolar lung epithelial cells and small airway epithelial cells was first described to occur via macropinocytotic events dependent on the utilisation of microfilaments, Rho GTPases and PI3K contractile mechanism which allows the transformation of membrane ruffles into intracellular compartments (Slevogt et al., 2007). In a later study, *M. catarrhalis* has been shown to utilise LOS and UspA1 proteins for internalisation into Chang epithelial cells (Spaniol et al., 2008). The process was governed by clathrin and actin polymerisation, fibronectin and $\alpha5\beta1$ integrin (Spaniol et al., 2008). The different findings from Slevogt et al and Spaniol et al studies suggest *M. catarrhalis* is able to invade different cell lines via multiple mechanisms.

M. catarrhalis presence has been evaluated in 40 children undergoing tonsillectomy or adenoidectomy. Using various techniques for detecting bacteria *in vivo*, Heiniger and colleagues determined *M. catarrhalis* is able to pass the host epithelial barrier and invade sub-epithelial lymphoid tissue (Heiniger et al., 2007). *M. catarrhalis* can reside in sub-epithelial tissue and invade host cells, suggesting the carrier rate of the bacterium could be higher than so far detected by culture methods and may also be a source for endogenous future reinfections (Heiniger et al., 2007).

1.3.3.3 Host colonisation

Colonisation rates in children and adults differ but it is considered *M. catarrhalis* early and high cell density colonisation rates in infancy lead to a greater chance of developing otitis media (Pearson et al., 2006; Goldstein et al., 2009). Colonisation of mucosal surfaces in the nasopharynx is central for such diseases because this location provides support and basis for perseverance (De Vries et al., 2009; Pearson et al., 2006; Luke et al., 2007). For instance, to cause otitis media, *M. catarrhalis* has to migrate from the nasopharynx to the middle ear via the Eustachian tube; to cause lower respiratory tract infections, *M. catarrhalis* needs to be inhaled into the lungs and escape immune cells in the lungs. In addition, for successful lower lung colonisation and infection *M. catarrhalis* has to avoid and neutralise the biochemical barrier of the respiratory epithelium *e.g.* immunoglobulins, lysozymes, defensins and protease inhibitors (see section 1.1.2.2).

Respiratory pathogens must first attach to its host mucosa in order to establish colonisation. Type IV pili (TFP) have been identified as important factors for colonisation. In the *in vivo* studies by Luke and co-workers, pili have been shown as being biologically important for colonisation and perhaps stabilisation of interbacterial interactions in the chinchilla nasopharynx (Luke et al., 2007). Using a *pilA* mutant, pili have been proved crucial for microcolony formation, density and three dimensional pillar formation. TFP presence were also found to contribute to *M. catarrhalis* biofilm formation with multicellular mushroom like structures, separated by water filled channels (Luke et al., 2007).

1.3.3.4 Biofilm formation

Biofilm formation is crucial for bacterial persistence and long term colonisation of the nasopharynx (De Vries et al., 2009). Biofilms are communities of multiple bacterial cells attached to surface, enclosed by a matrix of extracellular polymers that have protective function. Biofilms are often resistant to stress, host immune mechanisms, antibiotics and thus exhibit increased virulence. Biofilm formation is dependent on environmental factors such as nutrient availability, temperature and solute concentrations (Ni et al., 2016; Goldstein et al., 2009). The criteria for characterising infectious biofilms involves the identification of bacterial clusters, within an anatomical site, which are adhered to mucosal surface and are not susceptible to antibiotic treatment (Hall-Stoodley et al., 2006). There is a suggestion that chronic conditions could be due to infectious colonisation of the mucosa as *M. catarrhalis* infectious

biofilms have been reported in the middle ear of children suffering chronic otitis media (Hall-Stoodley et al., 2006).

The exact mechanism predisposing bacteria to biofilm formation has not yet been identified, but *in vitro* studies suggest genes involved in adhesion could also play a role in the formation of bacterial aggregates. Pearson and his colleagues tested different *M. catarrhalis* strains ability to form biofilms and found that strains differed in their capacity to aggregate (Pearson et al., 2006). Strains capable of forming biofilms successfully on epithelial cell lines possessed the *UspA1*gene, which has been confirmed important for biofilm formation. Similarly, strains which expressed the *hag* gene product have been negatively correlated with biofilm formation (Pearson et al., 2006). Wang and colleagues have also reported a number of *M. catarrhalis* genes were upregulated during growth in a biofilm mode (Wang et al., 2007). The maximally changed genes included respiratory nitrate reductase subunits beta, delta, gamma and alpha (*narH*, *narJ*, *narI*, *narJ*), which are important for the conversion and reduction of nitrate to nitrous oxide. However, deletion of *narGH* genes, encoding nitrate reductase in *M. catarrhalis* mutants did not have any effect on bacterial biofilm formation (Wang et al., 2007).

1.3.3.5 *M. catarrhalis* biofilm and interaction with other respiratory pathogens

There is growing evidence that *M. catarrhalis* is often isolated from patients in presence of other bacteria *e.g.* NTHI and *S. pneumoniae*. NTHI or *S. pneumoniae* occurrence with *M. catarrhalis* increases the risk of acute otitis media in children (Perez and Murphy 2017). The co-occurrence of *M. catarrhalis* with other respiratory pathogens has implications as it is challenging to treat polymicrobial biofilms with antibiotics (Perez and Murphy 2017). Co-infection and co-colonisation with different bacteria enhanced the incidence and severity of an otitis media infection model in the middle ear and nasopharynx of mice and chinchillas (Krishnamurthy et al., 2009; Perez et al., 2014).

β-lactamase positive *M. catarrhalis* has been shown *in vitro* to protect *S. pneumoniae* against penicillin and amoxicillin antibiotics (Budhani and Struthers 1998; Perez et al., 2014). The mechanism has been postulated to involve *M. catarrhalis* outer membrane vesicles (OMVs) carrying β-lactamase to protect other bacteria. Conversely, *S. pneumoniae* has been shown to passively protect *M. catarrhalis* biofilm from azithromycin killing (Perez et al., 2014). *S. pneumoniae* and NTHI can improve *M. catarrhalis* biofilm survival and persistence *in vitro* and *in vivo* (Perez et al., 2014;

Armbruster et al., 2010). In a chinchilla middle ear infection model *M. catarrhalis* biofilm biomass was found to be enhanced by NTHI through quorum signalling, which then lead to increase antibiotic resistance (Armbruster et al., 2010). *S. pneumoniae* also can help to increase *M. catarrhalis* biofilm biomass, which is characterised by dense bacterial clusters surrounded by open spaces thought to be water filled channels; the biofilm then contributed to increased antibiotic resistance (Perez et al., 2014). In addition to these findings, when in a co-infection model both *S. pneumoniae* and *M. catarrhalis* colonisation and bacterial load increased in the nasopharynx of chinchillas and mice (Perez et al., 2014).

1.3.4 Host immune response to *M. catarrhalis* infection

The capacity of human immune cells to sense pathogens and microbial secretions is essential for the immune system to respond to infections (Xie and Gu 2008). Immune cells secrete a range of cytokines and chemokines to fight infections, initiate phagocytosis and successfully clear pathogens from the lungs. Immune cells can fight microbial pathogens trough phagocytosis and the release of cytokines but could also lead to excessive inflammation that can alter the clearance of pathogens (Xie and Gu 2008).

In COPD patients, immune cells are actively recruited to the lungs in response to *M. catarrhalis* infection (Sue et al., 2012; Rosseau et al., 2005, Heinrich et al., 2016). Evidence suggests *M. catarrhalis* binds to immune cells causing the release of cytokines and chemokines, enhancing local and systemic inflammation (Heinrich et al., 2016; Rosseau et al., 2005; Krishnaswamy et al., 2003). Importantly, *M. catarrhalis* can induce heightened inflammatory responses triggering exacerbations in COPD patients (Sue et al., 2012). *M. catarrhalis* binds to mast cells and actively aggregates around their surface (Krishnaswamy et al., 2003). This interaction of *M. catarrhalis* with mast cells leads to activation of NF-kB and in turn to the active secretion of MCP-1/ CCL2 and IL-6, which have pro-inflammatory properties. Neither LPS nor bacterial culture supernatant trigger the release of MCP-1/ CCL2, suggesting direct contact with bacteria is required for mast cells activation. Despite NF-kB activation, *M. catarrhalis* hasn't stimulated the secretion of IL-13, IL-4, IL-8/ CXCL8 or GM-CSF/ CSF-3 (Krishnaswamy et al., 2003). *M. catarrhalis* has also been shown to activate B lymphocytes isolated from healthy donors. Purified MID outer membrane protein of *M. catarrhalis* is able to increase the proliferation of B lymphocytes *in vitro* through binding to IgD present on B cells (Gjorloff-Wingren et al., 2002). Th2 cytokines *e.g.* IL-4 and IL-10 and MID stimulated B lymphocytes increase IgA and IgG secretion.

Moreover, the Th1 specific IL-2 enables increased IgM secretion from B lymphocytes upon MID binding (Gjorloff-Wingren et al., 2002)

Accumulation of monocytes in the lungs is considered detrimental for patients with a chronic lung disease as it is associated with amplified inflammatory response and lung tissue damage, characterised by large numbers of neutrophils, macrophages and the release of cytokines and chemokines (Rosseau et al., 2005). *M. catarrhalis* infected human alveolar epithelial cells recruit human monocytes, allowing adhesion and transmigration of monocytes supported by MCP-1/ CCL2 secretion, ICAM-1 and vascular adhesion molecule – 1 (VCAM-1) upregulated expression on the epithelium. The process is accompanied by cell damaging superoxide production and monocyte oxidative burst dependent on epithelial protein kinase C (PKC) activation, and autocrine platelet activating factor (PAF) signalling in monocytes. Oxidative burst of monocytes is specific to *M. catarrhalis* stimulated epithelium compared to non-infected or TNF-α stimulated epithelium (Rosseau et al., 2005). Further, *M. catarrhalis* interaction with human primary monocytes causes upregulation in expression of ICAM-1 receptors on monocytes, IL-8/ CXCL8 and TNF-α secretion, which are involved in the induction of pro-inflammatory pathways in respiratory epithelial cells (Xie and Gu 2008). In addition, activated monocytes, through ICAM-1 upregulation and IL-8/ CXCL8 secretion, stimulated neighbouring naïve monocytes to release more pro-inflammatory TNF-α.

As mentioned earlier, increased numbers of neutrophils have been detected in COPD patients (Hogg et al., 2004) (see section 1.2.3.1). There is evidence that human granulocytes phagocytose *M. catarrhalis* via the CEACAM3 receptor present on the granulocytes. The CEACAM3 mediated process is associated with activation of small GTPase Rac, which is important for actin polymerisation and phagocytosis (Schmitter et al., 2004). More recently, human granulocytes isolated from peripheral blood from healthy volunteers were infected with *M. catarrhalis* (Heinrich et al., 2016). *M. catarrhalis* has been taken up by granulocytes upon interaction of UspA1 with CEACAM3 receptor, resulting in granulocytes degranulation, ROS and IL-8/ CXCL8 production. To characterise better the mechanism of induced cytokines, Heinrich and colleagues used a differentiated promyelocytic NB4 cell line, which demonstrated *M. catarrhalis* induced signalling occurs via CEACAM3 receptors, CARD9, the Syk pathway and activated NF-kB, which can modulate airway inflammation (Heinrich et al., 2016).

In a murine model of *M. catarrhalis* infection, massive neutrophilic influx, lower numbers of eosinophils, macrophages and CD4+ T cells resulted in high levels of TNF-α, IL-6 and moderate levels of IFN-γ and IL-17 secreted in BAL (Alhanas et al., 2017). Noteworthy, TNF-α neutralisation aided the lowering of systemic levels of IL-1β, IL-6 and IL-17, which was followed by reduced susceptibility to *M. catarrhalis* infection. IL-17 knockout mice infected with *M. catarrhalis* showed reduced numbers of neutrophils, eosinophils, macrophages and lymphocytes recruited to the lungs, implicating IL-17 not only in controlling influx of neutrophils but contribution to *M. catarrhalis* induced exacerbations in allergic airway inflammation state (Alhanas et al., 2017).

1.4 Rhinovirus

1.4.1 Clinical importance and characteristics

Rhinoviruses are the most frequent cause of the common cold worldwide. They account for about half of all colds in adults and about a quarter of all colds in children (Bella and Rossmann 1999; van der Zalm et al., 2011). Rhinoviruses have been long known as relatively benign upper respiratory tract pathogens until they were found to initiate exacerbations in COPD and asthma patients (Cox and Le Souef 2014). Rhinoviruses can in certain circumstances cause lower respiratory tract infections such as pneumonia and bronchitis, and children who suffer rhinovirus induced wheezing illness at early age of life have been shown to have a high risk for developing asthma (Bochkov and Gern 2016).

1.4.1.1 Structure

Rhinovirus is a small non-enveloped virus which belongs to the *Picornaviridae* family of Enteroviruses. It has an icosahedral capsid that envelopes a single stranded positive ribonucleic acid (RNA) with more than 160 known serotypes (Bochkov and Gern 2016). The rhinovirus capsid consists of 60 viral proteins (VP). Proteins VP1, VP2, VP3 constitute the exterior of the capsid, whilst VP4 is in the interior where it is in contact with the viral RNA (Bella and Rossmann 1999; Jacobs et al., 2013). Five VP1 proteins form a fivefold vertex which is surrounded by a deep depression on each site, with each depression having 5 pits known as ‘canyons’ (60 molecules per virus) (Figure 1-6). Canyons are hypothesised to be the region of rhinovirus interaction with its host cell receptor (Jacobs et al., 2013).

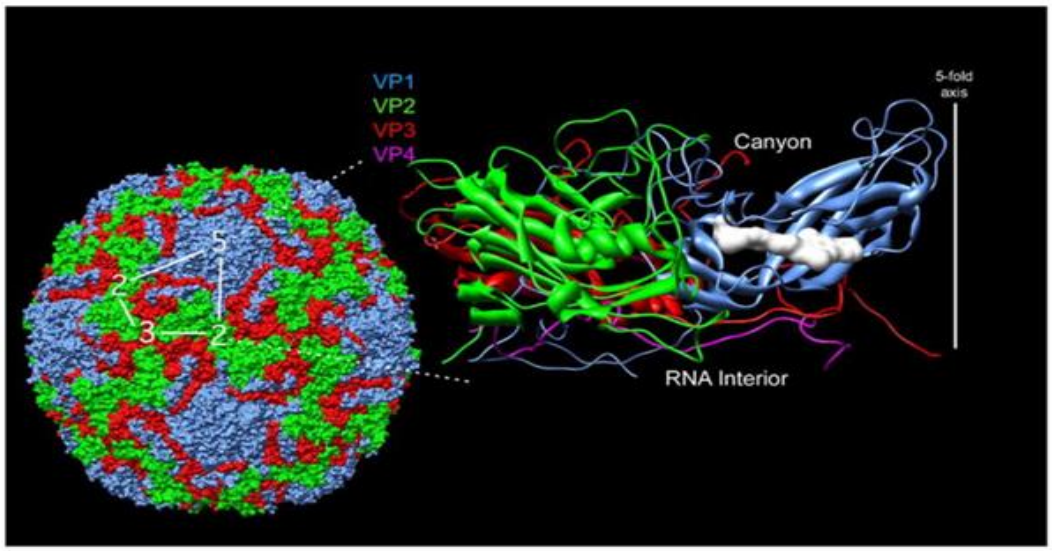

Figure 1-6: Rhinovirus structure.

The capsid consists of VP1, VP2, VP3, VP4 forming icosahedral structure which surrounds the viral RNA. A canyon on the VP1 protein is thought to be the place of interaction between the virus and its cellular receptor (adapted from Gonçalves et al., 2007).

1.4.1.2 Virus Classification

Rhinoviruses are classified into different groups according to their structural and biological properties. Based on their receptor specificity they are grouped into major and minor groups (Bella and Rossmann 1999). The major group accounts for 90% of all known serotypes and binds to ICAM-1 found on endothelial and epithelial cells. The minor group binds to the low density lipoprotein receptor (LDLR) expressed on bronchial epithelial cells (Bella and Rossmann 1999; Jacobs et al., 2013). In addition, members of the rhinovirus genus can be subdivided into types A, B and C according to VP1 and VP4/VP2 nucleotide and amino acid sequence (Bochkov and Gern 2012). The most common RV serotypes isolated from children belong to genetic group A (van der Zalm., 2011; Savolainen et al., 2006). *In vitro* studies have looked at both types A and B serotypes including RV16, RV1b, RV2, RV14, RV39 (Papadopoulus et al., 2000; Subauste et al., 1995). Genome sequencing of newly identified rhinoviruses has designated a novel rhinovirus type C. Rhinovirus C has been suggested to be more pathogenic than types A and B in children with acute wheezing illness (Cox and Le Souef 2014). Most recently, the cadherin-related-family-member 3 receptor (CDHR3) has been shown to enable rhinovirus C entry into host cells (Bochkov et al., 2015).

1.4.1.3 Rhinovirus Replication

Following rhinovirus binding to a cellular receptor, the viral genome is uncoated and translocated across the cell membrane into the host's cytoplasm (Johnston et al., 1993). Viruses replicate by hijacking cell's host machinery for translation (Johnston et al., 1993; Bochkov and Gern 2016). The rhinovirus genome replication depends on the VPg (virion protein genome linked) protein which is covalently linked to the 5' coding region (Johnston et al., 1993; Cordey et al., 2008). Upon its urilydylation it acts as a protein primer for RNA synthesis. The rhinovirus genome consists of approximately 7200 base pairs and replicates rapidly in 6h with an yield of about 100,000 virions per cell (Johnston et al., 1993; Cordey et al., 2008).

1.4.2 Rhinovirus infection of the airway epithelium

1.4.2.1 Rhinovirus infection of cell lines or human basal respiratory airway epithelial cells

Rhinovirus infection in airway epithelial cells has been investigated in a number of studies (Subauste et al., 1995; Papadopoulos et al., 2000; Edwards et al., 2006; Jakiela et al., 2008). It has been shown *in vitro* to replicate in human epithelial cells from both upper and lower respiratory tracts (Bochkov and Gern 2016). The peak of rhinovirus replication occurs between 24h and 48h post infection and has been documented *in vitro* in human nasal monolayers (Winther et al, 1990) and in human bronchial epithelial cells (Papadopoulos et al., 2000). Primary bronchial basal epithelial cells have been suggested to be more susceptible to rhinovirus 16 and 1A due to high viral replication compared to that within suprabasal cells (Jakiela et al., 2008). Rhinovirus's ability to directly infect the lower respiratory epithelium has been demonstrated in monolayers of human bronchial epithelial cells of healthy and asthmatic subjects (Papadopoulos et al., 2000). Rhinovirus 16 titres were low in the first 6 hours of infection but steadily increased over 24h and 48h (Papadopoulos et al., 2000).

Studies have confirmed respiratory epithelial cells are an important site for rhinovirus infection and induction of airway inflammation (Papadopoulus et al., 2000; Subauste et al., 1995; Winther et al., 1990). Infection of the bronchial epithelial cell line, BEAS-2b, with rhinovirus types 2 and 14 *in vitro* was found to stimulate the production of cytokines and chemokines (Subauste et al., 1995,). Cytokines and chemokines are known to recruit inflammatory cells such as neutrophils and eosinophils and prolong the inflammatory state within the cells (Subauste et al., 1995). Some of the pro-inflammatory molecules secreted by epithelial cells in response to rhinovirus infection

are IL-1β, IL-6, IL-8/ CXCL-8, IP-10/ CXCL10, ENA-78/ CXCL5, RANTES (regulated on activation, normal T cell expressed and secreted)/ CCL5, GM-CSF (granulocyte-macrophage colony stimulating factor)/ CSF (Subauste et al., 1995; Edwards et al., 2006; Lopes Souza et al., 2009). Undifferentiated cells treated continuously with rhinovirus 16 for 6h at multiplicity of infection (MOI) of 10^6 $TCID_{50}$/ml and left to recover for 24h, produced increased mRNA levels of pro-inflammatory cytokines IL-1, IL-6, IL-8 / CXCL8, RANTES/ CCL5, TNF-α in conjunction with increased viral RNA levels (Lopes-Souza et al., 2004).

1.4.2.2 Rhinovirus infection of differentiated epithelial cells

Human airway epithelial cells are the primary target of rhinovirus (Bai et al., 2015). Most of the studies on rhinovirus infection have been documented *in vitro* in cell lines and non-differentiated monolayers in submerged conditions (Subauste et al., 1995; Edwards et al., 2006; Jakiela et al., 2008). However, recent studies in airway well-differentiated epithelial cells grown at air-liquid interface have become a more suitable model to investigate rhinovirus infection (Jakiela et al., 2014; Griggs et al., 2017; Jing et al., 2019). The pseudostratified nature of ALI cultures represents better the *in vivo* respiratory epithelium, providing structural and functional characteristics (Bai et al., 2015). Initially, human differentiated pseudostratified tracheal and nasal cells have shown resistance to rhinovirus 16 infection compared to squamous undifferentiated monolayers of tracheal and nasal cells (Lopes-Souza et al., 2004). The level of pro-inflammatory molecules has been shown to be related to the degree of viral infection as no pro-inflammatory cytokines were detected at mRNA levels in well-differentiated cells (Lopes-Souza et al., 2004). Rhinovirus 16 replication has also been suggested to be higher in human bronchial epithelial cultures than in human nasal epithelial cultures based on viral load findings (Lopes-Souza et al., 2009).

Recent research suggests rhinovirus infects fully differentiated cultures and it targets predominantly ciliated cells (Jakiela et al., 2014; Chen et al., 2006; Griggs et al., 2017; Jing et al., 2019). For instance, rhinovirus 16 infection of human bronchial ciliated cultures of seven healthy donors and thirteen asthma donors resulted in a reduced number of ciliated cells and downregulation of ciliary genes expression including the ciliary dynein *DNAH9*, *DNAI1* and *FOXJ1* ciliogenesis transcription factor (Jakiela et al., 2014). Additionally, ICAM-1, the receptor for rhinovirus entry in epithelial cells was found apically expressed on both ciliated and non-ciliated cells, suggesting that greater receptor availability is not the reason for preferential infection of ciliated cells, but perhaps represents a more efficient replication in this cell type (Jakiela et al.,

2014). In the Jakiela study, induced mucous metaplasia by stimulation with IL-13 and IL-4 of differentiated airway cells was also found to be associated with reduced rhinovirus replication.

Further, rhinovirus C infection of human bronchial mucociliary cultures was found to be associated with viral replication in ciliated cells, with little rhinovirus replication found in non-ciliated cells and no detected replication in secretory cells (Griggs et al., 2017). This study found enhanced culture ciliation resulted in greater viral susceptibility and increased viral replication in the epithelial cells. Interestingly, rhinovirus C binding and replication was found positively correlated with the high expression of its receptor- CDHR3 in bronchial differentiated cultures (Griggs et al., 2017). Different types of rhinovirus have been linked to different degrees of replication and induction of virus associated cytokines in fully differentiated cultures. For instance, rhinovirus A and the newly discovered rhinovirus C have been shown to replicate faster in ciliated cultures, compared to the minor rhinovirus B group (Nakagome et al., 2014). Epithelial infection with rhinovirus A and C was associated with greater cytotoxicity in epithelial cultures and higher induction of pro-inflammatory cytokines such as IP-10/ CXCL10, IP-9/ CXCL11, RANTES/ CCL5 and IFNλ (Nakagome et al., 2014).

Well differentiated cells form tight junctions and have transepithelial resistance which is important for the barrier integrity of the respiratory epithelium against inhaled particles and pathogens (Looi et al., 2016). Rhinovirus 16, 1B and 39 serotypes have been shown to decrease epithelial resistance of human differentiated tracheal cells through dissociation of ZO-1 from tight junction complexes, causing increased paracellular permeability (Sajjan et al., 2008). The finding has been lately confirmed by Looi and his colleagues who found rhinovirus disrupted ZO-1 and occludin expression in differentiated tracheal cells, leading to increased epithelial permeability (Looi et al., 2016). Rhinovirus can change the expression of a variety of genes in the differentiated epithelium (Bai et al., 2015). They are specific to inflammatory pathways, epithelial function and cilia structure and include RANTES/ CCL5, IP-10/ CXCL10, Fractalkine/ CX3CL1, MUC5AC, CDHR3, CCRL1, IP-9/ CXCL11 (Bai et al., 2015; Looi et al., 2016; Nakagome et al., 2014).

1.4.3 Specific antiviral response to rhinovirus infection

The main inflammatory mediators associated with rhinovirus infection in human epithelial cells are interferons (IFNs), IL-1, IL-6, IL-8/ CXCL8, eotaxin 8, RANTES/

CCL5, IP-10/ CXCL10, Protein Kinase R (PKR), Myxovirus resistance (Mx) proteins, 2'-5'-oligoadenylate synthase (OAS) and virus inhibitory protein, endoplasmic reticulum associated IFN inducible (viperin) (Khaitov et al., 2009; Chen et al., 2006; Sykes at el., 2013). These antiviral proteins can interfere with viral assembly, replication, translation and protein trafficking (Vareille et al., 2011; Goubau et al., 2013). *In vivo* studies using a mouse model of RV1B infection found that bronchoalveolar lavage samples (BAL) collected 24h post infection had a high percentage of neutrophils, lymphocytes and myeloperoxidase relative to sham Hela cell lysate control. Macrophage inflammatory protein-1α and 2 (MIP1α ad MIP2), RANTES/ CCL5, Interferons-α and β expression were also increased compared to sham controls (Newcomb et al., 2008).

1.4.3.1 Interferons

Interferons are strong mediators of immunomodulatory, antiviral and anti-proliferative function on cellular level which cooperatively regulate cell susceptibility to picornaviruses infections (Rotbart, 2000). They can mediate robust anti – viral responses against rhinovirus by preventing viral growth and spread (Edwards et al., 2006). Retinoic acid inducible gene-1 (RIG-1), melanoma differentiation-associated gene 5 (MDA5) and toll like receptor 3 (TLR3) have been specifically reported to sense rhinovirus RNAs and are thought to mediate interferon expression in primary human bronchial cells (Sykes et al., 2013). The first stimulated interferons in human airway epithelial cells upon viral infection are IFNα1 and IFNβ (Peng et al., 2006; Sykes et al., 2012). It has also been documented that viruses trigger initial expression of both type I and type III IFNs (IFN λ1 and λ2/3) in human airway cells *in vitro*. In a study by Khaitov and colleagues, bronchial epithelial BEAS-2b cells and human primary bronchial cells expressed IFN type I (α and β) and type III (λs) in response to rhinovirus 16 and 1B *in vitro* infection (Khaitov et al., 2009). In a study by Lopes-Souza rhinovirus initiated a more pronounce interferon response in human non-differentiated tracheal cultures compared to differentiated tracheal cultures (Lopes-Souza et al., 2004).

The clinical relevance of interferons during rhinovirus infections has been demonstrated in several studies. The calculated efficacy of intranasal IFN-α2 in preventing rhinovirus infection was 100% (Farr et al., 1984). However, the long term dosing with IFN-α2 resulted in side effects such as frequent episodes of symptoms and nasal irritation (Farr et al., 1984). The results suggested IFN-α could prevent colds due to rhinovirus. In another experimental study, of Australian family groups,

IFN-α2 was intranasally administered for 7 days when symptoms of respiratory illness (runny nose, sore throat, muscle pain, fever) occurred within family members (Douglas et al., 1986). 76% of participants treated with IFN-α2 experienced less days of symptoms after rhinovirus infection while 86% of participants experienced a 'less definite' illness after exposure to rhinovirus (Douglas et al., 1986). These findings suggest a protective role of interferon in rhinovirus induced colds and highlights the interferon immunomodulatory function in patients. Despite the stimulation of interferons during the trials, severity of symptoms and clearance of virus from nasal secretions did not change rapidly (Douglas et al., 1986) suggesting interferons as protective rather than therapeutic against rhinovirus colds.

Interestingly, asthmatic bronchial cells infected with rhinovirus 16 lacked interferon response but RNA sensors expression remained the same (Sykes et al., 2013). In COPD patients infected with rhinovirus 16, BAL measurements indicated decreased IFN α and λ suggesting an impaired IFN-response when compared to healthy subjects infected with rhinovirus. In addition, increased neutrophil levels, IL-6, IL-8/ CXCL8 were detected in COPD sputum samples post rhinovirus infection revealing the virus had induced an increased inflammatory state (Mallia et al., 2011). Recent discoveries have identified novel genes associated with the interferon pathway exhibiting antiviral function (Chen et al., 2006). A study with differentiated tracheobronchial cells from healthy subjects has reported 52 induced genes in response to rhinovirus; strikingly, 32 of these genes have been directly related to the interferon pathway (Chen et al., 2006).

1.4.3.2 Anti-viral proteins

A member of the interferon stimulated genes (ISG) induced proteins – 2'-5' Oligoadenylate synthase (OAS) senses single and double stranded RNAs. It is suggested it prevents viral infections by activating ubiquitous ribonuclease L (RNAse L) (Silverman, 2007). In a study examining OAS's role together with RNase L, OAS was reported to reduce viral replication (Chebath et al., 1987, Samuel, 2001). Chinese hamster ovary cells (CHO) negative for dehydrofolate reductase (DHR^-) or co-transfected with OAS have been compared during Mengo (*Picornaviridae)* viral infection. Cells constitutively expressing OAS showed a thousand fold decrease in viral replication and resistance to the virus compared to control CHO cells (Chebath et al., 1987; Samuel, 2001).

Another protein induced in response to rhinovirus infection is the Mx protein (Samuel, 2001; Vareille et al., 2011). The human genome expresses two versions of the antiviral Mx protein – MxA stimulated by IFNα and MxB stimulated by IFNβ (Samuel, 2001; Chen et al., 2006). MxA has been shown to impair viral protein trafficking and thus to inhibit viral synthesis in various DNA and RNA viruses (Samuel C 2001). Chen and colleagues (Chen et al., 2006) have shown highly elevated OAS and Mx gene expression in human tracheobronchial cells after rhinovirus 16 *in vitro* infection.

Induced NO in epithelial cells is also playing a defensive role during viral and microbial infections (Vareille et al., 2011; Samuel, 2001). It is highly abundant in airways as NO synthases (NOS-1, NOS-2, NOS-3) contribute to its production. NOS-2 overexpression is triggered by pro-inflammatory mediators during respiratory viral infections (Vareille et al., 2011). In rhinovirus infection, NO stops viral replication and cytokine expression by blocking interferon regulatory factor 1 (IRF1) (which promotes interferon induction) and NF-kB pathways (Goubau et al., 2013; Vareille et al., 2011).

Protein Kinase R is another important cytokine in viral infections as it activates cellular proteins which stop translation of viral mRNAs, it initiates apoptosis in infected cells and stimulates NOS-2 expression in epithelial cells (Vareille et al., 2011; Samuel, 2001; Chen et al., 2006). Chen and colleagues have shown significantly increased PKR levels in primary human tracheobronchial cells infected with rhinovirus 16 or rhinovirus 1B. In addition, the group has reported the dsRNA-PKR pathway as essential for rhinovirus inducible genes (Chen et al., 2006).

1.4.4 Rhinovirus during COPD exacerbations

Chronic airway inflammation is a feature of the COPD epithelium (Schneider et al., 2010). The pro-inflammatory phenotype of the COPD epithelium has been reflected in tracheal differentiated cells *in vitro*, where the cytokines IL-8/ CXCL8, IL-6, GRO-α/ CXCL1 have been confirmed to have a higher initial baseline levels compared to differentiated airway cultures from healthy subjects (Schneider et al., 2010).

Airway inflammation is known to be a key feature of the aetiology of COPD exacerbations, which are often driven by rhinovirus infection (Seemungal et al., 2001; Schneider et al., 2010). In response to rhinovirus, COPD differentiated cultures exhibit higher oxidative stress and cytokine release despite high interferon production (Schneider et al., 2010; Baines et al., 2013). It has been shown that heightened inflammatory response correlates with increased cellular signalling through the IL-1 and toll like receptor (TLR) pathways via IL-1 receptor associated kinase 2 (IRAK2)

and Pellino 1 receptor (Pell1) (Baines et al., 2013). Experimental rhinovirus infection of COPD patients produced prolonged airway inflammation characterised by higher counts of blood and sputum neutrophils, neutrophil elastase concentrations, lymphocyte numbers, BAL IL-6 and IL-8/ CXCL8 levels in infected patients compared to control non-infected patients (Mallia et al., 2011). The viral load in COPD patients was also higher, and those infected had more severe lower respiratory tract symptoms compared to non-infected COPD controls (Mallia et al., 2011). Moreover, respiratory exacerbations in COPD patients, triggered by rhinovirus infection are characterised by highly induced serum IP-10/ CXCL10 levels (Quint et al., 2010). Marked increase of systemic C-reactive protein (CRP) and blood leukocytes, along with sputum increased IL-6, IL-8/ CXCL8 and IP-10/ CXCL10 levels have been detected in COPD patients during acute exacerbations in the presence of respiratory viruses (Rohde et al., 2008; Seemungal et al., 2000). Overall, acute COPD exacerbation, caused by rhinovirus, results in a significant decrease in FEV_1 and FVC and increased levels of inflammatory mediators, particularly IL-6, IL-8/CXCL8 and IP-10/ CXCL10, indicating the heightened inflammatory state of the COPD epithelium (Mallia et al., 2011; Rohde et al., 2008; Seemungal et al., 2000; Seemungal et al., 2001; Schneider et al., 2010; Quint et al., 2010).

Mucus lines the airway epithelium, supporting epithelial barrier function through active trapping of inhaled particles and pathogens (De Rose et al., 2018). Increased mucus production however, could result in airway obstruction in patients with lung diseases (Jing et al., 2019). Rhinovirus infection of differentiated tracheobronchial cells from COPD patients has been recently shown to increase mucins expression, goblet cells number and FOXA3 goblet cell transcription factor, all essential for the induction of goblet cell hyperplasia (Jing et al., 2019). Goblet cell hyperplasia was dependent on NOTCH3 activated signalling following rhinovirus infection of COPD ciliated cultures, which is central for the process of epithelial differentiation, suggesting that rhinovirus could be remodelling the airways (Jing et al., 2019).

These studies emphasise the importance of rhinovirus in initiation of exacerbations in COPD patients. However, the very early cytotoxic effects of rhinovirus on the host epithelium and the associated inflammatory response have not been completely elucidated.

1.5 Pathogen recognition, inflammatory signalling and cytokine production

1.5.1 Pathogen recognition receptors

The innate immunity against pathogens and microorganisms is important for pathogen recognition followed by induction of a pro-inflammatory response (Takeuchi and Akira 2010). The host innate defence system relies on the recognition of different microorganisms by germline-encoded pattern recognition receptors (PRRs) (Akira et al., 2006). PRRs are expressed on host immune cells and are not dependent on immunologic memory. PRRs can therefore detect and eliminate bacterial and viral invading pathogens via pathogen associated molecular patterns (PAMs) and damaged associated molecular patterns (DAMPs) (Akira et al., 2006; Takeuchi and Akira 2010). The ability of different PRRs to recognise specific PAMs initiates distinct signalling pathways which induce pathogen specific response, with stimulation of pro-inflammatory cytokines, interferons and antimicrobial proteins (Akira et al., 2006). Currently, there have been identified four different families of PRRs: transmembrane proteins involve TLRs and C-type lectin receptors (CLRs), cytoplasmic proteins involve retinoic-acid-inducible gene-1 (RIG-1) and NOD-like receptors (NDRs) (Takeuchi and Akira 2010). One of the best studied anti-viral and anti-bacterial PRRs are TLRs expressed differentially on different immune and airway epithelial cells (Takeuchi and Akira 2010).

1.5.1.1 TLRs

TLRs are membrane glycoproteins, located on the cell surface of immune cells or on endosomes, which recognise PAMPs and DAMPs and stimulate different kinases into signalling pathways to eliminate invading pathogens (Sun et al., 2012; Goubau et al., 2013). Thirteen different TLRs have been identified in mammals, ten of which (TLR 1-10) are expressed on airway epithelial cells (Vareille et al., 2011). TLR3 recognises viral double stranded RNAs (dsRNAs) whilst TLR7 and TLR8 recognise viral single stranded RNAs (ssRNAs). Bacterial diacylated lipoproteins are recognised by TLR2, bacterial oligodeoxyribonucleotides activate TLR9 while bacterial lipopolysaccharides activate TLR4 and bacterial flagellin is detected by TLR5 (Sykes et al., 2013; Sun et al., 2012; Parker and Prince 2011).

Once TLRs are activated by bacterial or viral PAMPs, the receptors dimerise and recruit Toll/interleukin-1 receptor-domain-containing-adaptor-inducing-interferon–β (TRIF) or Myeloid differentiation primary response gene 88 (MyD88). Specifically, TLR3 recruits the adaptor TRIF; TLR4 can use both TRIF and MyD88 while TLR7,

TLR8 and TLR9 recruit only MyD88 (Vareille et al., 2011). When activated the primary adaptors phosphorylate a number of key transcription factors (Sun et al., 2012). These include IRF 3 or 7 and NF-kB (See Figure 1-7). When activated they translocate to the nucleus where they induce expression of IFN α/ β (Vareille at al., 2011; Sun et al., 2012).

1.5.1.2 Cytosolic TLRs for sensing viruses

As well as cell surface and endosomal TLRs, pattern recognition receptors are also found in the cytosol (Goubau et al., 2013; Vareille et al., 2011). These receptors include RIG-1- like family – RIG-1, the melanoma differentiation-associated gene 5 (MDA-5) and laboratory of genetics and physiology 2 (LGP2) (Vareille at el., 2011, Goubau et al., 2013). Other identified cytosolic receptors are cyclic-GMP-AMP synthase (cGAS), Interferon-gamma-inducible protein 16 (IFI16), DNA-dependent activator of IFN-regulatory factors (DAI) (Goubau et al., 2013). RIG-1 family receptors detect viral intracellular ssRNAs and dsRNAs and thus regulate interferon type I signalling (Vareille et al., 2011). Specifically, the N-terminal domains - caspase activation and recruitment (CARDS) of the RIG-1 receptor sense negative ssRNAs with 5' triphosphate end such as respiratory syncytial virus (RSV) and influenza. MDA5 uses CARD domains to sense smaller but relatively long dsRNAs such as picornaviruses during infection. LGP2 is thought to facilitate recognition via its ATPase domain, however its role in sensing intracellular RNA remains unclear (Vareille et al., 2011; Goubau et al., 2013).

Activation of RIG-1 like family receptors initiate downstream signalling pathways via mitochondrial antiviral signalling (MAVs) adaptors located on the surface of mitochondria and mitochondria-associated endoplasmic reticulum (ER) membrane (Goubau et al., 2013). For instance, viral RNAs cause the assembly of large aggregates of MAVs. This results in amplified signal transduction that enables recognition of small amounts of viral RNA - less than 20 viral RNA molecules are capable of activating the RIG-1 – MAVs pathway (Goubau et al., 2013). MAVs recruit protein kinases responsible for activation and phosphorylation of IRF3 and IRF7, which leads to the expression of IFN α and β genes in the nucleus (Goubau et al., 2013; Vareille et al., 2011). The RIG-1 like family receptors are highly induced in a positive-loop feedback manner which reinforces antiviral immunity (Goubau et al., 2013).

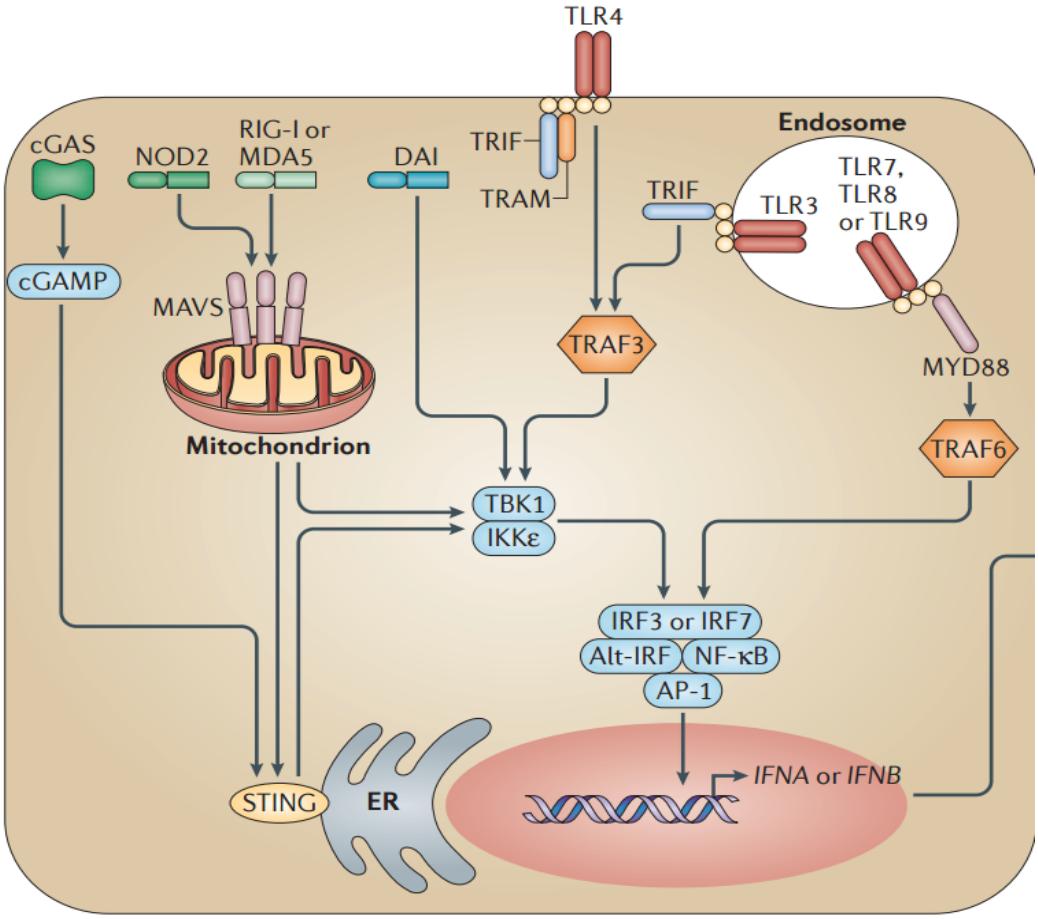

Figure 1-7: Signalling pathways in Type I Interferon induction.

Microbial agents are recognised by pattern recognition receptors including TLR3, RIG-1 and MDA5. TLR3 signals through the primary adaptor TRIF. Activated TRIF recruit tumour necrosis factor (TNF) receptor – associated factor 3 (TRAF 3). RIG-1 and MDA-5 receptors signal through MAVs. TRAF3 and MAVs adaptors phosphorylate interferon regulatory factors 3 and 7 via TANK-binding kinase 1 (TBK1) or/and IkB kinase-ε (IKKε). IRF 3 and IRF 7 translocate to the nucleus and activate transcription of interferon α and β genes (adapted from: McNab et al., 2015).

1.5.1.3 Signal transduction

Cells have to respond to extracellular signals such as physical and chemical changes of growth factors, cytokines and nutrients by altering essential intracellular behaviours such as proliferation, survival, metabolism and homeostasis (Cuenda and Rousseau 2007, Zarubin and Han 2005). In order for the extracellular signal to reach the nucleus, a stimulus ligand must bind to its receptor, usually located on the cell membrane. Binding of a ligand to its receptor, can cause dimerization of the receptor and phosphorylation of the intracellular portion of the receptor tyrosine residues. Tyrosine

kinase activity is often associated with autophosphorylation at the carboxyl ($CHOO^-$) terminal of the receptor. The tyrosine kinases then turn into docking sites for proteins with Src Homology-2 (SH-2) units which can then phosphorylate a variety of proteins to initiate a signalling cascade (Lee and McCubrey 2002).

1.5.2 Important inflammatory cytokines in the airway epithelium

Cytokines are important modulators of inflammation in the human airways and to date more than 50 cytokines have been implicated in the pathogenesis of COPD, however their distinctive role in diseases is often unclear (Barnes, 2008). Cytokines could have pro-inflammatory properties which can amplify and prolong the inflammation or anti-inflammatory properties to negatively modify the inflammation process. When activated, immune receptors such as TLRs stimulate cytokine and chemokine production (Barnes, 2008). Chemokines are a family of cytokines that drive directed chemotaxis of targeted cells. Chemokines mediate recruitment of immune cells from the circulation to the site of infection (Parker and Prince 2011).

The rapid immune signalling in tissues results in the stimulation of key pro-inflammatory cytokines such as IL-1β, IL-6, TNF-α, IL-8/ CXCL8, IP-10/ CXCL10, RANTES/ CCL5 and MCP-1/ CCL2 which can amplify inflammation, through the recruitment, activation and survival of immune cells (Barnes, 2009).

1.5.2.1 Interleukin -1β (IL-1β)

IL-1β is induced mainly by immune cells but can also be produced by endothelial and epithelial cells in response to microbial molecules through NF-kB signalling (Turner et al., 2014). IL-1β functions primarily as a potent pro-inflammatory cytokine (Turner et al., 2014) and can activate macrophages, which in turn secrete additional cytokines and chemokines (Barnes, 2009) Upon expression, IL-1β is synthesised in a precursor state and must be cleaved by IL-1 converting enzyme or caspase-1, located in the inflammasome, in order to become biologically active. IL-1β binds to IL-1 receptors – IL-1R1 and IL-1R2 on target cells to initiate downstream signalling cascades. IL-1 receptors are designated as ILR/TLR receptors and signal via Toll/IL-1R (TIR) domain and MyD88, leading to the activation of MAPK, NF-kB and pro-inflammatory cytokines (Turner et al., 2014).

The potency of IL-1β is thought to be regulated by IL-1 receptor antagonist –IL-1Ra which readily binds with great affinity to IL-1R1 and with lower affinity to IL-1R2.

Binding of IL-1RA to IL-1 receptors attenuates IL-1β signal transduction, thereby sequestering IL-1 into an anti-inflammatory function (Turner et al., 2014).

1.5.2.2 Interleukin- 6 (IL-6)

IL-6 can be produced by a range of immune and non-immune cells including macrophages, lymphocytes, fibroblasts, endothelial and epithelial cells and belongs to the hematopoetic family of cytokines (Turner et al., 2014). It is expressed upon NF-kB activation in response to PAMPs, DAMPs, IL-1β, TNFα and IFN-γ. IL-6 works with other cytokines to modulate a link between the innate and adaptive immunity (Barnes, 2008, Parker and Prince 2011). Amongst its many functions, IL-6 is involved in immune cells maturation, T cell activation and switching B cells towards IgE production and priming granulocytes (Turner et al., 2014; Barnes, 2008; Davoine and Lacy 2014). IL-6 function in the liver involves stimulation of C-reactive protein release, which indicates a current infection and an inflammation process (Barnes, 2008).

IL-6 binds to the heterotrimeric IL-6 receptor (IL-6R), triggering signalling pathways via the signal transducing gp130 proteins, leading to the recruitment of janus kinases (JAKs) which in turn phosphorylate the receptor and STAT3. STAT3 dimers are translocated to the nucleus where pro-inflammatory cytokines are transcribed together with intracellular adhesion molecules. Cytosolic gp130 proteins can bind to the cytosolic IL-6R form and thus function as an anti-inflammatory by inhibiting trans-signalling induction (Turner et al., 2014).

1.5.2.3 Interleukin 8 (IL-8)

IL-8 also known as CXCL8 is a crucial inflammatory chemokine, produced by an array of cells including monocytes, neutrophils, lymphocytes, fibroblasts, endothelial and epithelial cells (Turner et al., 2014). IL-8's/ CXCL8's most important function is to induce chemotaxis of neutrophils. IL-8/ CXCL8 can also recruit monocytes, lymphocytes and eosinophils to sites of infection (Turner et al., 2014). IL-8/ CXCL8 readily binds to the chemokine receptors CXCR1 and CXCR2 receptors, expressed on leukocytes and endothelial and epithelial cells, to trigger a cascade of events involved in chemotaxis and degranulation.

Upon binding to its designated receptors, IL-8/ CXCL8 triggers the activation of G-protein coupled receptors which initiate adenylate cyclase, generating cyclin AMP to activate protein kinase A (Turner et al., 2014). Alternatively, G-protein receptors can activate phospholipase β to produce inositol triphosphate (IP3) and diacylglycerol and

activate protein kinase C, leading to MAPK activation and change gene expression to promote cell survival, proliferation and inflammation. Inositol triphosphate is involved in degranulation processes by stimulating calcium ions release from intracellular stores (Turner et al., 2014).

IL-8/ CXCL8 is strongly associated with respiratory diseases such as asthma and COPD as high levels of the chemokine are detected in BAL from these patients (Barnes, 2008). High levels of IL-8/ CXCL8 correlate with increased numbers of neutrophils detected in COPD patients' lungs, and it has been found further elevated during COPD exacerbations (Barnes, 2008). Smoke exposure also upregulates TLR4 expression leading to heightened IL-8/ CXCL8 production in the airways (Parker and Prince 2011). The important role of IL-8 in COPD pathogenesis makes the chemokine of interest to investigate further.

1.5.2.4 Tumour Necrosis Factor alpha (TNF-α)

TNF-α is a potent pro-inflammatory cytokine which plays a crucial role in the induction of pro-inflammatory cytokines, activation and expression of adhesion molecules and stimulation of growth (Davoine and Lacy 2014). Additionally, it has been involved in lipid metabolism, insulin resistance and endothelial function. TNF-α is designated as one of the most important cytokines in initiation of airway inflammation (Davoine and Lacy 2014; Turner et al., 2014). TNF-α is produced mainly by activated macrophages, monocytes, T cells, fibroblasts and airway epithelial cells.

The TNF receptor 1 (TNFR1) is expressed widely on different cell types including airway epithelia whereas TNF receptor 2 (TNFR2) is predominantly expressed on endothelial cells and leukocytes (Parker and Prince 2011; Turner et al., 2014). Signalling via TNFRs induces a pro-apoptotic cascade or recruitment of adaptor molecules that activate MAPK and transcription factors (Parker and Prince 2011). Transcription factor activation ultimately results in elevated transcription of other pro-inflammatory cytokines, amplifying the inflammatory cell state (Parker and Prince 2011; Turner et al., 2014).

1.5.2.5 RANTES

RANTES or CCL5, produced by eosinophils, neutrophils, macrophages, mast cells, T cells and airway epithelial cells, is an important eosinophil and lymphocyte chemoattractant to regions of inflammation (Turner et al., 2014). RANTES/ CCL5 exerts its function by binding to different CC receptors such as CCR1, CCR3 and

CCR5 (Barnes, 2008). Of interest, CCR5 is distributed on T cells, more specifically on Th1 and Tc1 cells and initiate recruitment of T cells in COPD patients. T cells expressing CCR5 have been found increased in COPD patients and RANTES/ CCL5 levels are upregulated in the sputum of COPD patients (Barnes, 2016). It is therefore thought RANTES/ CCL5 has a role in the recruitment of T cells, eosinophils and macrophages during exacerbations in COPD patients (Barnes, 2008).

1.5.2.6 Interferon – γ – inducible protein (IP-10)

IP-10 or CXCL10 is an IRF-3 stimulated protein, induced by IFN-γ and produced by variety of cells including monocytes, keratinocytes, lymphocytes, fibroblasts, endothelial and epithelial cells (Barnes, 2016). IP-10/ CXCL10 is a CXC chemokine which has affinity for the G-protein CXCR3 receptor. CXCR3 is expressed specifically on type 1 T lymphocytes, which are known to infiltrate the lungs of patients with COPD disease (Saetta et al., 2002; Barnes, 2008). Along with the CXCR3 positive cells in the peripheral airways of COPD patients, IP-10/ CXCL10 was found to be increased in bronchial epithelium, particularly in the wall of pulmonary arteries in COPD subjects. The CXCR3/ IP-10 axis is thought to be important in the preferential recruitment of T lymphocytes, which produce IFN-γ that could further increase IP-10/ CXCL10 levels and thus cause amplification predominantly of Th1 hyper inflammatory state (Saetta et al., 2002).

1.5.2.7 Monocyte Chemoattractant Protein 1 (MCP-1)

MCP-1 also known as CCL2 is a potent CC chemokine that can activate CCR2 expressed on monocytes (Barnes, 2009). MCP-1/ CCL2 is secreted by monocytes, T cells and epithelial cells induced by oxidative stress, other cytokines or growth factors. MCP-1/ CCL2 is highly expressed in sputum, BAL and lungs of COPD patients. MCP-1/ CCL2 regulates monocytes migration to the lungs and thus is thought to cause increased macrophages accumulation in COPD patients (Barnes, 2008).

1.6 Hypothesis and aims

The hypothesis of this study is that co-infection of airway ciliated epithelium with rhinovirus and *M. catarrhalis* leads to greater ciliary dysfunction and greater epithelial inflammatory response than either infection alone in ciliated cultures from healthy individuals and COPD patients.

The main aims of the study were:

- To investigate the initial interaction of *M. catarrhalis* / rhinovirus with the airway epithelium
- To determine the effect of rhinovirus pre-infection followed by *M. catarrhalis* infection
- To compare the effect of *M. catarrhalis* infection alone, rhinovirus infection alone and co-infection with *M. catarrhalis* and rhinovirus in ciliated epithelial cells from healthy and COPD subjects

This is the first study to investigate the role of rhinovirus and *M. catarrhalis* co-infection of the ciliated healthy and COPD epithelium. More detailed hypotheses and aims are included in each results chapter, in order to more specifically address the research questions.

Chapter 2. Materials and methods

2.1 Materials

Detailed information about media, reagents, solutions and buffers used in this thesis is provided in Supplementary Tables 1, 2 & 3 in Appendix 4.

2.2 Culture of human airway epithelial cells

2.2.1 Ethical approval

Human respiratory nasal and bronchial samples from healthy volunteers and COPD patients were collected with written consent being obtained prior sample collection. All samples were collected through the Airway Living Biobank ethical approval with reference number 14/NW/0128, granted by the North West Liverpool-East Research (NRES) committee.

2.2.2 Collection of airway epithelial cells

Human respiratory nasal or bronchial epithelial cells were isolated from the airways of healthy and COPD donors according to British Thoracic Society (BTS) guidelines (British Thoracic Society 2016). Nasal or bronchial brush biopsies were obtained by nasal (CytoSoft, USA) or bronchial cytology brushes (Olympus, USA) by brushing the epithelium in a forward and backward direction. After the procedure the brush head was placed into 2ml of 20mM HEPES buffered medium 199 (Invitrogen, UK) containing 100IU/ml penicillin (Invitrogen, UK), 100μg/ml streptomycin (Invitrogen, UK) and 2.5μg/ml fungizone (Invitrogen, UK). To resuspend the captured cells on the brush, the cell strips were shaken off well into the medium. The nasal/bronchial cell strips were cultured within 2h immediately after collection or kept at 4^0C until the next day.

2.2.3 Collagen coating of flasks/wells/inserts

Collagen coating of flasks/wells/inserts (Fisher Scientific UK, Invitrogen UK) was completed at least one day before use. PureCol (3mg/ml) (Cellsystems, Germany) was prepared as a 1% solution in sterile phosphate buffered saline (PBS). Sufficient volume was added to completely cover the surface of the flasks/wells/inserts and incubated for at least 1 hour at room temperature. The flasks/wells/inserts were washed once with sterile tissue grade water to remove any acidity on the collagen

coat. The flasks/wells/inserts were air dried in a safety cabinet and stored in sealed plastic bags.

2.2.4 Airway epithelial cell culture

To completely remove the HEPES 199 buffered medium before culture, the cells were centrifuged at 200 x *g* for 5min in a 15ml falcon tube (Fisher Scientific, UK) using an Eppendorf centrifuge (Eppendorf, UK). The cell pellet was resuspended in 1ml of F-medium (co-culture media). Co-culture medium contained 3 parts of 10% foetal bovine serum (Invitrogen, UK), 1% penicillin/streptomycin DMEM and 1 part F-12 nutrient mix (Invitrogen, UK) supplemented with 5μg/ml insulin (Sigma, UK), 5μM Y-27632 (ROCK inhibitor) (Enzo Life Sciences, USA), 25ng/ml hydrocortisone (Sigma, UK), 0.125ng/ml epidermal growth factor (ThermoFisher, UK), 0.1nM cholera toxin (Sigma, UK), 10μg/ml gentamicin (Invitrogen, UK), 250ng/ml amphotericin B (Invitrogen, UK). The cells were propagated using a newly proposed co-culture method.

2.2.5 Co-culture of human basal cells

The co-culture method was adapted from Butler (Butler et al., 2016) to enable rapid expansion of the human airway epithelial cells. This method shows the use of a ROCK (Rho-kinase, coiled coil containing protein kinase) inhibitor in the basal cells growth medium and mitotically inactivated fibroblast feeder layers helps support the growth and multipotent differentiation capacity of the basal cells.

2.2.5.1 Preparation of mouse epithelial fibroblasts feeder layer

Mouse embryonic fibroblasts (J2F) gifted from Dr Rob Hynds (Lungs for Living Research, London) were grown in submerged conditions in 8% bovine serum (BS) (Invitrogen, UK) and 1% penicillin/streptomycin (Invitrogen, UK) supplemented Dulbecco's modified Eagle's medium (DMEM, Life technologies, UK) at 37^0C with 5% CO_2. The J2F fibroblasts were grown to 80-90% confluency and were routinely inactivated for the preparation of feeder layers.

Inactivation medium was prepared by adding mitomycin C (Sigma, UK) into 8% BS, 1% penicillin/streptomycin DMEM media at a final concentration of 10μg/ml. Active fibroblasts were exposed to 10ml inactivation medium for 2h at 37^0C with 5% CO_2 after which rinsed with 10ml sterile PBS and dislodged by 0.05% trypsin/EDTA for 3-5 min. Trypsin action was neutralised by 5ml 8% BS DMEM and the fibroblasts collected by centrifugation at 200 x *g* for 5min were stained with trypan blue (Sigma,

UK) and counted by a c-chip (NanoEnTek, Korea). $1.5x10^6$ fibroblasts were plated out in one T75 cm^2 flask and incubated overnight to attach. On the next day the inactivated J2Fs were used as a feeder layer.

2.2.5.2 Co-culture of human basal cells with J2F inactivated fibroblasts

The co-culture of human basal cells with J2F inactivated fibroblasts prolonged the passaging of cells for differentiation and improved the cell yield with better proliferation features and provided good populations of epithelial cells which functionally differentiated into a ciliated phenotype.

To grow human basal cells, they were transferred from the collection tube into a feeder layer with 9ml co-culture medium and incubated for 5-7 days at 37^0C with 5%CO_2. The basal cells at that stage were labelled as passage 1+1 and fed every other day with 10ml co-culture media. For further passaging of the co-cultures differential trypsinisation was applied (Butler et al., 2016). Due to the high sensitivity of the mouse fibroblasts to trypsin they were detached by 2ml 0.05% of trypsin/EDTA for 30sec which was then washed away completely by PBS. The strongly adherent basal cells were then dislodged by 5ml TrypLE (mixture of recombinant enzymes) (Life Technologies, UK) for a maximum of 10min at 37^0C with 5% CO_2 which was then neutralised by addition of 5ml of co-culture media. The pure population of basal cells was collected by spinning at 200 x *g* for 5min. For routine passaging, the basal cells were seeded into T75cm^2 feeder layer flasks at a concentration of $0.5x10^6$ cells/ml.

2.2.6 Differentiation of basal cells at air – liquid interface

The basal cells collected by the procedure above were resuspended in 1ml of co-culture media, and their viability and cell numbers were assessed by trypan blue and a c-chip. Around $0.5x10^6$ cells/ml were seeded onto 24 well collagen coated transwell clear inserts with 0.4μm pore size (Corning, USA) under co-culture media (Hirst et al., 2010). The cells were in submerged conditions for 2 days at 37^0C with 5% CO_2 in a high humidity incubator. At day 2 post seeding, air-liquid interface was created by exposing the cells to air at the apical site while feeding them from the basolateral compartment with air-liquid interface (ALI) media (Hirst et al 2010). For ALI media preparation was used basal epithelial base medium (BEBM, LONZA, UK) referred as bronchial epithelial growth medium (BEGM) when complemented with SingleQuots supplements (LONZA, UK) - 500μl hydrocortisone, 500μl gentamicin/ amphotericin B, 500μl retinoic acid, 1ml bovine pituitary extract, 500μl human insulin, 500μl transferrin, 500 μl triiodothyronine, 500μl epinephrine and 500μl human epithelial growth factor

or basal growth medium Promocell™ (Promocell, UK) supplemented with – 0.5 μg/ml hydrocortisone, 0.1 ng/ml retinoic acid, 0.0004ml/ml bovine pituitary extract, 5 μg/ml human insulin, 10 μg/ml transferrin, 6.7 ng/ml triiodothyronine, 0.5 μg/ml epinephrine and epidermal growth factor 10 ng /ml. ALI media consisted of 50% DMEM and 50% BEGM (or 50% Promocell™ growth media supplements) with the same amount of the above supplements without gentamicin. This stage was considered as day 0 of the ALI cultures (Hirst et al., 2010). Thereafter, ALI media was prepared weekly and further supplemented with 10nM retinoic acid to induce mucociliary differentiation. The cells were fed three times a week at the basolateral site as the apical surface was washed once a week with 50μl of BEBM. Apical washes from one donor were pulled together, clarified at 11400 x *g* for 3min and stored -80^{0}C for future analysis. The cultures were grown for 5 weeks in an ALI state to initiate full differentiation.

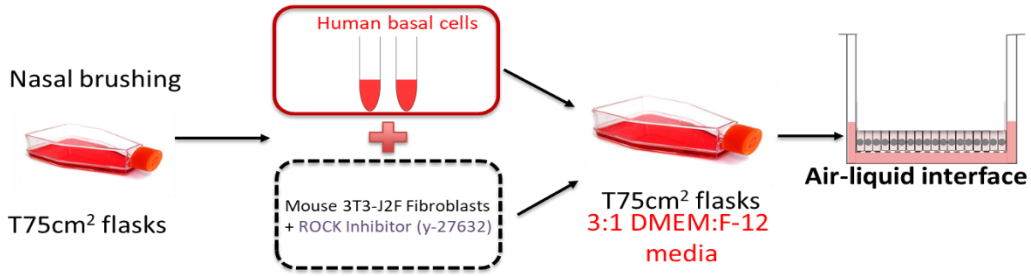

Figure 2-1 Flowchart of the co-culture method of nasal/bronchial basal airway cells with inactivated fibroblasts.

Co-culture of airway basal cells with mitotically inactivated fibroblasts by ROCK inhibitor (Y-27632). This allowed expansion of airway basal cells. Primary airway cells from healthy and COPD donors were then seeded on transwell inserts to allow differentiation.

2.2.7 Transepithelial electrical resistance (TEER) measurement

TEER was determined by use of an EVOM^2 voltmeter and a pair of STX2 chopstick electrodes (World Precision Instruments, USA). Chopstick electrodes tips were cleaned in pure methanol prior to use for a couple of minutes and then suspended in BEBM medium. The voltmeter was switched on and the function was switched to Ohms. The meter reading of an empty insert was used to set a baseline value. All readings were in a digital format which provided a range of 1-9,999 Ohms (Ω). To measure TEER of ALI cultures, 0.2ml of BEBM medium was added to the apical surface where the electrodes were placed for 2 seconds. After the measurement the BEBM medium was removed from the apical surface.

2.2.8 Ciliation score and quality control test

To check the quality of differentiated epithelial cultures within a study, a ciliation score check was implemented prior experiments to ensure similarity between the wells used. The stage was essential due to inter and intra donor variability in the ciliation level and the condition of the epithelial cells from different donors. The test consisted of observational assessment of the quality of each well using a high speed video system which allowed to score the ciliation level, and acknowledge additional details such as mucus production and leakiness of the culture. The degree of ciliation appearance involved 5 levels: from no moving cilia observed, indicated by 0 to a fully ciliated condition, indicated by 5, where cilia lawn covered the entire epithelial surface. The full quality control assessment sheet is included in Appendix 2.

Further, due to the variability of ciliation and appearance of differentiated cultures from healthy volunteers and COPD patients, the quality assessment stage was also implemented to chose similar wells with epithelial cells for experiments where a compasiron between the two groups had to be made. Thus, the ciliation level of epithelial cells from healthy donors was matched with the ciliation level of epithelial cells from COPD donors.

Date of seeding										
Date of ALI										
Ciliation Score										
0	No moving cilia observed									
1	A few individual ciliated cells scattered around the transwell (1-20 ciliated cells/well)									
2	Several ciliated cells in small groups but not forming extensive patches.									
3	Extensive patches of cilia (usually around edges). Cilia are usually absent in the centre of the transwell.									
4	A lawn of cilia all around the edges of the transwell. Cilia usually sparse in the middle of the transwell.									
5	Fully ciliated on edges and in the middle. A continuous lawn of cilia covering the entire surface of the transwell.									
Well number	I	II	III	IV	V	VI	VII	VIII	IX	X

Figure 2-2: Assessment of ciliation appearance.

2.3 Pathogen propagation

2.3.1 *M. catarrhalis* cultivation

2.3.1.1 Preparation of master stocks

M. catarrhalis was purchased from ATCC (#25238, ATCC, UK) and cultured on blood agar base (BAB) (Oxoid, UK) supplemented with 5% sheep blood (subsequently referred to as sheep blood agar) (Sigma-Aldrich, UK) and incubated overnight at 37^0C with 5% CO_2. The purity of the culture was established by visual inspection for a diplococcus monoculture appearance. Periodically, 1-2 single colonies were emulsified in sterile H_2O to confirm bacterial morphology by a Gram staining procedure (described below). Subsequently, *M. catarrhalis* was sub-cultured onto fresh sheep blood agar plates from 1-2 distinct colonies and incubated overnight at 37^oC with 5% CO_2. The confluent plates were examined for colony purity after which one entire plate was harvested and resuspended into 20ml brain heart infusion (BHI) broth supplemented with 10% glycerol. The bacteria were aliquoted into 1ml vials and frozen at -80^oC.

2.3.1.2 The Miles and Misra viable count

Miles and Misra counting (Miles et al., 1938) was used to determine the number of viable microorganisms in the glycerol stocks ($5.2x10^{11}$ CFU/ml). Briefly, a vial of *M. catarrahlis* was washed 3x in PBS and 10 fold serial dilutions were prepared in a flat bottom 96 well plate (Corning, Life Technologies, UK); 10ul of each dilution was plated out in triplicate onto a sheep blood agar plate and incubated overnight at 37^0C with 5%CO_2. On the next day colonies were counted and stock density was calculated according to equation 1:

Equation 1: CFU/ml= average number of colonies x dilution factor x 100

2.3.1.3 Preparation of working stocks

To ensure characteristics of bacteria are the same for all infection experiments, *M. catarrhalis* was cultured until mid-exponential phase at optical density (OD) of 1. A preliminary growth curve was performed in duplicate to determine *M. catarrhalis* mid-exponential phase. Assessment of bacterial growth was performed using a BioPhotometer 2000 (Eppendorf ltd, USA). Simply, 4ml BHI broth was inoculated with *M. catarrhalis* at a concentration of $1x10^6$ CFU/ml from frozen stocks. The suspension was incubated overnight at 37^{o}C with constant shaking at 225 rpm. Then, 200µl from the overnight inoculum was diluted 1/50 in BHI broth and incubated at 37^{0}C with constant shaking and bacterial OD readings were recorded hourly at 600nm. Growth curve was continued until *M. catarrhalis* reached stationary phase at OD of 2.4. The stocks were supplemented with 10% glycerol, frozen at -80^{o}C and used within 12 months.

2.3.1.4 Gram staining

Gram staining was performed to check for correct bacterial morphology and Grams classification. On a microscope slide (Life Technologies, UK) 1-2 distinct colonies were emulsified until a thin film of microorganisms was formed. The film was heat fixed for 5min at 85^{0}C using a heating block (Techne Dri-block DB 20, UK). The film was stained for 1-2 min with crystal violet solution and excess dye was removed. Gram's iodine solution was applied for 1-2 min and excess stain was removed. The slide was decolorized quickly with acetone and rinsed thoroughly with tap water. Safranin stain was applied for 2 min to counterstain after which the film was rinsed with tap water. Any excess water or dye were wiped off and the slide was dried for 5min at 85^{o}C on a heating block. Bacteria were visualised at 100x objective using Leitz Dialux 22 bright field microscope (Leitz Wetzlar, Germany).

2.3.2 Rhinovirus 16 stock preparation

Major group rhinovirus (RV) type 16 was tested for strain validity by neutralisation with specific anti-sera antibodies, which were gifted from Dr Gary McLean (Cellular and Molecular Immunology Research Centre, London, UK) and expanded to 25ml to yield virus stocks through passaging in cell culture. Hela H1 cells passage 22 were also a gift from Dr McLean and were further propagated in 10% foetal calf serum (FCS) (Sigma, UK) and 1% penicillin/ streptomycin DMEM media. A confluent T175cm^2 flask of Hela H1 cells was washed twice in 5ml PBS and infected with 5ml of $1.35x10^7$

$TCID_{50}$/ml (50% tissue culture infectivity dose) rhinovirus 16 made up to 12.5ml with rhinovirus infection medium consisting of 2% FCS, 1% penicillin/streptomycin, 15mM HEPES (Sigma-Aldrich, UK) and 15mM Sodium bicarbonate (Sigma-Aldrich, UK) in DMEM media. Cells were incubated for 1h on a platform shaker at room temperature to spread the rhinovirus gently within the flask (Walker et al., 2013). An extra 12.5ml of rhinovirus infection medium was added to the Hela stock which was then transferred to an incubator (set at 37^0C and 5% CO_2) for 16-24 hours until >80% cytopathic effects were observed and cells were fully disrupted (Walker et al., 2013).

2.3.2.1 Purification and concentration of rhinovirus stock

Hela H1 cell lysates from 10 x T175cm^2 flasks (200ml) infected with rhinovirus 16 were harvested at 24h post infection. To collect live virus, contents of the flasks were lysed through 2-3 freeze/thaw cycles. The infectious inoculum was purified by centrifugation at 2500 x *g* for 15min at 4^0C to eliminate cell debris and filtered through 0.2μM filters to remove damaged particles unable to infect *in vitro* (Papi and Johnston 1999), followed by clarification centrifugation to remove cells debris at 3000 x *g* for 15min. The supernatants were filtered through 0.2μ vacuum filters and transferred into 4 x 50ml Amicon ultra (100 000 NMCO) (AmiconUltra, Merck, U centrifugal filtration devices, which concentrated virus into 15ml through centrifugation at 3000 x *g* at 4^0C. The virus was then precipitated using 7% polyethylene glycol (PEG) 6000 (Sigma-Aldrich, UK) and 0.5M sodium chloride (NaCl) (Sigma-Aldrich, UK) on ice with occasional mixing for 1 hour. The precipitated virus was pelleted by centrifugation at 3000 x *g* for 1 hour at 4°C and then resuspended in 15ml of PBS with vigorous pipetting and occasional vortexing to ensure the virus had dispersed evenly. Insoluble matter was removed by an additional centrifugation at 3000 x *g* for 15min at 4^0C and filtration through 0.2μ syringe filter. The virus was further concentrated using Amicon Ultra centrifugal filtration devices (100,000 NMCO) to a volume of around 0.5ml. To wash the virus, 10ml of PBS was added and pipetted thoroughly to mix well the concentrated virus in the filtration device and the concentration step was repeated. The virus was harvested, and the filtration devices were washed with additional 2 x 1ml PBS. The washes were afterwards combined with the concentrated virus in the 0.5ml to obtain a total of 2.5ml purified and concentrated virus stocks. Efficacy of rhinovirus infectivity was evaluated by comparing it mock-medium controls. Viral titres were determined by titration assays and stocks were stored at -80^0C.

2.3.2.2 Titration assay of rhinovirus 16

Titration of rhinovirus stocks was accomplished by seeding 1.5 x 10^4 Hela H1 cells in 150μl/well in a flat bottom 96 well plate. 10 fold serial dilutions of the rhinovirus stocks were prepared to infect 6 replicates of Hela cells with 50μl of each dilution. Control wells of Hela cells with media (no RV) were included for each 96 well plate. Infected/non-infected cells were cultured in rhinovirus infection medium for 4-5 days at 37^0C atmosphere with 5% CO_2 (Papi and Johnston 1999). The cytopathic effects of rhinovirus were visually assessed every day by a light microscope. At day 4 post infection, wells with cells showing cytopathic effects were scored and the titre was calculated using the Spearmen-Karber equation expressed as $TCID_{50}$/ml (Papi and Johnston 1999) (see equation 2).

Equation 2

$TCID_{50}/ml = xk + d\ [0.5-(1/n)\ (r)]$

Where xk- dose of the highest dilution, r= sum of negative responses, d= spacing between dilutions, and n=wells per dilution

2.3.2.3 Crystal violet staining

Continuity of infected monolayers was also assessed 4 days post infection by staining them with 0.1% crystal violet (Sigma, UK) in water for 10 minutes (Papi and Johnston 1996). The cells/dye were dissolved in 1% sodium dodecyl sulphate (SDS, Fisher Scientific, UK) in water for 1h with constant shaking at room temperature. Absorbance was read at 560nm (FLUOstar Omega microplate reader, BMG, Labtech) and values were plotted as a standard curve using GraphPad Prism v 7.1 (GraphPad software, USA).

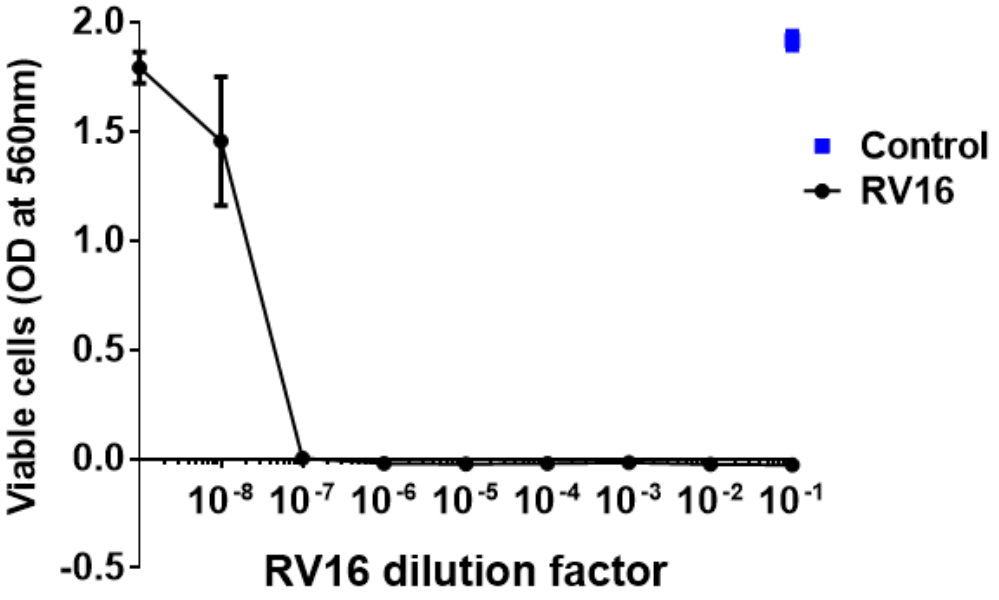

Figure 2-3: Infectivity of purified and concentrated rhinovirus 16 stock, determined by a titration assay and crystal violet staining.

2.4 Bacterial / viral infection and co-infection of ciliated airway epithelial cultures

2.4.1 Infection of ALI cultures with *M. catarrhalis*

When nasal/ bronchial epithelial cells were identified as being fully differentiated, typically at week 4 or 5 of air-liquid interface, cultures were deemed to be ready to use for experiments. One day prior to infection, the ALI cultures were fed with antibiotic-free media (BEBM: DMEM, SingleQuots supplements with hydrocortisone, retinoic acid, transferrin, epinephrine) and the apical surface was rinsed with 50μl of BEBM media. The following day a Nikon's Eclipse Ti-E microscope and the attached high speed video camera were switched on one hour before use and the humidified incubation chamber was set to 37^0C and 5% CO_2. The TEER of the ciliated epithelium was measured as described in 2.2.7. The ALI plate was positioned for viewing on a heated stage and ciliated epithelial cells were visualised by Nikon NIS Elements Software v. 4.12 using 20x objective. At least 5 areas of interest (ROI=512x512) that contained at least 5-6 ciliated cells were randomly selected and their respective X and Y coordinates were saved using the NIS software. High speed video recordings were captured as described below (section 2.5.1). Apical fluid of the ALI culture was

collected by washing with 50μl of BEBM and then spun at 11400 x *g* for 3min; this supernatant was then stored at -80^{0}C for future analysis.

For infection studies, the cultures were removed from the microscope, the basolateral fluid was exchanged with fresh ALI media and 5x10^6 CFU/ well of live *M. catarrhalis* were added in 200μl of BEBM. The plate was returned to the humidified incubator for 15min after which the bacteria were removed and cultures were washed 2x in 200μl BEBM. Ciliary beat frequency was recorded at 15min post infection and at 24h post infection. At 24h post infection TEER of cultures was measured by adding 200μl of BEBM to the apical chamber of the cultures and 20μl from both apical and basolateral fluids were taken for Miles and Misra viable counts. For signalling pathway activation pathways the basolateral fluid of ALI cultures was not changed prior the addition of *M. catarrhalis* to avoid signal interference from growth factors contained in the media.

2.4.2 Adherence and invasion of *M. catarrhalis* into ciliated respiratory cultures

The apical surface of infected and non-infected ciliated cultures was gently washed 3 times with 200μl BEBM to wash loosely bound or mucus bound bacteria and the number of adhered and intracellular bacteria was determined by a method described previously (Slevogt et al., 2007). For washing, 200μl of BEBM or 200μl of BEBM containing 200μg/ml Imipenem (Sigma, UK) was added to the apical chamber of the ciliated ALI cultures, in the basolateral chamber the fluid was exchanged with 500μl of BEBM. The plate was returned for 2h to the humidified incubator at 37^{0}C+5% CO_2. The media from the apical and basolateral chambers was removed and the epithelial surface was washed another 3 times with 200μl of BEBM to remove dead extracellular bacteria. This was followed by the addition of 180μl Trypsin/ EDTA, basolateral site received 500μl of Trypsin/ EDTA for 15min at 37^{0}C with 5% CO_2. After the incubation time, epithelial cells were detached from the inserts by careful pipetting and transferred into 1.5ml Eppendorf tubes, where Trypsin/ EDTA was inactivated by addition of 10% (v/v) volume foetal calf serum (Sigma, UK). Epithelial cells were pelleted by centrifugation for 5min at 5100 x *g* and resuspended in 200μl PBS or in 200μl of 0.2% (v/v) saponin in PBS (Sigma, UK) to lyse the epithelial cells for 20min at room temperature. Adhered and intracellular *M. catarrhalis* was determined by Miles Misra viable counts as described earlier.

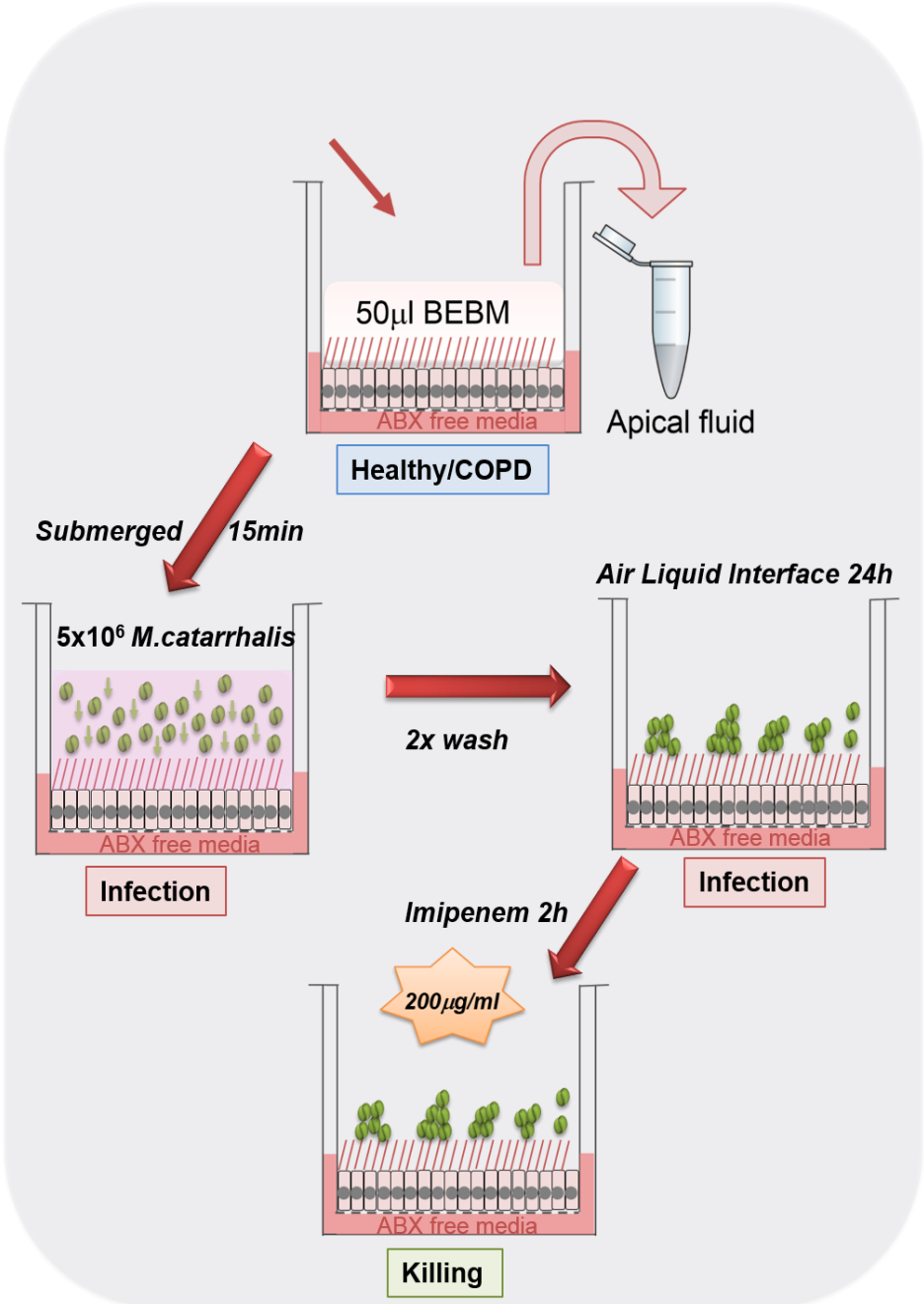

Figure 2-4: Schematic diagram *of M. catarrhalis* infection of primary airway epithelial cells at air-fluid interface.

Gefitinib and PAN PI3K inhibition of *M. catarrhalis* invasion of primary airway epithelial cells

Once fully differentiated, epithelial cells from healthy and COPD subjects were washed apically once with plain BEBM media and the basolateral fluid was exchanged with ALI culture media without antibiotics. Quality of epithelial cultures was checked by measuring TEER as described in 2.2.7 previously. 10mg Gefitinib (Tocris, UK) inhibitor was obtained in a powder form and reconstituted in 2.24ml DMSO to obtain a 10mM stock, aliquoted and stored at -20^{0}C. For assays, 10mg PAN PI3K (GSK987740A) was used and was obtained from GlaxoSmithKline's Refractory Respiratory Inflammation-DPU in a powder form and reconstituted in 2.52ml DMSO to obtain a 10mM stock, which was aliquoted and stored at -20^{0}C. Serial dilutions of Gefitinib or PAN PI3K inhibitors were performed in BEBM plain media and used at 1μM final concentration which were added to the basolateral chamber of the epithelial cells. Alternatively, vehicle controls had DMSO added only. Epithelial cells were pre-treated with the inhibitors for 1h at 37^{0}C with 5% CO_2. Meanwhile, *M. catarrhalis* stocks were retrieved, washed 3 times and diluted to 2.5 x 10^7 CFU/ml as described previously. Then 200μl from the bacterial stock (5x10^6 CFU) were added apically to designated wells, while uninfected controls received 200μl of plain media. Differentiated cultures were flooded with bacteria / media for 15min at 37^{0}C with 5% CO_2 and the inoculum was then removed. The epithelial layers were washed 2 times with plain media to remove unbound bacteria. The plate was subsequently returned to the incubator and the infection was progressed at an air-fluid interface condition for 24h at 37^{0}C, 5% CO_2 in a humidified environment. At the end of the infection, 200μl of BEBM was added apically and TEER was measured again. Apical and basolateral fluids were collected and stored at -80^{0}C for further analysis. The apical site of epithelial cultures was gently washed 3 times with 200μl of BEBM media and 200μl of plain media containing 200μg/ml Imipenem (Sigma-Aldrich, UK) was added apically for 2h at 37^{0}C and 5% CO_2; the basolateral site received 500μl of plain media. The apical site of the cultures was gently washed another 3 times with plain media, followed by the addition of 180μl Trypsin/ EDTA, the basolateral media was exchanged with 500μl of Trypsin/ EDTA for 15min at 37^{0}C and 5% CO_2. After the incubation time, epithelial cells were dislodged from the plastic inserts through careful pipetting and Trypsin/ EDTA was inactivated by 10% (v/v) volume foetal calf serum (Sigma-Aldrich, UK). The cells were transferred into 1.5ml Eppendorf tubes and spun down for 5min at 5100 x *g*, the supernatants were removed and the pellets resuspended in 200μl of 0.2% (v/v) saponin in PBS (Sigma-Aldrich, UK) to lyse the

epithelial cells for 20min at room temperature. Miles Misra viable counts were performed as described in 2.3.1.2 previously to determine intracellular bacterial counts.

2.4.3 Rhinovirus infection of air-liquid interface cultures

Fully differentiated ALI cultures from healthy volunteers and COPD patients were washed once with plain media BEBM prior to the viral infection. TEER of cultures was measured in 200μl of plain media by a voltmeter as explained above (section 2.2.7). Purified rhinovirus with stock concentration of $9.18x10^8$ $TCID_{50}$/ml was diluted to $1.5x10^7$ $TCID_{50}$/ml in plain media and 100μl of diluted virus was added to the apical site of ALI cultures at a final concentration of $1.5x10^6$ $TCID_{50}$/culture. Infection in flooded conditions was allowed for 1h at 37^0C with 5% CO_2 in a humidified incubator to allow viral attachment to mucociliary cultures. The inoculum was then removed and the infection was progressed for 24h at 37^oC and 5% CO_2. Control/ mock infected cultures received 100μl of plain media and were processed in the same manner as infected wells.

2.4.4 Long term (7 day) rhinovirus infection of respiratory epithelial cultures

Once fully differentiated at ALI conditions at 37^0C and 5% CO_2 in a well humidified environment, epithelial cultures were infected with rhinovirus as described in 2.4.3. The infection was allowed to progress for up to 7 days at ALI conditions. On days 1, 2, 3 and 7 ciliary beat frequency was recorded as described below (section 2.5.2), without washing the apical site of the cultures. This method determined if mucus build up in the period of 7 days affected the beat frequency of cultures. Additionally, at different days post-infection in designated wells 200μl of plain media to the apical chamber of ciliated cultures was added and TEER was measured by a voltmeter. Infected and non-infected cultures were then sacrificed by scraping the epithelial cells from the insert membrane, followed by collection in 1.5ml Eppendorf tubes. The epithelial cells were pelleted by centrifugation at 8500 x *g* for 5min and pellets were stored for western blot analysis at -20^0C. In a different set of wells, 100μl of plain media was added to the apical chamber and epithelial cells were scrapped off the membranes by a spatula and subsequently transferred into 1.5ml Eppendorf tubes and stored at -80^0C until live virus was titred in Hela H1 cells as previously described (section 2.3.2.2).

2.4.5 PI4KIIIβ inhibition of rhinovirus replication in airway epithelial cells

Fully differentiated cultures from healthy and COPD subjects were maintained at 37^0C with 5% CO_2 in a well humidified environment. Prior the inhibition assay, the apical chamber of epithelial cultures was washed once in 200μl of plain media and quality of cultures was assessed by measuring TEER as previously described. The basolateral chamber media was exchanged with fresh 500μl ALI medium. For assays, 10mg of the PI4KIIIβ inhibitor (GSK2998533) was used and was obtained from GlaxoSmithKline's Refractory Respiratory Inflammation-DPU in a powder form and reconstituted in 2.12ml DMSO to obtain a 10mM stock, aliquoted and stored at -20^0C. Serial dilutions of the compound were prepared in BEBM plain media and epithelial cultures were pre-treated with PI4KIIIβ at a final concentration of 100nM basolaterally for 1h at 37^0C with 5% CO_2. Vehicle control received DMSO only, prepared in the same manner as the inhibitor compound. Rhinovirus stock (9.14×10^8 $TCID_{50}$/ml) was retrieved and cultures were infected with 1.5×10^6 $TCID_{50}$/ well apically in 100μl of plain media for 1h at 37^0C with 5% CO_2. Mock infected controls received plain media only and were treated in the same manner as infected wells. Following incubation, the inoculum was removed, and the virus infection was allowed to progress at air-fluid interface at 37^0C with 5% CO_2 for 24h in a well humidified incubator. At the end of the experiment, 100μl of BEBM plain median was added to the apical chamber and TEER was measured again. Epithelial cells were scraped by a small spatula and then collected into 1.5ml Eppendorf tubes. The epithelial cells were subsequently frozen at -80^0C or quick frozen in dry ice/ thawed 3 times to release live virus in the supernatant. Cell debris were pelleted by centrifugation at 5100 x *g* for 5min. The basolateral fluid from the infected cultures was collected into 1.5ml Eppendorf tubes and stored at -80^0C for further analysis. Live virus in epithelial cells treated with/ out PI4KIIIβ inhibitor was assessed by titration assays in Hela H1 cells as described previously.

2.4.6 Co-infection of ALI cultures with rhinovirus 16 and *M. catarrhalis*

Co-infections of human ciliated cells were similarly performed to the *M. catarrhalis* infection. Briefly, fully differentiated cultures were fed with antibiotic free ALI media 24h before infection. Briefly, 1.5×10^6 $TCID_{50}$/ well rhinovirus was added apically to airway differentiated cells 1h at 37^0C with 5% CO_2. Mock infected controls and *M. catarrhalis* alone condition received plain media only and were treated in the same manner as infected wells. Following incubation, the inoculum was removed, and the virus infection was allowed to progress at air-liquid interface conditions at 37^0C with 5% CO_2 for additional 24h in a well humidified incubator. The following day, CBF was

recorded as described below (section 2.5.1) and the cultures were washed apically with 50μl of BEBM, the apical fluid was stored at -20^{0}C for further analysis. Epithelial cultures were infected with 5x10^6 CFU/well *M. catarrhalis* for 15min at 37^{0}C with 5% CO_2 and then washed 2x in BEBM. At 24h post co-infection TEER measurements and bacterial viability were obtained.

2.4.7 Respiratory epithelial cultures' apical fluid role on *M. catarrhalis* viability

Fully differentiated cultures from healthy and COPD subjects were maintained at 37^{0}C with 5% CO_2 in a well humidified environment. Apical fluid is defined as the apical rinse, collected in 50μl of plain media added to the apical surface of epithelial cultures, treated without antibiotics for 24h prior the wash. To determine the effect of apical fluid role on the growth of *M. catarrhalis*, fluid from ciliated cultures non/ infected with rhinovirus was collected and stored at -20^{0}C. *M. catarrhalis* stocks (3 x 10^8 CFU/ml) were retrieved from freezer storage and washed 3 times as described before (section 2.4.1). Stock was diluted to 3.3 x 10^7 CFU/ml and 150μl of bacteria were transferred onto a flat bottom 96 well plate. To each well with bacteria was added 50μl of apical fluid obtained from healthy / COPD cultures infected and non-infected with rhinovirus to a final volume of 200μl/ well. Mock control wells received BEBM plain media only and were treated in the same manner as wells with apical fluid treated bacteria. The assay was recorded as a time-lapse over 24h, where images of pre-selected areas with co-ordinates X, Y and Z from within a well were acquired every 10min. Time-lapses were recorded with an inverted Nikon Tie Eclipse microscope at a 20x objective in a humidified chamber at 37^{0}C with 5% CO_2. Movies of biofilm formation over 24h were created by the NIS Elements software v 4.12. In the end of the experiment, bacteria were gently pipetted up and down to dislodge adhered to the plastic biofilm. Miles Misra counts were performed as previously described in section 2.3.1.2 to assess bacterial viability following treatment with apical fluids.

2.5 Live video microscopy of ALI cultures

2.5.1 High speed video recording

Respiratory epithelial ciliated cells were grown and maintained in a humidified incubator at 37^{0}C with 5% CO_2 for 4-5 weeks in ALI media as describe previously (section 2.2.6). High speed video recording of cilia beating was carried out after complete differentiation of the cells (motile cilia were observed). Videos were recorded with a Hamamatsu ORCA digital camera C11440 attached to an inverted

phase-contrast Nikon Eclipse Ti-E microscope equipped with long distance 20x objective. The microscope was connected to a HP Z440 computer. Digital video recording was performed at 394 frames per second (fps) at 512 x 512 pixel resolution with 2ms of exposure time. The temperature of recording was 37^0C and was maintained by a temperature controller (OKOLab). CO_2 levels were controlled by a CO_2 unit with active humidity controller (OKOLab). For analysis, 5 to 10 areas of each sample were selected upon good resolution, perfect focusing and good distance from insert edges. X, Y and Z-axis coordinates of selected areas were saved using NIS-Elements software version 4.12. Nikon's perfect focusing system (PFS) allowed for focus correction in real time overcoming focus drift. Recorded video sequences were played back at a lower frame rate (slow motion) to assess quality. Videos were recorded as ND2 files and converted to non-compressed AVI files by NIS-Elements software v 4.12.

2.5.2 Ciliary beat frequency measurement

Ciliary beat frequency was determined from AVI files using Image J software and the ciliaFA plugin as described previously (Smith et al., 2012). CiliaFA calculates the change in average pixel intensity of an AVI file over time and exports this data to Excel (Microsoft Office 2007) which performs a Fourier transformation in order to obtain a CBF value in Hertz. At least 5 -10 videos were analysed per sample.

2.5.3 Manual assessment of ciliary beat frequency

Ciliary beat frequency was evaluated by the high speed video system and high speed videos recorded as described in section 2.5.1. Beat frequency of cilia was assessed by playing recorded ND2 files at reduced frame rates. Ciliated cells were identified and beat frequency was calculated by assessing the number of frames required for the completion of 5 full beating cycles. Frequency was converted to Hertz units by using the formula:

Equation 3:

$$CBF = \frac{394 \text{ frames / second (speed of recording)}}{\text{Number of frames required for 5 beating cycles}} \times 5 \text{ (conversion/beat cycle)}$$

Beat frequency of cultures was calculated for 10 ciliated cells per donor and a total of 6 donors per group were included in the assessment.

2.5.4 Ciliary beat amplitude

Ciliary amplitude is the distance a cilium travels from the beginning to the end of a stroke, viewed from above. The methodology used to measure beat amplitude involves the high speed video system and high speed videos recoded at high magnification (60x objective) at 198 fps at 1024x1024 pixel resolution with 2ms of exposure time at 37^0C with 5% CO_2 in a well humidified incubation chamber. Playing recorded videos in slow motion enabled the analysis of the amplitude of beating cilia to be determined. The precise distance travelled by cilia was evaluated by plotting a horizontal line from the beginning of a cilium stroke all the way to the end of the same stroke. The distance was calculated in μM in NIS Elements software version 4.1. For experiments with *M. catarrhalis* infection, ciliary beat amplitude was measured for non-infected ciliated cultures and infected cultures, where cilia had either *M. catarrhalis* bound or unbound. Five ciliated areas per video were selected to measure beat amplitude for each condition. Three different donor cultures were assessed for healthy and COPD groups.

2.5.4.1 Variability of analyses

To test variability of CBF and ciliary amplitude manual assessment between different assessors, CBF measurements and ciliary beat amplitude were obtained for 2 pre-selected ciliated cells in 10 high speed videos. The results from 3 different assessors are included in Appendix 2.

To test the variability between manual CBF and automated CBF assessment by the CiliaFa™ software, CBF measurements of 2 pre-selected ciliated cells from 10 videos were compared to the CBF measurements of ciliated cells from 10 videos obtained by the CiliaFa software. Analysis are included in Appendix 2.

To calculate the reproducibility of manual CBF measurements, the beat frequency of 20 ciliated cells from 10 high speed videos (2 ciliated cells/ video) was measured in 3 different days and the obtained results were compared. Standard deviation results are included in Appendix 2.

2.5.5 Ciliary activity analysis of epithelial cultures using the CiliaFa software

Ciliary activity is defined as the field with moving ciliated cells when looked down on the microscope. To assess rhinovirus effect on ciliated cells activity, infected with rhinovirus epithelial cells were placed in a humidified chamber at 37^0C with 5% CO_2 on an inverted Nikon Tie Eclipse microscope. The X, Y, Z co-ordinates of areas of

interest were saved in the NIS elements software prior the start the infection, where at least 5 ciliated cells were counted per area. High speed videos were recorded at 394fps using a 20x objective, by focusing on the ciliated cells; 10 areas per well were recorded for each condition prior the infection and 24h later. High speed videos were subsequently converted from ND2 files to AVI files without compression using the NIS Elements software. The AVI format of the videos allows comprehensive analysis of ciliated areas where ciliary beat frequency and percentage (%) of ciliary activity per area were automatically calculated (Smith et al., 2012).

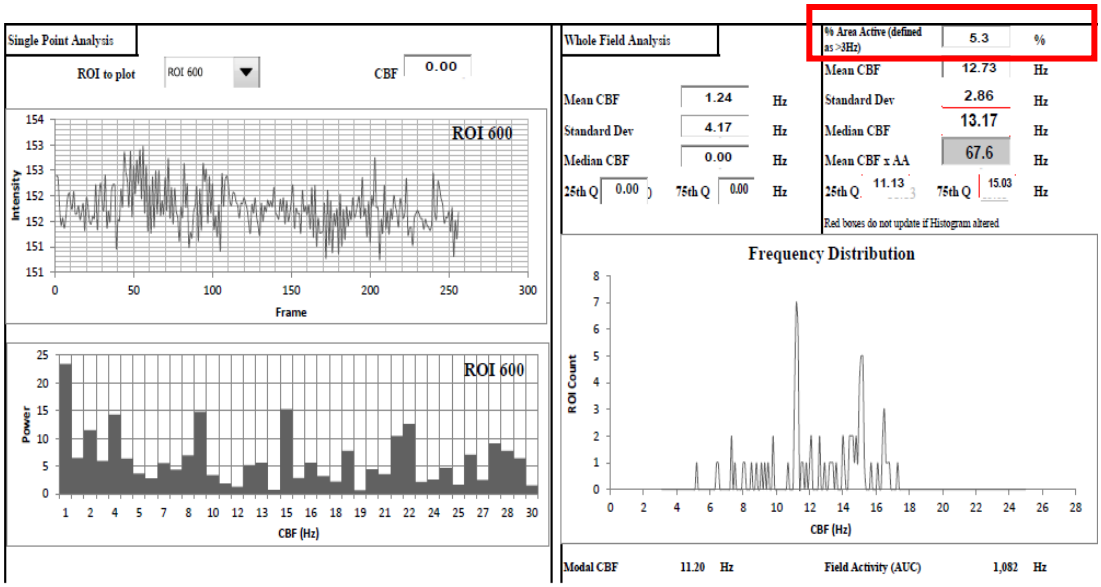

Figure 2-5: Screenshot of CiliaFa analysis report of ciliary function of epithelial cultures.

High speed videos were recorded for 512 frames at 394 frames/ second with 2ms of exposure time and saved as ND2 files. ND2 files were converted to non-compressed AVI files, which were run on the freely available ImageJ plug in CiliaFa (Smith et al., 2012). CiliaFa carries out Fourier transformation of pixel movement and presents ciliary function and % active area of the whole field.

All AVI files were run on the CiliaFa software using the same settings. Ciliary activity before and after rhinovirus infection was calculated by using the % area activity, calculated by the CiliaFa software. Ciliary activity from 10 videos per condition was averaged and plotted as a column chart.

2.5.6 Confocal imaging of live ALI cultures infected with *M. catarrhalis*

Fully differentiated ALI cultures fed with antibiotic-free ALI media 24h prior infection were stained with cell mask solution (ThermoFisher, UK). Briefly, on the day of infection ALI cultures were washed apically once with BEBM, 1000X concentrated cell mask stock solution was diluted to a final concentration of 1.5X in BEBM, 200µl of the working solution stain was added apically to cultures for 30min at 37^0C with 5% CO_2 and then washed 3x in BEBM. *M. catarrhalis* stock vial was labelled with 10µM CFSE cell tracker dye (Cell Trace, UK) for 30min at 37^0C with 5% CO^2 with gentle agitation. The stained bacteria were washed 2 times in BEBM and diluted to $2.5x10^7$ CFU/ml in BEBM. Inserts with primary human ciliated cultures were transferred into glass bottom dishes (WillCo, Intracell, USA) containing 1ml ALI media without antibiotics and fixed to edges with tape (FisherScientific, UK). After sealing the apical site with parafilm (AlfaLab, UK) cultures were carefully transferred to a Zeiss LSM 710 confocal microscope (Carl Zeiss ltd, Germany) where placed onto 25x water dipping objective. Correct microscope settings were adjusted by changing condenser height, upper and lower polarizer and phase contrast. A constant temperature of 37^0C was maintained by a temperature controller unit (OKOLab, UK).For inoculation, $5x10^6$ CFU of live or heat inactivated (65^0C for 30min) *M. catarrhalis* per well were added to the ciliated cells in a 200µl volume by a syringe. The initial interaction between cells and bacteria was captured live at 5 fps using Zen 2009 software (Carl Zeiss ltd, Germany) at 488nm and 650nm excitation wavelengths. Z-stack images were taken by focusing at top and bottom of the culture. Unbound bacteria were washed off within 15 minutes and the cells were rinsed twice in BEBM medium. After 24h incubation at 37^0C with 5% CO_2 cultures were returned to the confocal microscope, short videos and z-stack images were taken. Alternatively, ALI ciliated cultures were stained with Dextran dye (10, 000MW, A647, Sigma-Aldrich, UK) and *M. catarrhalis* were stained with 10µM CFSE cell tracker dye (Cell Trace, UK), and diluted to $2.5x10^7$ CFU/ml in BEBM. Epithelial cultures were infected with *M. catarrhalis* for 24h at 37^0C with 5% CO_2 in a well humidified incubator. Following the incubation time, dextran dye was removed, epithelial cells were washed in BEBM, scraped off from the insert membranes and transferred onto glass dishes and videos were recorded. Videos and images were initially recorded in lsm format then converted to avi/jpeg files and rendered with maximum intensity projection filters by Imaris v 7.2.3 (Bitplane AG, Switzerland) or by Volocity v 5 (Quorum Technologies, Canada).

2.6 Imaging of airway epithelial cells

2.6.1 Scanning Electron Microscopy of the ciliated epithelium infected with *M. catarrhalis*

Human ciliated cultures infected with $5x10^6$ CFU *M. catarrhalis* for 1h and incubated for 24h at 37^0C with 5% CO_2 were fixed in 2.5%Glutaraldehyde/0.1M cacodylate buffer (Agar Scientific, UK) in water for 24h at 4^0C and handed to Mrs Ania Iwanowska-Straatman, EM facility at the University of Leicester. The samples were subsequently washed twice in cacodylate buffer and cut out from the well inserts. Samples were washed three times in double distilled water within 95min and dehydrated using a series of increasing ethanol concentrations to 100% as follows - 30%- 40 minutes, 50% - 55 minutes and 70% - overnight, 90% - 30min and 100% - 55min, followed by 35min incubation with 100% anhydrous ethanol (Sigma-Aldrich, UK). The specimens were critical point dried by loading the material into a Critical Point Drier (Bal-Tec CPD030) and mounted onto aluminium stubs using carbon sticky tabs and sputter coaters (Quorum Q150T ES coating unit Au/Pd target, 20nm). Samples were visualised on a Hitachi S3000H Scanning Electron Microscope with an accelerating voltage of 10kV. Representative images were taken at various magnifications to effectively display the epithelium layer.

2.6.2 Transmission Electron Microscopy (TEM) of the ciliated epithelium infected with *M. catarrhalis*

Human ciliated cultures infected with $5x10^6$ CFU *M. catarrhalis* for 1h and incubated for 24h at 37^0 with 5% CO_2 were fixed in 2.5%Glutaraldehyde/0.1M Cacodylate buffer in water for 24h at 4^0C and handed to Ms Ania Iwanowska-Straatman, EM faicility at the University of Leicester. All steps were performed at room temperature on a rotor. Transwells processed for TEM were extra cut into two pieces and transferred into processing vials. Samples were post fixed with 1% osmium tetroxide with 1.5% potassium ferricyanide in 0.1M cacodylate buffer for 90min. This was followed by washing in 0.1M cacodylate buffer four times in 70min and the samples were stained in 1% tannic acid in 0.05M sodium cacodylate in the dark for 45 minutes, washed in 1% sodium sulfate in 0.05M cacodylate for 5 minutes and then four times with distilled deionised water within 90min. Samples were then dehydrated using a series of increasing ethanol concentrations to 100%, followed by dehydration in 100% anhydrous ethanol (Sigma-Aldrich, UK) 2x in 50min. The TEM samples were embedded in green coffin moulds in propylene oxide (VWR, UK): TAAB 812 (TAAB, UK) mixtures, followed by fresh resin (100% TAAB 812 resin) embedding and

polymerisation at 60ºC for 24 hours. Samples were sectioned into 70nm thick slices using a Reichert Ultracut E ultramicrotome, collected onto copper mesh grids and stained for 5 minutes in lead citrate. Samples were visualised on a JEOL JEM-1400 transmission electron microscope with an accelerating voltage of 100kV. Digital images were obtained by an EMSIS Xarosa digital camera with Radius software.

2.6.3 Immunofluorescence microscopy of ALI cultures

Fully differentiated ALI cultures were infected with *M. catarrhalis* or rhinovirus for selected times. Following infection, ALI cultures were fixed with 4% PFA for 20min at room temperature, and the fixative was then exchanged with PBS. Fixed cultures were kept at 4^0C and plates were sealed with parafilm until stained with specific antibodies. Staining procedure of ALI cultures was carried out in the inserts as previously described (Smith et al., 2014). Prior staining with antibodies, ALI cultures were permeabilised with 0.1% (v/v) Triton X (Sigma-Aldrich, UK) in PBS and non-specific binding was blocked with 3% (v/v) BSA (Sigma-Aldrich, UK) in PBS for 1h at room temperature with constant shaking at 150rpm (IKA Horizonal shaker 260, UK). Primary antibodies were prepared in 0.1% (v/v) triton X and 1% (v/v) BSA solution and diluted to a desired concentration according to manufacturer's instructions. Table 2-4 summarises all antibodies used. Primary antibodies were added apically in 50μl volume and incubated for 2-3h at room temperature with constant shaking at 150rpm. The antibodies were then washed 3 times to ensure non-bound antibodies were removed from the cultures. Secondary antibodies were prepared in 0.1% (v/v) triton X and 1% (v/v) BSA solution and diluted to a desired concentration recommended by suppliers' information. Secondary antibodies were added in 50μl apically to cultures and incubated at room temperature with constant shaking at 150rpm for 1.5h. Phalloidin staining was carried out for selected cultures for 1h at room temperature with constant shaking. The cultures were washed twice apically and Hoechst stain solution (Sigma-Aldrich, UK) was incubated on ALI cultures apically for 30min at room temperature, while constantly shaking. Unbound antibodies and dyes were removed by washing the cultures 3 times in the end of the procedure. To visualise stained epithelial cells, membranes were gently cut from their plastic holders and mounted onto glass slides with n-propyl gelate. The membranes were sealed with cover slips on top and stored at 4ºC until imaged.

Table 2-1: Immunofluorescence staining antibodies

Primary antibodies (Abs)	Originating species	Primary Ab working dilution	Secondary Abs	Secondary Ab working dilution
Human anti-β-tubulin (Abcam, ab15568)	rabbit	1:100	Anti-rabbit , Alexa Fluor 488 (abcam, ab150077)	1:1000
Acetylated α–tubulin (Sigma, T6793)	mouse	1:2000	Anti-mouse. AlexaFluor 594 (Invitrogen, A-11020)	1:250
Anti-VP2 rhinovirus (QED biosciences, 18758)	mouse	1:600	Anti-mouse, Alexafluor 647 (Abcam, Ab150103)	1:500
Anti-PI4P (Echelon Biosciences, Z-P004)	mouse	1:200	Anti-mouse AlexaFluor 488 (Ab150121)	1:200
Anti-*M. catarrhalis* (antibody sera sypplied by GSK)	mouse	1:500	Anti-mouse, Alexafluor 647 (Abcam, Ab150103)	1:500
Phalloidin (Abcam, Ab235138)	-	1:1000	-	-
Anti-VP2 rhinovirus (QED biosciences, 18758) conjugated to APC/ Cy7 using a conjugation kit (Ab102859)	mouse	1:600	10μg of rhinovirus antibody was conjugated by 10μl modifer in APC colour	-

2.7 Protein analysis and immunophenotyping

2.7.1 Preparation of samples for SDS-PAGE electrophoresis

Human primary epithelial cells from 2 replicate T24-well plate inserts were harvested by scraping. Protein samples were prepared by lysing the cells for 1h on ice with 30μl RIPA (Radioimmunoprecipitation assay) buffer (Merck, UK) containing a 1% (v/v) cocktail of protease inhibitors (Sigma-Aldrich, UK), and 1% (v/v) phosphatase cocktails inhibitors 2 and 3 (Sigma-Aldrich, UK). Samples were sonicated for 5min with intervals for cooling and then spun down at 10,500 x *g* for 5min to pellet cell debris. Protein amount was determined by using colorimetric BCA assay (bicioninick acid assay) (Pierce, ThermoFisher, UK). Briefly, samples diluted 1 in 10 in distilled water, were mixed with working reagents according to manufacturer's instructions and incubated for 30min at 37^0C. The absorbance from the reaction was read at 562nm by a spectrophotometer (FLUOstar Omega microplate reader, BMG, Labtech). The protein concentration of extracts was determined by plotting blank corrected absorbance values and standards' concentrations as a linear curve on Excel and using a relative linear equation:

Equation 5:

E.g. Y= 0.0003X + 0.0212

where y= absorbance and x= unknown concentration

Alternatively, protein concentrations were determined according to blanked absorbance values using a polynomial curve fit by the Omega Analysis software v4.3 (FLUOstar Omega BMG, Labtech).

For protein separations 10μg of samples were mixed with 5x laemmli buffer containing DTT (dithiothreitol, Sigma-Aldrich, UK) and boiled for 10min at 95^0C in a heating block (Bioport solutions); 10μl of sample/per lane were loaded per well onto a 12% polyacrylamide SDS gels (Bio-Rad, UK). SDS-PAGE was carried out in a Mini PROTEAN system (Bio-Rad, UK) in 1x running buffer at 140V using a Bio-Rad power pack (Bio-Rad, UK) until all molecular size proteins were separated.

2.7.2 Transfer of proteins to a polyvinylidene fluoride (PVDF) membrane

Protein samples were electro-blotted onto a solid support matrix *e.g.* a PVDF membrane (Millipore, UK) by creating a sandwich in a cassette (Saraswathy and Ramalingam 2011). The elecroblotting tank (Bio-Rad, UK) was filled with 1x transfer buffer and a cooler insert, to consume heat produced, and transfer of protein bands was carried out for 1h at constant 100V or at 4^0C overnight at 30V.

Following transfer of protein samples, the blot was blocked with 5% milk in PBS-Tween 20 (0.05%) or 5% BSA in TBS-Tween20 (0.1%) for 1h at room temperature to prevent nonspecific binding of antibody probes. Proteins were then complexed with a specific antibody against total EGFR (Cell signalling technologies, UK) / phospho EGFR (Cell signalling technologies, UK) / pan AKT (Cell signalling technologies, UK) / phospho AKT (Cell signalling technologies, UK) / DNAI2 (Invitrogen, UK) and/or GAPDH (Sigma-Aldrich, UK) in blocking buffer at 4^0C overnight on a roller shaker (manufacturer). To remove excess unbound antibody, blots were washed 4 x 5min in TBS-Tween20. To detect primary antibodies, blots were probed with appropriate detection HRP-linked (horseradish peroxidase) (Sigma-Aldrich, UK) antibody in blocking buffer for 1h at room temperature with constant shaking. Blots were finally washed 4 x 5min in 0.1% TBS-Tween 20 and stained with chemiluminescence – ECL (BioRad, UK) solution for 5 min to detect the position of the target protein and identify its abundance. Excess solution was drained onto tissue and PVDF membranes were placed into a cassette for imaging as described below (section 2.7.3).

2.7.3 Imaging the target proteins

Immuno-reactive protein bands of interest were detected by exposure of the blot to an X-ray film for 1min to 20min inside the cassette, in a dark room with a red lamp on. The film was then exposed in an audiograph machine (Amersham, UK). Proteins of interest were visualised as dark bands, the size of which was determined by laying over the blotted membrane with proteins. Alternatively, proteins of interest were visualised by a Chemi-Doc imaging machine (Bio-Rad, ImageLab software version 5.6), where protein bands were visualised by exposing PVDF membranes to UV light, and protein ladder was visualised by exposing the membrane to white light. Acquired images were saved as individual JPEG files.

2.7.4 Densitometry analysis of proteins of interest

Density and abundance of protein bands were determined by ImageJ software version 1.51j8 (National Institutes of Health, USA). JPEG images of western blots

were analysed by labelling each protein band as a separate lane of interest and plotting individual lanes as graph peaks. Area of peaks and percent values were automatically determined by the Image J software. To determine the abundance of the target proteins, percent values were normalised to relative GAPDH percent values or normalised first to relative GAPDH percent value and then to relative total protein percent value. The following equations were used to calculate the abundance of target proteins:

Equation 6:

$$\text{Relative expression of DNAI2} = \frac{\text{DNAI2 percent value}}{\text{GAPDH percent value}}$$

OR Equations 7, 8 and 9:

$$\text{Relative expression of phosphorylated AKT} = \frac{\text{phosphorylated AKT percent value}}{\text{GAPDH percent value}}$$

$$\text{Relative expression of total AKT} = \frac{\text{Total AKT percent value}}{\text{GAPDH percent value}}$$

$$\text{Normalised AKT expression} = \frac{\text{Relative expression of phosphorylated AKT}}{\text{Relative expression of total AKT}}$$

2.7.5 Flow cytometry to determine epithelial apoptosis following rhinovirus infection

Differentiated epithelial cells from healthy volunteers and COPD patients, infected with rhinovirus for 24h were washed once apically with 50μl of plain BEBM media, the wash was used for immediate subsequent analysis (see section 2.7.5.1). Basolateral fluid was removed, and epithelial cells were incubated apically and basolaterally with cell dissociation buffer (Life Technologies, California, US) for 15min at 37^0C with 5% CO_2. Epithelial cells were collected by gentle pipetting and resuspended in 10% FCS media to inactive the dissociation buffer and spun down at 5100 x *g* for 5min. UV zombie dye (live / dead stain) brilliant violet 405nm (BioLegend, UK) was diluted 1:500 in 1x Annexin V binding buffer (0.1M HEPES, 1.4M NaCl and 25mM $CaCl_2$) (BD Pharmingen, UK), diluted 1:10 in H_20. The cells were resuspended in 100μl of UV zombie dye for 15min at room temperature in the dark. The epithelial cells were then washed once in 1x Annexin V Binding Buffer, followed by the addition of 5μl of Annexin V dye FITC (BD Pharmingen, UK) for additional 15min, protected from direct light. Samples were washed twice in 1x Annexin V binding buffer, followed by fixation

with 1% paraformaldehyde (PFA) (Sigma-Aldrich, UK) for 20min at room temperature. Single stained samples were used for gating purpose. Samples were stored at 4^0C until processed on BD LSRII flow cytometer using BD FACS Diva software v8.0.1 (Becton Dickinson, New Jersey, US). All data were analysed in FlowJo v10 software (Treestar Inc, Oregon, US).

2.7.5.1 Detection of apoptosis in detached epithelial cells following rhinovirus infection

Apical washes from two 24-well inserts were combined and spun down at 5100 x *g* for 5min. Pellets were washed once in PBS and stained with 1:500 diluted UV zombie dye (BioLegend, UK), diluted in 1x Annexin V Binding Buffer (0.1M HEPES, 1.4M NaCl and 25mM $CaCl_2$) (BD Pharmingen, UK) for 15min at room temperature, protected from light. Samples were then washed once in 1x Annexin V Binding Buffer and stained with 5μl/sample Annexin V dye in a final volume of 100μl in 1x Annexin V Binding Buffer. Samples were incubated with Annexin V for 15min in the dark and washed once in 1x Annexin Binding Buffer. This was followed by fixation in 1% PFA for 20min at room temperature and an additional wash in PBS. Samples were resuspended in 50μl of 1x Annexin V Binding buffer and cytospun at 120 x *g* for 5min onto glass slides. The samples were mounted with N- propyl gelate (Sigma-Aldrich, UK) and a cover slip, and imaged using high magnification (100x objective) on a Nikon TiE Eclipse 100 microscope. 25 images per donor were acquired and a total of 4 healthy and 4 COPD donors were used for analysis.

2.8 Metabolic assay

2.8.1 Reactive oxygen species/ hydrogen peroxide (H_2O_2) detection in epithelial cells infected with *M. catarrhalis* and rhinovirus

To estimate the amount of hydrogen peroxide produced by differentiated epithelial cells infected with *M. catarrhalis* and rhinovirus, hydrogen peroxide (H_2O_2) substrate (Promega, USA), diluted 1:80 in dilution buffer (Promega, USA) to a final concentration of 25μM, was added apically in 50μl volume to non/infected epithelial cells. A H_2O_2 substrate solution was incubated with epithelial cells for the final 3h of the infection at 37^0C + 5% CO_2. Lyophilized lucifer detection reagent was resuspended in reconstitution buffer (Promega, USA) and prior use was enhanced with D-cysteine and signal enhancer solution at 1:100 dilution to produce the ROS-Glo detection solution. Then 50μl ROS-Glo detection solution was added to each well and incubated for 20min at room temperature, followed by 50μl of substrate and detection solution from each sample, containing produced reactive oxygen species, were then transferred in duplicates into 96 well white opaque plates. Luminescence was read by a FLUOstar Omega microplate reader (BMG Labtech, USA).

2.9 Epithelial inflammatory response to *M. catarrhalis* / rhinovirus pathogens

2.9.1 Luminex plex immuno-assays to measure cytokines IL-1β, IP-10/ CXCL10, IL-6, IL-8/ CXCL8, TNF-α, RANTES/ CCL5, MCP-1/ CCL2, ENA-78/ CXCL5, MIP-3α/ CCL20, GRO-α/ CXCL1, CSF-3/ GM-CSF, IL-15 in apical and basolateral fluids from differentiated airway epithelial cells

Pro-inflammatory IL-1β, IP-10/ CXCL10, IL-6, IL-8/ CXCL8, TNF-α, RANTES/ CCL5, MCP-1/ CCL2, ENA-78/ CXCL5, MIP-3α/ CCL20, GRO-α/ CXCL1, CSF-3/ GM-CSF, IL-15 were quantified by Luminex plexes (custom multiplex assay, Invitrogen, UK). The assay was performed according to manufacturer's instructions. The 96 well plates were coupled with antibody specific beads diluted 1:50 in wash buffer (Invitrogen) for 2 minutes and then washed twice with wash buffer while constantly placed on a Hand-held magnet plate washer. Luminex plexes were provided with lyophilized calibrated standards, prepared in a 4 fold serial dilutions and loaded onto 96 well microplates in duplicates. Then 50μl of neat apical and basolateral fluids or calibrators were incubated on microplate plates overnight at 4°C with constant shaking at 500rpm. After the incubation, samples and standards were removed and plates were washed

twice with wash buffer while placed on a Hand-held magnet plate washer. Detection antibodies provided at a 50x concentration were diluted in detection antibody diluent (Invitrogen) to a 1x and added to all wells for 30min at 500rpm at room temperature. The same washing step was repeated as described earlier and streptavidin – PE solution was added to all wells and incubated additionally for 30min on a plate shaker at 500rpm. The microplate was washed as before and reading buffer was added onto each well and incubated for 5min, shaking at 500rpm at room temperature. Plates were read by a Bio-Plex 3D Suspension Array instrument (Bio-Rad, UK). The concentration of the samples was calculated by plotting the expected standards concentration against their mean fluorescence intensity. Each analyte had a specific working range, entered in the software prior reading the plate. A best curve fit was generated by the BioPlex Manager Software v6.0 and samples concentrations were calculated.

2.9.2 Meso Scale Discovery (MSD) assays to measure IFN-α, IFN-β, IFN-λ, IFN-γ, IL-17c, TARC/ CCL17

The interferons IFN-α, IFN-β, IFN-λ, IFN-γ were quantified by U-plex plates and the pro-inflammatory cytokines IL-17c and TARC/ CCL17 were quantified by V-plex plates (MSD, UK). The multiplex assays were performed according to manufacturer's instructions. 10 spot U-plex and V-plex plates were coated with biotinylated antibodies, coupled with unique U-plex / V-plex linkers. The plates were coated overnight at 4^0C with constant shaking. Plates were washed 3 times with PBS+0.05% Tween-20. Calibrators, containing a range of recombinant proteins lyophilized in a buffer diluent were provided with the multiplex assay kit. The 5 fold dilutions of the stock calibrators were performed in Diluent 43 (MSD) to a final concentration 1x and 4-fold dilutions were prepared for the subsequent 6 calibrator dilutions. Calibration ranges were 10,000pg/ml to 0pg/ml and were loaded in duplicate in the 96 well plates. For U-plexes basolateral fluid samples were loaded neat and apical fluid samples were loaded at a 1:3 dilution in Diluent 43. For V-plexes basolateral fluid samples were loaded neat and apical fluid samples were loaded at a 1:4 dilution in Diluent 43. 25μl of samples or calibrators were loaded into the multiplex plates, which were sealed with adhesive foil and incubated overnight with constant shaking at 4^0C. Plates were washed 3 times with PBS+0.05% Tween 20. Stock concentration of SULFO-TAG detection antibody was diluted 100 times to a final concentration of 1x in Diluent 3 (MSD) and 50μl was added into each well. The plates were sealed again and the detection antibody was incubated at room temperature for 1h while shaking. The

plates were washed 3 times in PBS+0.05% Tween 20. 150μl/ well of 2x reading buffer (MSD) was added into each well and the plates were analysed immediately on a MSD plate reader Sector Imager 3000 (MSD, UK). Data were calculated by the Discovery Workbench software version 3.0 (MSD) by plotting the standard curves of calibrators and samples absorbance readings against the relevant standard curves.

2.9.3 Enzyme-linked ImmunoSorbent assay (ELISA) to quantify CXCL14 and IL-36g in apical and basolateral fluid samples

Specific antibodies to CXCL14/ BRAK and IL-36g (Thermofisher, UK) were coated on 96 well plates at 1μg/ml concentration in 100μl volume, diluted in PBS and incubated overnight with constant shaking at 4^0C. Coated plates were washed 3 times with PBS+0.05% Tween 20. Plates were blocked with reagent diluent, containing 10% bovine serum albumin (Thermofisher, UK) for 1h at room temperature, while placed on a shaker, followed by a wash step as described earlier. Human CXCL14/ IL-36g recombinant protein standards were diluted in reagent diluent (1% BSA in PBS) (Thermofisher, UK) in a 2 –fold manner from 4000pg/ml to 0pg/ml and 50μl from each standard concentration was added in duplicates in the plates. Apical fluid samples were diluted 1:8 in reagent diluent and basolateral fluid samples were added neat in 50μl in duplicates in 96 well strip plates. Samples/ standards were incubated overnight at 4^0C with constant shaking at 500rpm. This was followed by additional 3 washes with PBS+0.05% Tween 20. 100μl of specific CXCL14 / IL-36g detection antibody (Thermofisher, UK), diluted in reagent diluent to 250ng/ml concentration as to manufacturer's instructions was added to all wells for 2h while shaking at 500rpm at room temperature. The washing step was repeated and 100μl of working dilution of Streptavidin – HRP linked was added to the wells for 20min, while the plate was covered with aluminium foil adhesive to protect it from light. Then 100μl of substrate solution (1:1 mixture of H_2O_2 and Tetramethylbenzidine) (Thermofisher, UK) was added to the wells which were incubated for 20min in dark, until colour started developing in background wells. To stop the reaction, 50μl of Stop solution (2N H_2SO_4) (Thermofisher, UK) was added to all wells. Plates were read immediately in a plate reader SpectraMax i3 (Molecular Devices Corporation, USA) to determine the absorbance of the samples. Two readings were acquired per plate to correct for plate imperfections, at 450nm and 540nm. The 540nm readings were then subtracted from the 450nm optical density readings. Concentration of samples was determined by plotting standards' curves in GraphPad Prism software v7.0.

2.10 Statistical analyses

Statistical analyses were performed using the statistical programming language R (R-core team 2018), Version 3.5.1, with Dr Tanja Hoegg – principal statistician from the Research Statistics group at GSK Medicines Research Centre in Stevenage. The details of the statistical analyses vary according to the experimental design and the hypotheses for the specific studies. An overview of the statistical methods is summarised below.

2.10.1 Data pre-processing

For some studies, data from primary airway epithelial cells exhibited a positive relationship between the mean and the variance of measurements. Measurements were therefore log10 transformed, where necessary, prior to the statistical analysis to stabilize the variance and to ensure that the variability of measurements was of comparable size amongst all experimental conditions. The latter is a key assumption for most statistical modelling techniques. Additionally, log transformations can support interpretation of findings as changes in the endpoint are expressed as percent changes rather than unit changes. For experiments where measurements of zero were observed, a small constant of 1 was added to all measurements to enable the log transformation. Technical replicates were averaged prior to modelling, where available.

2.10.2 Statistical methods

2.10.2.1 Statistical modelling

For experiments involving different treatments or time points, data was pooled for all experimental conditions and relevant disease groups were analysed jointly using linear modelling techniques. All models included separate means (*e.g.* fixed effects) per experimental condition and disease group. For studies where only one observation per donor was collected, standard linear regression models were fitted. For studies where multiple observations per donor were collected, linear mixed effect models were applied. In addition to the fixed effects for treatment, time point and disease group, linear mixed effect models further included a random effect for each donor to acknowledge that the data are not independent but correlated within donors. All fitted models were visually assessed for violations of the underlying assumptions such as normality and equal variance of residuals and, if applicable, normality of the random effects.

For endpoints analysed on the log scale, differences between groups, time points or treatments are reported as relative changes from baseline, with a value of one corresponding to no change. For endpoints analysed on the original scale, differences between groups, time points or treatments are reported as absolute (*e.g.* unit) changes, with a value of zero corresponding to no change. Absolute and relative changes are accompanied by the lower and upper bounds of 95% confidence intervals and p-values for the test of no change in the endpoint. To reduce the chance of obtaining false positive findings, multiple comparison correction using the Benjamini-Hochberg (BH) method was applied to all p-values. The method controls the false discovery rate, meaning that if p-values below 5% are considered statistically significant, 5% of findings are expected to be false (Benjamini and Hochberg 1995).

2.10.2.2 Two-sample *t- tests*

For experiments involving only one experimental condition, differences between disease groups were compared using two-sample *t- tests* with the assumption of equal variances for both groups. Unadjusted p-values were provided for these results for the test of no difference between groups.

2.10.2.3 Paired t-tests

Paired t-tests were applied for experiments with only two experimental conditions where differences for each disease group were of interest. P-values for the test of no change between treatments are reported.

Table 2-2: Summary of analyses performed.

	Pre-processing		
Study	**Log transform**	**Replicates**	**Method**
Ciliary amplitude	yes	average	mixed model
Manual ciliary beat frequency	No	average	mixed model
Viability of single *M.cat* infection	yes	raw	mixed model
Viability single *M.cat* infection + inhibitor	yes	NA	mixed model
TEER of Healthy vs COPD	No	average	two-sample t-test
TEER folloing *M. cat* infection	No	average	paired t-test
TEER following *M. cat* infection + inhibitor	yes	average	mixed model
Phosphorylated protein expression following *M. cat* infection	yes	NA	mixed model
Total protein expression following *M. cat* infection	yes	NA	mixed model
Cytokines following *M. cat* infection	yes	NA	mixed model
CiliaFa Ciliary activity rhinovirus 24h post infection	yes	average	mixed model
CiliaFa Ciliary beat frequency following 24h *M. catarrhalis* infection	yes	average	mixed model

Titre of rhinovurus (apical/ intracellar) 24h post infection	yes	NA	Linear regression model
Titre of rhinovirus + inhibitor at 24h post infection	yes	NA	mixed model
CiliaFa ciliary beat frequency rhinovirus+inhibitor post 24h infection	No	yes	mixed model
ciliary activity rhinovirus 7 day post infection	No	yes	mixed model
Titre of rhinovirus 7 day post infection	yes	NA	mixed model
Protein expression 7 day post rhinovirus infection	yes	NA	mixed model
Apoptosis of ciliated cultures post rhinovirus infection	No	NA	paired t-tests
Comparisons of shed epithelial cells in apical secretions post rhinovirus infection	No	NA	paired t-tests
Cytokines post 24h rhinovirus infection	yes	NA	mixed model
CBF after 24h co-infection with *M. catarrhalis* and rhinovirus	No	average	mixed model
Ciliary acitivity after 24h co-infection with *M. catarrhalis* and rhinovirus	Yes	average	mixed model
Ciliary activity variability	No	average	mixed model
TEER of cultures after 24h co-infection with *M.*	No	average	mixed model

catarrhalis and rhinovirus			
M. catarrhalis viability post treatment with apical fluids	Yes	average	linear regression
M. catarrhalis viability post treatment with apical fluids obtained from rhinovirus infected cultures	Yes	average	mixed model
ROS after co-infection	yes	NA	mixed model
Co-infection study *M. catarrhalis* viability counts	yes	NA	mixed model
Cytokines after 24h co-infection with *M. catarrhalis* and rhinovirus	yes	NA	mixed model

Chapter 3. *Moraxella catarrhalis* interaction with healthy and COPD respiratory epithelium

3.1 Introduction

This research project aimed to investigate the initial interaction of *M. catarrhalis* with the ciliated epithelium. We chose to investigate the healthy ciliated epithelium and the COPD epithelium because *M. catarrhalis* is known to drive exacerbations in COPD patients. The underlying cellular and molecular mechanisms of *M. catarrhalis* infection and acute exacerbations have not been completely elucidated. Thus, using a number of individual donors allowed us to see the variation in response between healthy and COPD individuals.

Epithelial migration, proliferation, differentiation and extracellular matrix synthesis are promoted by epidermal growth factors (EGFR, EGF, TGF-α, betacellulin, heregulin, HER-2, HER-3) in the respiratory epithelium, however overexpression of these may lead to squamous metaplasia and mucous hyperplasia. The epidermal growth factor family expression has been shown to be higher in bronchial specimens from ex-smokers with COPD when compared to ones without COPD (de Boer et al., 2006), suggesting EGFR could be linked to remodelling of the airways. Further, EGFR expression has been confirmed to co-localize with mucous producing cells in bronchial biopsies from smokers with and without COPD (O'Donell et al., 2004). Even though EGFR is mainly expressed on basal and goblet cells in healthy, COPD and asthmatic airway epithelium (Takeyama et al., 2000; de Boer et al., 2006; Shaykhiev et al., 2013), its activation by cigarette smoke has been correlated with reduction of ciliation in human bronchial epithelial ciliated cultures (Valencia-Gattas et al., 2016). In addition to inducing changes in differentiation, EGFR has also been reported to disrupt epithelial cell junctions in organotypic cultures of primary bronchial epithelial cells and bronchial epithelial cell lines (Zhang et al., 2013; Petecchia et al., 2009) and to skew the fate of basal epithelial cells to a more squamous and epithelial mesenchymal transition (EMT) phenotype (Shaykhiev et al., 2013; Zuo et al., 2017).

There is increasing evidence that different bacteria are present in the lungs of COPD patients, when their condition is thought to be stable and during exacerbations, causing adverse effect on patients' lung function and overall health status (Sethi, 2004; Murphy et al., 2005; Garcha et al., 2012; Wang et al., 2016; Wang et al., 2018). Lately, *M. catarrhalis* has been recognised to trigger 10-15% of all COPD pulmonary

exacerbations, becoming the third most prevalent detected pathogen in COPD patients, behind *S. pneumoniae* and NTHI (Sethi, 2010; Ngo et al., 2016). *M. catarrhalis* exacerbations are often associated with the acquisition of a new strain of *M. catarrhalis*, with corresponding high levels of IL-8/ CXCL8, TNF-α and neutrophil elastase (Sethi et al., 2007).

M. catarrhalis has been found to initiate an inflammatory response in A549 pulmonary epithelial cells via TLR-2 and NOD-1 signalling (Slevogt et al., 2007). In addition, in BEAS-2B bronchial epithelial cells, *M. catarrhalis* stimulates the pro-inflammatory cytokines IL-8/ CXCL8 and GM-CSF/ CSF-3 via activation of the MAP kinases p38 and extracellular receptor kinase 1/2 (ERK1/2) (Slevogt et al., 2006). Isolated LOS (lipooligosaccharide) from *M. catarrhalis* is detected by a CD14-TLR4 complex, which was first identified in a monocytic cell line - THP-1 (Xie and Gu 2008) and later in murine macrophages (Hassan et al, 2012). The whole bacterium is detected by TLR-2, TLR-9 and TLR-4 receptors via MyD88 and TRIF signalling in murine macrophages (Hassan et al., 2012). This was supported by the strong activation of IFN-β and RANTES/ CCL5, both TRIF dependent (Hassan et al., 2012). As it is established that multiple TLRs are involved in *M. catarrhalis* triggered host inflammatory response, TLR-4 can also function in host defence to help clear *M. catarrhalis* at early time-points of infection *in vivo* (Hassan et al., 2012).

Further to these earlier findings, more recently *M. catarrhalis* has been found to enhance host inflammatory responses by stimulating EGFR (N'Guessan et al., 2014). *M. catarrhalis* can activate EGFR in a time-dependant manner in BEAS-2B bronchial epithelial cells where pro-inflammatory cytokines release is dependent on ERK and NF-kB signalling (N'Guessan et al., 2014). As the direct binding of *M. catarrhalis* to EGFR seems unlikely, several TLRs *e.g.* TLR-1/2, 3, 5 and 6 have been reported to trans-activate EGFR via a complex signalling cascade which involves TGF-α, a protein that directly binds EGFR, the metalloprotease-TNF-α converting enzyme (TACE), dual oxidase-1 (DUOX-1) and ROS (Koff et al., 2008). In addition to signalling via TLRs, *M. catarrhalis* has been found to also induce PI3K signalling (Slevogt et al., 2007). Activation of TLR-2 receptors of respiratory epithelial cells results in recruitment of p85a subunit of PI3K which mediates the activation of NF-kB transcription factor, responsible for the release of pro-inflammatory cytokines (Slevogt et al., 2007).

M. catarrhalis is a pathogen that can successfully escape the immune system via UspA1 binding to CEACAM1 receptors present on airway epithelia and suppressing

TLR-2 triggered NF-kB dependent cellular activation (Slevogt et al., 2008). The binding of UspA1 – *M. catarrhalis* outer membrane protein to CEACAM-1 receptor results in enhanced activation of tyrosine residues of the cytoplasmic ITIM domain, which in turn activates the Src-homology 2 domain – the cytoplasmic protein tyrosine phosphatase (SHP-1). SHP-1 inhibits p85a phosphorylation and ultimately the PI3K - Akt - NF-kB signal transduction and the pro-inflammatory release of cytokines (Slevogt et al., 2008). Thus, *M. catarrhalis* can counteract TLR-2 induced immune responses in the airway epithelium, which involves pathogen sensing and pro-inflammatory cytokine release that can recruit immune cells to the site of infection (Slevogt et al., 2008; Tekuchi and Akira, 2010). These findings suggest a mechanism by which *M. catarrhalis* is capable to colonise the respiratory epithelium without causing inflammation (Slevogt et al., 2008).

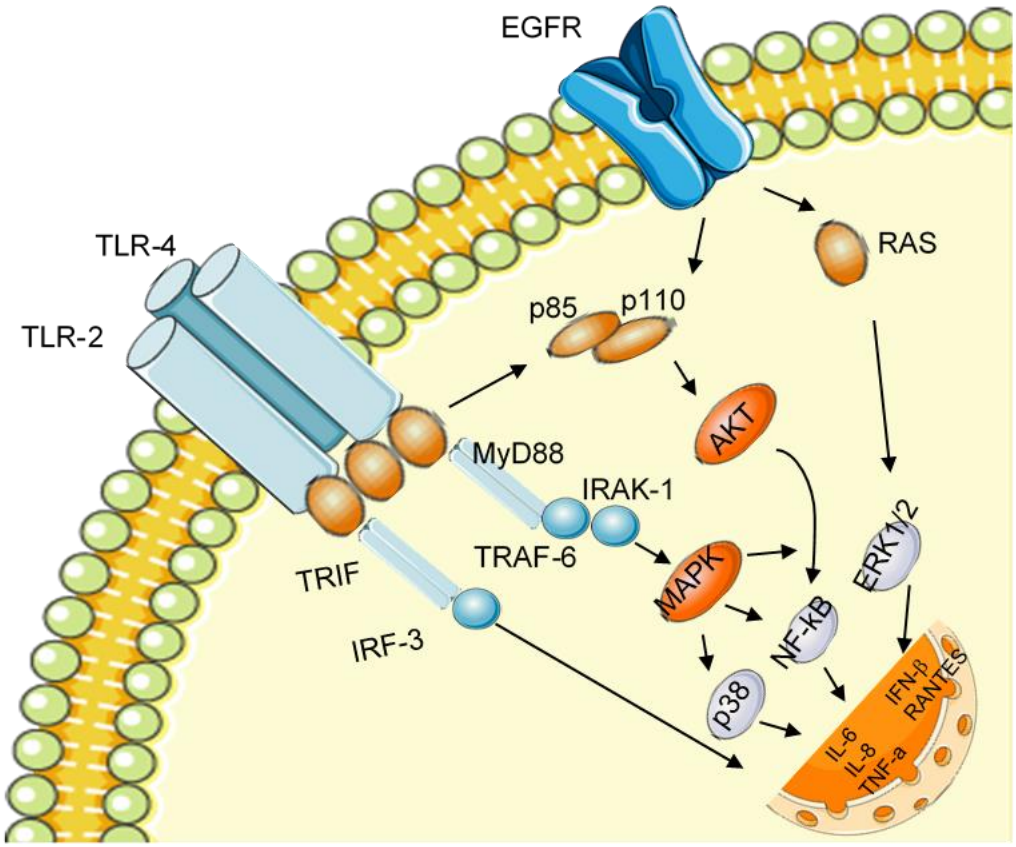

Figure 3-1: Schematic drawing of proposed inflammatory response to *M. catarrhalis* in respiratory epithelial cells *(original figure)***.**

Once *M. catarrhalis* is detected by TLRs, the MyD88 and TRIF adapter proteins are activated to further phosphorylate IL-1 receptor to IR-1R associated protein kinase (IRAK-1), tumour necrosis factor (TNF) receptor – associated factor 6 (TRAF-6) and mitogen activated protein kinase (MAPK) and extracellular receptor kinase (ERK), p38 and transcription factor NF-kB or interferon regulatory factor (IRF)-3 respectively which initiate the production of pro-inflammatory cytokines/chemokines in the nucleus. EGFR activation can stimulate the downstream ERK1/2 which can stimulate the release of inflammatory cytokines. TLR and EGFR activation can induce PI3K (p85 and p110) pathway signalling and AKT phosphorylation leading to NF-kB translocation to the nucleus where it stimulates the production of a range of cytokines and chemokines.

Up to date studies show *M. catarrhalis* adapts morphologically (Augustyniak et al., 2018; Blakeway et al., 2018; Murphy et al., 2017) to colonise the respiratory tract and cause a disease, but still very little is known about the host – pathogen interaction and the associated inflammatory response. In order to further the knowledge of early *M. catarrhalis* infection, this study aims to assess the changes of *M. catarrhalis* infection in primary epithelial cells from healthy and COPD individuals.

3.1.1 Hypothesis

M. catarrhalis preferentially adheres and invades airway differentiated cells from COPD donors compared to airway differentiated cells from healthy donors, initiating greater ciliary dysfunction and inflammatory state in these cultures.

3.1.2 Aims

1. To investigate the early initial stages of adherence of *M. catarrhalis* to respiratory ciliated cells and to assess the epithelial ciliary function of epithelial cultures.

2. To investigate the mechanism of internalisation of *M. catarrhalis* inside epithelial cells and the associated epithelial signalling.

3. To investigate the role of an EGFR inhibitor (Gefitinib) and PI3K pathway inhibitor (GSK987740) on reducing *M. catarrhalis* internalisation of epithelial cells.

4. To determine if *M. catarrhalis* infection of ciliated cultures changes the cytokine response in differentiated cells from COPD donors compared to differentiated cells from healthy donors.

3.1.3 Characteristics of patients

A total of 30 airway samples were collected in the period between January 2016 and January 2019 from 14 Healthy volunteers and 13 COPD patients, 2 COPD donors' samples have been excluded from research because of pre-existing microbial contamination. Upon collection of samples healthy volunteers reported a 3 week period free of respiratory cold symptoms. COPD patients were admitted to either of the hospitals (The Royal Free Hospital/ University College London Hospital/ University Hospitals Leicester / Papworth Lung and Transplantation Centre) where nasal and/ or bronchial airway swabs were collected. All of the participants in the study have given written consent for nasal/ bronchial samples to be used for research activities. The table below summarises the clinical characteristics of the donors

included in this study. Individual patients' details are included in Supplementary Table 1 in Appendix 1.

Table 3-1: Clinical characteristics of patients.

13 healthy volunteers and 10 COPD patients whose samples have been included in the study of *M. catarrhalis* interaction with the respiratory epithelium, data are presented as mean ± SEM or % except FEV_1 which is expressed as median ± interquartile range.

Clinical characteristics	Healthy	COPD
Age (years)	58.44 ±1.938	72.84 ±2.376
Gender (Male)	35%	50%
Exacerbations <2/last year	0	80%
Current smoker	0	22%
Chronic bronchitis	-	77%
FEV_1 (L)	-	1.25±0.73
FEV_1 (%)	-	46.67±5.24
FVC (L)	-	2.55±0.24
FVC (%)	-	79±6.61
FEV_1/FVC ratio	-	0.52±0.043

3.1.4 Nasal and bronchial primary cultures

All experiments in chapter 3 were carried out with nasal differentiated epithelial cells except the following experiments, which used bronchial differentiated epithelial cells.

Table 3-2: Human bronchial epithelial cultures used in *M. catarrhalis* single studies.

Group	Experiment	Assay	Figure
COPD	Adherence of *M. catarrhalis* to the ciliated epithelium	Live confocal imaging	3-3 A and B
COPD	Adherence of *M. catarrhalis* to the ciliated epithelium	Scanning Electron Microscopy	3-3 E and F

3.2 Results

3.2.1 Differentiation of airway epithelial cells at the air-liquid interface

Human nasal and bronchial epithelial cells were expanded in growth factors enriched co-culture media and differentiated at air-liquid interface to induce a ciliated epithelium resembling that found in the airways (Hirst et al., 2010). After seeding, the epithelium was composed of undifferentiated cells which attached to the inserts for a maximum of two days. The cells proliferated rapidly and various phases of growth were visually observed. At days 0 to 7 the cells formed a layer which became multi-layered in days 7 to 14. During this period, some microscopically darker areas of probably more stratified areas of cells were observed. At day 14 appearance of differentiated cells was apparent as short twitching cilia were detected. Mature cilia were visualised in days 21-28. Number of ciliated cells increased progressively over week 5 as patches of ciliated cells were identified after day 30.

Different donors showed different phenotypes in culture. For example, cells from healthy donors produced an apical layer of fluid during the first 2 weeks of differentiation whereas cells from some of the COPD donors consistently developed a layer of mucus secretion, which was removed regularly by washing the apical site of the cultures. These characteristics were consistently observed in 5 healthy donors passaged 4-5 times in co-culture and 4 COPD donors passaged 4 times in co-culture. ALI cultures were always used in experiments after full differentiation and assessment of ciliary activity and epithelial layer integrity. Figure 3-2 shows the surface layer of airway differentiated cultures of healthy (Figure 3-2 A) and COPD (Figure 3-2 B) donors imaged by confocal microscopy. Prior to experiments the differentiated epithelium was observed to have motile cilia that were seen to beat in a similar direction from cell to cell, using high speed video microscopy (Figure 3-2 C). Ciliated cultures from healthy donors had a TEER mean±SEM: 891 ± 90 Ω/cm^2 and ciliated cultures from COPD donors had a TEER 841 ± 105 Ω/cm^2 (Figure 3-2 D). The readings were obtained from 6 healthy donors (2 individual measurements/ donor) and 6 COPD donors (2 individual measurements/ donor).

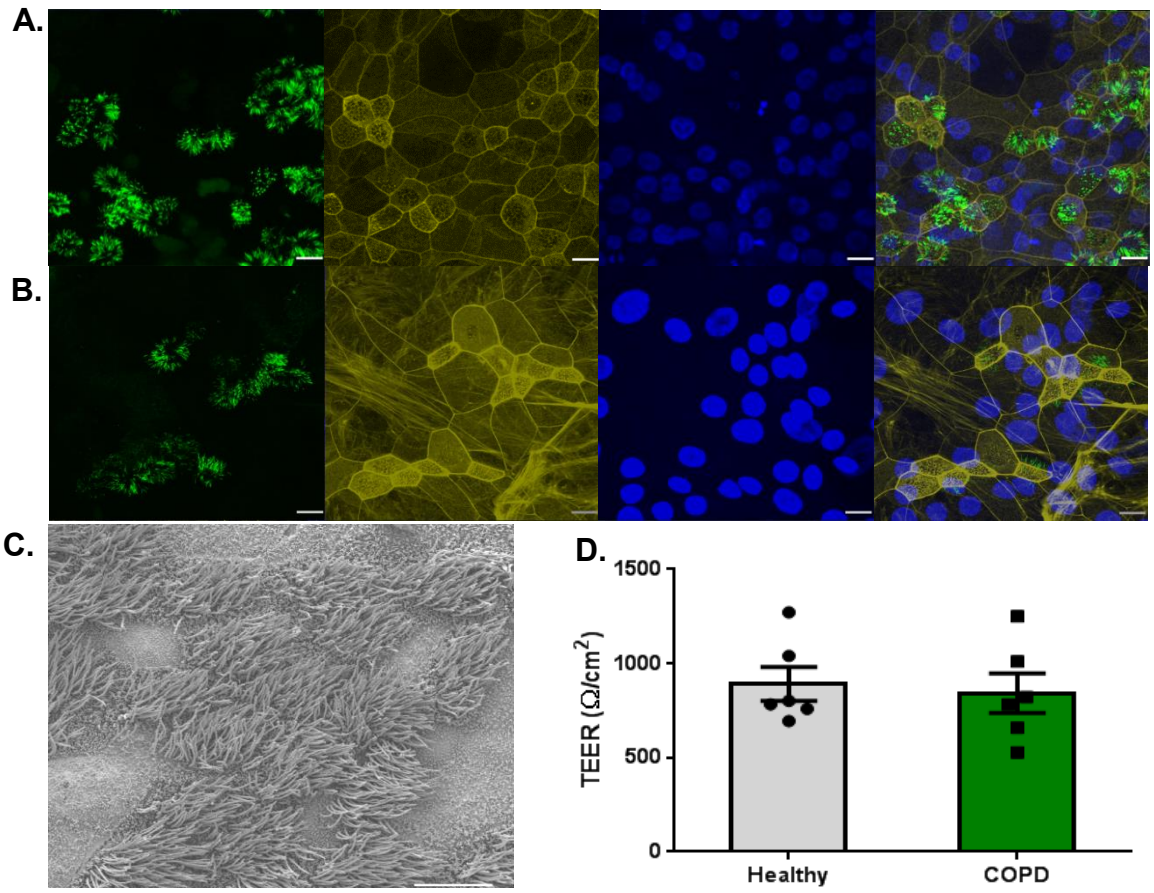

Figure 3-2: Expansion and differentiation of epithelial cultures from healthy and COPD donors.

A) Immunofluorescence image of differentiated primary healthy cells, scale bar = 17μM; B) Immunofluorescence image of differentiated primary COPD cells, scale bar = 17μM, A and B are stained for β-tubulin in green, showing cilia, phalloidin in yellow, showing F-actin and Hoechst solution in blue, showing nuclei. C) Scanning electron micrograph of a ciliated culture from a healthy donor, scale bar= 20μM. D) Integrity of epithelial cultures post 28 days of differentiation as measured by TEER, n=6 for both groups, error bars represent ±SEM

3.2.2 Adherence of *M. catarrhalis* to the respiratory epithelium

In order to assess the initial interaction of *M. catarrhalis* with the respiratory epithelium live confocal imaging was carried out to observe the process more closely (Figure 3-3 A and B). Addition of *M. catarrhalis* to primary nasal and bronchial differentiated cells was associated with instant binding to the tips of rapidly beating cilia (Supplementary Video 1 and 2 in Appendix 5, provided on an external hard drive). Short (20 sec) and

long (1min 40sec) videos demonstrated green fluorescent *M. catarrhalis* preferential binding to the cilia of epithelial cultures from a COPD donor (Figure 3-3 A and B screenshots of bacterial binding areas). Within seconds live individual *M. catarrhalis* and small aggregates adhered to the beating cilia (Figure 3-3 A, Supplementary Video 1 in Appendix 5, external hard drive). The binding gradually increased over time. *M. catarrhalis* adherence pattern was similar in ciliated cultures from both healthy and COPD subjects with individual bacteria binding and 'attracting' more to attach. Within 15 min of incubation, green fluorescent bacteria covered the ALI cultures, building aggregates on top of beating cilia (Figure 3-3 B, Supplementary Video 2, Appendix 5, external hard drive). High speed video microscopy enabled direct visualisation of the bacteria and of the number of ciliated cells that bacteria were bound to. A mean ±SEM of 27.3% ± 4.81% of all the ciliated cells observed in the pre-selected viewing areas of the cultures had *M. catarrhalis* bound to them within the first 15 minutes of infection (Table 3-2).

3.2.3 Scanning Electron Microscopy of adhered *M. catarrhalis* to the respiratory epithelium

To help characterise the interaction between live and heat inactivated (65^0C for 30min) *M. catarrhalis* and the epithelial cells, scanning electron microscopy of healthy nasal and bronchial cultures was processed as described previously (chapter 2, section 2.6.1). Electron microscopy of the infected cultures demonstrated *M. catarrhalis* tightly associated with cilia (Figure 3-3 C-F). Infection with live *M. catarrhalis* at 12h and 24h demonstrated the presence of multicellular grape-like aggregates adhered to the underlying cilia (Figure 3-3 C-E). Scanning electron micrographs at 12h (Figure 3-3 C-D) revealed the majority of *M. catarrhalis* were attached as clusters to cilia. Figure 3-3 D shows a strand between bacterial aggregates and an individual bacterial cell, suggesting a formation of a biofilm is occurring. At 24h of infection, aggregates of *M. catarrhalis* were seen as a biofilm attached to the cilia of airway epithelial cells (Figure 3-3 E). Aggregates associated with cilia were not seen with heat inactivated bacteria. Infection with heat inactivated *M. catarrhalis* at 24h showed individual bacteria attached to cilia (Figure 3-3 F).

Table 3-3: Adherence of *M. Catarrhalis* to cilia.

Total ciliated cells viewed in 5 areas and the number and percentage of ciliated cells with bacteria bound at 15 minutes are shown. Results from 6 cultures from healthy individuals, 6 cultures from COPD individuals.

Donor	Ciliated cells #/ 5 areas	# Ciliated cells with bound *M. catarrhalis* (%)
Healthy 1	199	49 (24.6%)
Healthy 2	67	13 (19.4%)
Healthy 3	84	9 (10.7%)
Healthy 4	154	52 (33.7%)
Healthy 5	28	10 (35.7%)
Healthy 6	23	12 (52.1%)
COPD 1	54	21 (33.7%)
COPD 2	123	31 (25.2%)
COPD 3	136	24 (17.6%)
COPD 4	74	24 (32.4%)
COPD 5	39	10 (25.6%)
COPD 6	25	19 (76%)
Total	1000	273 (27.3%)

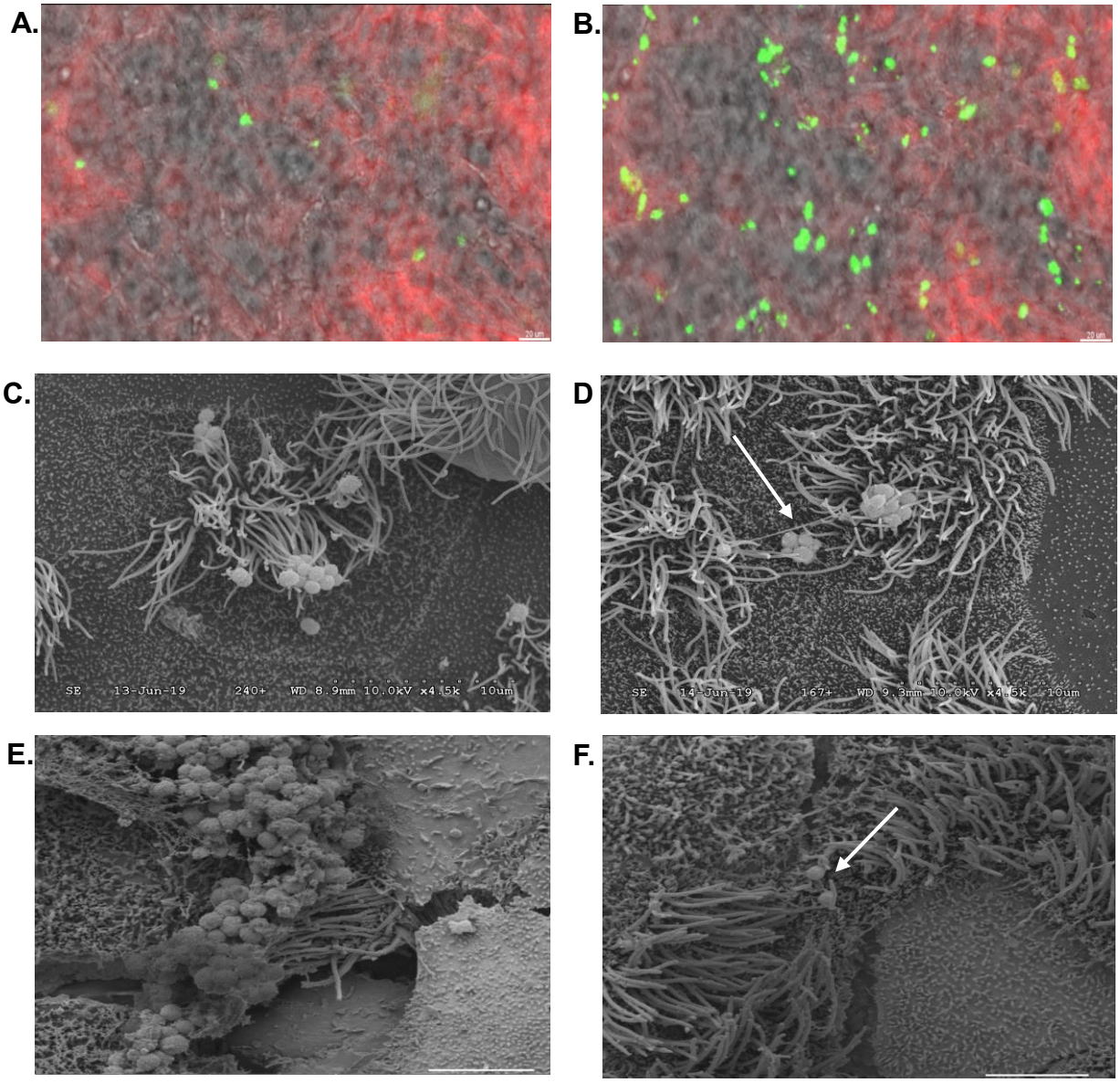

Figure 3-3: *M. catarrhalis* infected nasal and bronchial differentiated cultures.

A) A screenshot from live confocal video of COPD respiratory bronchial ciliated cells (labelled with CellMask™ Deep Red Plasma membrane Stain to highlight the plasma membrane, one focal plane) infected with $5x10^6$ *M. catarrhalis* (labelled with CellTrace™ CFSE Green) within seconds of addition and B) 15 minutes post addition of bacteria, scale bars =20μM; Electron micrographs of *M. catarrhalis* on ciliated respiratory cells C) Nasal epithelial cells from healthy donors associated with *M. catarrhalis* at 12h post infection, scale bar = 10μM; D) Nasal epithelial cells from COPD donors associated with *M. catarrhalis* at 12h post infection; white arrow pointing at a strand connecting bacteria, scale bar = 10μM; E) COPD bronchial epithelial cells associated with *M. catarrhalis* at 24h, scale bar = 5μM, F) COPD bronchial epithelial cells associated with heat inactivated *M. catarrhalis* showing individual bacteria (white arrow) scale bar = 5μM.

Scanning electron microscopy allowed closer examination of the interaction between bacteria and cilia at 12h post infection. The bacteria occurred predominantly as small aggregates or individual bacteria attached to the sides of the tips of multiple cilia from the same cell (Figure 3-4 A-D). The phenomenon occurred in both healthy (Figure Figure 3-4 A-B) and COPD (Figure 3-4 C-D) donor cultures. Figure 3-4 C-D shows cilia bound to *M. catarrhalis* at the side of the tip of the cilia. Even when bacteria appeared to be associated with the surface of non-ciliated cells, closer inspection revealed that they were also attached to the tips of cilia (Figure 3-4 E).

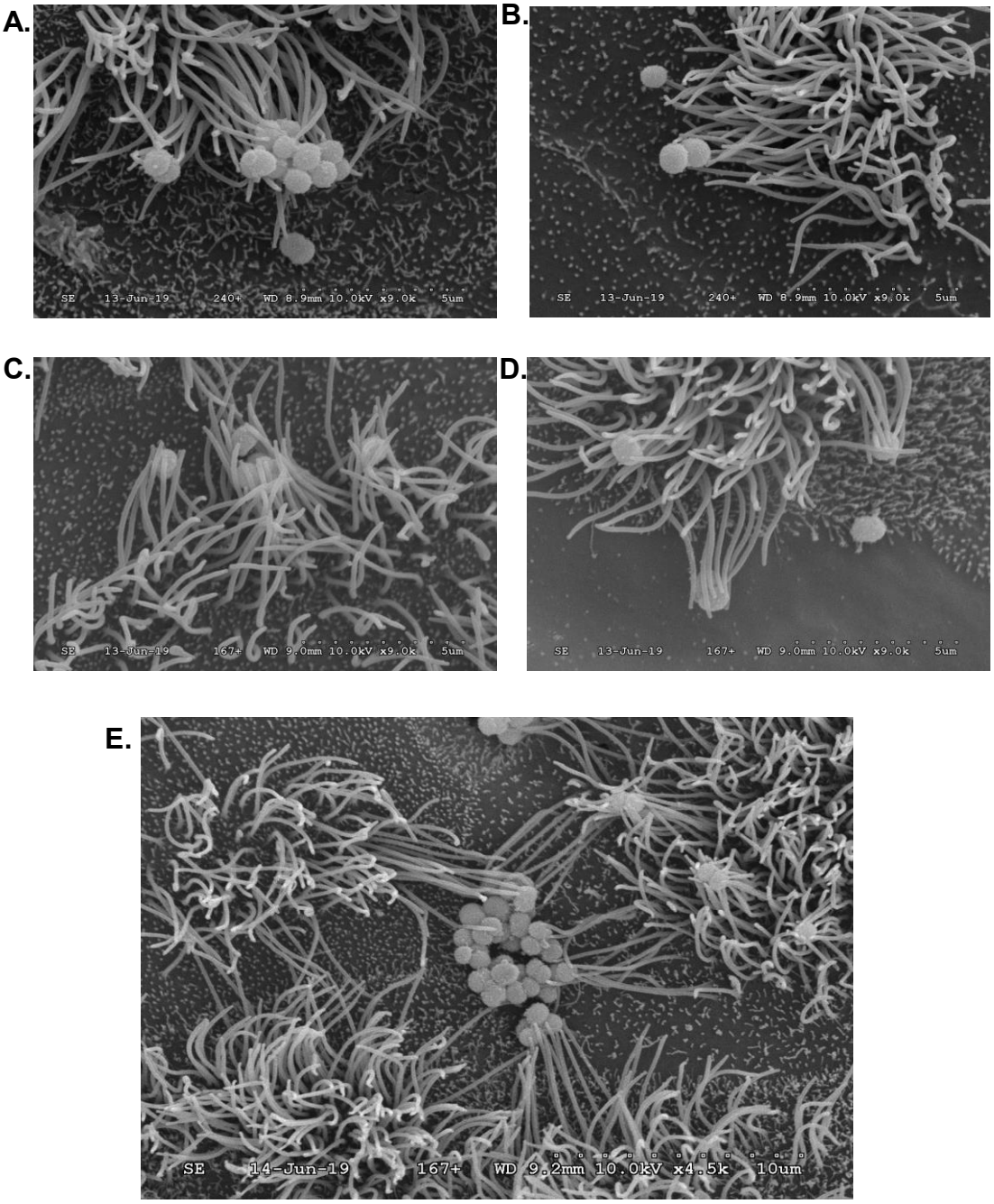

Figure 3-4: Scanning electron micrographs of nasal differentiated cultures infected with *M. catarrhalis* at 12h.

A-B) Electron micrographs of *M. catarrhalis* attached to the sides of the tips of cilia of healthy respiratory cells; C-D) Electron micrographs of *M. catarrhalis* attached to the sides of the tips of cilia of COPD respiratory cells, scale bars = 5μM; E) *M. catarrhalis* aggregates associated with the apical surface of non-ciliated COPD nasal respiratory cells. The aggregate also shows binding to cilia from adjacent cells 12h post infection, scale bar = 10μM.

3.2.4 Ciliary function of epithelial cultures following *M. catarrhalis* infection

To assess whether *M. catarrhalis* affects the ciliary function of epithelial cultures upon binding, ciliary beat frequency (CBF) and ciliary beat amplitude (CBA) were measured manually using high speed videos of epithelial cultures recorded during infection using methodologies described previously (Hirst et al., 2010). This allowed comparison of the ciliary function of a non-infected epithelial culture and the ciliary function of an infected culture, where cilia from the same culture did or did not have *M. catarrhalis* bound to them.

Because of the rapid interaction of *M. catarrhalis* with the respiratory cilia, CBF of differentiated cultures from 6 healthy and 6 COPD donors was measured immediately after addition of bacteria at 15 minutes and 24h later. There was a non-significant reduction of CBF of cilia with *M. catarrhalis* bound to them at 15 minutes ($p=0.39$, healthy and $p=0.39$, COPD) or at 24h ($p=0.92$, healthy and $p=0.99$, COPD) when compared to non-infected cultures. There was also a non-significant reduction of CBF of infected cultures after addition of *M. catarrhalis* compared to non-infected cultures (Figure 3-5 A - D) where there was no binding to cilia observed at 15 minutes ($p=0.39$, healthy and $p=0.99$, COPD) or at 24h ($p=0.58$, healthy and $p=0.39$, COPD).

The interaction of airway epithelial cells with *M. catarrhalis* resulted in a significant decrease of CBA in cultures from both healthy and COPD donors. In cultures from healthy donors, CBA was significantly reduced ($p=0.03$) at 15 minutes when *M. catarrhalis* was bound on top of cilia compared to the amplitude of non-infected cells (Figure 3-5 E). In cultures from COPD donors *M. catarrhalis* significantly reduced the amplitude of cilia where bacteria are bound compared to infected cells with no bound bacteria ($p<0.001$) or non-infected cultures ($p<0.0001$) (Figure 3-5 F). There were no significant differences between the healthy and COPD groups.

At 24h, binding of *M. catarrhalis* to the cilia of cultures from healthy donors significantly reduced their amplitude compared to non-infected cells ($p=0.007$) (Figure 3-5 G). In ciliated cells from COPD donors (Figure 3-5 H), *M. catarrhalis* binding at 24h decreased ciliary amplitude of ciliated cells with bound bacteria by 55% compared to non-infected cells' amplitude ($p<0.0001$). Amplitude of infected with *M. catarrhalis* cells with no bound bacteria was also significantly reduced compared to non-infected cells ($p=0.04$). There was also a significant decrease of ciliary amplitude between infected ciliated cells with and without bacteria bound ($p=0.002$). No significant changes between the healthy and COPD groups were observed at 24h post infection. Ciliary amplitude of infected cells from COPD donors with no bound bacteria was

decreased at 24h compared to 15 minutes, but statistical significance was not reached following Benjamini - Hochberg correction for multiple comparisons (p=0.1).

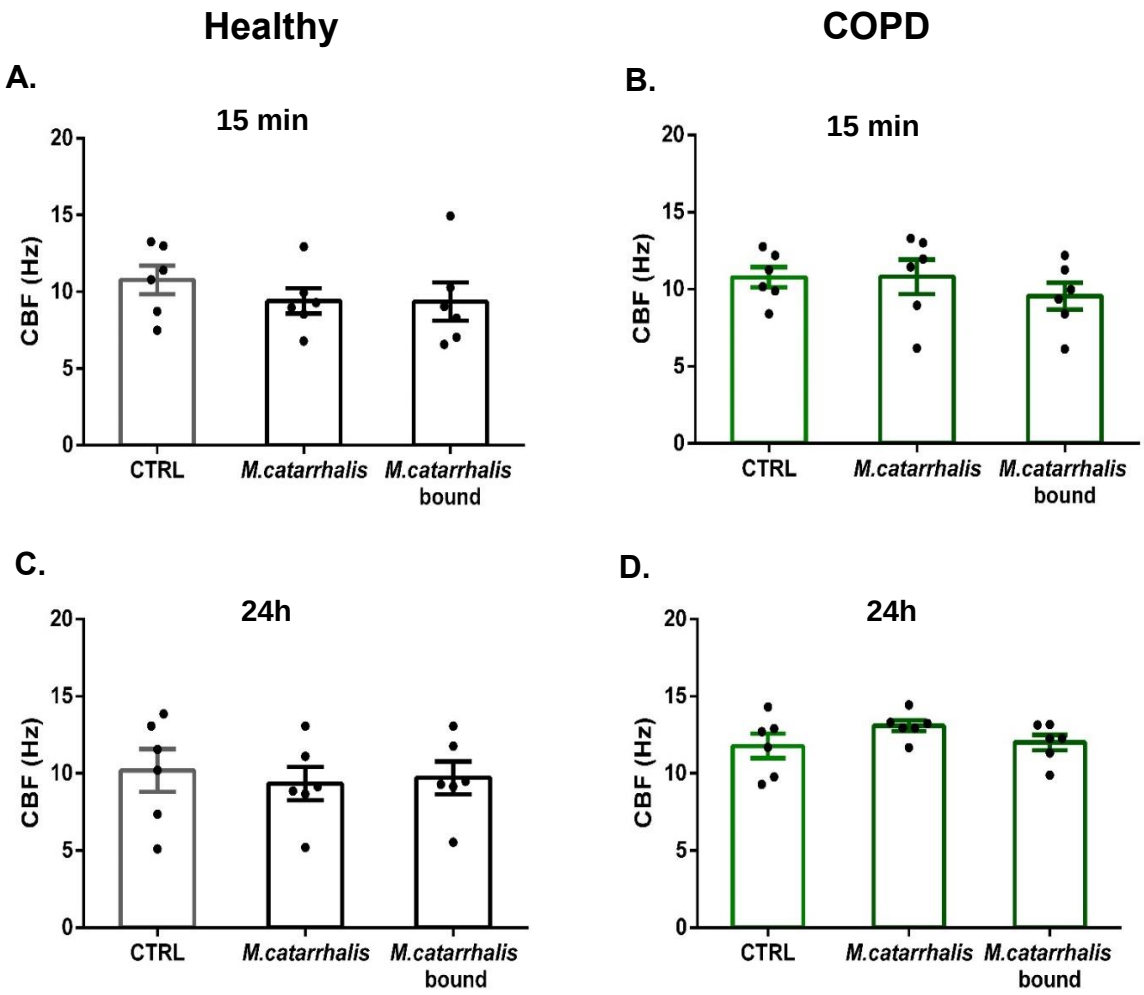

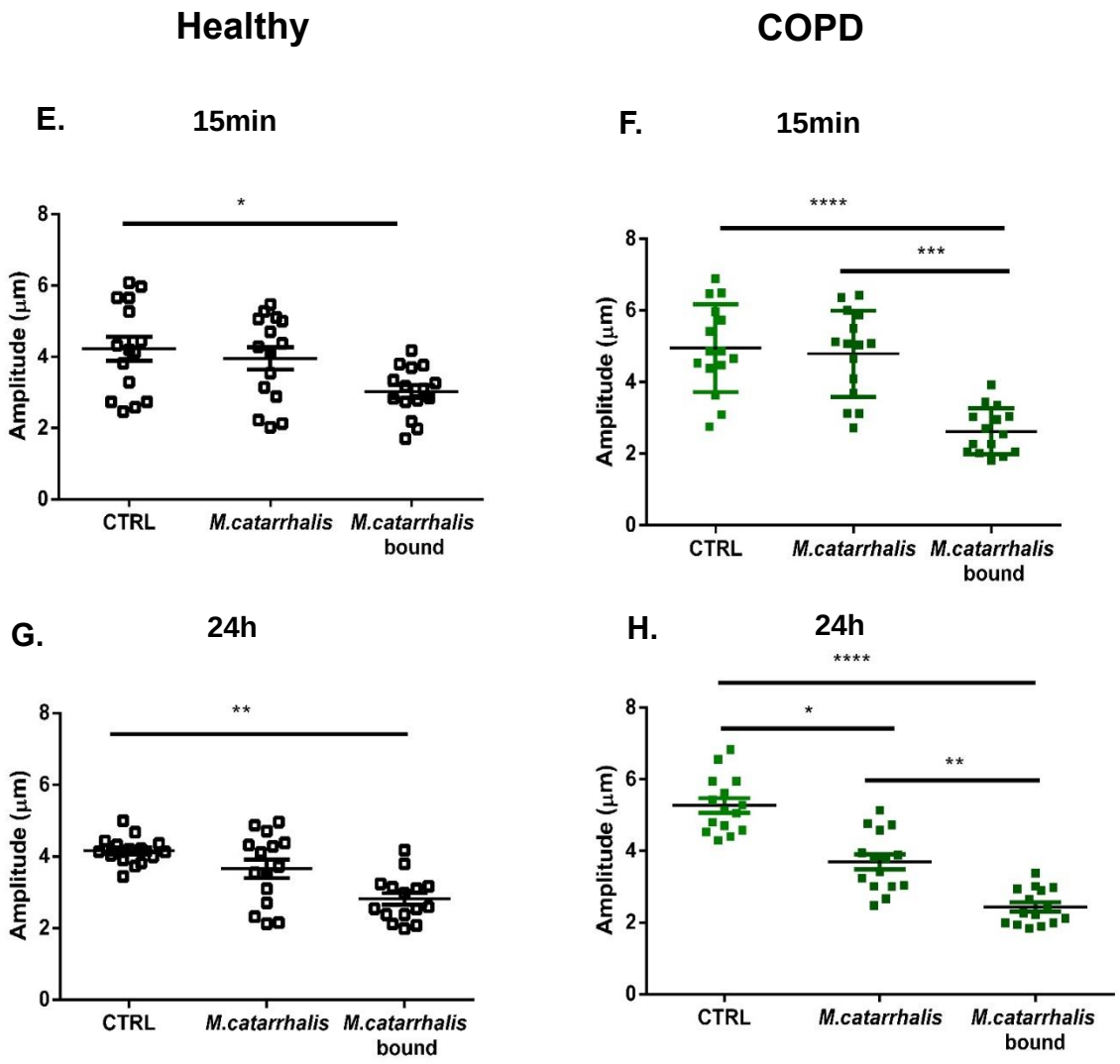

Figure 3-5: *M. catarrhalis* initial interaction with differentiated healthy and COPD nasal epithelial cells reduced their ciliary function.

CBF of epithelial cultures post infection (Figure 3-5 A-D). Results of ciliated cultures from A) healthy and B) COPD donors at 15minutes, analysed by manual counting. Results of ciliated cultures from C) healthy and D) COPD donors at 24h, analysed by manual counting, 6 healthy cultures, 6 COPD cultures, n=5 areas/culture. CBA (Figure 3-5 E-H) of ciliated cultures from E) healthy and F) COPD donors at 15min post infection, analysed by manual counting and results of ciliated cultures from G) healthy and H) COPD donors at 24h post infection, analysed by manual counting, 3 healthy, 3 COPD donors, n=5 areas/culture, error bars represent ±SEM, *=p<0.05, **=p<0.01, ***=p<0.001, ****=p<0.0001. CBF – ciliary beat frequency; CBA- ciliary beat amplitude

3.2.5 Bacterial growth in ALI cultures

To examine the viability of *M. catarrhalis* in ciliated cultures from healthy and COPD donors and to determine if it differs between the groups, viability CFU-based counts were performed at the end of the experiment (24h post infection). The bacterial colonies from the counts appeared grey-white and round, the colonies usually remained intact if pushed across the blood agar plate surface which is consistent with the bacteria being *M. catarrhalis* (Verduin et al., 2002). Each plate of bacterial colonies was examined closely and no signs of bacterial contamination were observed and no other bacteria other than *M. catarrhalis* were detected at the time of counting colonies or 2 days later when plates were sealed with parafilm and kept in a box at room temperature.

Viability of *M. catarrhalis* was measured from the apical washes of epithelial cultures collected at 24h post infection. Apical washes contained bacteria that were non-adhered to epithelial cells, loosely bound or mucous bound. When comparing bacterial viability between healthy and COPD groups (Figure 3-6 A), *M. catarrhalis* survival in epithelial cells from COPD donors seemed to be greater than in cultures from healthy donors, but the difference failed to reach statistical significance ($p=0.36$). Following washing of the cultures remaining bacteria were regarded as adhered to the ciliated cultures or internalised in cultured cells. The cultures were then trypsinised and sample suspensions, representing bound and internalised bacteria were plated on blood agar plates. CFU-based counts consistently indicated increased numbers of *M. catarrhalis* in ciliated cultures from COPD donors, which were significantly higher than in ciliated cultures from healthy donors ($p<0.01$) (Figure 3-6 B). Invasion of epithelial cultures by *M. catarrhalis* was assessed by an antibiotic-killing assay that killed extracellular bacteria (Slevogt et al., 2007). Although the results suggested that higher counts of intracellular bacteria were observed in ciliated cultures from COPD subjects, this just failed to reach a statistical significance ($p=0.053$) (Figure 3-6 C).

The barrier integrity of epithelial cultures infected with *M. catarrhalis* was monitored by TEER and was measured at 24h post infection. In ciliated cultures from both healthy and COPD donors, *M. catarrhalis* did not change the integrity of the differentiated cultures, compared to relative non-infected controls (Figure 3-6 D).

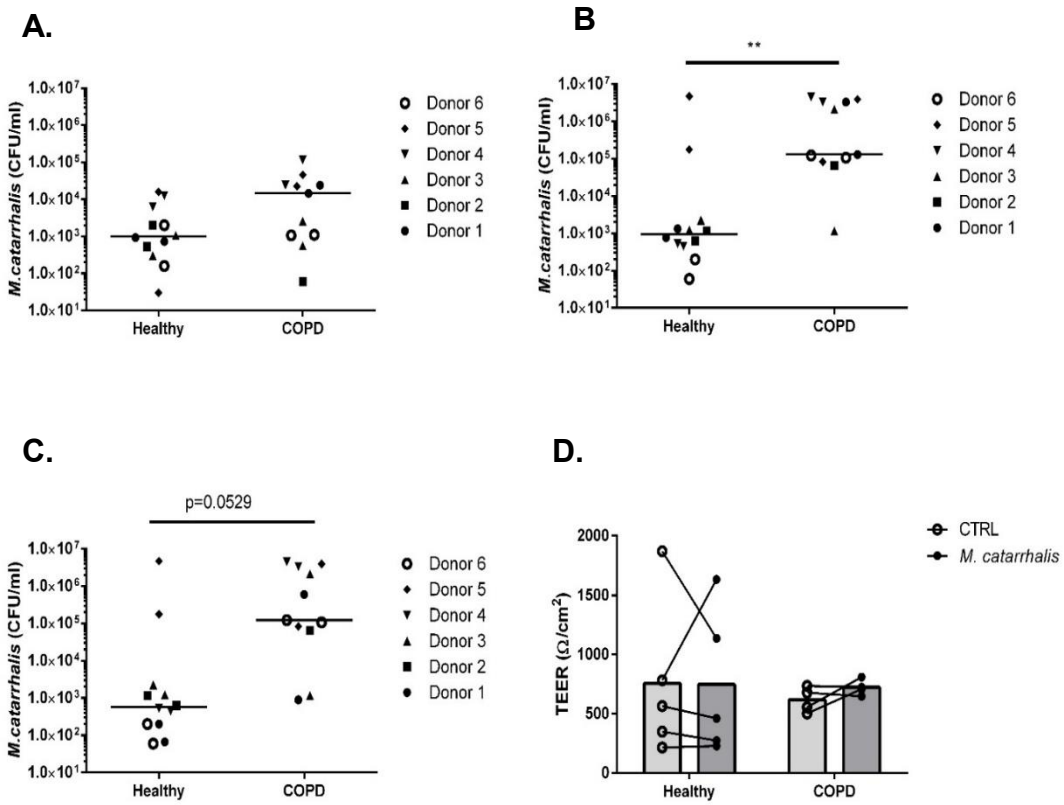

Figure 3-6: *M. catarrhalis* viability in differentiated nasal epithelial cells from healthy and COPD donors at 24h post infection.

Results from A) non-adhered, loosely bound or mucous bound bacteria collected from the apical site of cultures from healthy and COPD subjects; B) adhered to epithelial cells and intracellular bacteria in cultures from healthy and COPD donors **=p<0.01; C) Intracellular bacteria in cultures from healthy and COPD donors, 6 healthy and 6 COPD donors, n=2 replicate viability values/ donor; D) Integrity of epithelial cultures non-infected and infected with *M. catarrhalis* at 24h, 5 healthy, 4 COPD donors, dots represent means of replicate readings obtained from a TEER machine.

3.2.6 Intracellular bacteria in the respiratory epithelium

To confirm the presence of intracellular bacteria, epithelial cultures were immunofluorescently labelled with specific antibodies and imaged by confocal microscopy (Slevogt et al., 2007). Epithelial cultures from COPD subjects were selected for immunolabelling to increase the chance of visualising intracellular bacteria. At 24h post infection, *M. catarrhalis* were labelled in red with sera produced antibody against the outer membrane proteins of *M. catarrhalis*. Ciliated cells were stained for β-tubulin in green, actin organisation was determined by phalloidin in yellow and nuclei were visualised by staining with Hoechst solution in blue as described in section 2.6.3. Multiple red fluorescent bacteria were visualised bound to ciliary tips and inside epithelial cells (Figure 3-7 A and B). Different focal planes achieved by Z-stack images of the pseudostratified differentiated cultures, revealed that no ciliated cells had *M. catarrhalis* internalised within them.

Of interest was the determination of the pathway involved in the internalisation of *M. catarrhalis* in primary airway epithelial cultures. Ciliated cells were stained with dextran dye, a well-known liquid dye taken by macropinocytosis inside epithelial cells, at the time of infection (Love et al., 2010). CFSE labelled *M. catarrhalis* were found to co- localise with red labelled dextran (Figure 3-7 C) inside non ciliated epithelial cells 24h after infection suggesting that bacteria were partially if not completely taken up by a macropinocytotic mechanism. This finding was observed in ciliated cultures from 2 COPD donors. Consistent with ALI cultures experiments, green fluorescent bacteria were co-localised with red labelled dextran in airway primary basal cells, suggesting that macropinocytotic events occur during bacterial internalisation. This observation was found in human healthy and COPD basal cells (Supplementary Figure 1 Appendix 1).

3.2.6.1 TEM of *M. catarrhalis* and the respiratory epithelium

TEM enabled a closer and more detailed understanding of the host response to bacterial infection at 12h post-infection (Figure 3-8). TEM ultrastructural images confirmed the findings from confocal and electron microscopy, that bacteria are attached and internalised into epithelial cells. Attachment of *M. catarrhalis* to the apical surface of the epithelial cells (Figure 3-8 B) did not show ruffling of epithelial membrane or the formation of membrane vesicle around the bacteria. Bacteria were identified in some instances, internalised and free in the cell cytoplasm and in some instances enclosed into membrane bound vesicles or vacuoles. Nuclei remained unaltered and no obvious changes were observed between infected and non-infected

epithelial cells (Figure 3-8 B–C). Aggregated mitochondria and well-formed Golgi apparatus were observed in the infected with *M. catarrhalis* cells, suggesting the airway cells have become activated upon infection. Further some of the mitochondria appeared swollen when observed close to the site of internalised bacteria. Tight junctions of epithelial cells were identified as intact with no visual damage. In proximity to the epithelial layer, *M. catarrhalis* was observed in different sizes, in diplococcus or round shapes, surrounded by small outer membrane vesicles. Electron dense material was identified around the bacterial cell membrane and well-defined structures, which could be designated as bacterial pili (Figure 3-8 D). In some images it appeared that the bacteria were attached to the microvilli and held away from the cell surface (Figure 3-8 D).

A.

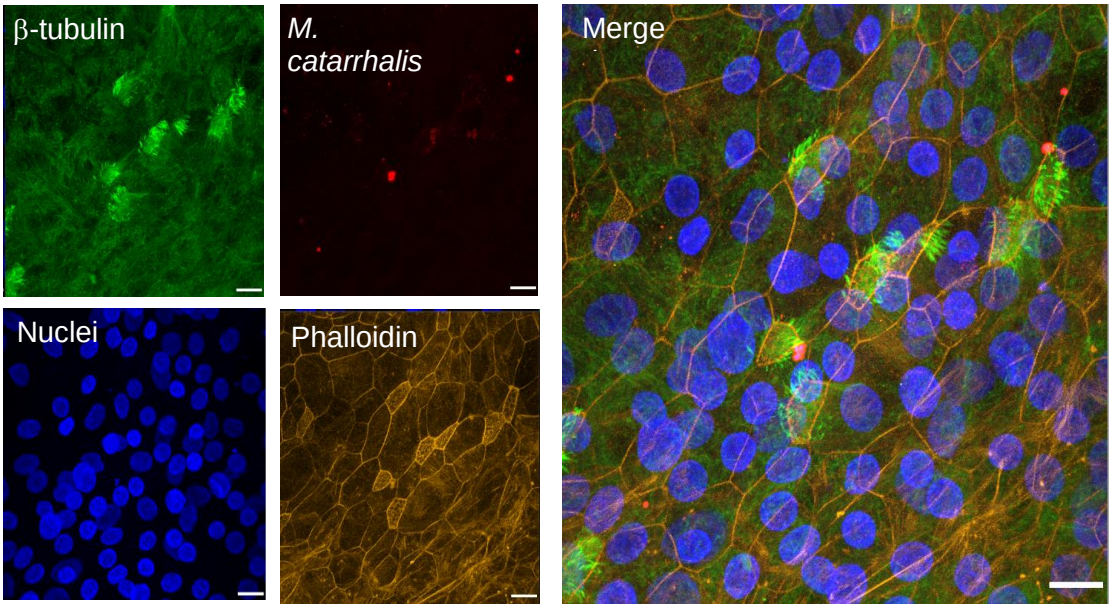

B.

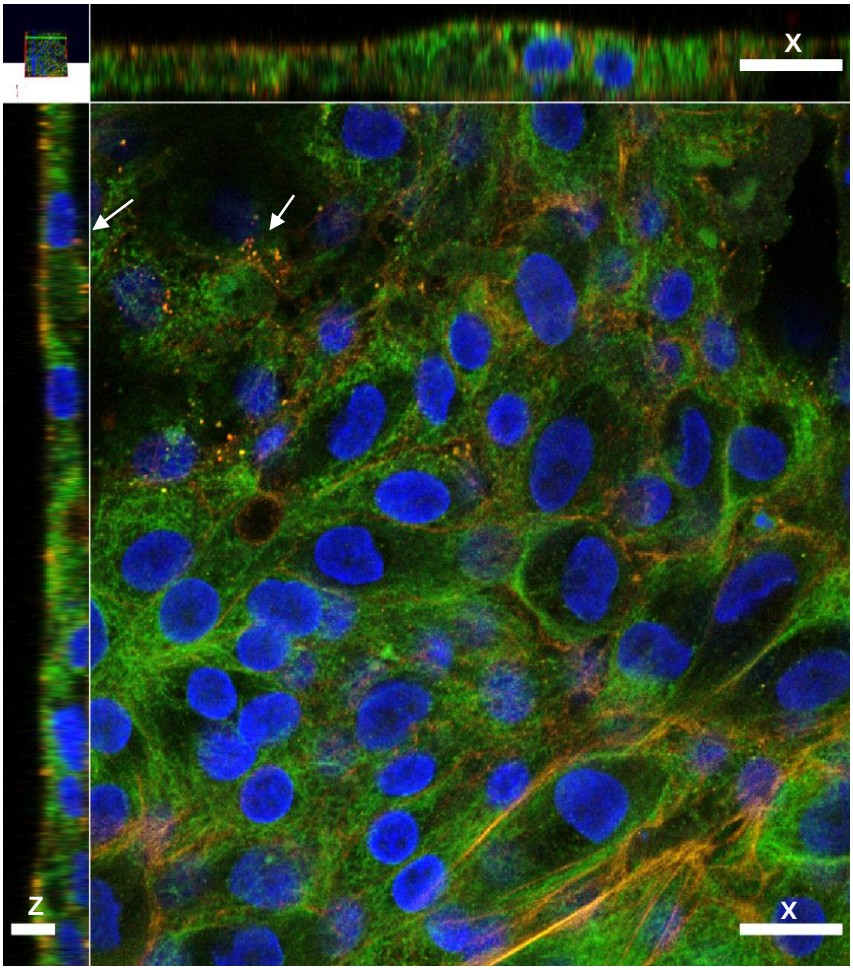

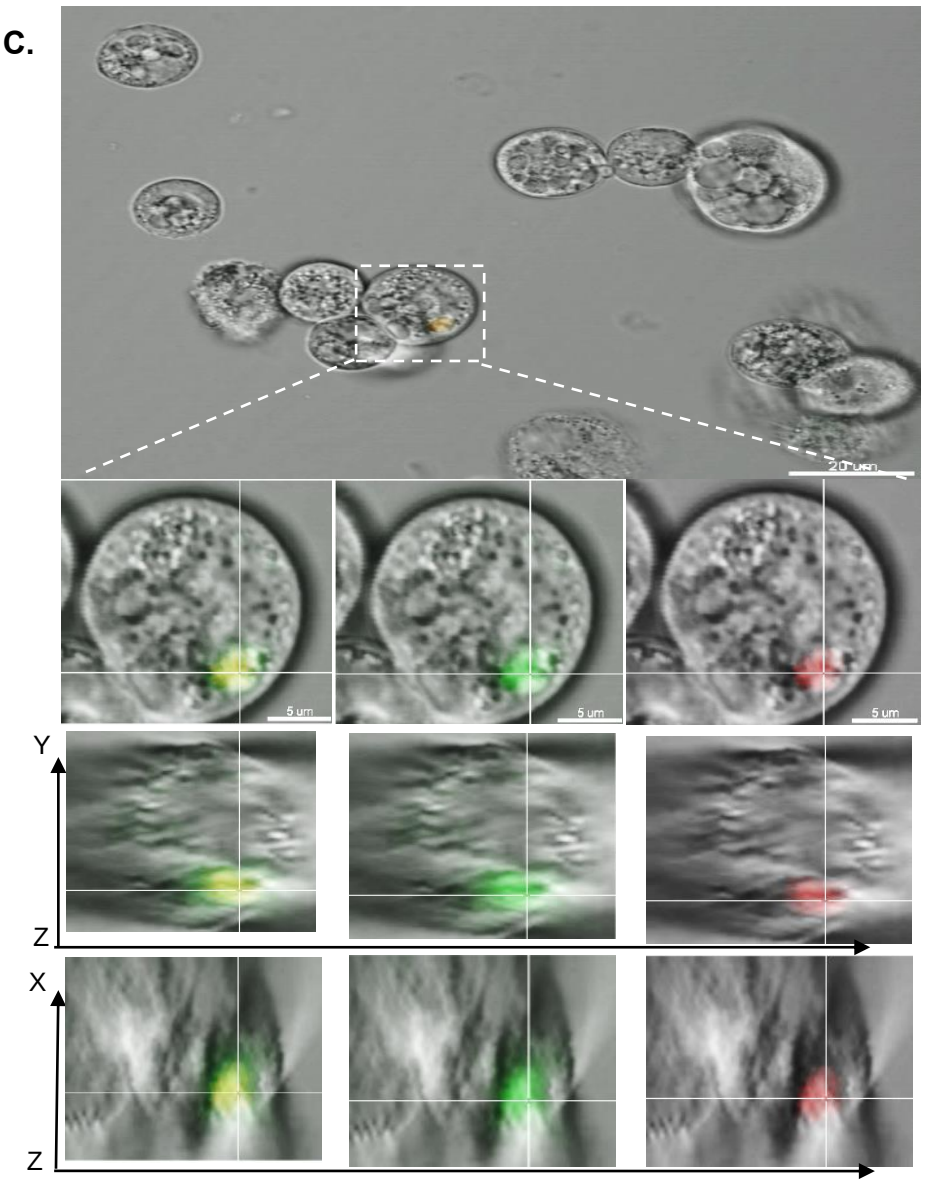

Figure 3-7: *M. catarrhalis* is internalised in primary airway epithelial cells.

A) Immunofluorescence image of nasal differentiated epithelial cells from a COPD donor with intracellular *M. catarrhalis* at 24h, detected by confocal microscopy. F-actin was labelled with phalloidin A555, *M. catarrhalis* with sera antibody in red A647, ciliated cells are labelled with β-tubulin in green A488, and nuclei are labelled with Hoechst A405, scale bar=21μM; B) Z-stack image of one focal plane from image (A), white arrows are pointing at intracellular bacteria, small scale bar = 8μM and big scale bar = 19μM; C) Z-stack image of detached COPD airway epithelial cells imaged in a glass bottom dish live by confocal microscopy at 24h post infection, red A647 dextran dye MW 10,000 is co-localised with green CellTrace™ CFSE *M. catarrhalis*, scale bar = 20μM and small scale bars = 5μM.

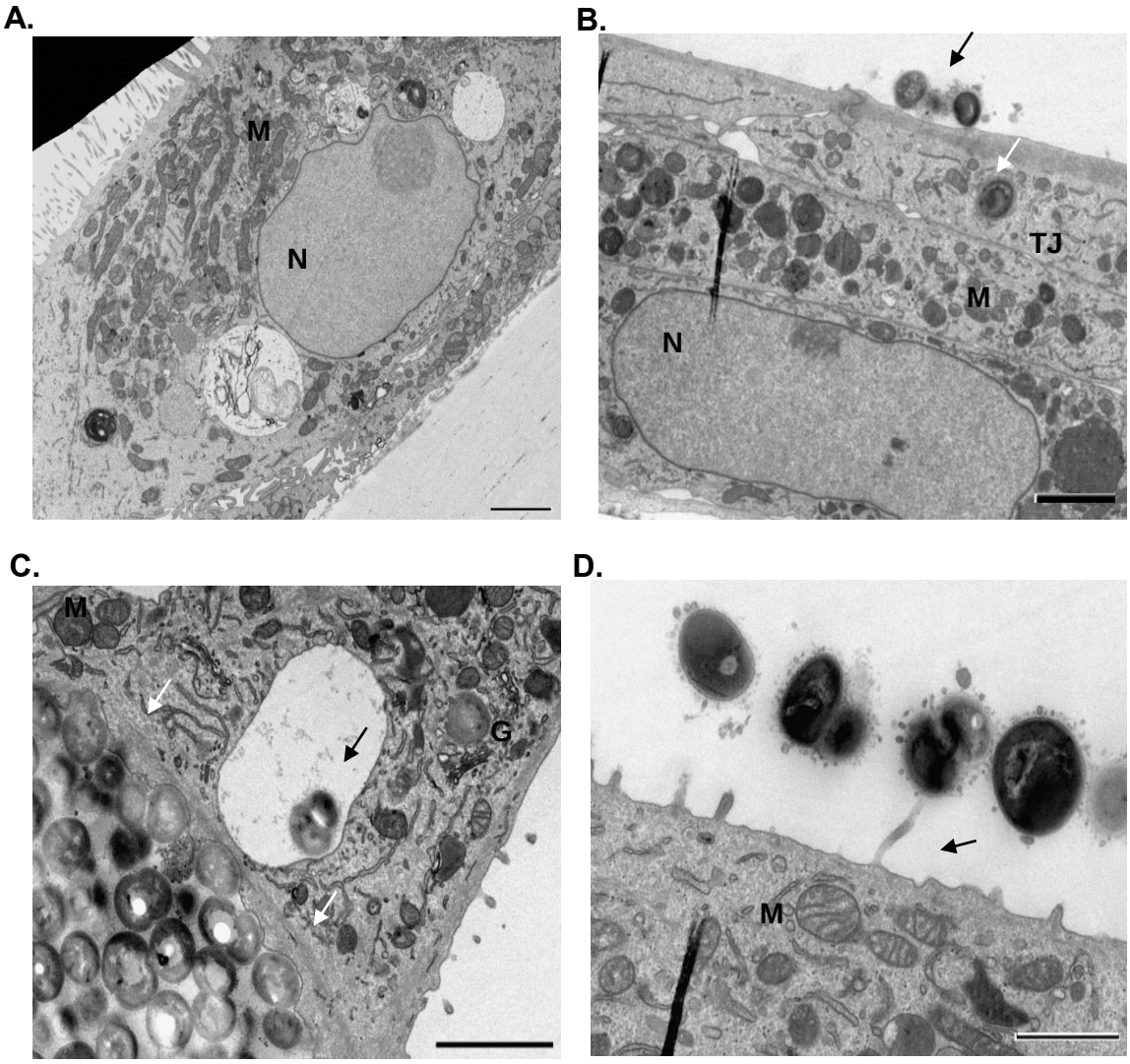

Figure 3-8: Fine structure of differentiated epithelial cultures grown at air-liquid interface.

A) Cross section of non-infected differentiated epithelial cells from a healthy donor, scale bar = 2μM; B) Cross section of infected differentiated cells, black arrow pointing at attached to the epithelium *M. catarrhalis*, white arrow pointing at internalised *M. catarrhalis*, scale bar = 2μM; C) Cross section of infected differentiated cells, arrow pointing at *M. catarrhalis* encapsulated into a vacuole, white arrows pointing at multiple internalised bacteria, scale bar=2μM; D) Closer image of *M. catarrhalis* in close proximity to the epithelium, black arrow pointing at microvilli, scale bar =1μM, M-mitochondria, N-nucleus, TJ-tight junctions, G-Golgi apparatus

3.2.7 Pro-inflammatory cellular pathways following *M. catarrhalis* addition

3.2.7.1 EGFR activation in ciliated cultures from healthy and COPD donors

To determine if *M. catarrhalis* activated pro-inflammatory pathways in airway epithelial cells and to observe whether there was a difference in the host epithelial response between healthy and COPD, proteins from ciliated cultures were profiled by SDS-PAGE electrophoresis, followed by western blotting. This is a classical method (Saraswathy and Ramalingam 2011) for analysing signalling proteins involved in epithelial cells' response, where the proteins from whole cell lysates are separated according to molecular weight and identified by specific antibody staining.

Initially, the expression and phosphorylation of EGFR at 15min and 24h post infection with *M. catarrhalis* was determined. The time-points were selected because *M. catarrhalis* binds very rapidly to the cilia of respiratory cells and because the aim of the study was to investigate the earliest time points of infection of the respiratory epithelium. Total relative expression of EGFR at the time of infection was measured in cultures from both healthy and COPD donors with no differences observed between time-points or between groups (Figure 3-9 A and B). To investigate whether a challenge with *M. catarrhalis* initiated EGFR activation, protein phosphorylation at tyrosine 1068, normalised to GAPDH house-keeping gene, was determined in reference to total EGFR expression and normalised to GAPDH house-keeping control (Figure 3-9 C and D).

In airway cultures from healthy subjects, no difference of phosphorylated EGFR was observed between infected and non-infected cultures at 15min (p=0.97) (Figure 3-9 C), though *M. catarrhalis* upregulated in all cultures phosphorylation of EGFR at the later time-point (24 hours), estimated change increase of 2.3 times (95% CI: 1.08 - 4.95), significance was not reached because of multiple comparisons (p=0.36) (Figure 3-9 C). In airway cultures from COPD donors, enhanced phosphorylation of EGFR was seen in five out of six donor cultures with relative estimated change increase of 2.12 times (95% CI: 0.99 - 4.52) compared to controls 15 minutes after contact with *M. catarrhalis* (p=0.41). Activation of EGFR in infected cultures from COPD donors increased in four patient cultures at 24 hours with relative estimated change increase of 1.3 times (95% CI: 0.61-2.78) (p=0.97) (Figure 3-9 D). Membrane images of phosphorylated proteins at different time-points, shown in Figure 3-9 E and F, represent densitometry findings from 6 and 6 COPD donor cultures. No significant changes were observed in the relative expression of phosphorylated EGFR following

M. catarrhalis addition between healthy and COPD donor cultures at 15min (p=0.99) or 24h (p=0.97).

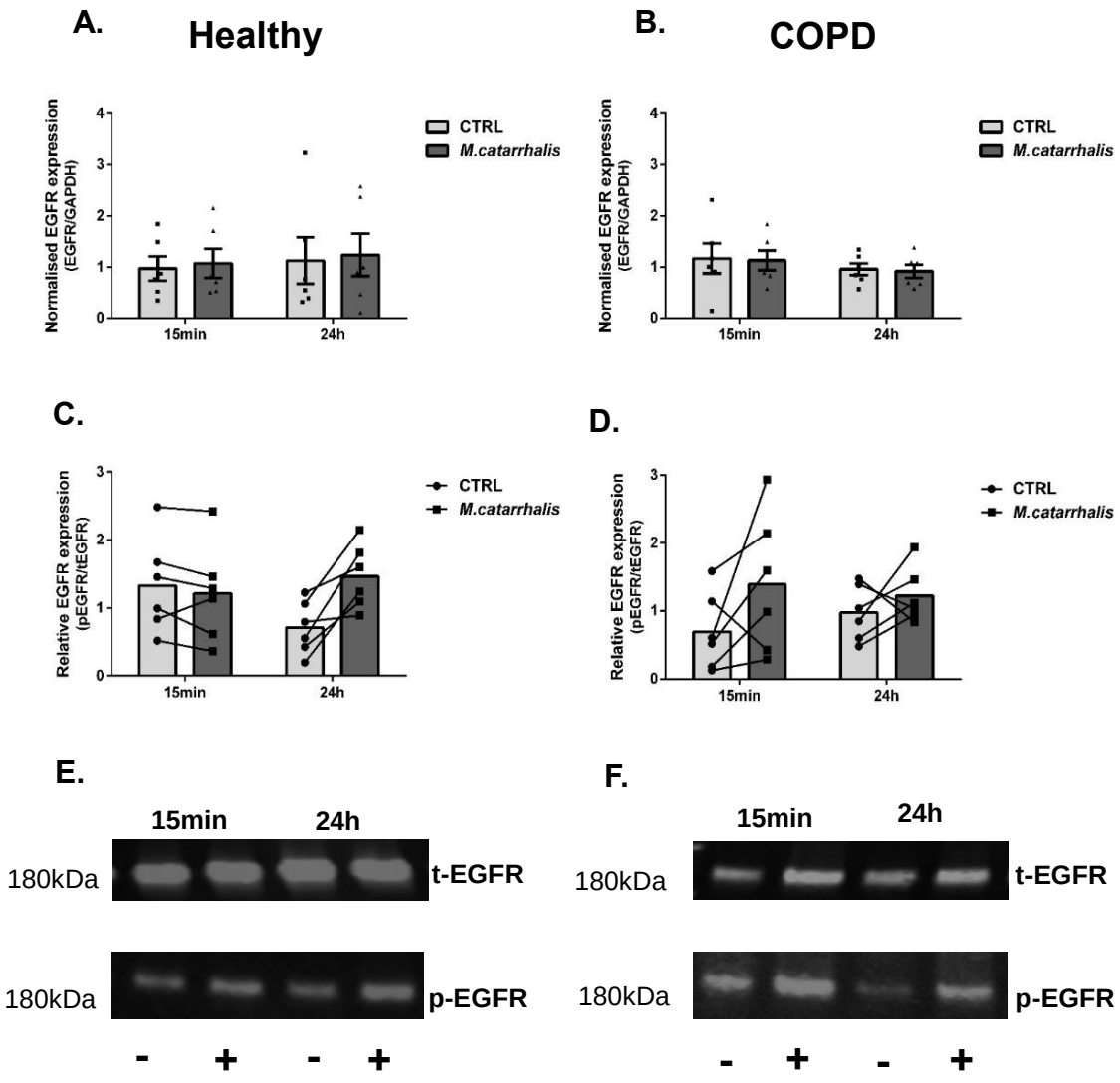

Figure 3-9: Western blot analysis of EGFR expression in response to *M. catarrhalis* initial interaction with the respiratory epithelium.

Protein expression of EGFR normalised to GAPDH expression in airway differentiated cells from A) healthy and B) COPD donors at 15min and 24h post infection. Relative protein expression of phosphorylated EGFR in airway differentiated cells from C) healthy and D) COPD donors at 15min and 24h post infection. Densitometry results are normalised to GAPDH and total EGFR protein expression for the relative time-points. Representative western blots of phosphorylated EGFR and total EGFR expression in airway differentiated cells E) healthy and F) COPD; N=6 healthy and 6 COPD donor cultures.

3.2.8 ERK activation in ciliated cultures from healthy and COPD donors

The findings from EGFR activation shown in Figure 3-9 were extended by further investigating downstream signalling in ciliated cultures upon *M. catarrhalis* infection. This part of the study focused on the downstream effectors ERK, involved in MAPK signalling and AKT, involved in PI3K signalling, both known to stimulate pro-inflammatory transcription factors such as NF-kB in the nucleus (N'Guessan et al., 2014). Downstream activation of EGFR was checked at the same time-points using the same cell lysates used for EGFR expression experiments following *M. catarrhalis* infection.

To determine the levels of phosphorylation of ERK1/2, the protein expression was evaluated in reference to total ERK1/2 expression in the cell lysates, both proteins of interest were normalised to GAPDH protein expression (Figure 3-10 A and B). The relative expression of phosphorylated ERK1/2 upon addition of *M. catarrhalis* at 15min remained unchanged compared to non-infected controls in ciliated cultures from healthy ($p=0.97$) and COPD ($p=0.97$) donors (Figure 3-10 C and D). There was no further activation of ERK1/2 at the later time point tested ($p=0.99$, healthy and $p=0.97$, COPD). There was no difference observed between the groups tested during *M. catarrhalis* infection at either time-point ($p=0.99$ at 15min, $p=0.43$ at 24h). Membrane images of proteins of interest (Figure 3-10 E and F) represent the findings from densitometry analysis from 6 healthy and 6 COPD donor cultures.

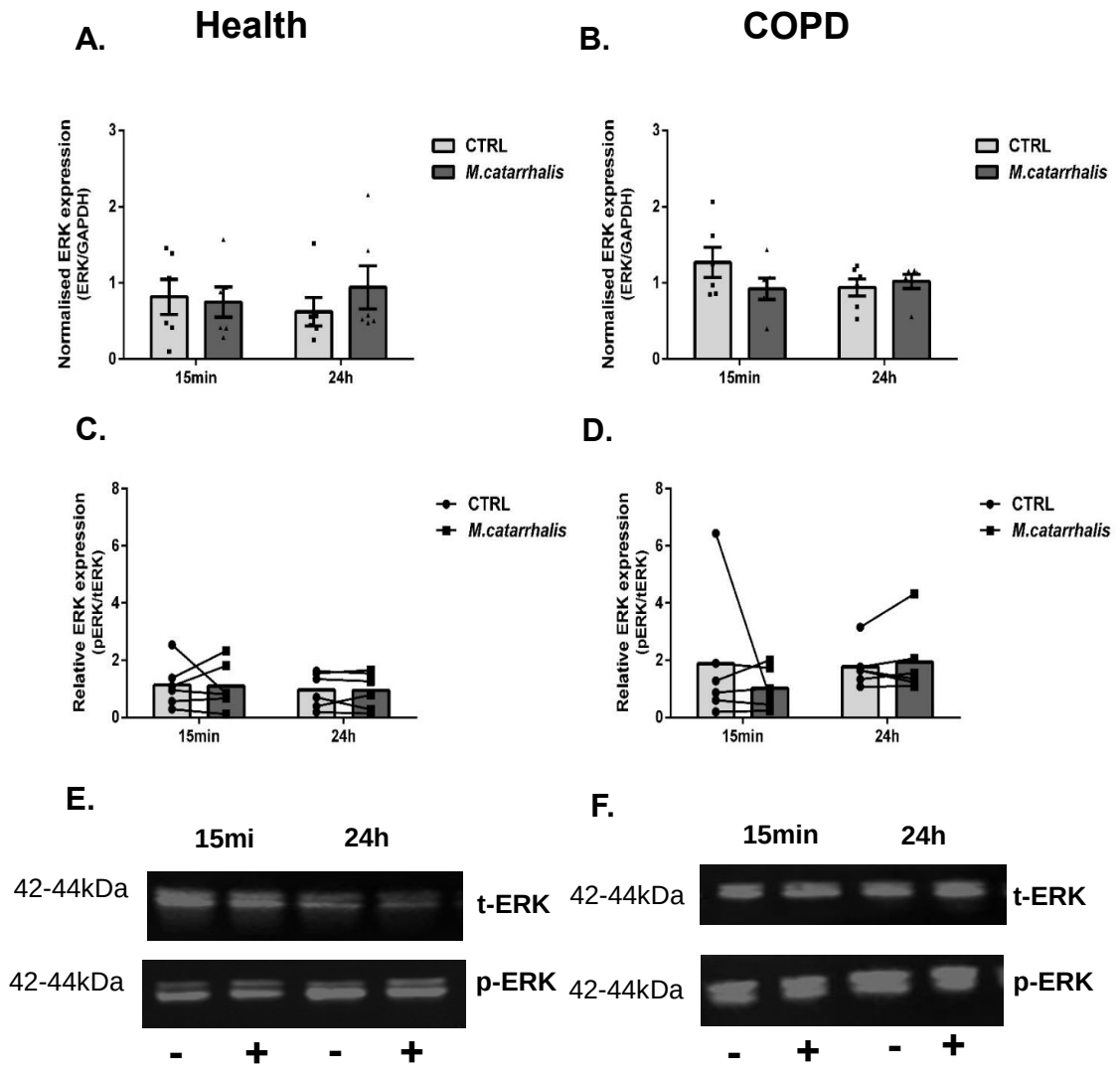

Figure 3-10: Western blot analysis of ERK1/2 expression in response to *M. catarrhalis* initial interaction with the respiratory epithelium.

Protein expression of ERK1/2 normalised to GAPDH expression in airway differentiated cells from A) healthy and B) COPD donors at 15min and 24h post infection. Relative protein expression of phosphorylated ERK1/2 in airway differentiated cells from C) healthy and D) COPD donors at 15min and 24h post infection. Densitometry results are normalised to GAPDH and total ERK1/2 protein expression for the relative time-points. Representative western blots of phosphorylated ERK1/2 and total ERK1/2 expression in airway differentiated cells from E) healthy and F) COPD donors; N=6 healthy and 6 COPD donor cultures.

3.2.9 AKT activation in ciliated cultures from healthy and COPD donors

As five out of six cultures in COPD showed activation of EGF receptors (Figure 3-9), AKT signalling was determined in the same donor cultures used for ERK1/2 signalling and in additional 3 healthy donor cultures. This was necessary because stripping of PVDF membranes and re-probing with antibodies is not always successful and could be difficult to evaluate expression of proteins. However, the same time points of infection – 15min and 24h were evaluated for signalling activation.

AKT activation was analysed by investigating phosphorylation of AKT serine residues at position 473 in relation to total AKT expression of this culture. AKT expression seemed to appear similar across different time-points in ciliated cultures from both healthy and COPD subjects (Figure 3-11 A and B) (p=0.97). In cultures from healthy subjects, *M. catarrhalis* infection at 15min and 24h did not have a significant effect on AKT phosphorylation (Figure 3-11 C) (p=0.77 and p=0.99, respectively). AKT activation in ciliated cultures from COPD donors following *M. catarrhalis* infection was variable with three out of six donor cell cultures showing an increase at 15min (p=0.97) and at 24h (p=0.77) (Figure 3-11 D). The PVDF membrane images of protein bands (Figure 3-11 E and F) are representative of AKT findings from 6 healthy and 6 COPD donor airway cultures.

To further elucidate the possible role of EGFR and PI3K pathways in *M. catarrhalis* infection we used an EGFR and a PAN PI3K inhibitor.

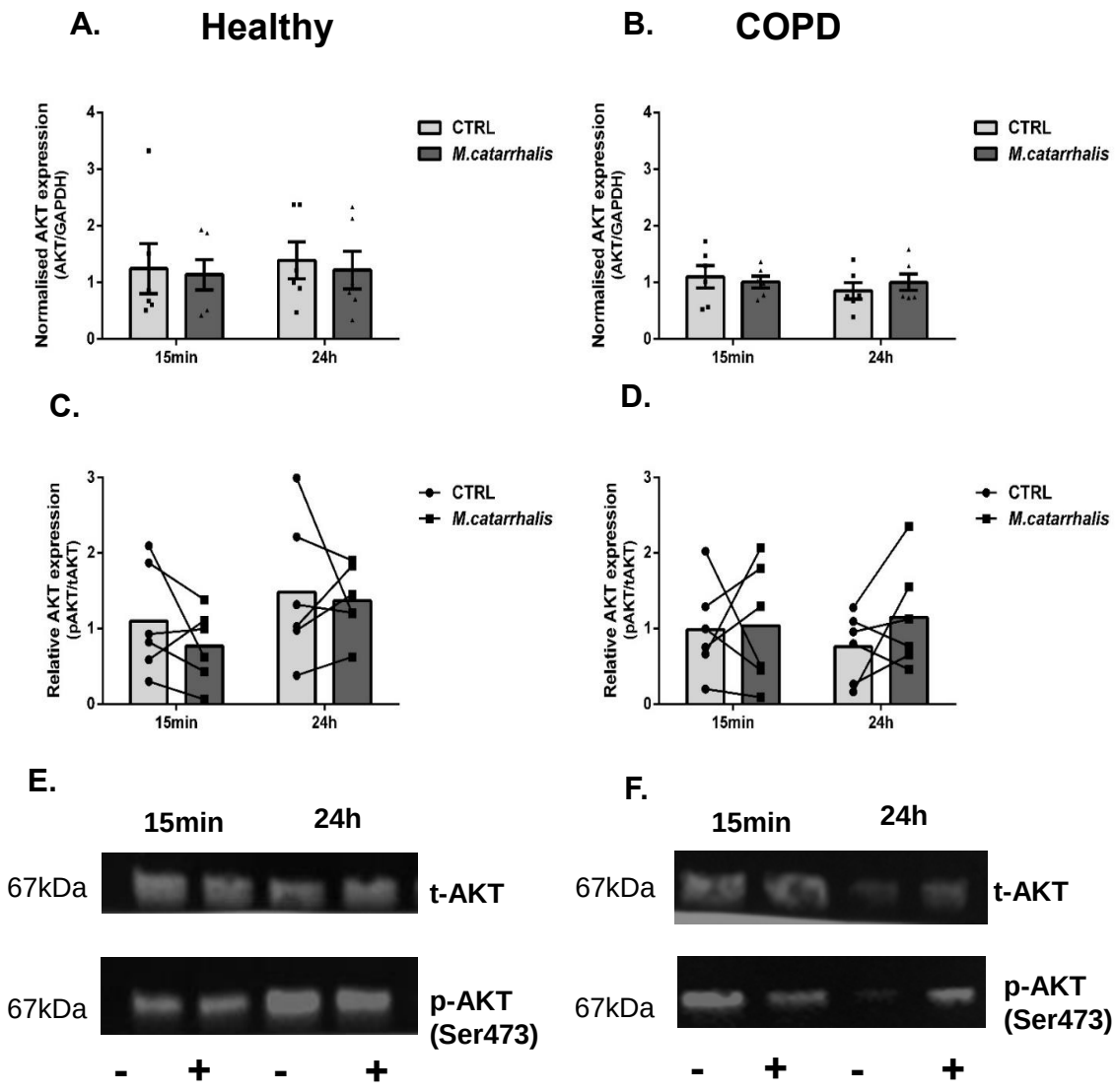

Figure 3-11: Western blot analysis of AKT expression in response to *M. catarrhalis* initial interaction with the respiratory epithelium.

Protein expression of AKT normalised to GAPDH expression in airway differentiated cells from A) healthy and B) COPD donors at 15min and 24h post infection. Relative protein expression of activated AKT in airway differentiated cells from C) healthy and D) COPD donors at 15min and 24h post infection. Densitometry results are normalised to GAPDH and total AKT protein expression for the relative time-points. Representative western blots of phosphorylated AKT and GAPDH expression in airway differentiated cells from E) healthy and F) COPD donors; N=6 healthy, 6 COPD donor cultures.

3.2.10 Gefitinib and PAN PI3K inhibitors role in *M. catarrhalis* internalisation in the respiratory epithelium

We investigated if the EGFR inhibitor – Gefitinib (Tocris, UK) or the PAN PI3K inhibitor (GSK987740) could decrease *M. catarrhalis* invasion in ciliated cultures from healthy and COPD donors. Impact of these compounds was explored at 24h post infection as this was the time-pointed initially tested for bacterial internalisation in ciliated cultures.

The role of Gefitinib and PAN PI3K inhibitors was tested at a concentration of 1μM added basolaterally for 1h prior infection with *M. catarrhalis*. This concentration was chosen based on preliminary results (available in Appendix 3 Supplementary Figure 3) and personal communication with GSK (1μM concentration was suggested to give high inhibition across the different PI3K isoforms). The experiments were performed as carried out for viability studies of bacteria described in section 3.2.5. In the current experiments at 24h cultures were exposed to imipenem to kill extracellular bacteria. In Figure 3-12 the intracellular viability of *M. catarrhalis* was determined following 1.5h of 200μg/ml imipenem treatment. Figure 3-12 shows viability counts of intracellular bacteria in cultures treated with or without Gefitinib or PAN PI3K inhibitors, and the relative integrity of the epithelial cultures at the time of the experiment. The data shows *M. catarrhalis* did not exhibit reduced viability following EGFR or PAN PI3K inhibitor treatment of epithelial cultures (Figure 3-12 A and C). During treatment with Gefitinib, intracellular bacterial viability was not reduced in cultures from healthy individuals relative to vehicle control, the estimated mean change was 8.84 with very large confidence intervals (95% CI: 0.88-88.5, p=0.77), in COPD, in four out of five cultures there was no reduction of bacterial viability, one culture showed a decrease, the estimated mean change was 1.52 (95% CI: 0.15-15.23, p=0.9). During PAN PI3K treatment, none of the cultures from healthy individuals showed a decrease in bacterial viability, mean relative change 4.11 (95% CI: 0.41-41.23, p=0.77), two out of five cultures from COPD individuals exhibited a reduction in bacterial variability with estimated mean change 0.76 (95% CI: 0.076- 7.65, p=0.9).

TEER of ciliated cultures from healthy and COPD donors (Figure 3-12 B and D) was non-significantly decreased by the carrier vehicle – DMSO (p=0.76 in healthy, p=0.83 in COPD) compared to TEER of *M. catarrhalis* infected cultures. Gefitinib did not affect TEER of cultures (p=0.58 in healthy, p=0.83 in COPD), while the PAN PI3K inhibitor non-significantly decreased TEER of epithelial cultures (p=0.11, healthy and p=0.76, COPD) compared to that of *M. catarrhalis* infected cultures.

Overall, for ciliated cultures from both healthy and COPD individuals, there is no evidence that Gefitinib or PAN PI3K inhibitors had any significant effect on *M. catarrhalis* internalisation or difference in internalisation between healthy and COPD donors for any of the treatments.

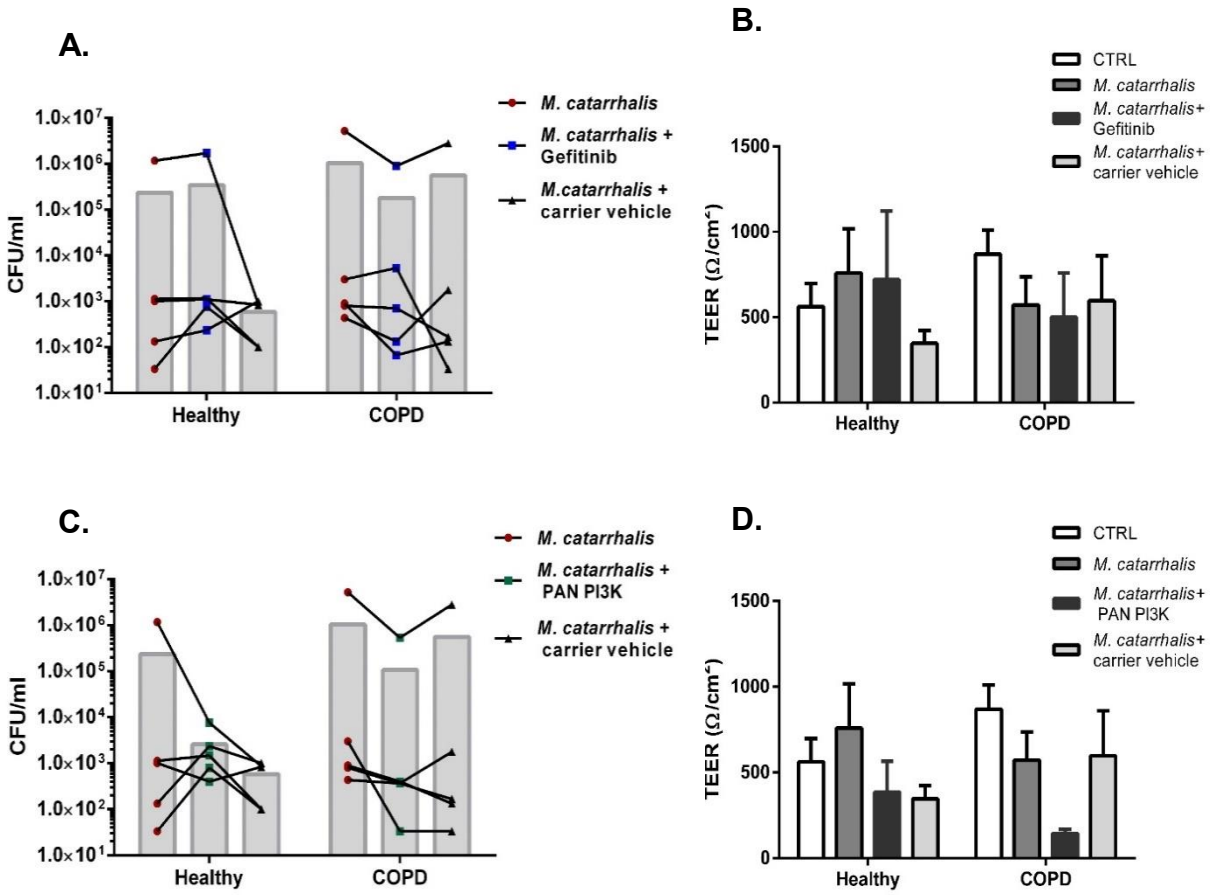

Figure 3-12: Viability counts of internalised bacteria in ciliated airway cultures treated with Gefitinib or a PAN PI3K inhibitor.

A) Bacterial counts of cultures treated with 1μM Gefitinib at the time of *M. catarrhalis* infection. B) Epithelial integrity of ciliated cultures treated with Gefitinib. C) Bacterial counts of cultures treated with 1μM PAN PI3K inhibitor at the time of *M. catarrhalis* infection. D) Epithelial integrity of ciliated cultures treated with the PAN PI3K inhibitor. Graphs represent the mean of cultures from 5 healthy and 5 COPD donor cultures, error bars represent ±SEM.

3.2.11 Induced cytokines and chemokines post *M. catarrhalis* infection of the respiratory epithelium

To assess the inflammatory response of ciliated cultures from healthy and COPD individuals to *M. catarrhalis* infection, the apical and basolateral fluids from cultures were collected at 24h post infection. Previous studies have reported increased levels of IL-6, IL-8/ CXCL8, TNFα, IFN-β and RANTES/ CCL5 in non-differentiated BEAS-2B and A549 epithelial cells in response to *M. catarrhalis* (Rosseau et al., 2005; Slevogt et al., 2006; Slevogt et al., 2007). In this study a panel of 20 cytokines was explored. Figure 3-13 and Figure 3-14 demonstrate the cytokines with the highest increase after infection with *M. catarrhalis* at 24h in basolateral and apical fluids, respectively, whereas Tables 3-4 and Table 3-5 summarise all cytokine measurement readings from basolateral and apical fluids.

3.2.11.1 Pro-inflammatory cytokines in basolateral fluids

Immunoassays demonstrated *M. catarrhalis* infection of the airway epithelium induced cytokines release in both apical and basolateral fluids from ciliated cultures. A greater than 50% increase was seen for the pro-inflammatory cytokines: IP-10/ CXCL10, IL-6, TNF-α, MCP-1/ CCL2, MIP3α/ CCL20, ENA-78/ CXCL5, CSF3/ G-CSF and IL-17c in the basolateral fluids of COPD donor cultures following *M. catarrhalis* infection when compared to non-infected cultures. Compared to non-infected controls, IP-10/ CXCL10 protein was 2.5 times higher (95% CI: 1.36 – 4.71, p=0.15), IL-6 protein was 2.7 times higher (95% CI: 0.86 – 8.46, p=0.55), TNF-α protein was 1.5 times higher (95% CI: 1.11 – 2.14, p=0.18), MCP-1/ CCL2 protein was almost 2 times higher (95% CI: 1.23 – 3.20, p=0.18) and CSF3/ G-CSF protein was 1.5 times higher (95% Cl: 1.00 – 2.34, p=0.44). A strong non-significant induction was observed for ENA-78/ CXCL5, 4.4 times higher (95% Cl: 1.63 – 11.62, p=0.15), and IL-17c, 3 times higher (95% Cl: 1.35 – 7.49, p=0.18) in COPD donor cultures infected with *M. catarrhalis* relative to non-infected controls. A significant induction was observed for MIP-3α/ CCL20 (p=0.042), 1.6 times higher (95% CI: 1.25 – 2.09) in the basolateral fluid of infected cultures compared to non-infected cultures from COPD donors. MIP-3α/ CCL20 was non-significantly increased, 1.3 times higher (95% CI: 1-1.68, p=0.46) in infected with *M. catarrhalis* cultures compared to non-infected cultures from healthy individuals.

In epithelial cultures from healthy individuals, protein levels in the basolateral fluids of cells infected with *M. catarrhalis* were relatively low (10-15% increased) and similar to baseline readings among the different analytes. An analyte is a component of a sample whose concentration is measured and identified. In infected cultures

compared to non-infected controls, estimated relative change increases were measured for TNF-α, 1.21 times (95% CI: 0.87 – 1.69, p=0.71), ENA-78/ CXCL5 proteins, 1.22 times (95% Cl: 0.45 – 3.26, p=0.9), MIP-3α/ CCL20, 1.30 times (95% Cl: 1.00 – 1.68, p=0.41), IL-17c, 1.43 times (95% Cl: 0.61 – 3.36, p=0.82) and CSF3/ G-CSF, 1.69 times (95% Cl: 1.10 – 2.59, p=0.23), though the increases did not reach significance. *M. catarrhalis* significantly induced IFN-β, with an estimated relative change increase 2.12 times (95% Cl: 1.47 – 3.06, p=0.034). IFN-β was also elevated in ciliated cultures from COPD donors 1.29 times (95% Cl: 0.92 – 1.81), but this did not reach significance (p=0.61).

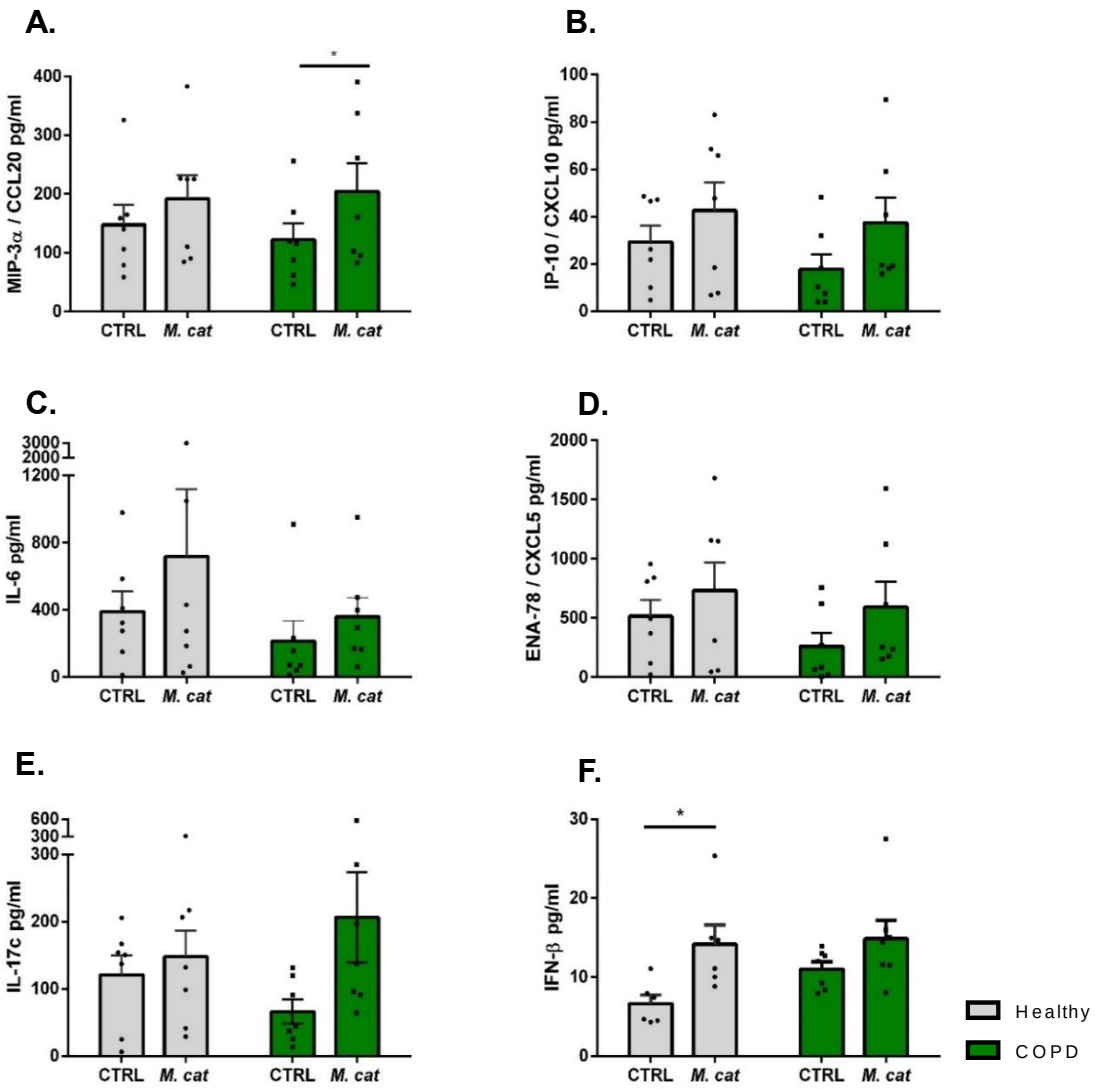

Figure 3-13: Inflammatory mediators secreted in the basolateral fluids from healthy and COPD donor cultures following *M. catarrhalis* infection for 24h.

Ciliated cultures from healthy and COPD were treated with $5x10^6$ CFU *M. catarrhalis* or plain media for 15min and inoculum was removed to allow infection at air-fluid interface. At 24h basolateral fluids were collected and cytokines were measured. A) MIP-3α / CCL20; B) IP=10/ CXCL10; C) IL-6; D) ENA-78/ CXCL5; E) IL-17c; F) IFN-β, n=6 healthy and 6 COPD donors, error bars represent ±SEM, *=p<0.05

Table 3-4: Inflammatory mediators secreted in the basolateral fluids of ciliated cultures following *M. catarrhalis* infection for 24h.

	Healthy			COPD		
pg/ml	**CTRL**	***M. catarrhalis***	**P value**	**CTRL**	***M. catarrhalis***	**P value**
IL-1β	1.04 ± 0.16	1.56 ± 0.42	0.70	0.9 ± 0.4	1.08 ± 0.40	0.79
IL-8 / CXCL8	1831.84 ± 187.90	2024.82 ± 152.12	0.79	1542.44 ± 245.57	2056.02 ± 268.56	0.31
RANTES / CCL5	1.67 ± 0.23	1.52 ± 0.28	0.83	1.48 ± 0.20	1.36 ± 0.15	0.89
TNF-α	93.13 ± 13.92	119.49 ± 22.69	0.71	63.85 ± 13.15	94.18 ± 16.54	0.19
MCP-1 / CCL2	418.13 ± 97.02	454 ± 108.88	0.93	298.88 ± 143.24	549.82 ± 215.93	0.18
CSF-3 / G-CSF	15.28 ± 2.33	31.25 ± 8.94	0.24	13.96 ± 2.92	21.98 ± 4.75	0.45
GRO-α / CXCL1	439.32 ± 100.62	313.93 ± 46.44	0.56	305.80 ± 30.24	268.17 ± 19.01	0.89
IL-15	4.89 ± 0.30	5.28 ± 0.38	0.83	5.40 ± 0.40	4.95 ± 0.54	0.75
IFN-α	2.52 ± 0.02	2.57 ± 0.03	0.75	2.57 ± 0.02	2.52 ± 0.04	0.71
IFN-γ	1.50 ± 0.20	1.79 ± 0.29	0.90	1.96 ± 0.23	1.49 ± 0.24	0.71
IFN-λ	0.57 ± 0.07	0.88 ± 0.26	0.56	0.55 ± 0.041	0.67 ± 0.05	0.73
TARC / CCL17	0.24 ± 0.05	0.31 ± 0.10	0.86	0.26 ± 0.07	0.31 ± 0.05	0.56
CXCL14	1066.79 ± 10.70	1082.16 ± 18.20	0.83	1121.49 ± 14.84	1134.17 ± 18.37	0.86
IL-36g	32.90 ± 6.13	29.21 ± 5.08	0.83	20.98 ± 1.58	21.66 ± 2.04	0.96

3.2.11.2 Pro-inflammatory cytokines in apical fluids

Consistent with the findings from basolateral fluids, *M. catarrhalis* induced pro-inflammatory cytokines secreted in the apical chamber of ciliated cultures from COPD patients. At 24h post infection trends for higher induction of pro-inflammatory cytokines were observed for IP-10/ CXCL10, TNF-α, MCP-1/ CCL2, MIP-3α/ CCL20, ENA-78/ CXCL5, CSF3/ G-CSF, IL-17c and IFN-β, though these did not reach significance. In infected cultures compared to non-infected controls, IP-10/ CXCL10 protein was 2.7 times greater (95% CI: 0.83 – 9.12, p=0.55), TNF-α was 1.78 times greater (95% CI: 0.88 – 3.60, p=0.55) and MCP-1/ CCL2 was ~ 1.7 times greater (95% CI: 0.76 – 3.75, p=0.70), MIP-3α/ CCL20 protein was 2 times greater (95% CI: 0.78 – 5.14, p=0.62), IL-17c protein was 2.8 times greater (95% CI: 0.81 – 9.71, p=0.55). A very strong increase of proteins was measured for ENA-78/ CXCL5, 4.5 times higher (95% CI: 0.78 – 45.71, p=0.55) and CSF3/ G-CSF, 3.8 times higher (95% CI: 0.95 – 15.48, p=0.48) relative to apical fluids from non-infected cultures. Interestingly, IFN-β was also stimulated in the apical site of infected cultures from COPD patients, with 76% increase or estimated change of 1.76 (95% CI: 1.29 – 2.39) compared to non-infected control and a significance value of p=0.04 (Figure 3-14).

Similar to the cytokines induced in the basolateral fluids of cultures from healthy individuals, apical fluids from cultures from healthy individuals infected with *M. catarrhalis* showed low and relatively similar increases in cytokine response. Estimated relative change increases of 1.39 (95% CI: 0.99 – 1.95, p=0.46), 1.44 (95% CI: 0.65 – 3.02, p=0.79), 1.54 (95% CI: 0.27 – 8.74, p=0.88) and 2.39 (95% CI: 0.59 – 9.67, p=0.71) were observed for IFN-γ, MCP-1/ CCL2, ENA-78/ CXCL5 and CSF3/ G-CSF proteins respectively (Figure 3-14), however statistically significant differences were not reached.

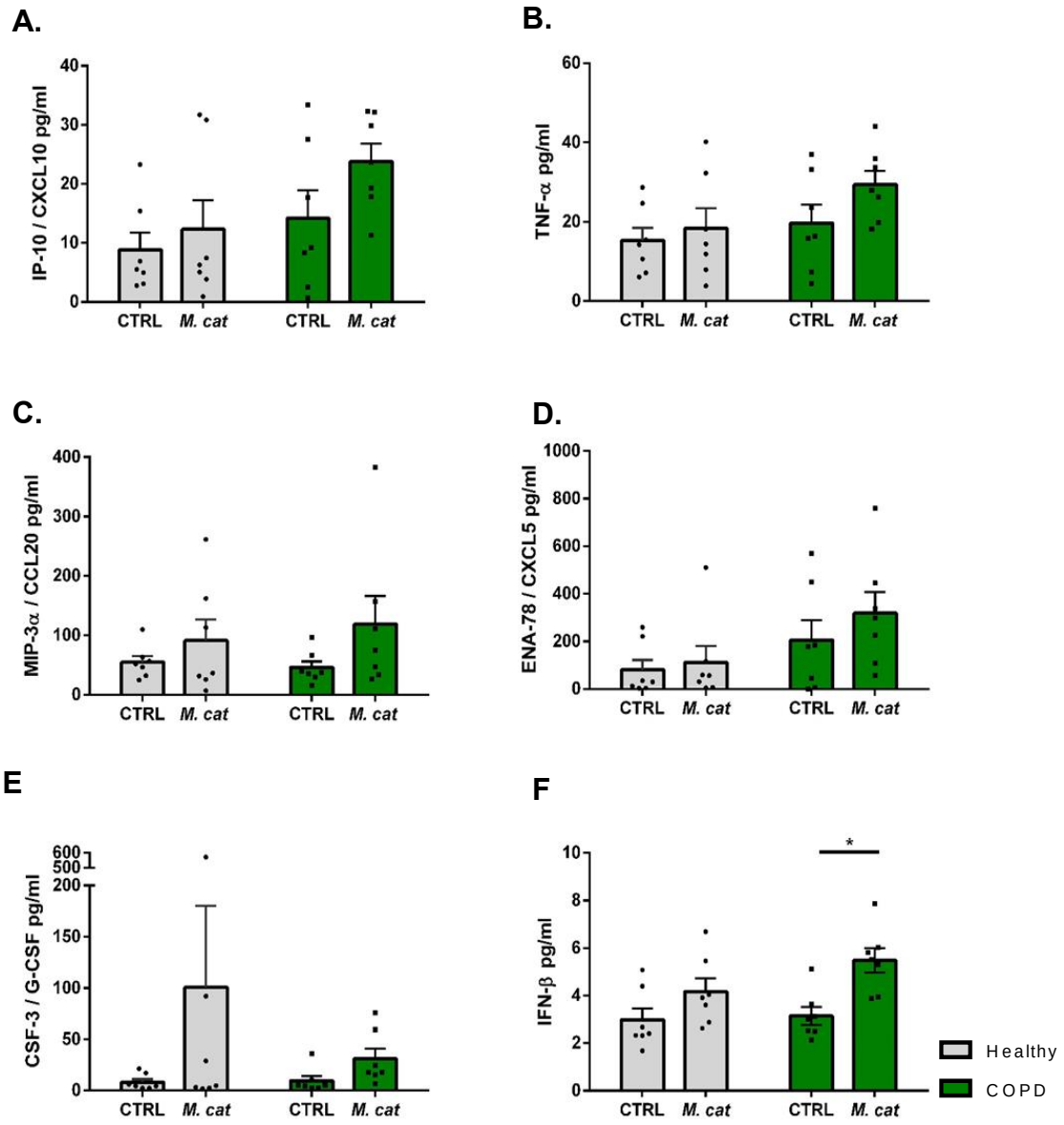

Figure 3-14: Inflammatory mediators secreted in the apical fluids of ciliated cultures following *M. catarrhalis* infection for 24h.

Ciliated cultures were treated with 5x10^6 CFU/ml *M. catarrhalis* or plain media for 15min and inoculum was removed to allow infection at air-fluid interface. At 24h apical fluids were collected and cytokines were measured. A) IP-10/ CXCL10; B) TNF-α; C) MIP-3α / CCL20; D) ENA-78/ CXCL5; E) CSF-3/ G-CSF; F) IFN-β, n=6 healthy and 6 COPD donors, error bars represent ±SEM, *=p<0.05

Table 3-5: Inflammatory mediators secreted in the apical fluids of ciliated cultures following *M. catarrhalis* infection for 24h.

	Healthy			COPD		
pg/ml	**CTRL**	***M. catarrhalis***	**P value**	**CTRL**	***M. catarrhalis***	**P value**
IL-1β	0.10 ± 0.03	0.12 ± 0.06	0.94	0.25 ± 0.14	0.17 ± 0.04	0.90
IL-6	154.68 ± 73.95	143.98 ± 66.36	0.86	1123.33 ± 917.017	342.79 ± 148.80	0.93
IL-8 / CXCL8	840.32 ± 154.94	966.62 ± 349.92	0.94	616.09 ± 96.52	647.49 ± 126.60	0.96
RANTES / CCL5	0.53 ± 0.08	0.82 ± 0.20	0.83	0.91 ± 0.30	0.75 ± 0.14	0.99
MCP-1 / CCL2	47.07 ± 20.58	46.98 ± 8.12	0.79	79.25 ± 27.31	91.72 ± 21.93	0.70
CSF-3 / G-CSF	8.28 ± 2.89	100.69 ±79.42	0.71	9.49 ± 4.54	31.08 ± 9.76	0.48
GRO-α / CXCL1	143.91 ± 22.87	131.99 ± 32.41	0.73	105.36 ± 11.74	91.27 ± 12.60	0.79
IL-15	0.68 ± 0.07	0.58 ± 0.13	0.71	0.693 ± 0.11	0.87 ± 0.16	0.84
IFN-α	1.09 ± 0.01	1.12 ± 0.02	0.73	1.13 ± 0.01	1.12 ± 0.026	0.95
IFN-γ	1.09 ± 0.12	1.52 ± 0.17	0.46	1.13 ± 0.14	1.75 ± 0.09	0.19
IFN-λ	0.28 ± 0.01	0.32 ± 0.01	0.70	0.31 ± 0.03	0.38 ± 0.04	0.56
IL-17c	4.63 ± 2.41	6.63 ± 3.41	0.93	2.413 ± 1.05	7.03 ± 2.67	0.56
TARC / CCL17	4.63 ± 2.41	6.63 ± 3.41	0.93	2.41 ± 1.05	7.03 ± 2.67	0.61

3.2.11.3 Comparison of apically and basolaterally induced cytokines

Initial statistic tests involved individual comparisons of cytokines released in the basolateral and apical fluids between infected and non-infected cultures from healthy and COPD donors. A global test which is more powerful than individual comparisons (combines readings from disease groups and types of fluids) was then performed to compare infected and non-infected. When p=0.05 or <0.05, the results from the basolateral fluids were compared to the results from the apical fluids. If the comparison ratio was greater than 1, then it was considered that greater release of cytokines was observed in the basolateral fluid of cultures.

Greater cytokine release in basolateral fluids of cultures from healthy individuals was seen for IP-10/ CXCL10 protein (p=0.92), TNF-α protein (p=0.92), MIP-3α/ CXCL5 protein (p=0.88), IFN-β protein (p=0.55) and IL-17c protein (p=0.93). As in cultures from COPD donors, greater cytokine release in basolateral fluids was observed for MCP-1/ CCL2 (p=0.92) and IL-17c (p=0.95) proteins only, suggesting that cytokine secretion on the apical surface of cultures plays a key role on the induction of inflammatory response in epithelial cells of COPD individuals.

3.3 Discussion

The experiments in this chapter aimed to investigate the early initial interaction of *M. catarrhalis* with the ciliated respiratory epithelium and to determine if bacterial viability and initiation of signalling cascades varies in the ciliated epithelium of healthy and COPD individuals. It also aimed to investigate whether the inflammatory response of airway ciliated cells to *M. catarrhalis* is similar between the two groups. It was hypothesised that *M. catarrhalis* preferentially adheres and invades respiratory epithelial cells from COPD donors, leading to greater ciliary dysfunction and inflammation.

3.3.1 *M. catarrhalis* and epithelial ciliary function

This is the first investigation to provide evidence that *M. catarrhalis* attaches, within seconds of addition, to rapidly beating cilia in airway cultures from both healthy and COPD individuals. Binding of *M. catarrhalis* was further confirmed by live confocal

microscopy, a method developed in this project to specifically to look at the initial interaction of the bacterium with the ciliated respiratory epithelium. Two previous studies have also suggested that *M. catarrhalis* binds to cilia *in vitro* and *in vivo* (Balder et al., 2009; Brockson et al., 2012), however, neither study looked at epithelial defence mechanisms following bacterial addition to the epithelial cells. Balder and colleagues (Balder et al., 2009) examining fixed slides, demonstrated *M. catarrhalis* strain O35E to have tropism for the apical site of cilia in human bronchial cells grown at ALI, mediated by the adhesin MID/Hag of the bacterial membrane. Further, *M. catarrhalis* tropism for ciliated cells has been demonstrated in the middle ear of a chinchilla where *M. catarrhalis* was tightly associated with cilia following intranasal challenge with the bacteria for 11 days (Brockson et al., 2012). Of interest, a different respiratory bacterial pathogen - *Bordatella bronchiseptica* was similarly shown to attach rapidly to ciliated cells of cultured primary rabbit differentiated tracheal cells within 30 seconds of addition (Edwards et al., 2005). The direct ciliary binding of *Bordatella bronchiseptica* to the host epithelium was facilitated by the expression of bacterial adhesins and toxins, but attenuated by the antimicrobial factor surfactant protein-A (SP-A). These findings were suggested as a determining step of bacteria to overcome mucociliary clearance and colonise the conducting airways (Edwards et al., 2005). In the current study *M. catarrhalis* was observed to form clumps of bacterial cells on the apical surface of cultures within 15min of initial attachment (Figure 3-3 B). The very rapid binding of *M. catarrhalis* affected ciliary function of epithelial cultures, significantly reducing ciliary beat amplitude as early as 15min post infection (Figure 3-5). Binding of *M. catarrhalis* to cilia decreased beat amplitude in cultures from healthy individuals by 35% and by 55% in cultures from COPD individuals at 24h. *M. catarrhalis* slowed the beat frequency of airway cultures by ~1 Hz when bound to cilia at 24h, though significant differences of CBF between the conditions and studied groups were not observed (Figure 3-5). However, other bacteria have been associated with slowing of CBF. For example, Hirst et al reported the CBF of brain ependymal brain slices is slowed upon infection with *S. pneumoniae*, within 90 min of infection (Hirst et al., 2000). The current study has shown for the first time that the immediate interaction of *M. catarrhalis* with host ciliated cells from healthy and COPD donors can interfere with ciliary function. It has been suggested that individuals with COPD may have shorter cilia and reduced CBF which may also affect mucociliary clearance (Yaghi et al., 2012; Piatti et al., 2005; Hessel et al., 2014). Thus, immediate attachment of *M. catarrhalis* to ciliated cells, can further impair innate respiratory defence mechanisms.

3.3.2 *M. catarrhalis* and invasion of differentiated epithelial cells

Once adhered to the host cell surface, bacteria can enter epithelial cells by different mechanisms (section 1.3.3.2). One of the main findings in this study is that *M. catarrhalis* can adhere and invade airway ciliated cultures when observed at 24h after addition of bacteria (Figure 3-6), in parallel with an increased bacterial viability in cultures from COPD donors. Bacteria with the potential to cause invasive disease can colonise the respiratory tract and escape host immune recognition by PRRs located on innate cells (Slevogt et al., 2007). A study by Slevogt et al suggested *M. catarrhalis* can invade the epithelial cells lines BEAS-2B and A549 through a macropinocytosis mechanism that involved ruffling of the epithelial membrane, formation of lamellipodia, macropinocytotic vacuoles (macropinosomes) and actin re-arrangement inside epithelial cells (Slevogt et al., 2007). Several other studies reported bacteria including NTHI, *Salmonella typhimurium* and *Shigella flexeri* initiate macropinocytosis to enter epithelial cells (Cossart and Sansonetti 2004; Ketterer et al., 1999; Weiner et al., 2016). Importantly, for the first time this study has observed by TEM that *M. catarrhalis* can be internalised into differentiated epithelial cells *in vitro* and be visualised independently in the cytoplasm or in vacuoles 12h post infection (Figure 3-8). In addition, use of dextran with a molecular weight of 10,000 Da which is known to be internalised in epithelial cells by a macropinocytosis mechanism (Love et al., 2010; Ketterer et al., 1999), expanded the electron microscopy findings. Confocal live images of ciliated cultures from COPD donors infected with *M. catarrhalis* for 24h and stained with dextran, showed that *M. catarrhalis* staining appeared to co-localise with the appearance of dextran in a few nonciliated cells. The time selected in this study (24h) may not be indicative of the initial mechanism of bacterial internalisation in the epithelial cells. In addition, because of the induced epithelial stress, *M. catarrhalis* could use alternative mechanisms for internalisation that does not involve endocytosis such as host – receptor binding (Su et al., 2012). No further investigations were carried out in this work for time constraints, but to definitively determine the mechanism of bacterial internalisation into epithelial cells, earlier time-points, higher bacterial concentrations and markers for clathrin and caveolae dependent endocytosis such as transferrin and cholera toxin B (Love et al., 2010) might reveal the routes of bacterial internalisation and epithelial changes associated with bacterial invasion.

3.3.3 *M. catarrhalis* and activation of EGFR in differentiated cells

To begin addressing the mechanism of the inflammatory response of epithelial cells to *M. catarrhalis* infection and to see whether it was dependent on the expression of receptors and their downstream activators, ciliated cultures from healthy and COPD donors were infected for 15min or 24h. Previous data suggested that *M. catarrhalis* induces IL-6, IL-8/ CXCL8 and TNF-α cytokines through the phosphorylation of EGFR in the bronchial BEAS-2B cell line (N'Guessan et al., 2014). In accordance with this finding, the current study also showed that *M. catarrhalis* stimulated EGFR phosphorylation in differentiated airway cells. Infected cultures from healthy and COPD donors presented differential expression of phosphorylated EGFR at 15min of infection, with highly induced receptor activation pattern in COPD contrasting with no activation in healthy cultures. At 24h phosphorylated EGFR was not as strongly expressed in COPD as in healthy, but it is possible activated EGF receptor may have been internalised through endocytosis and subject to lysosomal degradation, thus reducing its epithelial expression (Henriksen et al., 2013; Garay et al., 2015). Similar to *M. catarrhalis, Neisseria meningitis* has been reported to activate EGFR in endothelial cells 3h post infection, mediating meningococcal invasion of endothelial cells through EGF receptor activation (Slanina et al., 2014). EGFR expression is known to be increased in the airway epithelium of COPD patients and has a direct effect on goblet cell hyperplasia and mucous metaplasia through the secretion of mucins and stimulation of pro-inflammatory cytokines (Rogers, 2003; Casalino-Matsuda et al., 2006; Crystal et al., 2008; Turner et al., 2001). It may be that *M. catarrhalis* steadily activates EGFR in the COPD epithelium, contributing to over production of mucus and stimulation of inflammatory mediators, leading to airway obstruction and heightened inflammatory state. It is beyond the scope of this study but it would be of interest to investigate changes of the pathophysiology of COPD characteristics during established *M. catarrhalis* infection.

Downstream signalling of EGFR involves ERK 1/2 and PI3K signalling through AKT leading to NF-kB translocation to the nucleus and induction of transcription of genes, including cytokines associated with immune responses, proliferation, differentiation, cell survival and apoptosis (Lee and McCubrey 2002; Garay et al., 2015). In contrast to N'Guessan's (N'Guesan et al., 2014), findings that *M. catarrhalis* induces inflammatory mediators through ERK activation it was not possible to confirm this mechanism in primary airway epithelial cells as no increase in phosphorylation of ERK was evidenced in the cell donor cultures at either time-point (Figure 3-10). Furthermore, AKT activation regulates actin polymerisation and its inhibition by

wortmanin (PAN PI3K inhibitor) successfully reduced *M. catarrhalis* intracellular uptake (N'Guessan et al., 2014). The current findings propose that *M. catarrhalis* infections in cultures from healthy individuals is not associated with phosphorylation of AKT, though variable AKT activation has been reported in ciliated cultures from COPD individuals (Figure 3-11). To identify if EGFR and AKT activation associates with bacterial internalisation, pre-treatment of primary airway epithelial cells with the pharmacologic inhibitors Gefitinib (EGFR inhibitor) or the PAN PI3K compound (GSK987740) was carried out to determine the pathway of internalised bacteria. To date, no one has tested what would be the effect of such inhibitors on bacterial invasion in differentiated cultures, therefore the observation that neither inhibitor reduced bacterial invasion is novel and contradictory to the literature (Figure 3-12). It is possible that a larger number of donors may have to be used to observe the compounds' contribution to reduced bacterial uptake.

3.3.4 *M. catarrhalis* and epithelial inflammatory response

It is of interest that *M. catarrhalis* did not induce as many inflammatory mediators as it was expected. Surprisingly upon *M. catarrhalis* infection from the 20 cytokines tested, epithelial cells from healthy volunteers showed a significant increase of IFN-β levels, a 112% increase compared to non-infected control, and only a ~30% increase in epithelial cells from COPD patients. Of interest, IFN-β together with IFNα4 are known as the first Type I interferon stimulated genes upon viral infection, responsible for the induction of other interferons (Kovarik et al., 2016). Type I interferon response appears to be detrimental and at the same time protective against bacterial pathogens depending in which part of the body it is induced (Kovarik et al., 2016). In the lung, IFN-β promotes protection against epithelial barrier damage during bacterial infections (Kovarik et al., 2016). The induction of IFN-β during *S. pneumoniae* infection in the respiratory tract of mice reduced the transmigration of bacteria across the epithelium and ultimately to the bloodstream by upregulation of tight junction proteins such as claudin and cadherin, and downregulation of platelet activated receptor (PAF) receptor involved in bacterial endocytosis of epithelial cells (LeMessurier et al., 2013). In addition, mice deficient of the *IFNAR1* $^{-/-}$ gene exhibited enhanced transition of pneumococcus into the bloodstream and developed pneumococcal bacteraemia, despite the increased immune cell recruitment (LeMessurier et al., 2013; Parker et al., 2011). Further, mice pre-treated with IFN-β exhibited increased survival rate after *S. pneumoniae* infection (Weigent et al., 1986). To link the findings of enhanced production of IFN-β in cultures from healthy

individuals following *M. catarrhalis*, but not in cultures from COPD individuals from the current study with the recent discoveries on IFN-β host defence function, further investigations are needed.

Significantly induced MIP-3α / CCL20 in ciliated cultures from COPD patients, a 60% increase compared to non-infected control was detected, while epithelial cells from healthy individuals exhibited a 30% increase only compared to non-infected cultures. This increase is in accordance with gene expression data from undifferentiated Detroit 562 epithelial cells where *M. catarrhalis* induced a 129 fold increase of MIP-3α/ CCL20 mRNA expression (De Vries et al., 2013). De Vries and colleagues also saw an enhanced gene expression of IL-1β, IL-6, IL-8 / CXCL8, IL-17c, GRO-α/ CXCL1, GRO-β/ CXCL2 and CSF3/ G-CSF. In the current study the cytokine data failed to show an increase in IL-1β, GRO-α/ CXCL1 or RANTES/ CCL5 levels following *M. catarrhalis* infection, which is in disagreement with findings in macrophages (Hassan et al., 2012), but in agreement with Rosseau et al who also failed to see induction of IL-1β and RANTES/ CCL5 in epithelial cells (Rosseau et al., 2005). A mild increase (~36%) of IL-8/ CXCL8 was found in COPD cultures, as IL-6 and CSF3/ G-CSF differed with highly induced levels in infected ciliated cultures from COPD patients.

Recently, IL17c, which belongs to the IL-17 family of cytokines, has been suggested to be secreted by epithelial cells and to function in an autocrine manner to mediate immune response, stimulated directly by bacterial products or activated TLR and cytokine (TNF-α and IL-1β) pathways (Ramirez-Carrozzi et al., 2011). IL-17c has been found in my study as a unique cytokine with ~ 3 fold increase following *M. catarrhalis* infection, specifically in ciliated cultures from COPD donors. This in accordance with an *in vivo* study by Alhanas and colleagues, who found *M. catarrhalis* infection exacerbates airway allergic inflammation in house dust mite sensitised mice, primarily by IL-17 and TNF-α (Alhanas et al., 2017). Accordingly, high levels of IL-17 in asthma patients contribute to neutrophilic inflammation and the pathogenesis of the disease by stimulating neutrophil elastase, MMP-9 and recruitment of macrophages (Linden and Dahlen 2014). Conversely, IL-17 receptor deficient mice were shown more susceptible to bacterial infections with *Klebsiella pneumoniae* and *Mycobacterium tuberculosis,* suggesting protective properties of the cytokine (Curtis and Way 2009).

A non-significant increase of 4.4 fold was observed for ENA-78/ CXCL5 protein in ciliated cultures infected with *M. catarrhalis* relative to non-infected cultures from COPD subjects. Only one study has previously reported ENA-78/ CXCL5 to be induced following *M. catarrhalis* infection (Alhanas et al., 2017). ENA-78/ CXCL5 is a neutrophil chemotactic factor, found to be increased in COPD patients, which can mediate the recruitment of neutrophils to the airways and in turn together with neutrophil secreted proteases to cause alveolar destruction (Barnes, 2016). In my study, the cytokine data showed a marked increase of IP-10/ CXCL10 levels and MPC-1/ CCL2, in conjunction with a study by Rosseau, where a similar dose of *M. catarrhalis* ($1x10^5$ CFU/ml), stimulated MCP-1/ CCL2 in alveolar epithelial cells isolated from human lungs. MCP-1/ CCL2 is known to be involved in the recruitment of monocytes and the induction of pulmonary inflammation in COPD (Rosseau et al., 2005).

3.4 Summary

This is the first study to show the initial interaction of *M. catarrhalis* with the ciliated respiratory epithelium. The data demonstrates very rapid binding of *M. catarrhalis* to cilia, which is associated with reduced ciliary function. Preferential *M. catarrhalis* attachment and invasion of differentiated cells from COPD patients is associated at least partly with macropinocytotic events. Addition of *M. catarrhalis* to ciliated cultures from healthy and COPD donors is associated with activation of EGFR and AKT signalling cascades. The inflammatory response to *M. catarrhalis* included largely non-significant induction of pro-inflammatory cytokines, which is consistent with the inflammatory state and exacerbations in COPD patients.

Chapter 4. Rhinovirus interaction with the respiratory epithelium

4.1 Introduction

Rhinovirus frequently causes common colds in healthy individuals associated mainly with upper respiratory symptoms, however, it can also cause lower respiratory tract illnesses such as bronchitis and pneumonia (Bochkov and Gern 2016). It has been suggested children who suffer from wheezing in infancy due to rhinovirus infection are 10 times more likely to develop asthma in later childhood than children who do not wheeze during rhinovirus infections (Jackson et al., 2008). Rhinovirus can also initiate exacerbations in people with asthma and cystic fibrosis (Bochkov and Gern 2016). Rhinovirus is a major cause of severe and prolonged COPD exacerbations and account for 60% of all cases associated with respiratory viruses driven exacerbations (Wedzicha, 2003; Seemungal et al., 2001; George et al., 2014). It is thought rhinovirus infection spreads directly from person to person through infectious respiratory secretions or indirectly through contaminated surfaces (Wedzicha, 2003; Jacobs et al., 2013). Epithelial cells are recognised as the main site of rhinovirus infection, designated as the place of entry and replication (Lopes-Souza et al., 2004; Jacobs et al., 2013, Bochkov and Gern 2016). It has only been recently suggested that rhinovirus has a preferential cell type for infection and appear to target the respiratory epithelium by infecting ciliated cells (Griggs et al., 2017; Tan et al., 2018). The major group of rhinoviruses (types A and B) are thought to enter host cells intracellularly via binding to the ICAM-1 receptor that is present on the plasma membrane of airway epithelial cells. However, the ICAM-1 receptor has not been found present on ciliated or squamous epithelial cells (Winther et al., 1997). ICAM-1 expression has been shown to become upregulated upon rhinovirus infection in human bronchial epithelial cells via increased NF-kB transcription (Papi and Johnston 1999).

Upon infection, rhinovirus induces an inflammatory host response, characterised by signalling via TLRs and stimulation of release of a range of cytokines and chemokines, interferons and growth factors, collectively contributing to cellular inflammation (Bochkov and Gern 2016). Several experimental rhinovirus studies and *in vitro* experiments with cultured epithelial cells have confirmed rhinovirus initiates a strong Type I and type III interferon epithelial response in conjunction with the cytokines- RANTES/ CCL5, IL-6, IL-8/ CXCL8, IP-10/ CXCL10 and ENA-78/ CXCL5 (Papadopoulos et al., 2000; Wark et al., 2009; Jacobs et al., 2013; Mallia et al., 2014,

George et al., 2014; Bochkov and Gern 2016). In addition to activating TLRs *e.g.* TLR3 and TLR7, rhinovirus activates the PI3K pathway, leading to NF-kB transcription of cytokines including high IL-8/ CXCL8 expression, which is known to have a detrimental effect on COPD pathogenesis by recruiting neutrophils (Newcomb et al., 2005; Bentley et al., 2006; Bochkov and Gern 2016).

The phosphoinositides (PI) are present in the plasma membranes of many cell types across different tissues and are involved in cellular signalling and cascades as second messengers (Winkler et al., 2013). The lipid kinases involved in the generation of different PIs from phosphatadylinositols (PtdIns) are known as the PI3K family. In response to extracellular signals the PI3 kinase phosphorylates PtdIns and PIs at position 3 of the inositol ring to produce phosphatidylinositol-3-monosophoshate (PI3P), phosphadylinositol-(4,5)-bisphosphate ($PI(3,4)P_2$) and phosphatidylinositol-3,4,5-triphosphate ($PI(3,4,5)P_3$) (Winkler et al., 2013). In addition, the inositol ring of PtdIns and PIs can also be phosphorylated by phosphoinositide kinases at positions 4 and 5, producing phosphatidylinositol-4 phosphate (PtdIns(4)P or P4P) and phosphatidylinositol-5 phosphate (PtdIns(5)P or P5P). All of these signalling lipids are important for correct cellular function and maintenance including cell growth, proliferation, survival, cytoskeleton rearrangement, intracellular organelle trafficking, and the recruitment and activation of immune cells (Stokes and Condliffe 2018).

The PI4P lipid is employed specifically in Golgi apparatus function and intracellular trafficking, and its generation is dependent on the phosphatidylinositol – 4 (PI4) kinases PI4KIIα and PI4KIIIβ which regulate membrane transport from the trans-Golgi network to the plasma membrane (Tokuda et al., 2014). It has been recently reported that picornaviridae and flaviviruses utilise PI4KIIIβ enzymes and PI4P lipids for the formation of replication enriched platforms which serve as replication complexes in infected cells (Altan-Bonnet and Balla 2012; Ilnytska et al., 2013; Hsu et al., 2010). When RNA viruses hijack PI4K enzymes, they can enhance the production of PI4P lipids at the Golgi network and together with viral replication proteins and host cells molecules, build a machinery for efficient viral synthesis (Altan-Bonnet and Balla 2012; Hsu et al., 2010).

Current research on rhinoviruses is focused on whether they target the respiratory epithelium and induce a heightened host inflammatory response, contributing to amplification of inflammation which has a deteriorating effect on lung function and structure (Baines et al., 2013; Schneider et al., 2013). However, most of the investigations in the field have involved epithelial cell lines, which may not particularly

be informative of the precise biology of human host-pathogen interactions (Edwards et al., 2006; Lopez-Souza et al., 2004; Papadopoulos et al., 2000). Therefore, investigation of the ciliated pseudostratified epithelium, more closely resembling that found in the human airways, is needed to explore rhinovirus infection in healthy and COPD subjects. Studies are now needed to determine why rhinovirus shows a preference for infection of a specific cell type, how this affects the epithelial barrier function and how the virus replicates to produce a strong pro-inflammatory response.

4.1.1 Hypotheses

Rhinovirus replication is increased in cultures from COPD donors differentiated to a ciliated phenotype compared to cultures from healthy volunteers differentiated to a ciliated phenotype.

Rhinovirus infection of ciliated cultures from COPD donors promotes a greater inflammatory response than that seen in cultures from healthy individuals.

4.1.2 Aims

1. To investigate the early initial stages of rhinovirus interaction with the respiratory ciliated epithelium and to assess the epithelial ciliary function of differentiated cultures.

2. To investigate the effect of rhinovirus infection on epithelial barrier function in ciliated cultures from healthy and COPD individuals.

3. To investigate rhinovirus replication in differentiated cultures and the effect of a PI4KIIIβ inhibitor (GSK2998533) during rhinovirus infection.

4. To determine if the inflammatory response to rhinovirus infection in COPD differentiated cells differs from that in healthy differentiated cells.

4.1.3 Characteristics of patients

A total of 13 healthy and 10 COPD nasal samples were used to create cultures which I was able to differentiate into a mucociliary phenotype for rhinovirus infection studies. The baseline clinical characteristics of healthy volunteers and COPD patients are summarised in Table 3-1 in chapter 3 and also Supplementary Table 1 in Appendix 1. Ciliated cultures from a COPD bronchial epithelial sample were supplied by the Refractory Respiratory and Inflammation discovery unit at GSK, Stevenage. Airway bronchial COPD basal cells were initially obtained from Epithelix, Switzerland and differentiated in house using PneumaCult™ (ALI media, Stemcell™ technologies, UK).

4.1.4 Nasal and bronchial primary cultures

All experiments in chapter 4 were carried out with nasal differentiated epithelial cells except the following experiments, which used bronchial differentiated epithelial cells.

Table 4-1: Human bronchial epithelial cell cultures used in rhinovirus single studies.

Group	Experiment	Assay	Figure
COPD	7 day rhinovirus infection	Titration assay	In text results
COPD	7 day rhinovirus infection	High speed video microscopy- ciliary beat frequency	In text results
COPD	7 day rhinovirus infection	High speed video microscopy- ciliary activity	In text results
COPD	PI4KIIIβ inhibition of rhinovirus replication	Titration assay	In text results

4.2 Results

4.2.1 Rhinovirus targets the ciliated cells in the respiratory epithelium during infection

To visualise the respiratory epithelium during the early stages of rhinovirus infection, human nasal cultures differentiated at ALI for 30-50 days, were inoculated with $1.5x10^6$ $TCID_{50}$/ml rhinovirus for 1 hour after which the inoculum was removed to allow progression of the infection for another 24h at air-fluid interface. The time-points of immunostaining were chosen based on literature suggestions that rhinovirus replicates rapidly in epithelial cells within 6h of infection and that viral replication peaks at 24h – 48h of infection (Johnston et al., 2003; Winther et al., 1990; Papadopoulos et al., 2000).

At 6h post infection, the human nasal epithelial cells were immunofluorescently labelled with antibodies for β-tubulin, VP2 and Hoechst solution to visualise the ciliated cells, rhinovirus and cell nuclei. Rhinovirus staining appeared mainly in ciliated cells, predominantly localised on the apical surface of the cultures, determined by Z-stack imaging (Figure 4-1 A). Fixed epithelial cells infected with rhinovirus at 6h did not appear to be adversely affected by the rhinovirus and no evident structural changes of the respiratory epithelium were observed at the time of imaging. The epithelium appeared uniform and non-disrupted, similar to mock-infected differentiated cultures (Figure 4-1 A and B).

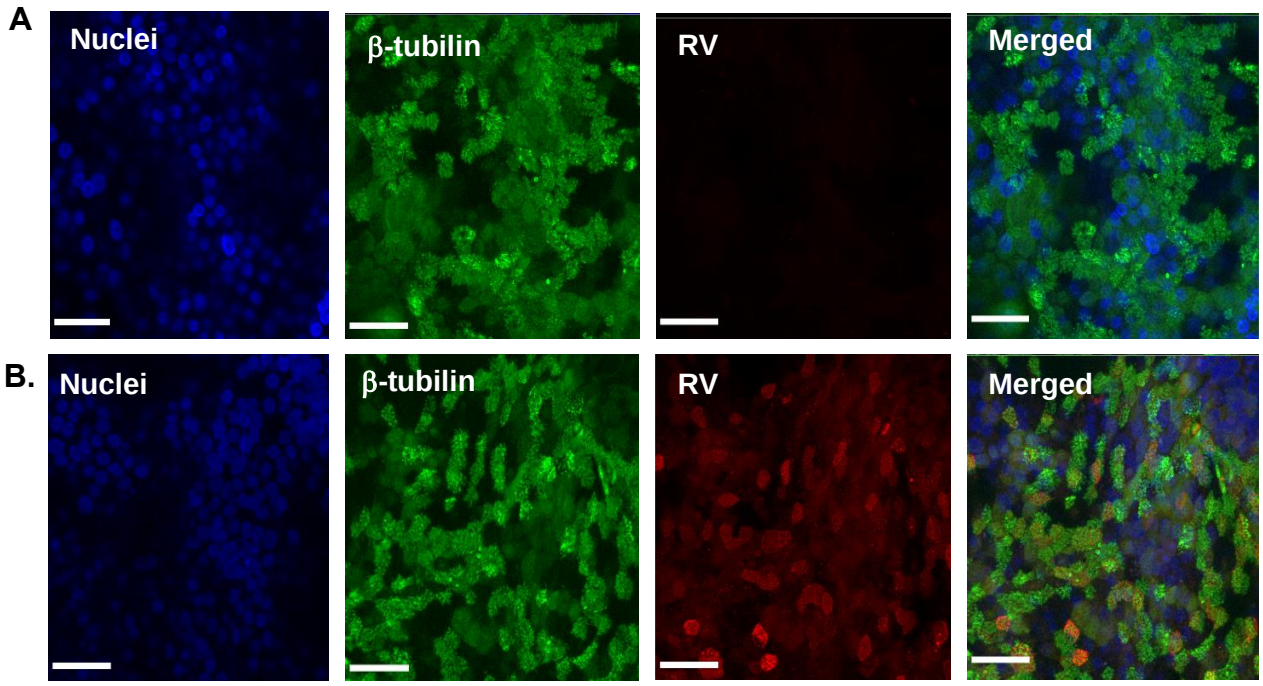

Figure 4-1 Immunofluorescence staining of airway epithelial cultures at 6h post rhinovirus infection.

A) Healthy uninfected epithelial layer imaged at 6h by a confocal microscope; B) Healthy epithelial layer infected with rhinovirus at 6h post infection imaged by a confocal microscope. Cilia are stained by anti- β-tubulin antibody in green, rhinovirus by anti- VP2 antibody in red, nuclei with Hoechst solution in blue. Scale bars for all images = 20μm.

To examine the differences of rhinovirus infection between healthy and COPD airway cells, epithelial cultures from the two groups were immuno-labelled with anti- β-tubulin and anti-VP2 antibodies, and imaged by a confocal microscope. Prior to immunofluorescence, high speed video microscopy experiments were designed to understand and monitor any cytotoxic/ cytopathic effects of rhinovirus on the differentiated cultures such as ciliary function and TEER change. Initially, rhinovirus infection was studied for 24h in ciliated cultures from healthy and COPD donors, with some experiments being prolonged for additional 24h.

Immunofluorescent staining of rhinovirus infected differentiated cultures from healthy and COPD donors at 24h (Figure 4-2) revealed that the viral infection was no longer localised predominantly to ciliated cells, but had spread to other cell types, showing that rhinovirus had established a widespread infection of the epithelium. In the non-infected cultures from healthy individuals the epithelium had cobblestone appearance with brightly fluorescent cilia clearly seen (Figure 4-2 A). However, following infection the cobblestone epithelium appeared with a significant change in the morphology of the epithelium. Staining of rhinovirus was no longer localised to ciliated cells (Figure 4-2 B). In COPD cells there was less cilia appearance and the cobblestone appearance was not observed (Figure 4-2 C). Following infection, there appeared to be a loss of ciliated cells and a suggestion that non-ciliated cells were also infected (Figure 4-2 D).

To characterise the dynamics of rhinovirus infection of the respiratory epithelium at the early time-points of infection more clearly, high speed video microscopy of epithelial cultures was carried out over 24 hours. Ciliated cells were observed to shed from the epithelium as early as 6h post infection. Shedding of epithelial cells gradually increased during the 24h time period. The phenomenon was observed in epithelial cultures from the healthy and COPD groups. Observational analysis of high speed videos revealed that the cilia of ciliated cells that had been shed from the epithelium continued to beat initially, but beating seen decreased over time stopping completely by 24h. When observed again at 48h of infection no cilia were seen to beat on detached cells. At 18h following infection (Figure 4-2 C), many rounded epithelial cells were observed detached from the epithelial layer. High speed video microscopy analysis did not allow the nature of the underlying epithelium to be visualised clearly. In summary, immunofluorescence and high speed video microscopy confirmed rhinovirus preferentially targets ciliated cells in the early time-points of infection and causes shedding of ciliated cells from the epithelium (Figure 4-2 E).

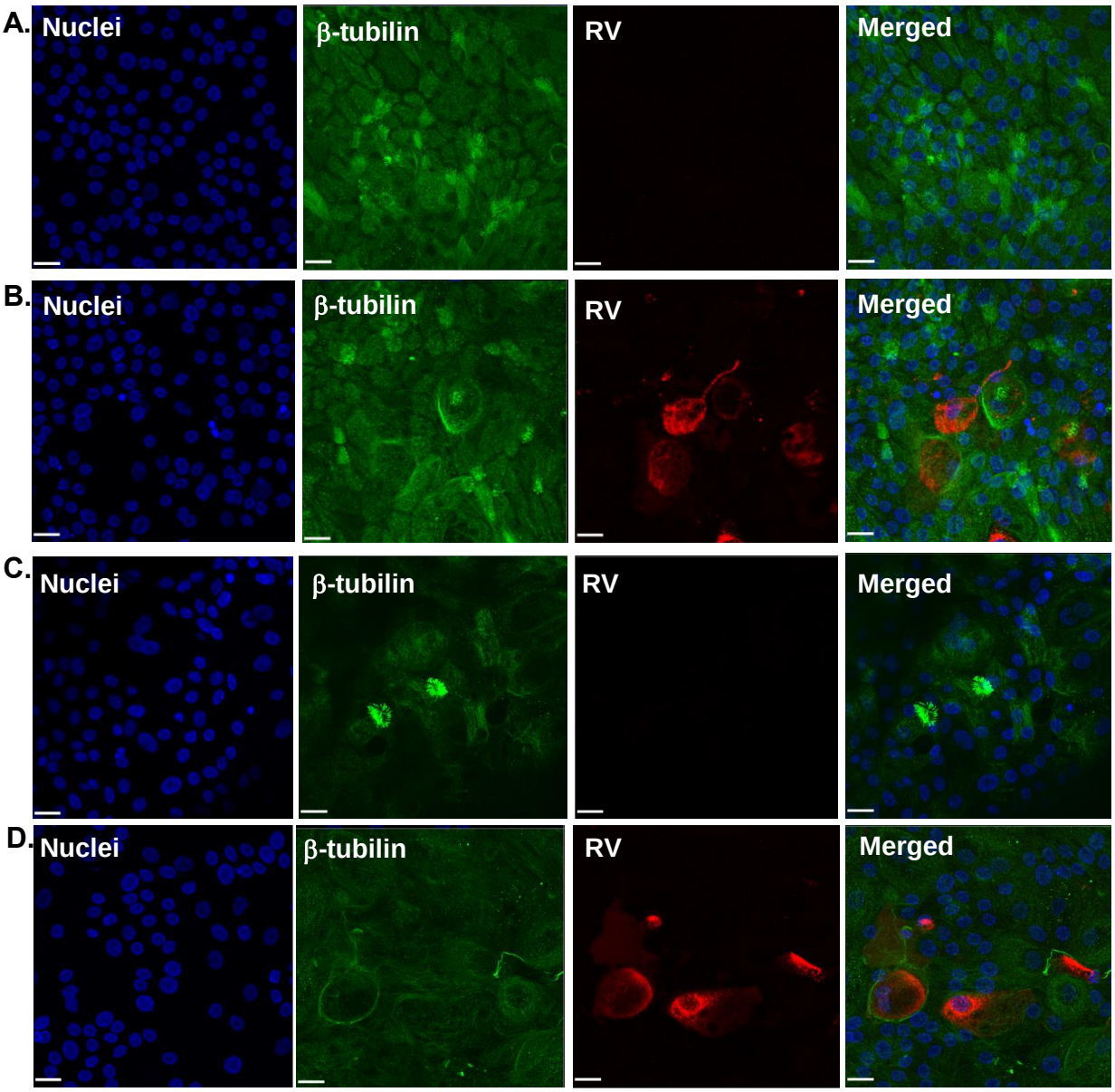
A.
Nuclei
β-tubilin
RV
Merged
B.
Nuclei
β-tubilin
RV
Merged
C.
Nuclei
β-tubilin
RV
Merged
D.
Nuclei
β-tubilin
RV
Merged

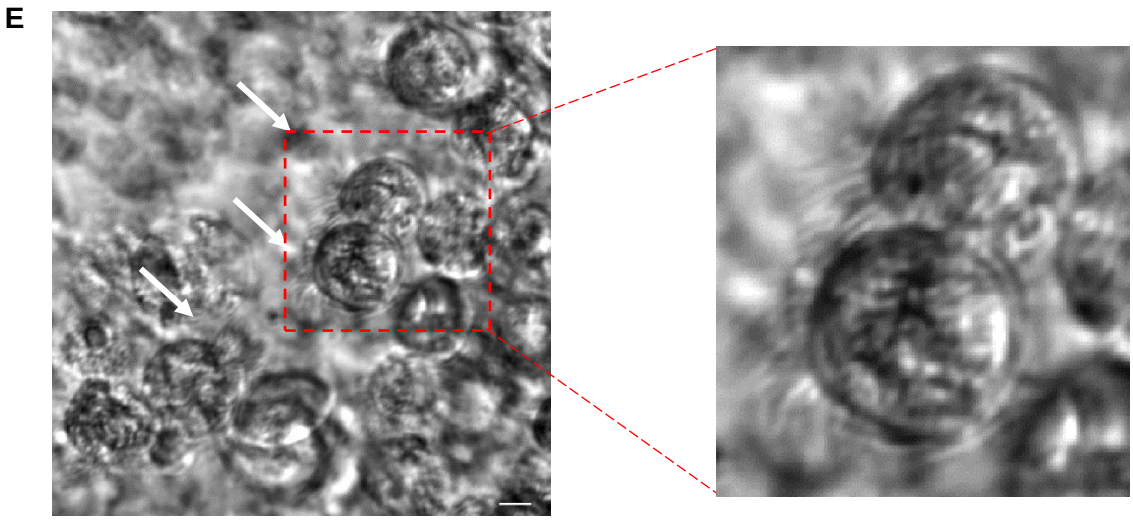

Figure 4-2: Rhinovirus infection of the ciliated epithelium at 24h.

A) Healthy epithelial layer control non-infected; B) Healthy epithelial layer infected with rhinovirus for 24h; C) COPD epithelial layer control non-infected: D) COPD epithelial layer infected with rhinovirus for 24h. A – D cilia are stained for β-tubulin in green, rhinovirus for VP2 in red, nuclei were stained with Hoechst solution in blue. Scale bars for all images = 20μm. E) A screenshot of a high speed video of a COPD epithelium infected with rhinovirus, imaged at 18h post infection, white arrows point at detached ciliated cells from the epithelial layer, scale bar = 10μm

4.2.2 Ciliary function of ciliated cultures following rhinovirus infection

High speed video microscopy allowed the examination of the first cytotoxic effects of rhinovirus on the epithelial layer. Videos of 10 pre-selected areas in airway cultures from 3 healthy and 3 COPD donors were included in the analysis of ciliary activity following 24h of rhinovirus infection. Videos of 10 pre-selected areas in ciliated cultures from 6 healthy and 6 COPD donors were included in the analysis of CBF following 24h rhinovirus infection. Rhinovirus significantly reduced the areas of active ciliary beating over 24 hours (Figure 4-3). A significant reduction in ciliary activity was seen between non-infected controls and infected cultures from healthy donors ($p< 0.0001$) and COPD donors ($p<0.05$) (Figure 4-3 A). Reduction in ciliary activity following rhinovirus infection was also evident by eye, in the cultures from the healthy and COPD groups, the majority of detached epithelial cells were ciliated cells. In epithelial cultures from healthy individuals, there was a non-significant increase in the CBF of rhinovirus infected cultures compared to non-infected cultures mean ± SEM: 10.5 ± 0.8 Hz vs 9.4 ± 0.9 Hz respectively ($p=0.2$). In cultures from COPD donors,

the CBF of rhinovirus infected cultures was similar to non-infected cultures mean ± SEM: 8.2 ± 1 Hz vs 8.1 ± 1 Hz respectively (p=0.89) (Figure 4-3 B). The differences did not reach significance in either group. These results indicate that shedding of ciliated cells from the epithelium results in significantly decreased ciliary activity of epithelial cultures from healthy and COPD donors. However, the CBF of cilia in cells that were not shed from the epithelium was not significantly affected by rhinovirus infection. CBF of the control cultures from healthy individuals and COPD patients were similar to each other (p=0.5).

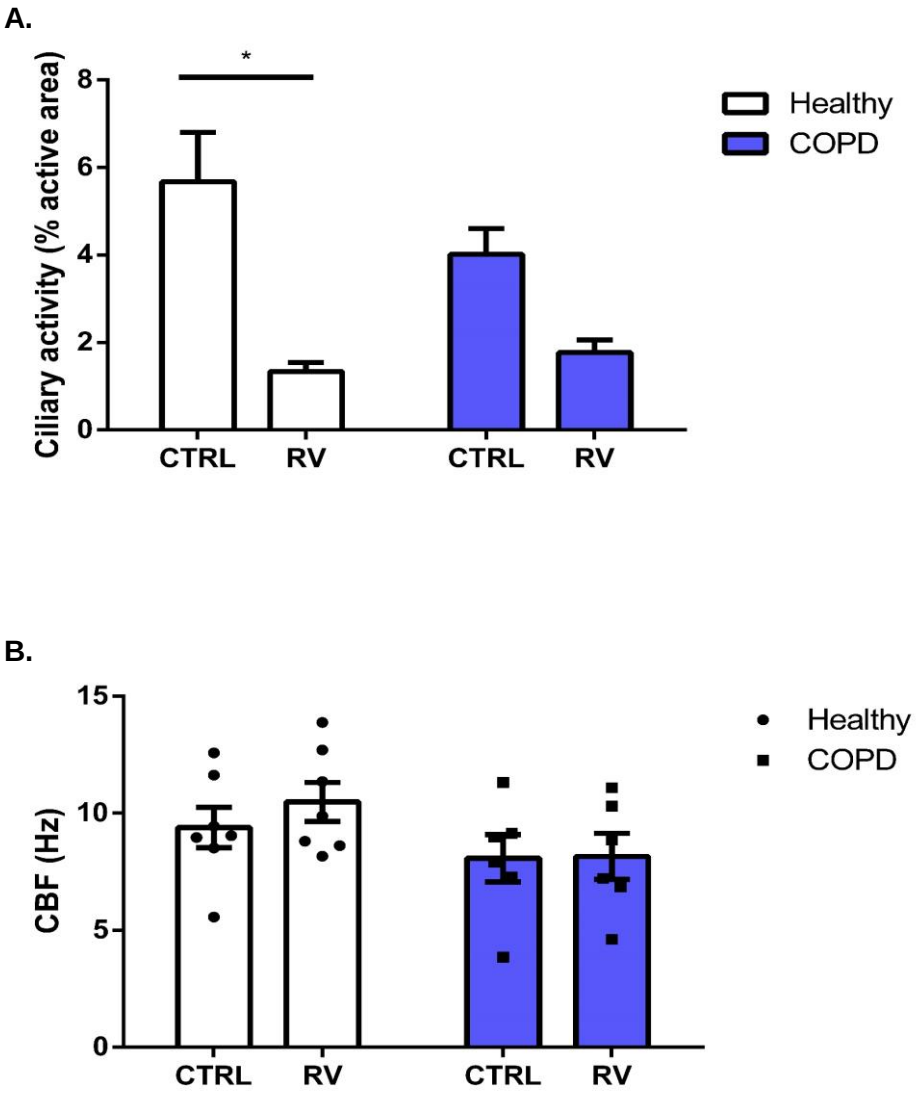

Figure 4-3: Ciliary function of rhinovirus infected epithelial cultures at 24h.
A) Ciliary activity of ciliated cultures expressed as % active area following rhinovirus infection, n=10 areas/ donor, 3 healthy and 3 COPD donors; B) Ciliary beat frequency of ciliated cultures following rhinovirus infection, n=10 areas/ donor, 6 Healthy and 6 COPD donors, error bars represent ±SEM, *=p<0.05, CBF-ciliary beat frequency

4.2.3 Rhinovirus replication in ciliated cultures at 24h

Having established that rhinovirus sheds off airway cells from the epithelium, the live virus titre was then investigated. To assess the viral replication in ciliated cultures from healthy and COPD individuals, rhinovirus infection was allowed for 24h, after which apical washes of epithelial cells and epithelial cells were collected. We measured rhinovirus titre in apical washes and epithelial cells. This was done for nasal epithelial cultures from 6 healthy and 6 COPD donors. Viral titres in the apical washes were quantified to determine if there was release of virus into the apical fluid that may enhance cell to cell spread. The mean ± SEM rhinovirus titre in healthy apical washes was $5.5x10^3 \pm 2.6x10^3$ $TCID_{50}$/culture and in COPD apical washes was $3.3x10^3 \pm 1.4x10^3$ $TCID_{50}$/culture. This difference did not reach significance (p=0.56) (Figure 4-4 A). Although the mean ± SEM rhinovirus titres in COPD epithelial cells were increased compared to healthy epithelial cells: $3.1x10^4 \pm 1.6x10^4$ $TCID_{50}$/culture and $2.3x10^4 \pm 4x10^3$ $TCID_{50}$/culture, respectively, this did not reach significance (p=0.56) (Figure 4-4 B). The mean ± SEM combined rhinovirus titre from apical washes and from epithelial cells in healthy was $2.9x10^4 \pm 3.4x10^3$ $TCID_{50}$/culture and $3.5x10^4 \pm 1.7x10^4$ $TCID_{50}$/culture in COPD (p=0.46) (Figure 4-4 C).

To examine whether rhinovirus alters epithelial integrity, TEER was measured in virus infected and non-infected epithelial cell cultures. Differentiated cultures from healthy individuals and COPD donors had a mean ± SEM TEER of 825 ± 52 Ω/cm^2 and 770 ± 36 Ω/cm^2, respectively. The cultures were flooded apically with a rhinovirus inoculum. After 1h of infection, the media was removed and the infection allowed to progress for another 24h at ALI. Voltmeter readings indicated that in the first 24h of infection, rhinovirus did not decrease TEER in cultures from either healthy (p=0.77) or COPD donors (p=0.69). Of interest, at 24h TEER readings from non-infected cultures of COPD donors were lower than those of non-infected cultures from healthy individuals (p=0.76) (Figure 4-4 D). The mean ± SEM TEER values at 24h of non-infected cultures from healthy individuals was 691 ± 241 Ω/cm^2 compared to 463 ± 139 Ω/cm^2 of non-infected cultures from COPD donors.

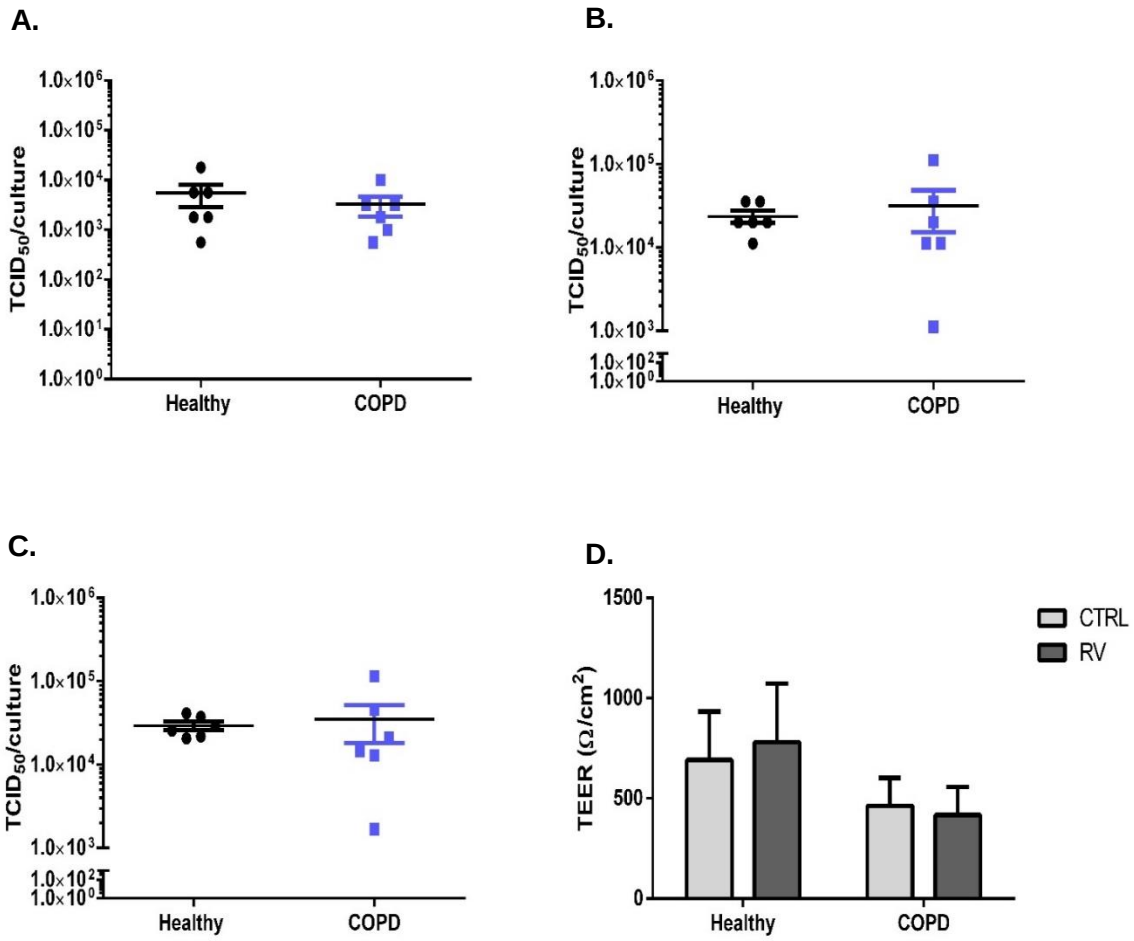

Figure 4-4: Rhinovirus replication in ciliated cultures at 24h post infection.

A) Live rhinovirus released in the apical washes of ciliated cultures, B) Intracellular live rhinovirus in ciliated cultures from healthy (black) and COPD (blue) donors; C) Combined intracellular and released live rhinovirus titre in ciliated cultures from healthy and COPD donors; D) TEER of epithelial cultures measured at 24h post infection, n=6 Healthy and 6 COPD donors, error bars represent ±SEM.

4.2.4 7 days rhinovirus infection of ciliated cultures

4.2.4.1 Rhinovirus replication in ciliated cultures over 7 days

Initial rhinovirus experimental studies were carried out for 24h only. Longer term viral infection of ciliated cultures from healthy and COPD donors was then studied over 7 days and epithelial integrity, ciliary activity and function, and rhinovirus load were assessed. To assess whether rhinovirus replication reduced or increased during this study, and whether there was a difference between the healthy and COPD groups, live viral replication was quantified in cell lysates by titration assays (section 2.3.2.2). Changes in rhinovirus titre over 7 days of infection were examined in ciliated cultures from 5 healthy and 4 COPD donors. The mean ± SEM rhinovirus loads at day 1 for cultures from healthy donors was $6x10^4 \pm 5x10^3$ $TCID_{50}$/culture and for cultures from COPD donors was $3x10^5 \pm 1.4x10^5$ $TCID_{50}$/culture which was 3.7 fold higher than in healthy ($p=0.18$) (Figure 4-5 A). As infection progressed, viral load gradually decreased. A significant reduction of replicating live virus, compared to day 1, was found in cultures from healthy individuals at day 2 ($p=0.011$), at day 3 ($p<0.001$) and day 7 ($p<0.001$) and in cultures from COPD donors at day 2 ($p<0.01$), at day 3 ($p<0.001$) and at day 7 ($p<0.001$). Viral load in ciliated cultures was mostly eliminated by day 7, the mean ± SEM load at day 7 was $2.8x10^2 \pm 1.6x10^2$ $TCID^{50}$/culture in healthy and $2.7x10^1 \pm 1.5x10^1$ $TCID_{50}$/culture in COPD. Significant differences between the healthy and COPD groups were not found at any of the different days of infection. These findings suggest that rhinovirus viral expression peaks at 24h and is almost eliminated by day 7 with the respiratory epithelium playing a pivotal role in the resolution of the virus infection.

To investigate further the capacity of rhinovirus to damage epithelial barrier function in longer term infections, the TEER of epithelial cultures was measured in airway epithelial cells treated with plain media that served as mock controls and in airway epithelial cells infected with rhinovirus. TEER measurements were taken prior to infection and before cells were sacrificed for viral titre analyses. The results of epithelial integrity are therefore expressed as fold decrease, relative to pre-infection levels. Rhinovirus reduced the TEER of cultures from healthy individuals by 60% over 7 days of infection (Figure 4-5 B) and by 50% in cultures from COPD donors (Figure 4-5 C), though no statistical significance was observed at the different time points or between infected and non-infected cultures. Epithelial integrity was lower in infected cultures for both groups at day 7 post infection compared to non-infected cultures.

To confirm the findings from nasal airway epithelial cells, bronchial COPD ciliated cells were infected for 7 days with rhinovirus. Only one experiment was possible with bronchial cells due to tissue availability. A similar trend to that found in the nasal epithelium was observed. Reduction in rhinovirus replication in bronchial ciliated cells was seen with titres - $1.12x10^5$ $TCID_{50}$/culture at day 1, $1.12x10^4$ $TCID_{50}$/culture at day 2, $3.5x10^3$ $TCID_{50}$/culture at day 3 and $2x10^2$ $TCID_{50}$/culture at day 7.

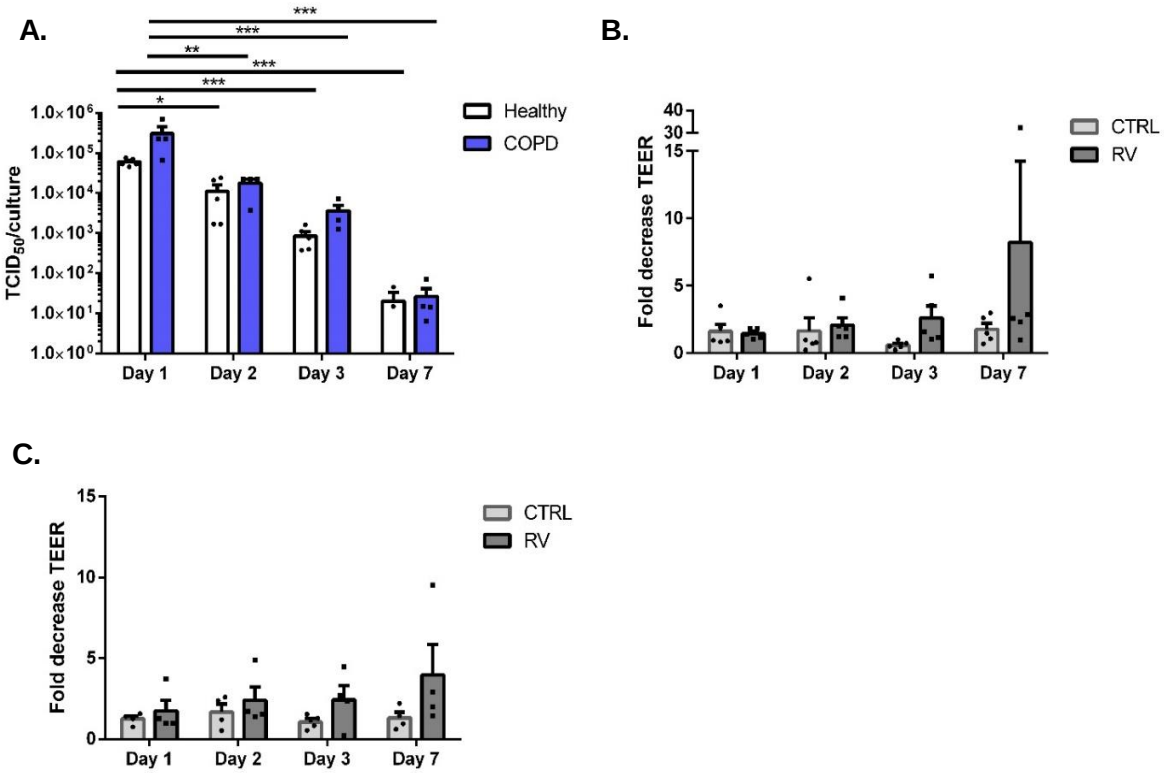

Figure 4-5: Rhinovirus replication during a 7 day infection of ciliated cultures from healthy individuals and COPD donors.

A) Live rhinovirus titre in nasal airway cultures at days 1, 2, 3 and 7 post infection, n=4 healthy and 4 COPD; B) TEER of nasal airway cultures from healthy volunteers at days 1, 2, 3 and 7 expressed as fold change relative to day 0 measurements, n=4 healthy and 4 COPD; C) TEER of nasal airway cultures from COPD donors at days 1, 2, 3 and 7 expressed as fold change relative to day 0 measurements, n=4 healthy and 4 COPD; error bars represent ±SEM, *=p<0.05, **=p<0.01, ***=p<0.001.

4.2.4.2 Ciliary function during 7 days of rhinovirus infection

4.2.4.2.1 Ciliary activity of ciliated cultures

To determine the effect of ciliary activity over time (Figure 4-6 A), high speed videos of infected cultures were recorded on days 1, 2, 3 and 7 using the same donor well to minimise the variation of ciliation levels between different wells. Ciliary activity in epithelial cultures infected with rhinovirus gradually decreased over 7 days. Marked reduction in ciliary activity was observed at the different days of infection between infected and non-infected cultures from healthy volunteers, however, statistical significance was not reached ($p=0.53$ at day 1, $p=0.69$ at day 2, $p=0.32$ at day 3, $p=0.09$ at day 7) (Figure 4-6 A). A marked decrease of ciliary activity was also observed in cultures from COPD donors at days 1, 2, 3 between infected and non-infected cultures ($p=0.09$ at day 1, $p=0.26$ at day 2, $p=0.09$ at day 3), however the reduction of ciliary activity reached significance only at day 7 ($p< 0.01$) (Figure 4-6 B).

To obtain more quantitative measurement of ciliation following rhinovirus infection, western blots of 3 rhinovirus infected and 3 non-infected airway cultures from healthy and COPD donors were performed to determine the relative expression of the ciliary specific protein DNAI2. Its expression was measured by normalising to internal GAPDH house-keeping control expression. DNAI2 expression was observed as reduced at day 1 of infection, compared to the mock treated control, reaching its lowest expression at day 7 for infected cultures for both healthy and COPD (Figure 4-6 C and D). In infected cultures from healthy subjects, DNAI2 expression was significantly reduced compared to mock infected cultures at day 3 ($p<0.001$) and at day 7 ($p<0.01$) (Figure 4-6 C). Further, a significant decrease of DNAI2 expression was measured between days 1 and 7 ($p=0.02$) and between days 2 and 7 ($p=0.014$). In cultures from COPD donors a significant reduction of DNAI2 expression between infected and non-infected cultures was also observed at day 3 ($p=0.03$) and at day 7 ($p=0.01$). Expression of DNAI2 in rhinovirus infected cultures from COPD donors was non-significantly reduced between different days of infection ($p=0.38$ at day 1 vs day 2, $p=0.53$ at day 1 vs day 3, $p=0.22$ at day 1 vs day 7, $p=0.86$ at day 2 vs day 3, $p=0.85$ at day 2 vs day 7, $p=0.65$ at day 3 vs day 7). Blot membrane images of DNAI2 relative expression of cultures from healthy (Figure 4-6 E) and COPD (Figure 4-6 F) individuals are representative of 3 donors from each group.

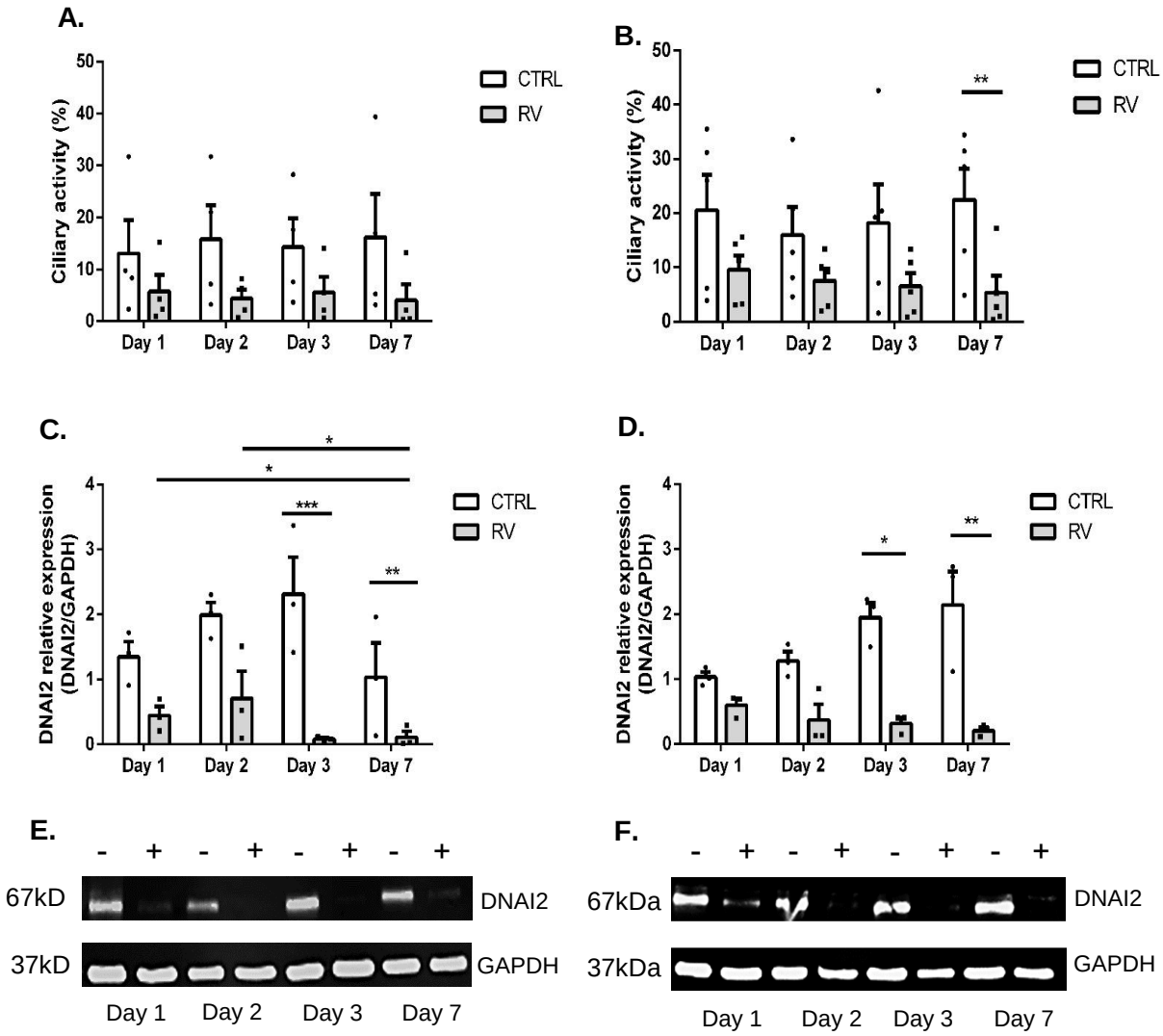

Figure 4-6: Ciliary activity during 7 day rhinovirus infection of ciliated cultures from healthy individuals and COPD donors.

A) Ciliary activity of ciliated cultures from healthy individuals at days 1, 2, 3 and 7 post infection, n=4/ group; B) Ciliary activity of ciliated cultures from COPD individuals at days 1, 2, 3 and 7 post infection, n=4/ group; C) DNAI2 expression relative to GAPDH expression in ciliated cultures from healthy individuals at days 1, 2, 3 and 7 post infection; D) DNAI2 expression relative to GAPDH expression in ciliated cultures from COPD individuals at days 1, 2, 3 and 7 post infection; E) Representative images of DNAI2 expression in cultures from healthy individuals from densitometry analysis; F) Representative images of DNAI2 expression in cultures from COPD individuals from densitometry analysis, error bars represent ±SEM, *=p<0.05, **=p<0.01, ***=p<0.001.

4.2.4.2.2 CBF of ciliated cultures

To investigate if long term rhinovirus infection affects the beating of airway ciliated cells, high speed videos of mock controls and rhinovirus infected cultures from healthy and COPD donors were recorded in the same donor wells during days 1, 2, 3 and 7. CBF of infected cultures from healthy individuals was similar to that of non-infected cultures at day 1 (Figure 4-7 A). The mean ± SEM CBF of cultures from healthy individuals was decreased following rhinovirus infection compared to non-infected at day 2 from 9.5 ± 1.3 Hz to 6.7 ± 0.4 Hz and at day 3 from 9.3 ± 0.5 Hz to 6.6 ± 1.1 Hz (Figure 4-7 A), however significance was not reached. In ciliated cultures from COPD patients, rhinovirus infection significantly reduced CBF for 7 days. The mean ± SEM CBF of rhinovirus infected cultures at day 1 was 11.8 ± 1.43 Hz and at day 7 was 7.5 ± 0.6 Hz ($p=0.01$). The mean ± SEM CBF of rhinovirus infected cultures at day 2 was 11.1 ± 1 Hz and at day 7 was 7.5 ± 0.6 Hz ($p=0.04$) (Figure 4-7 B). No significant differences were observed between infected and non-infected cultures at the different days.

To observe if rhinovirus infection for 7 days affected ciliary function and ciliation of lower airway cells, bronchial COPD ciliated cells were infected with rhinovirus for 7 days. Only one experiment with bronchial ciliated cells was carried out due to availability of tissue. Rhinovirus reduced the beat frequency of bronchial ciliated cultures in comparison to mock infected cultures from 11.1 Hz to 7.3 Hz at day 1, 8.8 Hz to 6.3 Hz at day 2, 9.7 Hz to 6.4 Hz at day 3 and 6.8 Hz to 6.5 Hz at day 7. Rhinovirus reduced the ciliary activity of bronchial ciliated cells from 41% of culture area with beating cells at day 1 to 6% at day 7.

Collectively, the findings from long term rhinovirus infection, suggest that rhinovirus alters the integrity of epithelial cultures, associated with shedding of ciliated cells, reduced ciliary beat frequency and ciliary activity of the epithelium to a level whereby either no ciliated cells were seen or just occasional few ciliated cells are left at the epithelium.

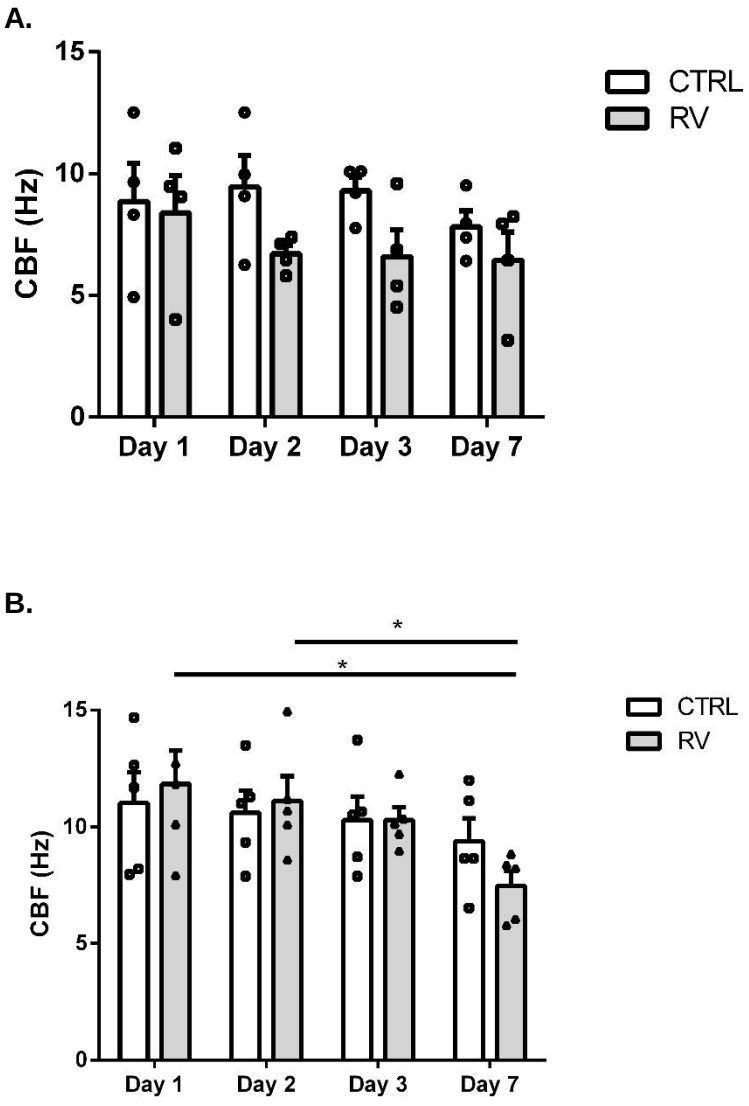

Figure 4-7: Ciliary beat frequency during 7 day rhinovirus infection of ciliated cultures from healthy and COPD individuals.

A) Ciliary beat frequency of nasal ciliated cultures from healthy individuals at days 1, 2, 3 and 7 post infection, n=4/group; B) Ciliary beat frequency of nasal ciliated cultures from COPD individuals at days 1, 2, 3 and 7 post infection, n=4/group; error bars represent ±SEM

4.2.5 Apoptosis in rhinovirus infected cultures

To investigate how airway ciliated cells were shed from the epithelium, apical washes from mock or rhinovirus infected cultures were collected at 24h post infection. Epithelial cells from the washes were labelled with Annexin V dye and Zombie UV dye to determine whether shedding occurred via apoptosis, a well-known mechanism of programmed cell death (Lotzerich et al., 2018). The high number of ciliated cells collected from apical washes of infected cultures suggests that the reduction in ciliary activity, on inspection, and DNAI2 protein expression was due to detachment of the ciliated cells from the epithelium.

Epithelial cells which are Annexin V FITC positive, UV zombie dye negative are identified as early apoptotic. Annexin V FITC and UV zombie dye positive cells are identified as late apoptotic. Annexin V FITC and UV zombie dye negative epithelial cells are considered as viable and UV zombie dye positive epithelial cells as necrotic. The cell counts from 4 healthy and 4 COPD apical washes revealed a consistent increase of detached airway cells in rhinovirus infected cultures compared to mock infected cultures (p=0.61, healthy and p=0.14, COPD) (Figure 4-8 C). Consistent with increased number of shed epithelial cells in the rhinovirus infected cultures, the count of detached ciliated cells from detached cell populations of infected cultures was also higher compared to mock controls, 37% vs 2% in healthy and 26% vs 6% in COPD (Figure 4-8 D). Interestingly, detached Annexin V positive cells were increased in rhinovirus infected cultures compared to mock infected cultures (p=0.14, healthy and p=0.61, COPD) (Figure 4-8 E and F). In addition, 45% of detached Annexin V positive cells in infected cultures from healthy individuals and 37% of detached Annexin V positive cells in infected cultures from COPD individuals were ciliated (Figure 4-8 E and F). In comparison to mock control, rhinovirus non-significantly increased the number of detached ciliated Annexin V positive cells in cultures from healthy individuals (p=0.14) and COPD individuals (p=0.25) (Figure 4-8 E and F). The findings suggest that rhinovirus selectively targets ciliated cells, causing detachment from the epithelium and apoptosis.

A.

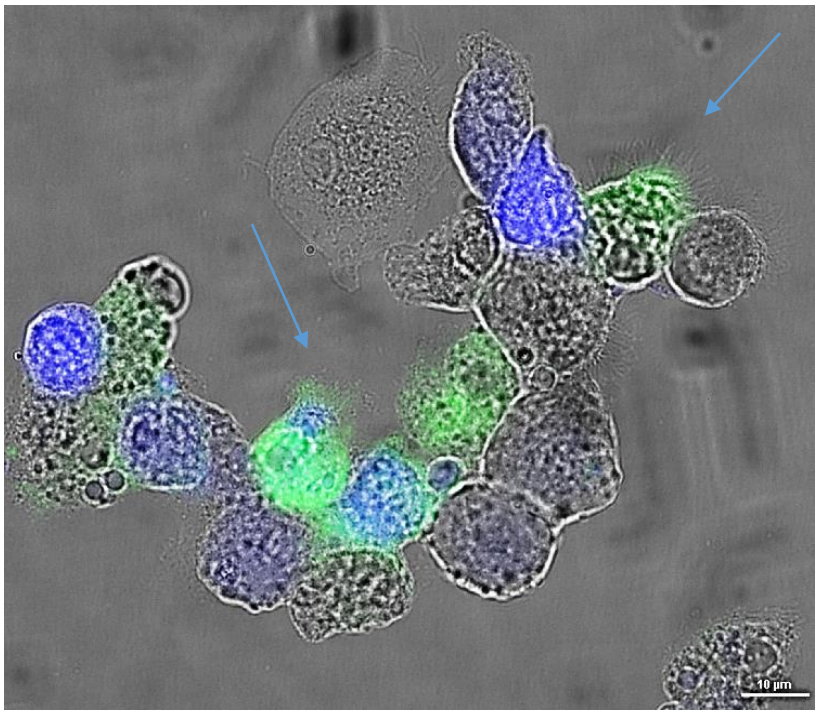

B.

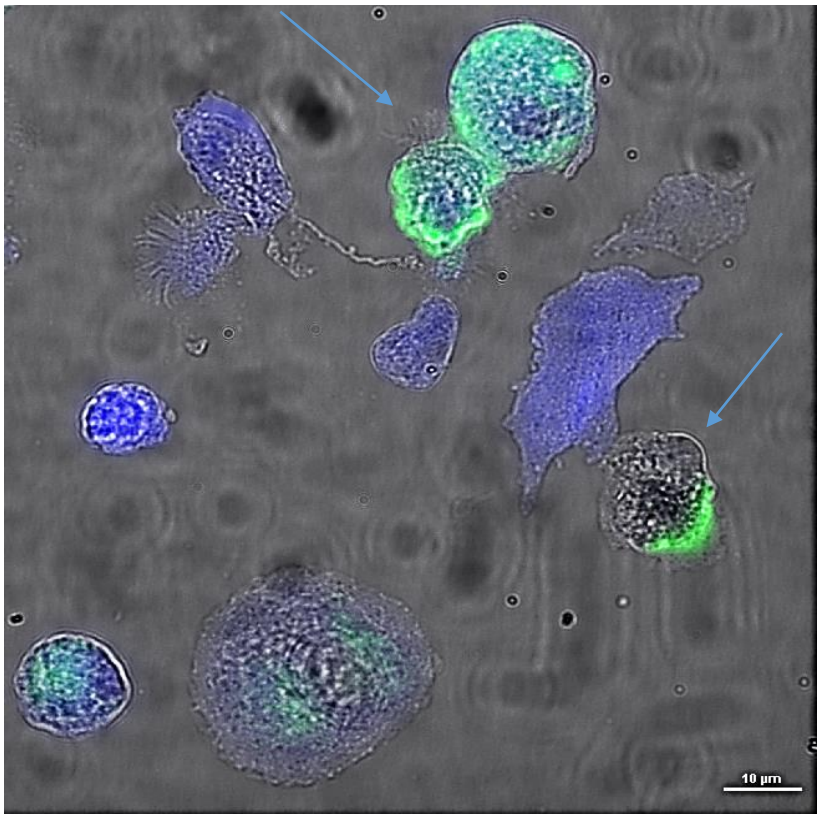

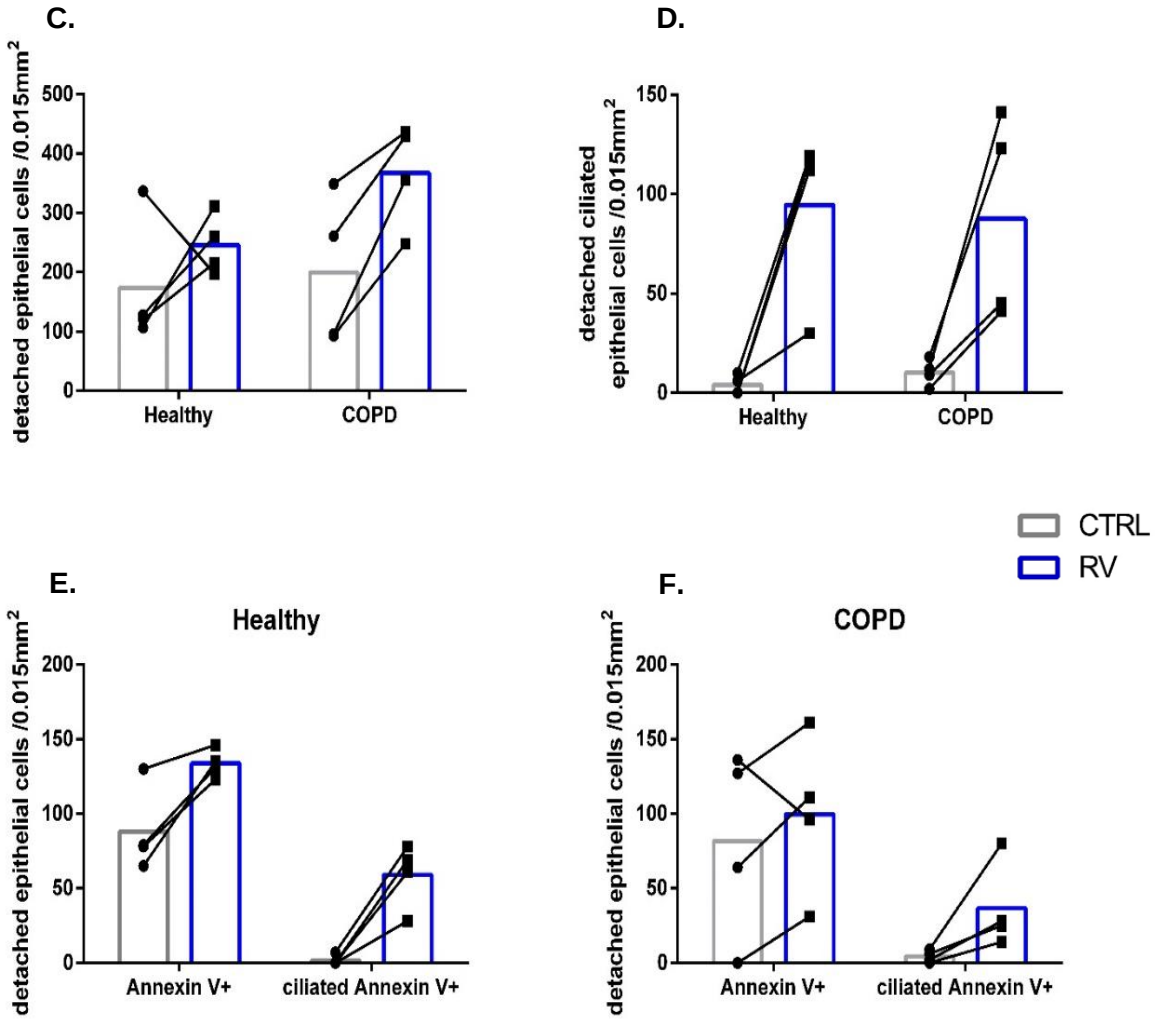

Figure 4-8: Epithelial cells detached from healthy and COPD epithelium infected with rhinovirus for 24h.

A and B) Representative images of epithelial cells in the apical washes of cultures following rhinovirus infection, apoptotic cells were indicated by green Annexin V marker, late apoptotic cells were indicated by green Annexin V and blue UV zombie markers, necrotic/ dead cells were indicated by blue UV zombie marker, scale bars=10μM; C) Number of detached cells counted per 0.015mm^2 field from 25 random images of each apical wash; D) Number of detached ciliated cells counted per 0.015mm^2 field from 25 random images of each apical wash; E) Number of all detached and ciliated epithelial cells positive for Annexin V dye post rhinovirus infection in healthy apical washes; F) Number of all detached and ciliated epithelial cells positive for Annexin V dye post rhinovirus infection in COPD apical washes.

The discussion below belongs to the cells remained to the epithelium that were not detached. Significant differences in early apoptosis between rhinovirus infected and non-infected conditions were not observed (p=0.43, healthy and p=0.43, COPD). Significant differences in late apoptosis between rhinovirus infected and non-infected cultures were also not observed (p=0.97, healthy and p=0.43, COPD) (Figure 4-9 B and C). Interestingly, independently of rhinovirus infection, larger cell populations undergoing late apoptosis (Annexin V+, UV zombie+), in comparison to early apoptosis (Annexin V+), were seen in cultures from healthy and COPD donors. In particular, the late apoptotic cell population in cultures from healthy donors was ~ 15% higher in mock control (p=0.43) and 22% higher in rhinovirus infected cultures (p=0.075) (Figure 4-9 B). In cultures from COPD donors, the late apoptotic population was ~ 14% higher in mock control (p=0.43) and 25% higher in rhinovirus infected cultures (p=0.43) (Figure 4-9 C). Of interest, the necrotic population (UV zombie+) in rhinovirus infected cultures from COPD individuals was ~ 9% higher than that in non-infected cultures (p=0.43) (Figure 4-9 C).

Overall, infection of ciliated cultures with rhinovirus causes shedding of epithelial cells from the epithelial surface. Programmed cell death was observed predominantly in ciliated cells detached from the epithelial layer following rhinovirus infection. It was of interest, that very few of the necrotic detached cells were ciliated (Appendix 1, Supplementary Figure 3). These results strongly suggest that the virus is inducing apoptosis in cells that are being shed from the epithelium. The cells remaining in the epithelium were also investigated for signs of apoptosis and necrosis. There was evidence of early, late apoptosis and necrosis. Even with mock infection there was evidence of early and late apoptosis and this was not different from infected epithelium.

A.

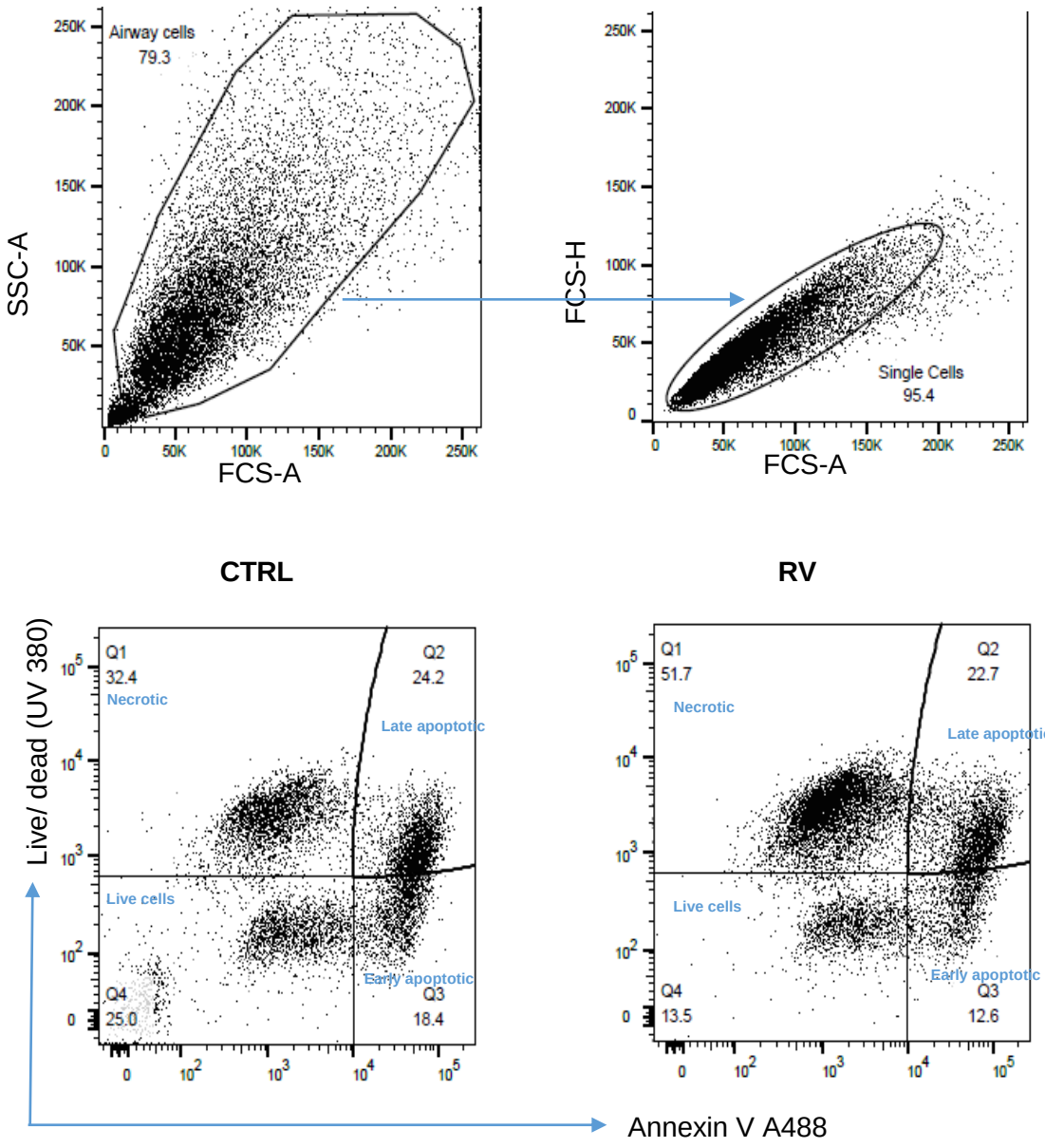
Airway cells
79.3
SSC-A
FCS-A
FCS-H
Single Cells
95.4
CTRL
RV
Live/ dead (UV 380)
Q1
32.4
Necrotic
Q2
24.2
Late apoptotic
Live cells
Early apoptotic
Q4
25.0
Q3
18.4
Q1
51.7
Necrotic
Q2
22.7
Late apoptotic
Live cells
Early apoptotic
Q4
13.5
Q3
12.6
Annexin V A488

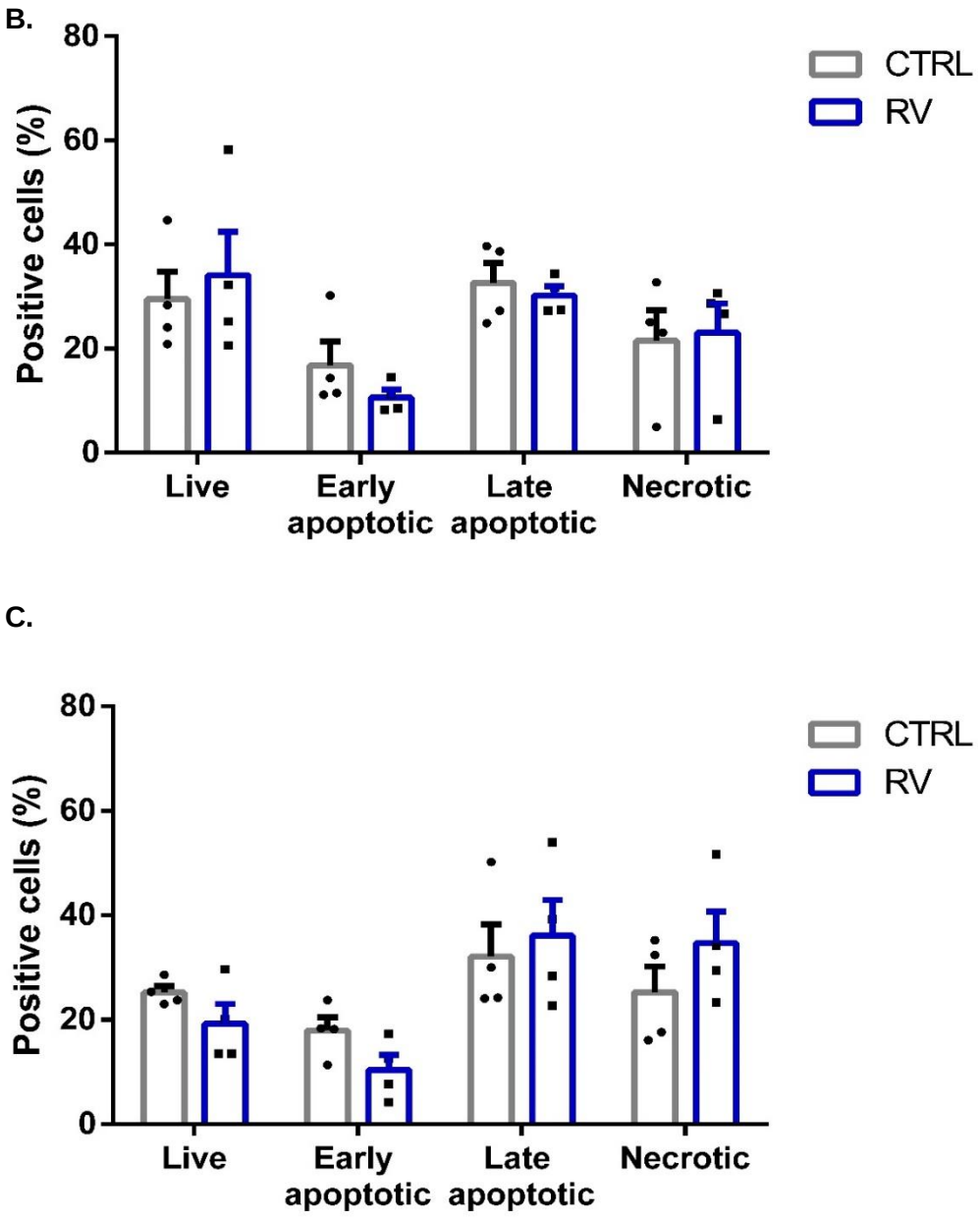

Figure 4-9: Characterisation of programmed cell death of airway ciliated cultures from healthy and COPD donors infected with rhinovirus at 24h.

A) Representative plots of flow cytometric analysis showing gated populations. Selection of primary airway single cells was gated based on the expression of apoptotic markers as follows: Annexin V + cells, Annexin V and UV zombie+ cells, UV zombie+ cells; B) Percentage of positive epithelial cells in cultures from healthy donors, using gating strategy as explained in A; C) Percentage of positive epithelial cells in cultures from COPD donors using gating strategy as explained in A, plots represent findings from 4 healthy and 4 COPD cultures, error bars represent ±SEM.

4.2.6 Inhibition of rhinovirus infection

After establishing an ALI culture model of rhinovirus infection of airway healthy and COPD differentiated cells we used the method to test a novel compound to determine its effect on rhinovirus viral replication. The GSK2998533 compound - PI4KIIIβ inhibitor was supplied by the Refractory, Respiratory and Inflammation Unit at GSK, Stevenage. Our secondary aims were to determine if the response to the inhibitor was similar in healthy and COPD and to determine if the compound affected shedding of ciliated cells following rhinovirus infection.

Ciliated cultures infected with rhinovirus and pre-treated with the PI4KIIIβ inhibitor showed a marked decrease of rhinovirus replication within 24h of infection compared to rhinovirus infected cells (Figure 4-10 A). As little as 100nM of PI4KIIIβ inhibitor was enough to significantly reduce the titre of live virus in ciliated cultures from both healthy ($p<0.0001$) and COPD ($p<0.0001$) donors compared to vehicle control. No differences were observed between the groups. Only one experiment was possible with bronchial ciliated cells due to the availability of tissue. At 24h the PI4KIIIβ inhibitor had a reduction effect on rhinovirus replication in bronchial ciliated cells compared to vehicle control ($1.1x10^4$ $TCID_{50}$/culture vs $3.6x10^5$ $TCID_{50}$/culture, respectively). TEER of nasal ciliated cultures was measured prior the experiment and at the end of the study. TEER changes were expressed as ratios based on pre-treatment readings, and no significant differences were observed between the treatments or the healthy and COPD groups (Figure 4-10 B).

The effect of the PI4KIIIβ inhibitor on ciliary function was assessed by the high speed video microscopy system, ciliary activity and ciliary beat frequency were measured. Ciliated cultures from healthy and COPD donors were infected with rhinovirus for 24h and pre-treated either with PI4KIIIβ inhibitor or vehicle control. In healthy, compared to control non-infected cultures, ciliary activity was significantly decreased by both rhinovirus ($p<0.01$) and vehicle control ($p<0.01$) (Figure 4-10 C). In contrast, the PI4KIIIβ inhibitor preserved the ciliary activity of cultures from healthy individuals following rhinovirus infection and maintained a higher percentage of active ciliated area compared to rhinovirus ($p=0.047$) and vehicle control ($p=0.122$). In COPD, there was a non-significant trend in ciliated cells treated with the PI4KIIIβ inhibitor prior to rhinovirus to have increased ciliary activity compared to rhinovirus infected cultures ($p=0.8$) and vehicle control ($p=0.85$) (Figure 4-10 C). There was no difference in ciliary beat frequency between the various conditions studied (Figure 4-10 D).

The data from this study showed the GSK2998533 compound significantly reduced rhinovirus replication in cultures from healthy and COPD donors and helped to preserve ciliary activity in cultures from healthy individuals with a similar trend seen in ciliated cultures from COPD donors.

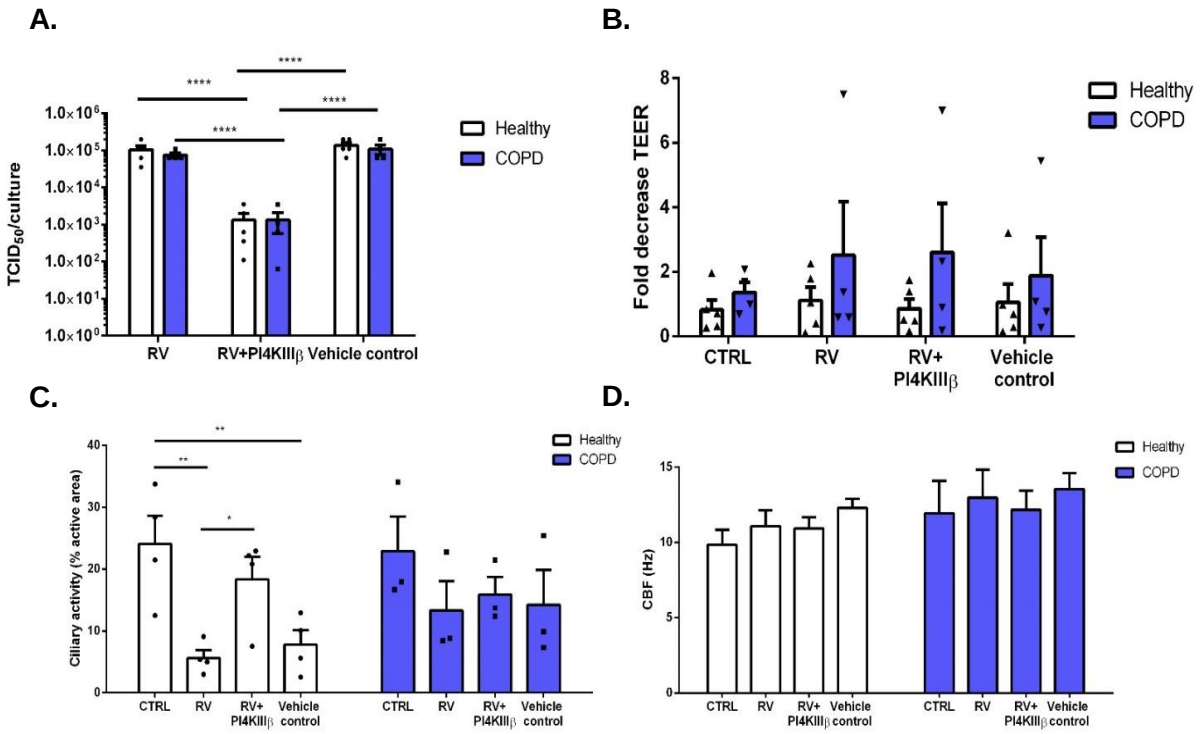

Figure 4-10: PI4KIIIβ inhibitor effect on rhinovirus replication and ciliary function of ciliated cultures from healthy and COPD individuals at 24h post infection.

A) Live virus titre was measured in nasal airway ciliated cultures following rhinovirus infection, PI4KIIIβ and rhinovirus infection, or vehicle control and rhinovirus infection, n=4 healthy and n=4 COPD donors; B) TEER of nasal ciliated cultures following rhinovirus infection, PI4KIIIβ and rhinovirus infection, or vehicle control and rhinovirus infection, relative to pre-treatment readings, n=4 healthy and n=4 COPD donors; C) Ciliary activity of nasal ciliated cultures following rhinovirus infection, PI4KIIIβ and rhinovirus infection, or vehicle control and rhinovirus infection, n=4 healthy and n=3 COPD donors, D) CBF of nasal ciliated cultures following rhinovirus infection, PI4KIIIβ and rhinovirus infection, or vehicle control and rhinovirus infection, n=4 healthy and n=3 COPD donors; error bars represent ±SEM, *=p<0.05, **=p<0.01, ***=p<0.001.

4.2.7 Expression of PI4P in ciliated cultures

Generation of successful panviral replication platform involves the recruitment of PI4KIIIβ enzyme to Golgi membranes and the enrichment of these membranes with PI4P lipids (Altan-Bonnet 2017). It has been demonstrated in this study that inhibition of PI4KIIIβ decreases replication of rhinovirus 16 in differentiated cultures from healthy and COPD donors. We therefore investigated whether differentiated cultures express PI4P lipids and if their expression changes with infection.

To confirm the presence of PI4P in respiratory epithelial cells, fully differentiated cultures were stained with an anti-PI4P antibody. A clear and dense expression of PI4P was seen in motile cilia, along the entire length of the ciliary membrane (two different cultures). PI4P expression was also visualised intracellularly with clear but less abundant expression (Figure 4-11 A). To observe where PI4P is located during rhinovirus infection, fully differentiated cultures were immunofluorescently labelled with β-tubulin to visualise cilia, PI4P, rhinovirus conjugated Ab and Hoechst solution. The staining allowed comparison of PI4P expression in the absence and presence of rhinovirus. Z-stack section images were acquired to make a composite of the epithelial layer. In control non-infected cultures (Figure 4-11 B) PI4P green fluorescent staining overlapped with β-tubulin red fluorescent staining, confirming findings in Figure 4-11 A. In infected cultures (Figure 4-11 C) PI4P expression was visualised inside epithelial cells, as extensive green staining. The images are representative from 2 ciliated cultures.

A.

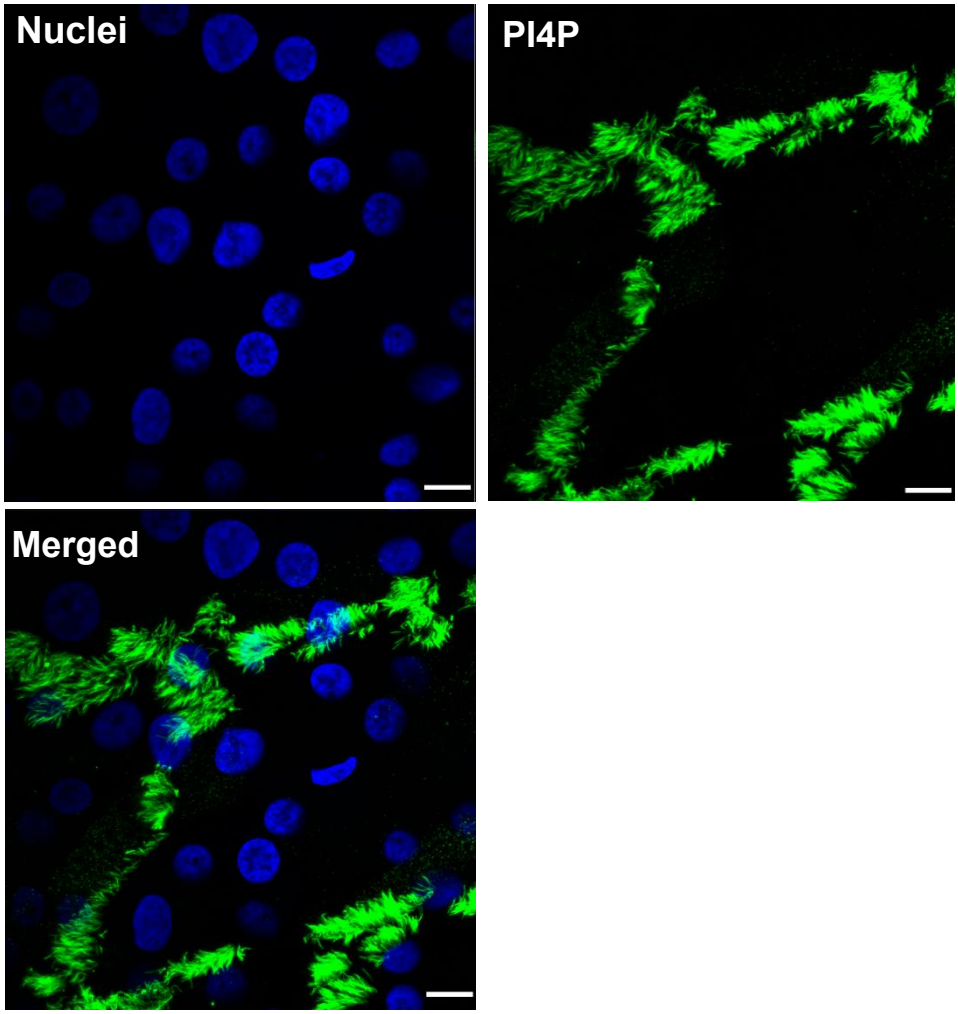

B.

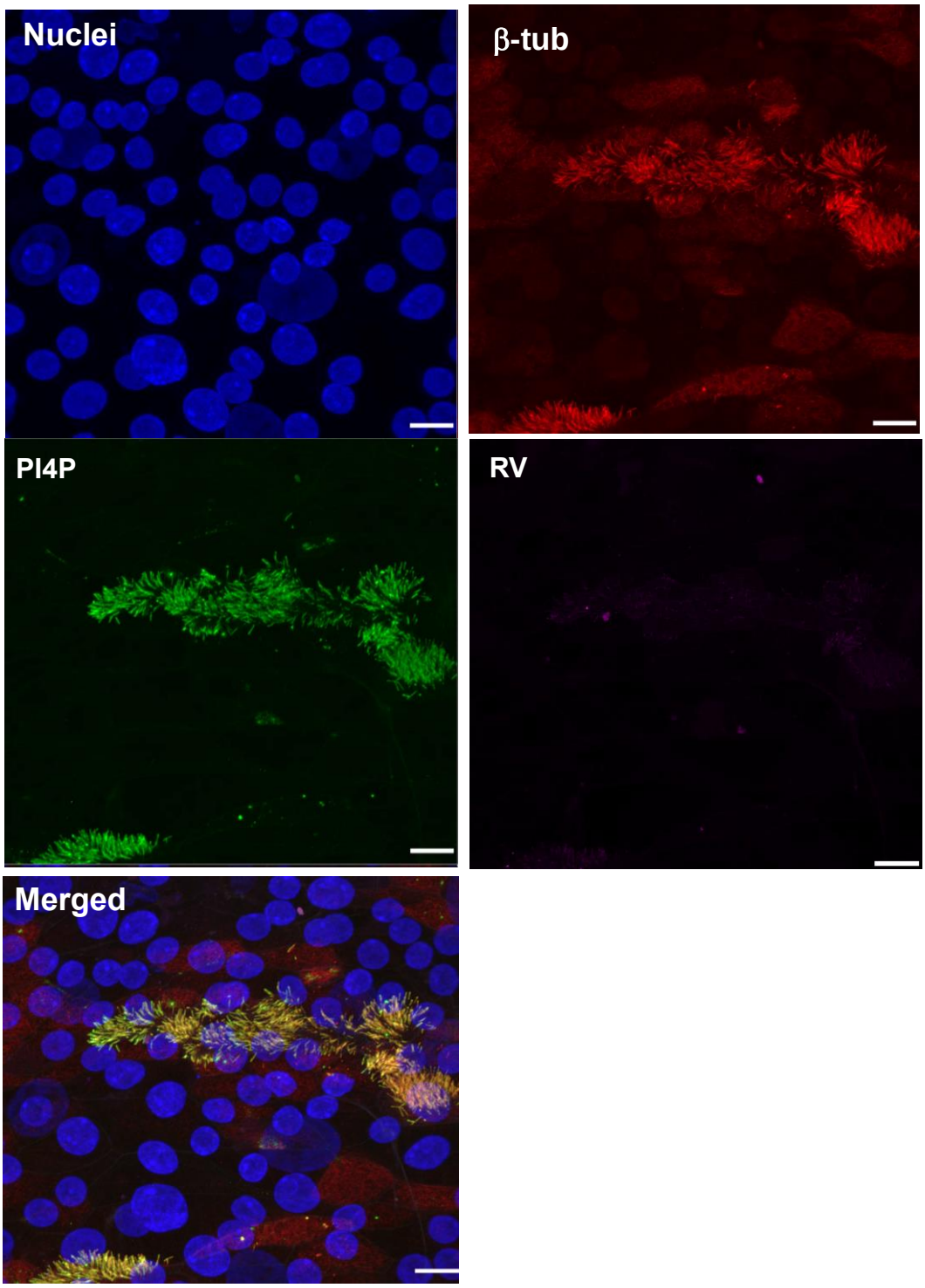

C.

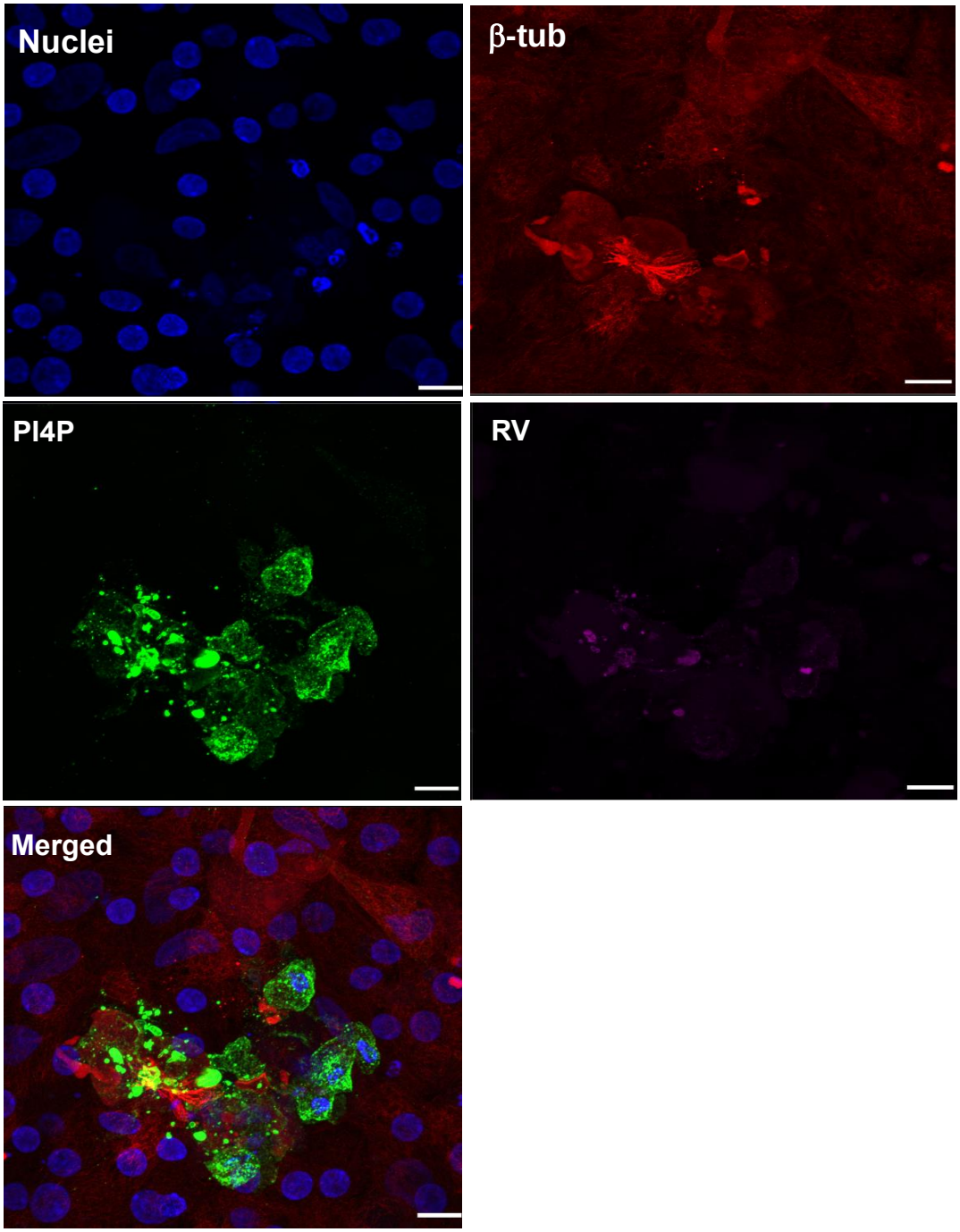

Figure 4-11: Immunofluorescent staining of PI4P expression in fully differentiated cultures.

A) Positive green fluorescent staining of PI4P expression was seen in motile cilia of differentiated cells; B) Positive green fluorescent PI4P staining overlaps with red fluorescent β-tubulin staining in non-infected control cells, confirming PI4P appearance in motile cilia; C) Positive green fluorescent PI4P staining is no longer seen in cilia but inside epithelial cells, where it overlaps with β-tubulin in red and rhinovirus in magenta colour staining. Scale bars = 16μM.

4.2.8 Inflammatory response of ciliated cultures to rhinovirus infection

To assess the effect of rhinovirus on the inflammatory response of differentiated cultures, apical and basolateral fluids were collected following 24h rhinovirus infection. A secondary aim of the study was to assess the differences between healthy and COPD groups and also differences of apical and basolateral secretion of cytokines. We selected the same panel of cytokines as for the *M. catarrhalis* study of interaction with the respiratory epithelium. Figure 4-12 shows cytokines that were significantly increased in the basolateral fluids of ciliated cultures from healthy and COPD individuals following rhinovirus infection, whereas Table 4-2 shows the measurements of cytokines which failed to reach significance in terms of their differences from controls.

4.2.8.1 Inflammatory mediators secreted in the basolateral fluids of ciliated cultures

Rhinovirus significantly increased IL-1β levels in ciliated cultures from COPD patients ($p=0.02$). A significant increase was seen for IP-10/ CXCL10 ($p<0.0001$), IL-6 ($p=0.006$), IL-8/ CXCL8 ($p=0.045$), RANTES/ CCL5 ($p<0.0001$) in ciliated cultures from both healthy and COPD individuals. A significant increase was observed for TNF-α protein in ciliated cultures from healthy donors ($p=0.003$), but a statistically significant increase in cultures from COPD donors was not observed ($p=0.052$). Likewise, CSF-3/ GM-CSF was significantly induced in cultures from healthy individuals ($p<0.001$), but not in COPD ($p=0.2$). MIP-3α/ CCL20 and MCP-1/ CCL2 were significantly increased in cultures from healthy individuals ($p=0.002$ and $p<0.001$, respectively) and in COPD ($p=0.02$ and $p=0.003$, respectively). A very strong increase was measured for IL-17c in ciliated cultures from both healthy and COPD donors ($p<0.0001$). No significant differences were observed between the two groups for any of the analysed cytokines.

Type I interferon response was not strongly induced by rhinovirus in any of the groups tested (Table 4-2). In contrast, a strong induction was observed for Type III IFNλ2/3 in ciliated cultures from healthy and COPD ($p<0.0001$) donors. No significant differences were observed between the healthy and COPD groups.

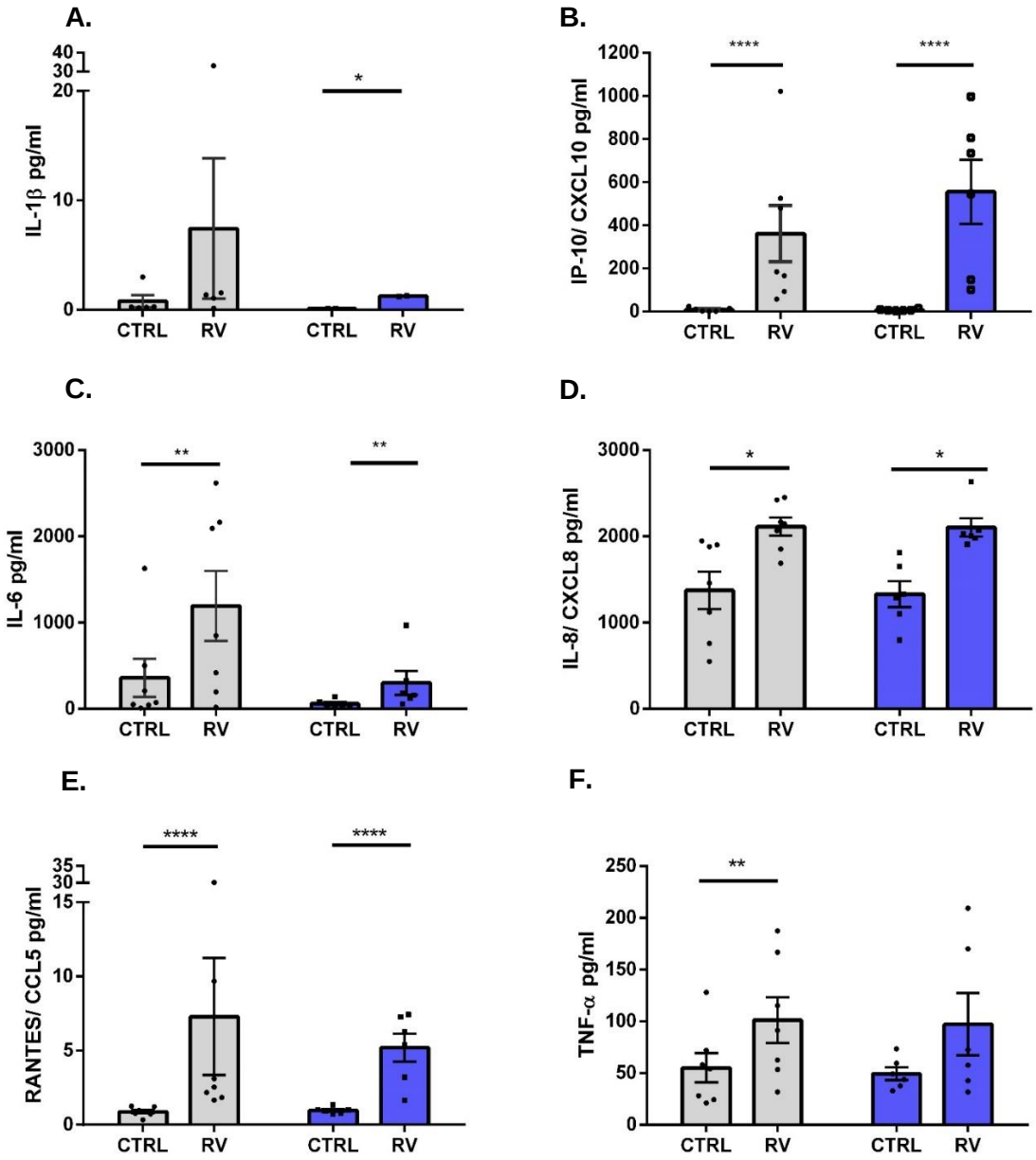
A.
IL-1β pg/ml
40
30
20
10
0
*
CTRL
RV
CTRL
RV
B.
IP-10/ CXCL10 pg/ml
1200
1000
800
600
400
200
0
****
****
CTRL
RV
CTRL
RV
C.
IL-6 pg/ml
3000
2000
1000
0
**
**
CTRL
RV
CTRL
RV
D.
IL-8/ CXCL8 pg/ml
3000
2000
1000
0
*
*
CTRL
RV
CTRL
RV
E.
RANTES/ CCL5 pg/ml
35
30
15
10
5
0
****
****
CTRL
RV
CTRL
RV
F.
TNF-α pg/ml
250
200
150
100
50
0
**
CTRL
RV
CTRL
RV

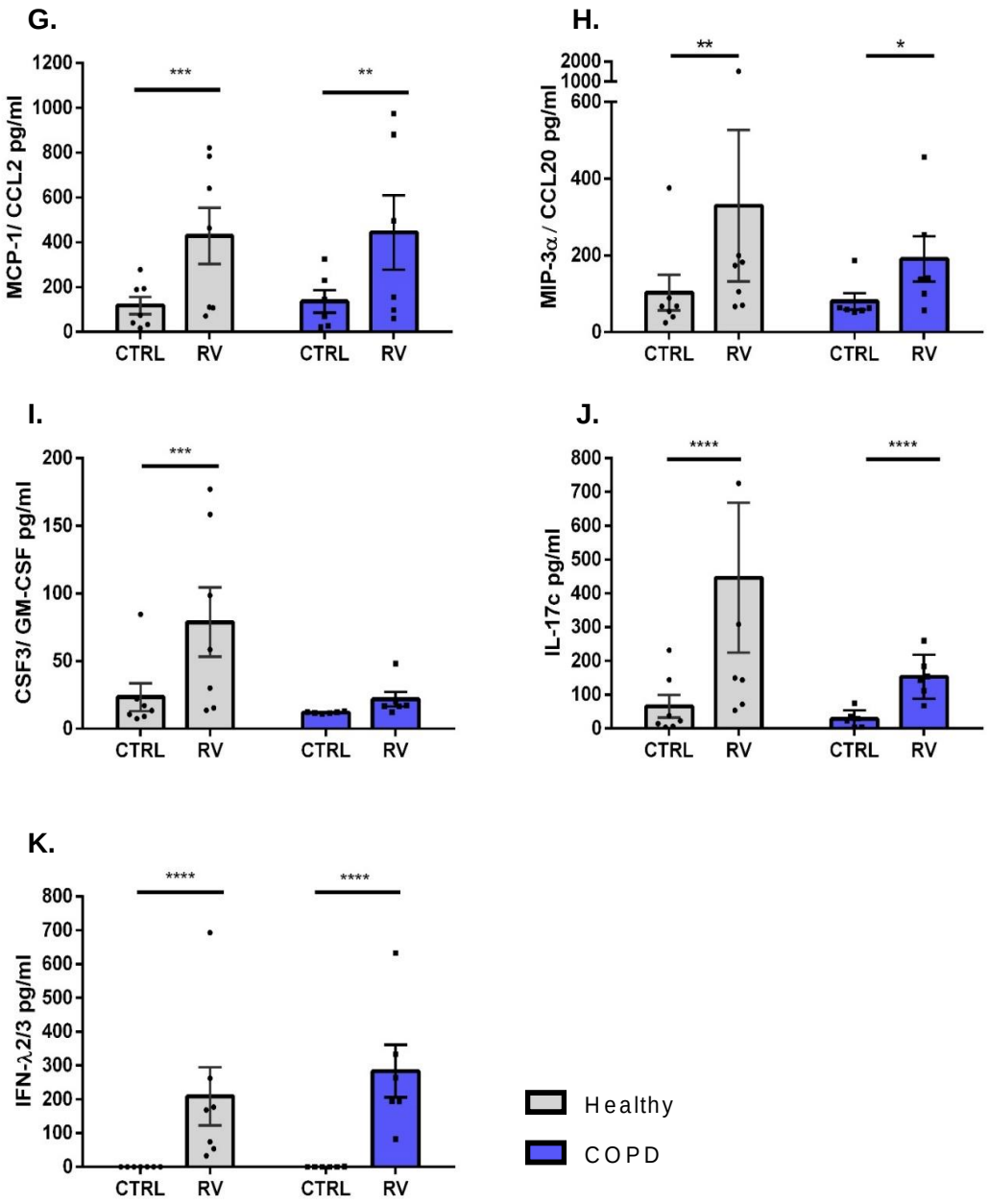

Figure 4-12: Inflammatory mediators secreted in the basolateral fluids of ciliated cultures from healthy and COPD donors following rhinovirus infection at 24h.

A) IL-1β, B) IP-10/ CXCL10, C) IL-6, D) IL-8/ CXCL8, E) RANTES/ CCL5, F) TNF-α, G) MCP-1/ CCL2, H) MIP-3α/ CCL20 , I) CSF-3/ GM-CSF, J) IL-17c, K) IFNλ2/3, grey denotes healthy cultures, blue denotes COPD culture, n=6 for each group, error bars represent ±SEM, *=p<0.05, **=p<0.01, ***=p<0.001, ****=p<0.0001.

Table 4-2: Inflammatory mediators secreted in the basolateral fluids of ciliated cultures following rhinovirus infection for 24h.

	Healthy			COPD		
pg/ml	**CTRL**	**RV**	**P values**	**CTRL**	**RV**	**P values**
ENA-78	161.61 ± 67.79	390.20 ± 98.94	0.14	65.73 ± 25.48	356.66 ± 190.20	0.2
GRO-α / CXCL1	390.15 ± 40.41	397.84 ± 22.17	0.89	401.71 ± 14.08	407.07 ± 21.14	0.99
IL-15	7.85 ± 0.68	9.86 ± 0.93	0.21	7.68 ± 0.55	9.30 ± 0.84	0.41
IFN-α	2.56 ± 0.07	2.67 ± 0.04	0.41	2.65 ± 0.06	2.80 ± 0.07	0.10
IFN-β	19.15 ± 2.51	18.11 ± 3.56	0.78	16.57 ± 2.14	15.70 ± 1.870	0.96
IFN-γ	1.88 ± 0.63	1.66 ± 0.38	0.99	2.05 ± 0.49	1.86 ± 0.32	0.98
TARC / CCL17	0.22 ± 0.06	0.25 ± 0.08	0.75	0.29 ± 0.06	0.36 ± 0.08	0.57
CXCL14	1175.97 ± 5.52	1192.03 ± 8.09	0.41	1200.04 ± 10.08	1207.90 ± 5.83	0.78
IL-36g	11.77 ± 1.00	15.27 ± 2.62	0.29	11.89 ± 0.44	13.35 ± 1.16	0.71

4.2.8.2 Inflammatory mediators secreted in the apical fluids of ciliated cultures

To establish whether inflammatory cytokines were also secreted in the apical fluids of rhinovirus infected cultures, protein levels of cytokines secreted in the apical fluids were measured 24h post infection. The same cytokine analysis panel was used as for basolateral fluids. The intention was to evaluate differences between the apical fluids with and without infection, and also differences in cytokine levels between healthy and COPD groups.

Cytokines with the highest increase in apical fluids are reported in Figure 4-13, while the rest of the measurements are summarised in Table 4-3. Similar to basolateral fluids, IL-1β was significantly induced in cultures from COPD donors ($p<0.01$), with slight increase in cultures from healthy individuals. Strong induction of IP-10/ CXCL10 and RANTES/ CCL5 were observed in ciliated cultures from healthy ($p<0.0001$ and $p<0.001$, respectively) and COPD donors ($p<0.0001$ and $p<0.0001$, respectively). IL-6 ($p<0.05$), CSF-3/ GM-CSF ($p<0.05$), IL-15 ($p<0.01$) and IL-17c ($p<0.05$) were also

significantly increased in cultures from COPD donors, but no statistical significance was reached in cultures from healthy individuals.

Variable levels were observed for type I interferon cytokines in apical fluids, with no induction post virus infection observed for IFN-α (Table 4-3) in culture fluids from healthy and COPD donors. A significant increase of IFN-β was detected for cultures from COPD individuals ($p<0.05$). A non-significant decrease of ~ 25% was observed for IFN-γ in both healthy and COPD stimulated cells ($p=0.75$ and $p=0.83$, respectively) (Table 4-3). Rhinovirus stimulation of IFN-λ2/3 significantly increased in both healthy and COPD groups ($p<0.0001$). No significant differences were reported between the groups.

4.2.8.3 Comparison between apical and basolateral secretion of inflammatory mediators

To evaluate the differences between apical and basolateral fluids, a global test was used to combine the data from the two groups and the two types of fluids to determine the effect of rhinovirus infection. If rhinovirus increased the concentration of a certain analyte in comparison to non-infected controls (when $p=0.05$ or $p<0.05$), then the results from apical fluids were compared to those from basolateral fluids. In the current study no statistically significant differences were reported between the apical and basolateral fluids for any of the cytokines measured. Greater stimulation of inflammatory mediators in the basolateral fluids of cultures from healthy individuals was observed for IL-1β (1.4 times, $p=0.85$), IL-6 (1.8 times, $p=0.8$), IL-8/ CXCL8 (1.7 times, $p=0.46$), TNF-α (1.4 times, $p=0.74$), MCP-1/ CCL2 (4.1 times, $p=0.2$), ENA-78/ CXCL5 (1.4 times, $p=0.95$), MIP-3α/ CCL20 (2.3 times, $p=0.28$), CSF-3/ GM-CSF (2 times, $p=0.23$). Larger stimulatory rhinovirus effect in the secretion of cytokines to the basolateral site of cultures from COPD donors was observed for IL-1β (2.2 times, $p=0.72$), IP-10/ CXCL10 (1.8 times, $p=0.68$), ENA-78/ CXCL5 (1.4 times, $p=0.89$), and MIP-3α/ CCL20 (1.1 times, $p=0.94$).

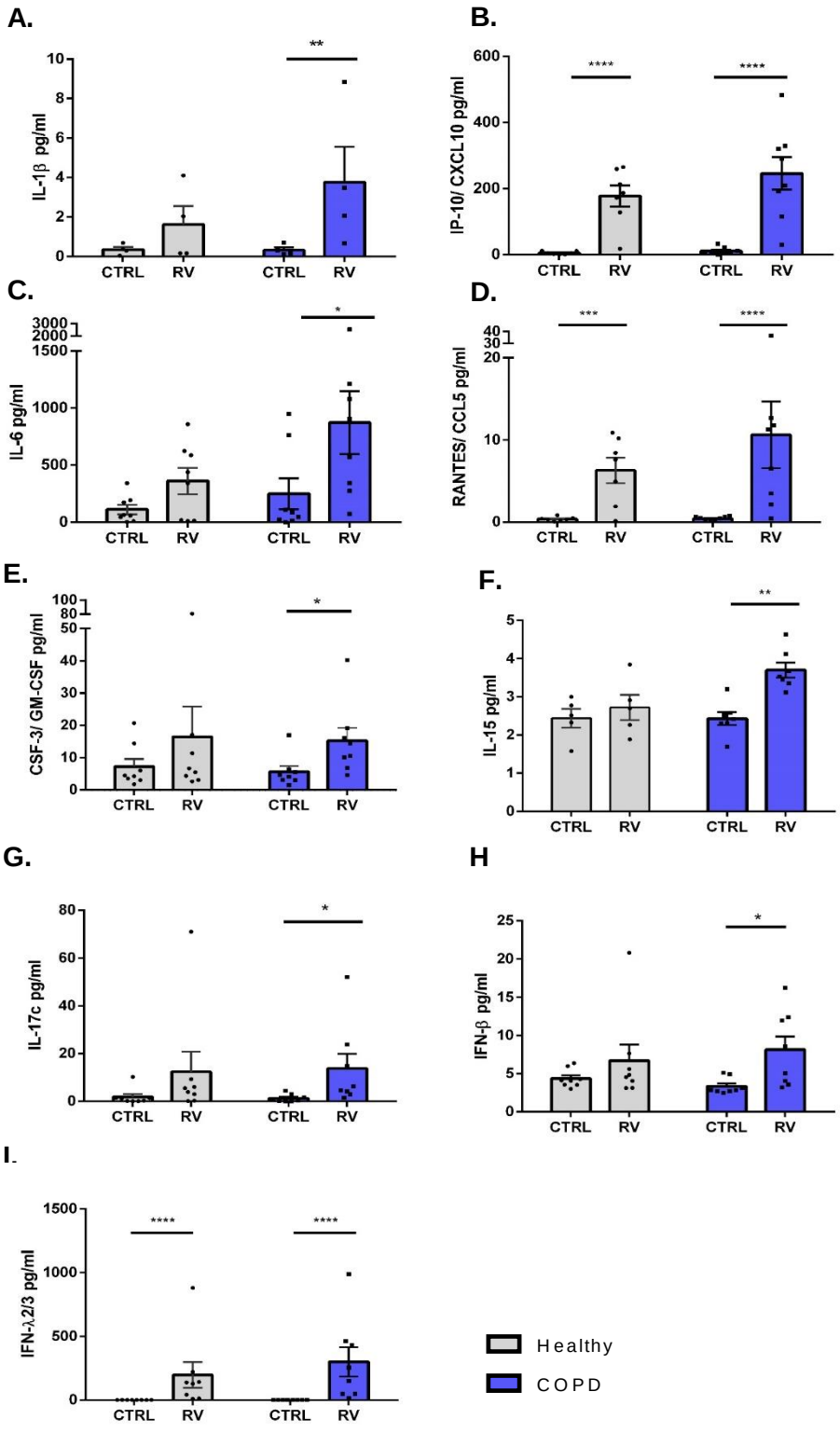

Figure 4-13: Inflammatory mediators in the apical fluids of ciliated cultures healthy and COPD donors following rhinovirus infection at 24h.

A) IL-1β, B) IP-10/ CXCL10, C) IL-6, D) RANTES/ CCL5, E) CSF-3/ GM-CSF, F) IL-15, G) IL-17c, H) IFN-β, I) IFNλ2/3, grey denotes healthy cultures, blue denotes COPD culture, n=6 for each group, error bars represent ±SEM, *=p<0.05, **=p<0.01, ***=p<0.001, ****=p<0.0001.

Table 4-3: Inflammatory mediators secreted in the apical fluids of ciliated cultures following rhinovirus infection for 24h.

	Healthy			COPD		
pg/ml	**CTRL**	**RV**	**P values**	**CTRL**	**RV**	**P values**
IL-8/ CXCL8	478.78 ± 107.86	432.04 ± 86.85	0.99	376.51 ± 59.73	718.25 ± 95.95	0.13
TNF-α	19.13 ± 4.46	25.83 ± 5.22	0.79	22.62 ± 5.96	46.07 ± 11.55	0.19
MCP-1/ CCL2	42.32 ± 13.94	45.57 ± 13.60	0.97	55.02 ± 21.96	145.27 ± 46.40	0.29
ENA-78	80.64 ± 39.83	104.69 ± 30.58	0.46	188.34 ± 103.67	356.20 ± 177.5	0.65
MIP-3α / CCL20	79.07 ± 50.27	46.49 ± 11.49	0.98	35.08 ± 11.07	63.37 ± 19.76	0.42
GRO-α / CXCL1	81.51 ± 11.75	76.10 ± 11.26	0.95	63.28 ± 7.82	88.03 ± 6.23	0.31
IFN-α	1.06 ± 0.02	1.12 ± 0.03	0.18	1.06 ± 0.01	1.27 ± 0.13	0.052
IFN-γ	0.87 ± 0.17	0.61 ± 0.09	0.75	0.82 ± 0.10	0.59 ± 0.15	0.83
TARC/ CCL17	0.08 ± 0.01	0.09 ± 0.02	0.98	0.07 ± 0.02	0.14 ± 0.05	0.39

4.3 Discussion

Previous studies have reported that epithelial cells are the main site of rhinovirus replication (Jacobs et al., 2013; Bochkov and Gern 2016). Jakiela et al suggested ciliated cells are the main target of rhinovirus, leading to their decreased number in human bronchial differentiated cells at 48h post infection (Jakiela et al., 2014). More recent publications have confirmed the findings of Jakiela et al for rhinovirus A in human nasal differentiated cells (Tan et al., 2018) and also suggested that rhinovirus C similarly targets the ciliated cell type in the bronchial ciliated cultures (Griggs et al., 2017). The current study is the first to report rhinovirus infection is characterised by initial selective infection of ciliated cells with a subsequent spread to other cell types at 24h in primary nasal ciliated cultures from healthy individuals and COPD donors (Figures 4-1 and 4-2).

The experiments described in this chapter aimed to observe the initial cytotoxic effects of rhinovirus on the airway epithelium and to compare rhinovirus infection in primary ciliated cultures from healthy and COPD individuals. Another aim was to determine if previously reported high secretion of inflammatory IL-6, IL-8/ CXCL8, TNF-α and IP-10/ CXCL10 in the sputum and serum of COPD patients (Mallia et al., 2014; Quint et al., 2010) is specific to the COPD patient group only. A heightened inflammatory state in COPD airways has been associated with severe exacerbations, leading to poor prognosis (Hogg and Timens 2009; Barnes 2016). Currently, no antiviral therapies are available against rhinovirus and the treatment is mainly supportive for cold symptoms (Jacobs et al 2013), however a better understanding of the pathogenesis of viral infection could help target new therapeutic approaches.

4.3.1 Rhinovirus infection and epithelial barrier function

This project has been particularly interested in the initial interaction of rhinovirus with the respiratory epithelium as this is the main target of the virus to replicate in the upper and lower airways (Gern et al., 1997; Lopes-Souza et al., 2009; Mosser et al., 2002). This study demonstrates that rhinovirus infection causes shedding of ciliated epithelial cells as early as 6h post infection. At 18h post infection, the respiratory epithelium was very damaged and covered by detached ciliated cells (Figure 4-2 C). The cilia on the detached cells continued to beat initially but over time they became static. The result was significantly reduced ciliary activity of airway cultures at 24h post infection (Figure 4-3 A). The positive link between rhinovirus infection and detachment of

infected cells was first reported by Mosser et al who infected airway bronchial tissue with rhinovirus 16 and reported that several detached epithelial cells stained positively for rhinovirus (Mosser et al., 2002). In the same study, 6h infection with rhinovirus 16 of adenoidal tissue showed a few ciliated cells from the epithelial layer became positive for rhinovirus (Mosser et al., 2002). Jakiela et al study, found detached epithelial cells from ciliated cultures when studied 48h post rhinovirus 16 infection and debris with cilia in the apical secretions of infected cultures at 48h post infection (Jakiela et al., 2014). Griggs et al also reported that cells expressing GFP labelled rhinovirus C were detached from the epithelium when observed 18h after infection (Griggs et al., 2017). My study used high speed video microscopy to image the respiratory epithelium allowing real time observation of the very early host-pathogen interactions. This showed rhinovirus appears to target ciliated cells and this is associated with very early shedding of ciliated cells resulting in a significant ciliated cells' depletion. In subjects with rhinovirus infection it is likely this is associated with reduction in mucociliary clearance.

The current study suggested that rhinovirus significantly impairs epithelial function through marked decrease of ciliary activity (Figure 4-4A and B). Indeed, the percentage of ciliated active areas of infected cultures from COPD donors was markedly reduced 7 days post rhinovirus infection (4-4 B). This observation was further confirmed by a marked reduction in the expression of the ciliary DNAI2 protein when measured 3 and 7days post infection. Of interest ciliary beat frequency of cilia on cells that were not extruded from the epithelium maintained their ciliary beat frequency 24h post rhinovirus infection (Figure 4-3 B). However, our group has previously shown that maintenance of a normal ciliary beat frequency does not mean ciliary function is preserved. For example, although ciliary bear frequency of nasal epithelial cultures infected with RSV was not affected in the first 72h of infection, extensive ciliary dyskinesia was an early feature of the infection (Smith et al., 2014). This is consistent with observation of nasal epithelial samples taken from healthy volunteers 3 days after nasal inoculation with coronavirus infection. Again, although ciliary beat frequency stayed within normal range following coronavirus infection marked ciliary dyskinesia was seen (Chilvers et al., 2001).

However, ciliary beat frequency was significantly reduced in cultures when measured seven days after rhinovirus infection. (Figure 4-5). The marked loss of ciliated cells and reduced ciliary function would impair the mucociliary escalator of the airway epithelium predisposing to a secondary infection (Tilley et al., 2015). In primary ciliary

dyskinesia uncoordinated and slow ciliary beating can lead to long term airway problems such as bronchiectasis and recurrent chest infections (Chilvers and O'Callaghan 2000).

Rhinovirus infection progressively reduced transepithelial electrical resistance of cultures. At day 7 rhinovirus had decreased TEER by more than 50% in infected cultures from healthy individuals and COPD patients (Figure 4-5 C and E). This could have a role on a potential subsequent bacterial infection (Sajjan et al., 2008). Reduced transepithelial resistance through dissociation of ZO-1 tight junction complex has been previously reported to initiate increase of NTHI transmigration across the airway epithelium (Sajjan et al., 2008).

4.3.2 Rhinovirus replication in the ciliated epithelium

COPD patients suffer from recurrent viral infections which initiate exacerbations (Mallia et al., 2014; George et al., 2014). In this study viral replication at 24h was only slightly increased in ciliated cultures from COPD donors compared to cultures from healthy individuals (Figure 4-6). This is consistent with Baines et al but in contrast to Schneider et al study (Baines et al., 2013; Schneider et al., 2010). Baines reported similar rhinovirus replication in healthy and COPD bronchial epithelial cells collected from patients and infected with rhinovirus 1B for 24h (Baines et al., 2013). Schneider's study differs from these findings finding a significant increase at 24h in viral replication of rhinovirus 39 in bronchial mucociliary cultures grown at air-liquid interface from 12 COPD patients (Schneider et al., 2010).

In our study 7 days of infection, ciliated cultures from healthy and COPD donors effectively reduced rhinovirus by 70% (Figure 4-7 A). The underlying mechanism for this is not completely clear, but it is possible that the epithelium removes virus infected cells through apoptosis and shedding from the epithelium. Other research groups have reported similar RSV infection kinetics of human airway cultures, with viral replication peaking at day 3 and with reduced viral titre by day 8 (Liesman et al., 2014). Liesman found clearance of RSV infection resulted in extrusion of infected ciliated cells and decline of mucociliary transport. Of interest, airway epithelial shedding into bronchial airway lumen resulted in accumulation of detached cells, leading to distal airway obstruction in hamsters (Liesman et al., 2014). In our study we also found that rhinovirus detaches epithelial cells from the epithelial layer that are likely to cause small airway obstruction.

One mechanism which could lead to shedding of epithelial cells is apoptosis, which controls the fate of cells and has been shown to be a defence mechanism against pathogens (Lotzerich et al., 2018). When the apical washes from infected cultures were investigated at 24h, ~30-50% of all counted cells were Annexin V positive cells, of which ~40% were ciliated (Figure 4-8 D). Evaluation of apoptosis in epithelial cells remained in the epithelium at 24h showed increased populations of late apoptotic and necrotic cells in COPD infected cells (Figure 4-9 C). The findings suggest apoptosis is the mechanism involved in the detachment of ciliated cells. A previous study has also reported an induction of apoptosis in human primary bronchial cells from COPD subjects following rhinovirus infection for 24h (Baines et al., 2013).

4.3.3 Rhinovirus replication and inhibition of the PI4KIIIβ enzyme

The data in this study suggests, for the first time, that PI4P is expressed on the entire ciliary membrane. The finding was reflected by β-tubulin staining, which indicated PI4P and β-tubulin fully overlap throughout the entire length of cilia, suggesting PI4P is part of the ciliary membrane composition. In addition to being expressed on cilia, PI4P has been also visualised intracellularly in cultures from healthy and COPD donors, however additional makers for different organelles are needed to define its precise location. Data from Garcia-Gonzalo and colleagues showed the primary cilium in murine inner medullary collecting duct cells (IMCDs) and mouse embryonic fibroblasts (MEFs) also express PI4P on their membrane. Further, PI(4,5)P2 was located at the base of the cilium, and together with PI4P, regulated by Inpp5e (phosphoinositude-5-phosphatase), are thought to enable hedgehog signalling (Garcia-Gonzalo et al., 2015). Previous studies revealed PI4P lipids are required for picornaviridae replication and formation of viral complexes for genome synthesis (Altan-Bonnet and Bella 2012, Altan-Bonnet 2017). First, the 3A viral proteins of coxsackievirus and poliovirus were observed at the Golgi membranes and trans-Golgi network of infected cells *in situ* (Hsu et al., 2010). PI4KIIIβ enzyme selective recruitment to the Golgi is initiated through the recruitment of RAS family small GTP-ase Arf1 and its guanine nucleotide exchange factor GBP1. PI4P lipids synthesis is catalysed by PI4KIIIβ, leading to transformation of secretory organelle membranes and assembly of viral replication organelles (Hsu et al., 2010). PI4P lipid whole cell concentration was rapidly increased over 4 hours of infection (Hsu et al., 2010). Utilization of the PI4P available viral platform at Golgi membranes is kinetically advantageous for early picornaviruses synthesis and replication (Altan-Bonnet and Balla 2012). To further examine whether PI4P located at the ciliary membrane is

important for viral synthesis and rhinovirus replication, and whether PI4P abundance in cilia is associated with the preferential infection of this cell type in differentiated airway epithelial cells initially in the early hours of rhinovirus infection, further experiments exploring PI4P expression during rhinovirus infection would be of interest.

The current study demonstrates rhinovirus replication is significantly reduced by the GSK2998533 compound which targets the PI4KIIIβ enzyme in both healthy and COPD epithelial cells. PI4KIIIβ has been previously shown to be the source for high PI4P lipid yield during rhinovirus replication in Hela epithelial cells (Illyntska et al., 2013; Spickler et al., 2013; Roulin et al., 2014). Other picornaviruses such as enterovirus, Aichi virus, severe acute respiratory syndrome (SARS) coronavirus, bovine kobuvirus have been revealed to depend on PI4KIIIβ and PI4P lipids for genome synthesis (Altan-Bonnet and Balla 2012), while PI4KIIIα has been reported to generate PI4P during Hepatitis C virus replication (Berger et al., 2011). Our findings are consistent with the Spickler et al study where a PI4KIIIβ inhibitor successfully inhibited rhinovirus replication (Spickler et al., 2013). It is also in accordance with the Arita et al., study where targeted PI4KIIIβ inhibition successfully supressed poliovirus replication (Arita et al., 2011). However, both studies used epithelial cell lines therefore the current study brings novel findings to the field of rhinovirus replication in the respiratory epithelium.

Having established that rhinovirus disrupts the epithelial barrier function, it was also important to validate the effect of the compound on ciliary function. High speed video microscopy showed the PI4KIIIβ inhibitor did not affect ciliary beat frequency and at the same time preserved the ciliary activity of the cultures. Ciliary activity protection reached significance in healthy cultures only although high protection of ciliary activity could have been possibly observed in COPD cultures if more donors were involved in the study. No significant differences were observed between the TEER of cultures treated with the PI4KIIIβ inhibitor and rhinovirus and rhinovirus infected cultures or vehicle control, suggesting the compound did not have a negative impact on transepithelial electrical resistance.

4.3.4 Rhinovirus induction of inflammatory mediators in ciliated cultures from healthy and COPD donors

The current study identified strong inflammatory response initiated in ciliated cultures from healthy and COPD donors following rhinovirus infection (Figures 4-12 and 4-13).

IL-1β, IL-6, IP-10/ CXCL10, RANTES/ CCL5 were found significantly increased in the apical and basolateral fluids of airway cultures from healthy and COPD donors. The findings are consistent with previously observed induction of these cytokines in COPD sputum, BAL samples and ciliated culture infections *in vitro* (Papadopoulos et al., 2000; Wark et al., 2009; Jacobs et al., 2013; Mallia et al., 2014; George et al., 2014; Bochkov and Gern 2016). In our infection model, statistically significant higher levels of chemokines IL-8/ CXCL8, MIP-3α / CCL20 and MCP-1/ CCL2 were observed in the basolateral fluids of infected cultures, known to be macrophages and neutrophil chemotactic. Interestingly, IL-17c was significantly induced in the apical and basolateral fluids of infected cultures. Recently, IL-17 has been linked with the development of COPD as high levels of IL17A and Th17 inflammatory cells have been detected in the sputum and bronchial mucosa of COPD patients (Pfeifer et al., 2013). In the present study, type I interferon proteins were not initiated in apical or basolateral fluids of ciliated epithelial cultures following rhinovirus infection, which is in contrast to previous studies (Newcomb et al., 2008; Tan et al., 2018). Tan et al. (2018) found strong induction of IFN-α and IFN-β mRNA expression in nasal differentiated cultures infected with rhinovirus 16 whereas Newcomb et al. (2008) found significant induction of protein IFN-α and IFN-β in mice infected with rhinovirus. On the other hand, in the current study significantly higher protein levels of Type III IFNλ2/3 were detected in the basolateral and apical fluids. Induced high levels of IFNλ2/3 following rhinovirus infection are in agreement with previous studies (Wark et al., 2009; Tan et al., 2018; Jakiela et al., 2014).

4.4 Summary

The aim of this chapter was to investigate the early cytotoxic effects of rhinovirus on the airway ciliated epithelium. My research was able to show that rhinovirus preferentially targets ciliated cells in cultures from healthy and COPD donors, and this is associated with active shedding of this cell type. Ciliary activity measurement and DNAI2 expression demonstrated that active shedding attributes with significantly reduced ciliation. Rhinovirus-induced shedding contributed to clearance of live rhinovirus from the respiratory epithelium. It is also proposed that the novel GSK2998533 compound can successfully reduce rhinovirus replication in airway ciliated cells and preserve the ciliary activity of cultures. Future studies are needed to explore whether the PI4KIIIβ inhibitor would reduce host inflammation triggered by rhinovirus.

Chapter 5. Rhinovirus and *M. catarrhalis* co-infection of the respiratory epithelium

5.1 Introduction

Bacterial-viral co-infections are thought to lead to acute infections in specific group populations such as the elderly population, immunocompromised individuals as well as healthy young people, children and healthcare workers in hospitals (MacIntyre et al., 2017). Factors such as geographical areas, vaccination and socio-economy status are also important for bacterial / viral respiratory tract infections. For example, children attending school and day care centres are at higher risk of co-infections with pathogens and subsequent transmission (MacIntyre et al., 2017). The significance of bacterial-viral co-infections in healthy populations has been recognised during the pandemic of influenza virus in 2009, with secondary bacterial infections (occurred 1 in 4 people, with major bacterial pathogen *S. pneumoniae*) associated with admission to intensive care and death (MacIntyre et al., 2018). Bacterial-viral respiratory co-infections are critical for people who suffer from lung diseases such as cystic fibrosis who are frequently colonised with pathogens and commensals (Kiedrowski and Bomberger 2018). For example, viral infections can impact pre-existing or subsequent bacterial infections in cystic fibrosis by modifying the host immune response and altering the bacterial community by changing the abundance of bacteria (Kiedrowski and Bomberger 2018).

The role of bacterial and viral co-infections in the aetiology of COPD exacerbations has been well recognised (Papi et al., 2006; Wilkinson et al., 2006). Co-infections contribute to acute exacerbations which are associated with decreased lung function, longer hospitalisation and increased risk for hospital readmission (Papi et al., 2006; Wilkinson et al., 2006). Rhinovirus is the most prevalent virus, and NTHI, *S. pneumoniae* and *M. catarrhalis* are the most prevalent bacteria detected during COPD exacerbations (Hutchinson et al., 2007; Papi et al., 2006; Perotin et al., 2013, Sethi, 2004; Murphy et al., 2005; Wilkinson et al., 2017). Clinical data from COPD patients and experimental human infection studies have identified that viral infections can predispose patients to secondary bacterial infections (George et al., 2014; Hutchinson et al., 2007; Mallia et al., 2011; Papi et al., 2006). In an experimental rhinovirus 16 infection, 60% of COPD patients developed a secondary bacterial infection, in particular *S. aureus, S. pneumoniae, H. influenzae or H. parainfluenzae* (Mallia et al., 2011). In a follow up study, in sputum samples collected before and after

the experimental infection of COPD patients was detected a significant outgrowth of *H. influenzae* at day 15 thought to originate from the pre-existing community in the airways of these patients. A supportive relationship between initial rhinovirus infection and secondary bacterial infections has been reported by George et al who investigated rhinovirus, *S. pneumoniae, M. catarrhalis* and *H. influenzae* loads in periods of naturally occurring COPD exacerbations (George et al., 2014). Interestingly, the bacterial load increase was recorded highest at day 14 post rhinovirus detection (George et al., 2014).

The main mechanisms by which the human airways respond to bacterial-viral infections are via mucociliary clearance, pathogen detection, antimicrobial peptides secretion and release of anti-inflammatory cytokines that also attract inflammatory cells (Crystal et al., 2008; De Rose et al., 2018). Culture based studies unveiled several mechanisms by which respiratory viruses negatively impact the respiratory epithelium and so promoting increased susceptibility for subsequent bacterial infections. These include enhanced interferon production, antimicrobial peptide alterations and upregulated cellular receptor expression, favouring bacterial adhesion and invasion (Hendricks et al., 2016, Sajjan et al., 2008; Smith et al., 2014; Wang et al., 2009).

Increased NTHI, *P. aeruginosa* and *S. aureus* bacterial adherence and invasion have been described in human nasal and bronchial epithelial cells infected with rhinovirus 16 (Sajjan et al., 2008; Wang et al., 2009). Rhinovirus-induced changes in epithelial cells included increased cellular expression of receptors important for bacterial adherence such as CEACAM, fibronectin and G protein-coupled platelet-activating factor receptor (PAFr) (Wang et al., 2009). In addition, rhinovirus 14 promoted *S. pneumoniae* binding to bronchial epithelial cells *in vitro* whilst rhinovirus 1B promoted *S. aureus* internalisation into alveolar epithelial cells which are normally non-permissive (Ishizuka et al., 2003; Passariello et al., 2006). Rhinovirus 1B facilitated also the transmigration of *H. influenzae* and *S. aureus* across the ciliated epithelium through disruption of tight-junction proteins (Sajjan et al., 2008). Further, RSV enhanced *S. pneumoniae* adherence and virulence in human ciliated nasal epithelial cells through direct RSV-G protein and *Streptococcus* penicillin binding protein 1a (PBP1a) interaction (Smith et al., 2014). Respiratory viruses can also dysregulate epithelial innate defence mechanisms and predispose to secondary bacterial infections through altered secretion of antimicrobial peptides such as elafin and secretory leukoprotease inhibitor (SLPI) (Mallia et al., 2014). Also, RSV enhanced

secondary *P. aeruginosa* infection in cystic fibrosis differentiated cells through dysregulation of airway nutritional immunity that promoted iron-bound transferrin release, ultimately stimulating biofilm formation (Hendricks et al., 2016).

Respiratory viruses are also responsible for dysregulation of host immune response to bacteria (Oliver et al., 2008). *In vitro* culture of isolated human macrophages showed rhinovirus suppressed macrophage cytokine response to bacteria and bacterial products such as lipopolysaccharides and lipoteichoic acid, providing a favourable environment for a secondary bacterial infection (Oliver et al., 2008; Jubrail et al., 2018). Further, a Type I interferon-stimulated response to influenza respiratory virus caused impaired airway production of CXCL1 and CXCL2 chemokines, resulting in a subsequent attenuated neutrophil and macrophage response to secondary *S. pneumoniae* infection leading to increased bacterial colonisation (Shahangian et al., 2009; Nakamura et al.,2011). Overall, these studies suggest that respiratory viruses can impair host defence against secondary bacterial infection. However, whether any of these effects contribute to rhinovirus and *M. catarrhalis* induced COPD exacerbations is unclear.

Despite the evidence that rhinovirus and *M. catarrhalis* are pathogens inducing exacerbations, which are often detected in bacterial-viral co-infection triggered severe exacerbations in COPD patients, studies exploring the causal link between acquisition of these pathogens and the increased risk for exacerbations are missing. Therefore, investigating the initial interaction of rhinovirus and *M. catarrhalis* with the ciliated respiratory epithelium, and the cellular and molecular mechanisms associated with rhinovirus and *M. catarrhalis* co-infection of the airway epithelium would contribute to a more comprehensive understanding of disease pathogenesis. For the first time this study investigated the effects of rhinovirus and *M. catarrhalis* co-infection in healthy and COPD ciliated respiratory epithelium.

5.1.1 Hypothesis

Co-infection the respiratory epithelium with rhinovirus and *M. catarrhalis* leads to greater ciliary impairment and a greater inflammatory epithelial response in ciliated cultures from healthy and COPD patients than either infection alone.

5.1.2 Aims

1. To investigate the ciliary function of epithelial cultures following rhinovirus pre-infection and subsequent *M. catarrhalis* infection.

2. To determine if rhinovirus pre-infection of the respiratory epithelium leads to enhanced *M. catarrhalis* growth in epithelial ciliated cultures from healthy and COPD donors.

3. To determine if apical secretions from rhinovirus infected ciliated cultures from healthy and COPD donors affect *M. catarrhalis* viability.

4. To determine if rhinovirus pre-infection changes the epithelial inflammatory response to *M. catarrhalis* infection in ciliated cultures from healthy and COPD donors.

5.1.3 Characteristics of the patients

A total of 30 nasal and bronchial samples were collected by airway brushings in the period between January 2016 and January 2019. Samples from 11 healthy volunteers and 9 COPD patients were included in this study. Essential requirement for sample collection was a minimum period of 3 weeks free of respiratory cold symptoms. None of the participants were active smokers at the time of the sample collection, except one COPD patient. A different COPD patient reported a Berger's disease. Table 5-1 summarises the characteristics of patients included in the study and Supplementary Table 1 in Appendix 1 provides the full details of the patients.

Table 5-1: Clinical characteristics of patients included in the co-infection study. 11 healthy volunteers and 9 COPD patients whose samples have been included in the study of rhinovirus and *M. catarrhalis* co-infection of the respiratory epithelium, data are presented as mean ± SEM or % except FEV_1 which is expressed as median ± interquartile range.

Clinical characteristics	Healthy	COPD
Age (years)	58.65 ±2.53	73.89 ±2.05
Gender (Male)	36%	66%
Exacerbations <2/last year	0	88%
Current smoker	0	11%
Chronic bronchitis	0	88%
FEV_1 (L)	-	1.06±1.02
FEV_1 (%)	-	39.63±6.10
FVC (L)	-	2.05±0.25
FVC (%)	-	68.67±6.90
FEV_1/FVC ratio	-	0.49±0.05

5.2 Results

5.2.1 Ciliary function of epithelial cells during co-infection with rhinovirus and *M. catarrhalis*

It was shown in chapter 3 that the initial interaction of *M. catarrhalis* with ciliated cells reduced the ciliary beat amplitude of airway cultures, while the pathogen had little effect on CBF. Then in chapter 4 it was observed that rhinovirus by itself did not alter the beat frequency of ALI cultures, but did reduce the percentage of areas with actively beating cilia in infected cultures. It was decided therefore to investigate whether a co-infection model with rhinovirus pre-infection and a *M. catarrhalis* subsequent infection would have an effect on ciliary function. To clarify, in Figure 5-1 the 24h time-point in the co-infection model equates to 48h of rhinovirus single infection. CBF and ciliary activity were analysed in 7 healthy and 6 COPD ciliated cultures during co-infection.

In healthy cultures at 15min, a single pathogen infection was not associated with reduction of CBF (Figure 5-1 A). There was no difference between rhinovirus or *M. catarrhalis* single infections or the type of pathogen infection relative to control non-infected cultures. A combination of rhinovirus with *M. catarrhalis* supressed significantly the CBF of healthy cultures by ~ 2 Hz compared to rhinovirus infection alone (p=0.046) and *M. catarrhalis* infection alone (p=0.037). In COPD cultures at 15min, rhinovirus with *M. catarrhalis* significantly suppressed by ~ 3 Hz CBF of co-infected cultures in comparison to non-infected cultures (p=0.004), by ~2.4 Hz in comparison to rhinovirus infected cultures (p=0.037) and by 1.8 Hz in comparison to *M. catarrhalis* infected cultures, though this failed to reach statistical significance (p=0.11) (Figure 5-1 A). At 15min post infection, in co-infection conditions we reported a strong difference between healthy and COPD, where a reduction of ~ 2 Hz was observed in the CBF of cultures from COPD donors in comparison to cultures from healthy individuals (Figure 5-1 A), the difference however did not reach statistical significance (p=0.27).

Figure 5-1 B shows there was a further reduction in CBF at 24h post co-infection of ciliated cultures from healthy and COPD donors. Co-infection with rhinovirus and *M. catarrhalis* led to a significant CBF decrease of cultures from healthy individuals in comparison to *M. catarrhalis* single infection (p=0.046) and rhinovirus single infection (p=0.037). Cultures infected with single pathogens presented with similar beat frequency (Figure 5-1 B). In contrast, rhinovirus single infection of cultures from COPD patients exhibited a significant CBF decrease of 2.3 Hz in comparison to *M. catarrhalis*

single infection (p=0.037). At 24h, a CBF reduction of ~1.7 Hz was observed in infected with rhinovirus and *M. catarrhalis* cultures from COPD donors in comparison to single *M. catarrhalis* infection. However, a direct comparison between co-infection and single rhinovirus infection revealed a higher CBF by ~ 0.6 Hz in co-infected cultures. These differences did not reach statistical significance. A difference of ~ 2 Hz in CBF was reported between cultures from healthy and COPD donors for co-infections at 24h, though it again did not reach significance. Comparisons of beat frequency between 15min and 24h time-points revealed a 1.6 Hz non-significant CBF reduction in non-infected cultures from healthy individuals at 24h, and a statistically significant 2.3Hz CBF reduction in non-infected cultures from COPD patients at the 24h time-point (p=0.037). In addition, a significant CBF reduction of 2.7 Hz was reported between 15min and 24h for rhinovirus single infection in cultures from COPD donors (p=0.024).

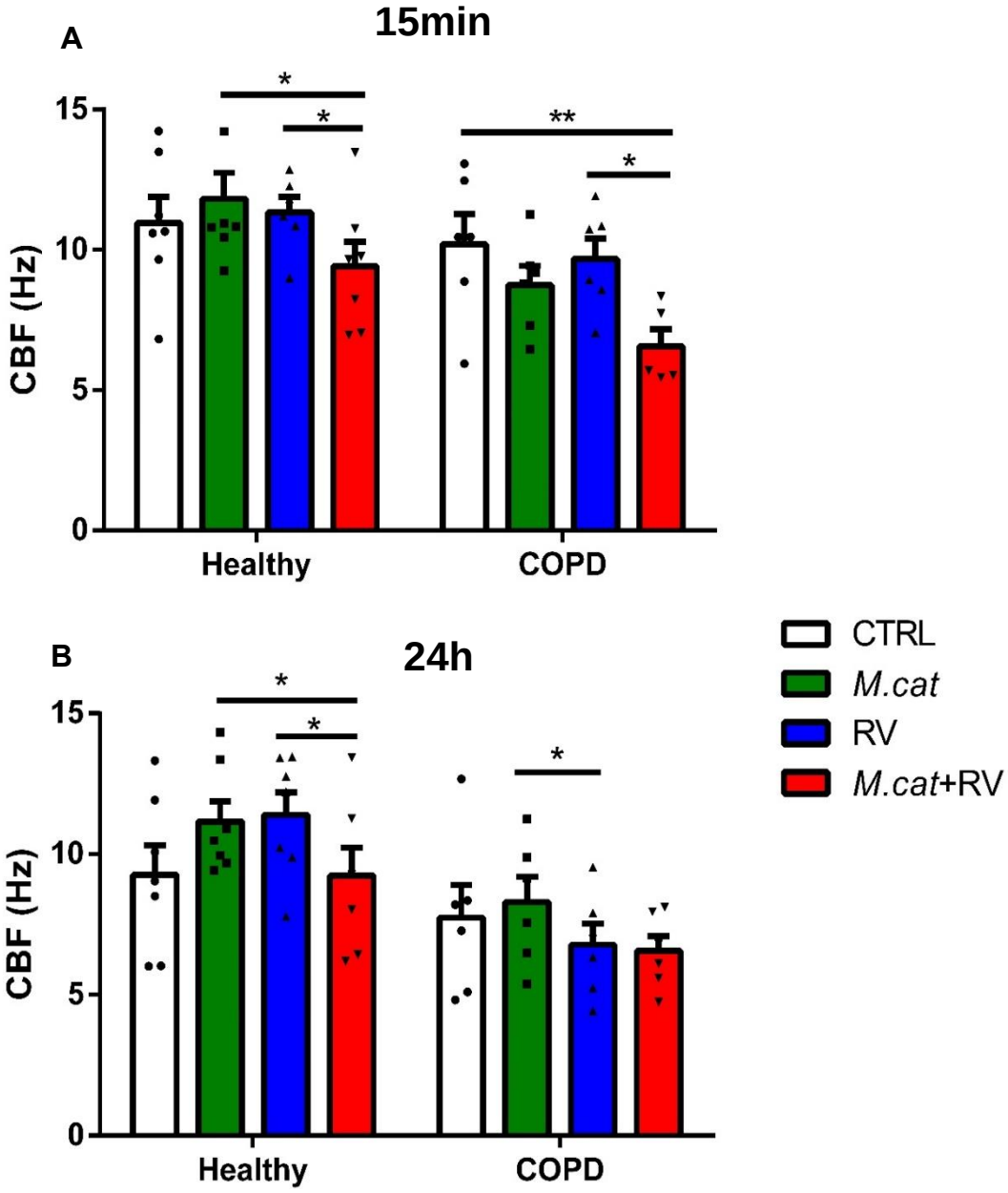

Figure 5-1: CBF of healthy and COPD ciliated cultures during co-infection with rhinovirus and *M. catarrhalis*.

A) CBF of ciliated cultures from healthy and COPD donors during co-infection with rhinovirus and *M. catarrhalis* at 15min (24h RV infection, 15min *M.cat* infection); B) CBF of ciliated cultures from healthy and COPD donors during co-infection with rhinovirus and *M. catarrhalis* at 24 hours (48h RV infection, 24h *M.cat* infection). Data points represent single mean values of 10 recordings/ donor in 7 healthy and 6 COPD donors, error bars represent ±SEM, *=p<0.05, **=p<0.01; CBF – ciliary beat frequency, *M.cat* - *Moraxella catarrhalis*; RV – rhinovirus

To assess whether a co-infection with rhinovirus and *M. catarrhalis* would affect the ciliary activity of epithelial cultures (Figure 5-2), the % active area was calculated from the same high speed videos recorded for CBF analysis. We have already shown that single rhinovirus infection significantly reduced the ciliary activity of cultures from healthy and COPD donors at 24h post infection (chapter 4 Figure 4-3) and by 7 days of infection, ciliation of infected cultures was vastly decreased to a level that would severely impair ciliary function (chapter 4 Figure 4-7). In the co-infection model the 24h time-point corresponds to 48h of rhinovirus infection. Although statistical comparisons, that included taking into account corrections for multiple comparisons, did not reach significance when ciliary activity was evaluated some trends did appear.

Similarly to rhinovirus single infection experiments, in the current co-infection model ciliary activity of rhinovirus pre-infected cultures was found reduced compared to control measurements (Figure 5-2). At 15min post co-infection in cultures from healthy individuals, pre-infection with rhinovirus already exhibited a ~30% decrease of ciliary activity in comparison to non-infected cultures (p=0.71) and a ~40% decrease in comparison to *M. catarrhalis* infected cultures (p=0.71). In cultures from COPD patients, a difference between ciliary activity in non-infected cultures and rhinovirus infected cultures was not observed, however *M. catarrhalis* infected cultures presented with a higher ciliary activity in comparison to rhinovirus infected cultures (~30% difference) (p=0.71). Ciliary activity of epithelial cultures infected with rhinovirus and *M. catarrhalis* was found to be around 30% decreased to that of *M. catarrhalis* infected cultures (p=0.71). No difference of ciliary activity was seen between rhinovirus and *M. catarrhalis* infected cultures and non-infected control (p=0.86) or rhinovirus infected cultures (p=0.95). None of the reported differences reached statistical significance (Figure 5-2 A).

At 24h post co-infection, differences in ciliary activity of cultures from healthy individuals between infections with *M. catarrhalis* or rhinovirus or the two together remained similar to the ones reported for the 15min time-point. In cultures from healthy individuals, rhinovirus infected cultures showed a ~40% decrease in ciliary activity compared to non-infected (p=0.71) and *M. catarrhalis* infected cultures (p=0.71) (Figure 5-2 B). In ciliated cultures from healthy individuals, infection with both pathogens presented with a ~20% decrease in ciliary activity compared to non-infected (p=0.88) and *M. catarrhalis* infected cultures (p=0.86). In cultures from COPD patients, rhinovirus induced a reduction of ~40% in ciliary activity compared to non-infected cultures (p=0.71) and ~60% reduction compared to *M. catarrhalis* infection

(p=0.49) (Figure 5-2 B). Similarly, a co-infection of cultures from COPD donors with the two pathogens caused a ~35% reduction of ciliary activity compared to non-infected cultures (p=0.71) and 55% reduction compared to *M. catarrhalis* only infection (p=0.55). *M. catarrhalis* did not suppress the ciliary activity of cultures from healthy or COPD donors at either time-point, suggesting that this is a feature specific to rhinovirus infection only. In addition, no difference of ciliary activity was observed between rhinovirus and *M. catarrhalis* co-infection and rhinovirus single infection, except at 24h in cultures from healthy individuals when ciliary activity of co-infected cultures was higher by 30% than that of rhinovirus infected cultures (p=0.78). Reductions of ciliary activity from 15min to 24h were observed in COPD donor cultures infected with rhinovirus and rhinovirus and *M. catarrhalis* together, accounting for ~ 30% (p=0.71) and 20% decrease (p=0.86) respectively. At 15min approximately 2 times lower ciliary activity was observed in healthy donor cultures infected with rhinovirus (p=0.71) or rhinovirus and *M. catarrhalis* (p=0.71) compared to COPD donor cultures. Ciliary activity of cultures from COPD donors during *M. catarrhalis* infection was found about 2 times higher compared to healthy at 24h.

Overall, the healthy and COPD epithelial cultures presented with severely impaired ciliary function following a co-infection with rhinovirus and *M. catarrhalis*. The beat frequency of cultures infected with the two pathogens was significantly reduced at both time-points investigated. In addition, there was a trend of reduced ciliary activity that appeared to be due to rhinovirus infection, suggesting that a combination of viral-bacterial infection could lead to inefficient mucociliary clearance, due to reduced number of ciliated cells in a combination with decreased beat frequency.

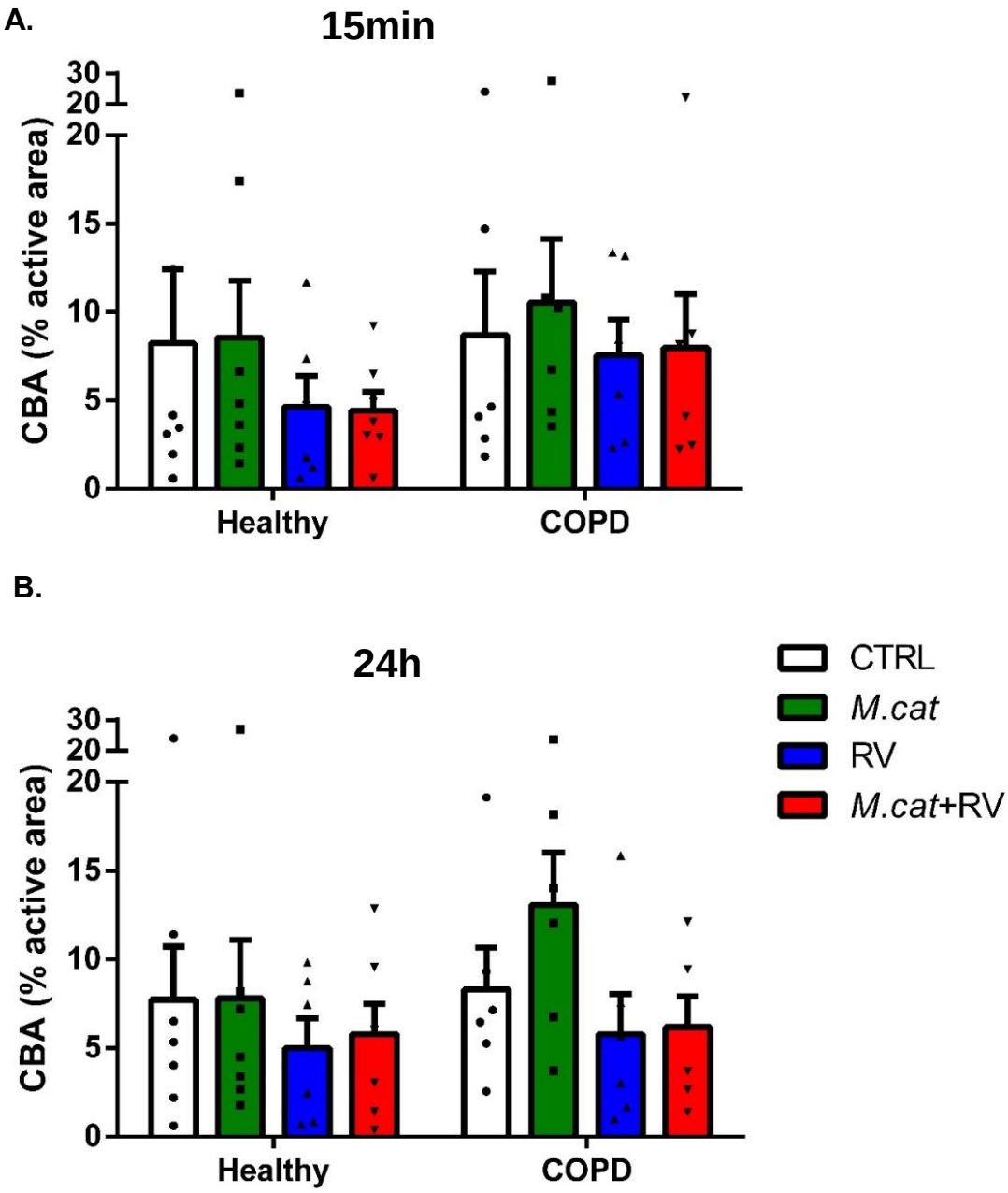

Figure 5-2: Ciliary activity of healthy and COPD airway cultures infected with rhinovirus and *M. catarrhalis*

A) Ciliary activity of airway cultures from healthy and COPD donors infected with rhinovirus and *M. catarrhalis* at 15min post co-infection (24h RV infection, 15min *M. cat* infection), B) Ciliary activity of airway cultures from healthy and COPD donors infected with rhinovirus and *M. catarrhalis* at 24 hours post co-infection (48h RV infection, 24h *M.cat* infection). Data points represent single mean values of 10 recordings/ donor in 7 healthy and 6 COPD donors, error bars represent ±SEM; CBA – ciliary beat activity, *M.cat* - *Moraxella catarrhalis*; RV – rhinovirus

5.2.2 *M. catarrhalis* viability during co-infection with rhinovirus

It was previously shown that *M. catarrhalis* viability was increased in COPD epithelial cultures compared to healthy epithelial cultures at 24h post infection (chapter 3 Figure 3-5). To evaluate whether bacterial adherence and invasion in epithelial cultures is upregulated following rhinovirus infection, bacterial viability was assessed in cultures infected with *M. catarrhalis* only or *M. catarrhalis* and rhinovirus together at 24h post infection. CFU counts were taken to enable a comparison between the two models of infection and to assess whether there was a difference between the healthy and COPD groups.

In Figure 5-3 *M. catarrhalis* viability was assessed in washes from the apical surface of infected cultures, thought to contain loosely bound or mucous bound bacteria. In cultures from healthy volunteers, the response to rhinovirus varied greatly between donors and no consistency of effect for apical CFU counts was demonstrated (p=0.86) (Figure 5-3 A). In cultures from COPD donors, a more constant trend of reduced bacterial viability was observed in the presence of rhinovirus infection, though no statistical significance was reached in terms of the numerical data (p=0.86). *M. catarrhalis* adherence and intracellular viability in healthy donor cultures was increased following rhinovirus infection by approximately ~30%, however no consistency of data amongst the different donors was achieved, and no statistical significance was reached (p=0.85) (Figure 5-3 A). An increase of *M. catarrhalis* adherence and invasion of epithelial cells was not found in rhinovirus infected cultures from COPD donors (Figure 5-3 B). There was a suggestion of decline in *M. catarrhalis* viability of adhered and intracellular bacteria for all COPD donors (p=0.45). Bacterial invasion in cultures from healthy individuals in response to rhinovirus was again variable whereas in cultures from COPD donors only one out of six cultures showed a slight increase in intracellular bacteria following rhinovirus infection (p=0.2) (Figure 5-3 B). None of these results reached statistical significance, suggesting more donors need to be included in the study to reach statistical biological relevance.

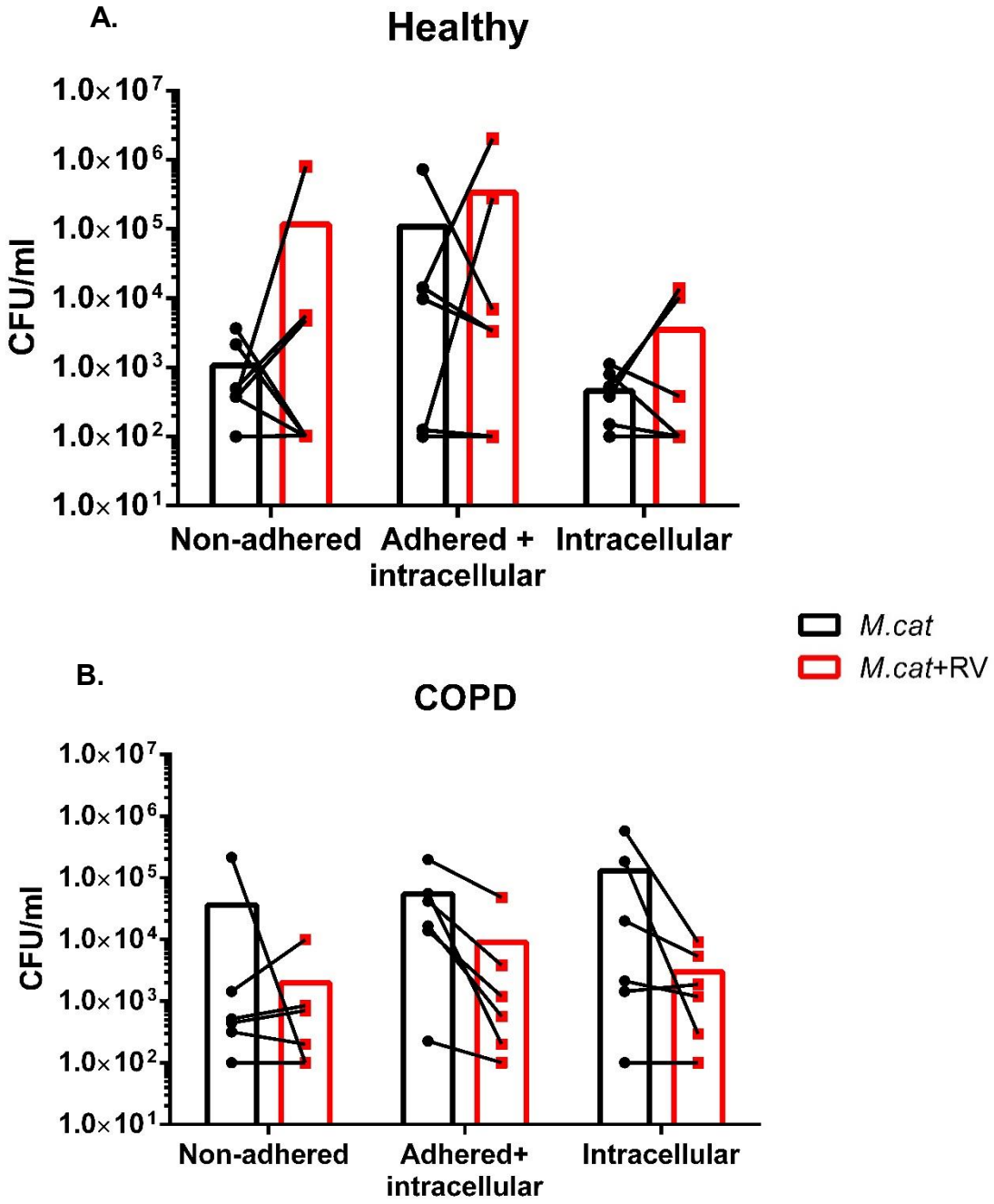

Figure 5-3: *M. catarrhalis* viability in ciliated cultures from healthy and COPD donors during co-infection at 24h .

A) *M. catarrhalis* viability in cultures from healthy individuals during co-infection with rhinovirus or single *M. catarrhalis* infection, B) *M. catarrhalis* viability in cultures from COPD donors during co-infection with rhinovirus or single *M. catarrhalis* infection. Data points represent means of 2 technical repeats in ciliated cultures from 7 healthy and 6 COPD donors.

5.2.3 TEER of primary airway epithelial cells infected with *M. catarrhalis* and rhinovirus

Immediately after the apical surface of ciliated cultures was flooded with culture media to check the bacterial viability, TEER measurements were carried out to evaluate whether a co-infection with rhinovirus and *M. catarrhalis* impaired the epithelial resistance of ciliated cultures. Figure 5-4 A demonstrates that the mean ± SEM TEER of non-infected cultures from healthy individuals was 1147 ± 317 Ω/cm^2 and that of infected with *M. catarrhalis* cultures was 1122 ± 300 Ω/cm^2. The mean ± SEM TEER of cultures from healthy individuals infected with rhinovirus was reduced to 855 ± 169Ω/cm^2 and the mean ± SEM TEER of cultures infected with rhinovirus and *M. catarrhalis* was 713 ± 190 Ω/cm^2. In cultures from COPD donors, the mean ± SEM TEER of non-infected cultures was 988 ± 239 Ω/cm^2 and that of *M. catarrhalis* infected cultures was 944 ± 168 Ω/cm^2. The mean ± SEM TEER of cultures from COPD donors infected with rhinovirus was 1107 ± 102 Ω/cm^2 and the TEER of cultures infected with *M. catarrhalis* and rhinovirus was 941 ± 261 Ω/cm^2 (Figure 5-4 B). TEER measurements findings were more variable in COPD cultures, less definitive decreases amongst conditions were observed. The results suggest that in all but one case (COPD: Rhinovirus + *M. Catarrhalis* - 260 Ω/cm^2) the cultures remained with good epithelial resistance during experiments.

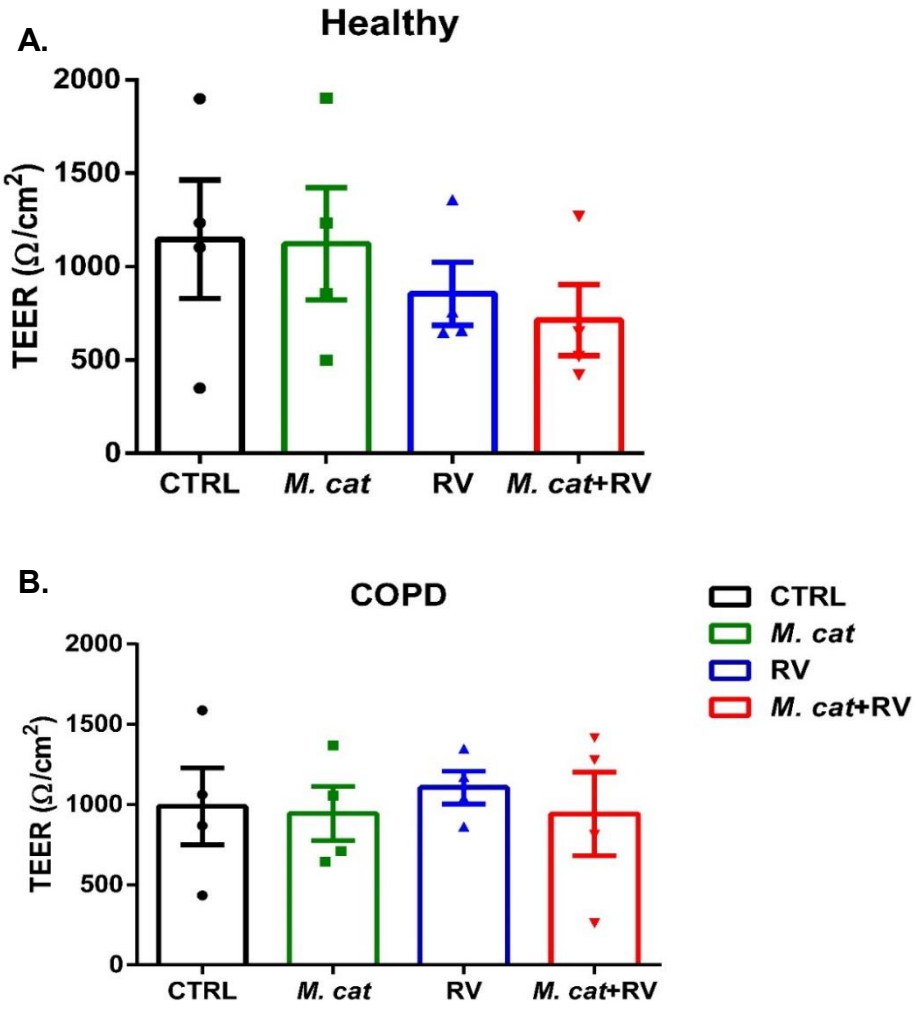

Figure 5-4: TEER of airway cultures from healthy and COPD donors at 24h post co-infection with *M. catarrhalis* and rhinovirus at 24h.

A) TEER of airway cultures from healthy individuals infected with rhinovirus and *M. catarrhalis* at 24h post-co-infection, B) TEER of airway cultures from COPD donors infected with rhinovirus and *M. catarrhalis* at 24h post-co-infection. Data points represent single mean values of 2 technical replicate measurements in 4 healthy and 4 COPD donors, error bars represent ±SEM. *M. cat* – *M. catarrhalis*, RV - rhinovirus

5.2.4 Shedding of epithelial cells following co-infection with *M. catarrhalis* and rhinovirus

Our findings for *M. catarrhalis* viability in rhinovirus infected cultures from COPD donors were not in agreement with previous experimental studies that suggest respiratory viruses increase bacterial growth (Sajjan et al., 2008; Hendricks et al., 2016). Therefore, I investigated whether the ability of rhinovirus to detach ciliated cells from the epithelial layer was associated with reduced bacterial adherence. It was previously shown in chapter 3 that *M. catarrhalis* rapidly binds to ciliated cells.

Figure 5-5 shows that observational assessment of recorded high speed videos from co-infection studies confirmed the presence of detached ciliated cells with *M. catarrhalis* bound to them. The screenshots in Figure 5-5 are representative examples of cultures infected with rhinovirus and *M. catarrhalis* and show detached ciliated cells with attached bacteria: although the cells became round in shape when detached from the epithelium, bacteria could be seen to be attached to cilia. This is the first *in vitro* study describing that rhinovirus can shed ciliated cells with attached bacteria. Detachment of ciliated cells with *M. catarrhalis* bound to the cilia could potentially facilitate spread of bacteria with coughing and also further dissemination throughout the respiratory tract. Future experiments, investigating the infectivity of detached airway cells with bound bacteria, would confirm infectivity with both virus and bacteria.

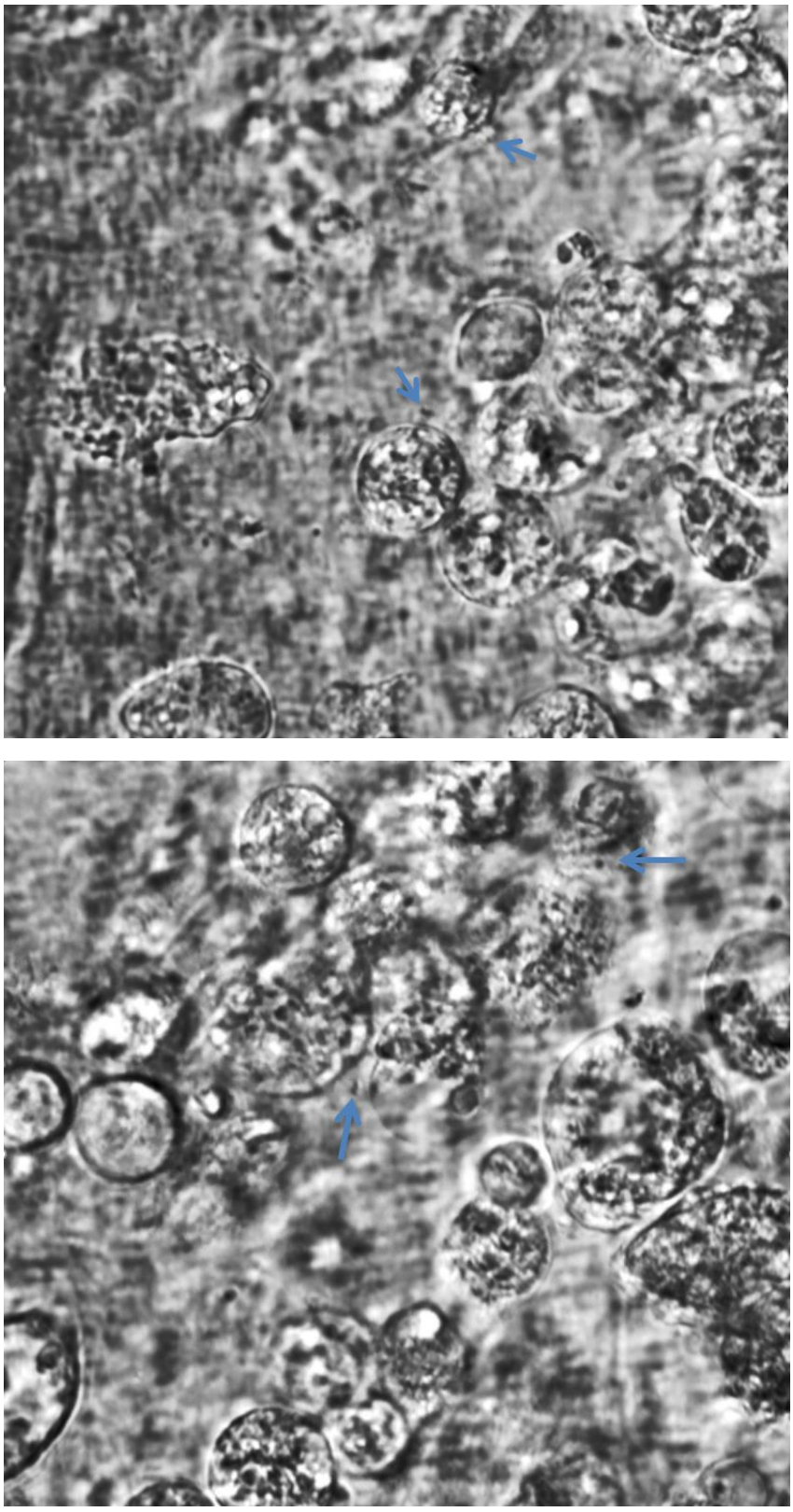

Figure 5-5: Screenshots of high speed recorded videos of ciliated cultures infected with rhinovirus and *M. catarrhalis* at 8h post co-infection.

Blue arrows pointing at detached ciliated cells with bound *M. catarrhalis.*

5.2.5 The effect of apical secretions from ciliated cultures from healthy and COPD donors on bacterial growth

Antimicrobial peptides are major factors in the epithelial barrier defence mechanism and host innate immunity against pathogens (De Rose et al., 20018). It has been suggested that respiratory viruses may decrease the concentration of antimicrobial peptides predisposing to subsequent bacterial infections (Mallia et al., 2012). To evaluate whether rhinovirus infection affects the apical secretions from ciliated cultures, an assessment was made of impact of apical fluids collected from rhinovirus infected and non-infected cultures on the growth of *M. catarrhalis* (Figure 5-6). Apical fluids were collected from ALI cultures and prepared as described in section 2.4.7. Significant suppression of bacterial growth was observed when *M. catarrhalis* was treated with apical fluids from cultures from healthy individuals for 24h compared to an equivalent volume of BEBM media control (p=0.02) (Figure 5-6 A). In contrast, apical fluids from cultures from COPD donors did not reduce the growth of *M. catarrhalis* and no difference was observed in viable counts compared to plain BEBM media (Figure 5-6 B). A direct comparison between apical fluids from cultures from healthy and COPD donors showed a non-significant difference of *M. catarrhalis* viability during treatments (p=0.1) (Figure 5-6 C). Representative screenshots of bacteria treated with BEBM, apical fluids from cultures from healthy and COPD donors are attached in Appendix 1, Supplementary Figure 5.

Assessment of apical fluids collected from rhinovirus infected cultures was carried out to evaluate whether rhinovirus infection would have an effect on *M. catarrhalis* growth (Figure 5-6 D). In the current study BEBM plain media and rhinovirus control media, which contained rhinovirus concentration similar to that measured previously in the apical washes of rhinovirus infected cultures (chapter 3 Figure 3-5), were used as negative controls. Bacterial viability was not found to be changed in the presence of apical fluids collected from cultures of either healthy or COPD donors infected with rhinovirus. A significant decrease in *M. catarrhalis* viability was observed between treatments with apical fluids from cultures from healthy individuals and plain BEBM media (p=0.01). There was a significant decrease in *M. catarrhalis* viability between treatments with apical fluids from rhinovirus infected cultures from healthy individuals and rhinovirus control media (p=0.04). No difference was observed between treatments with apical fluids from rhinovirus infected cultures from COPD donors and rhinovirus control media. Apical fluids from rhinovirus infected cultures from COPD donors did not decrease or increase the growth of *M. catarrhalis*.

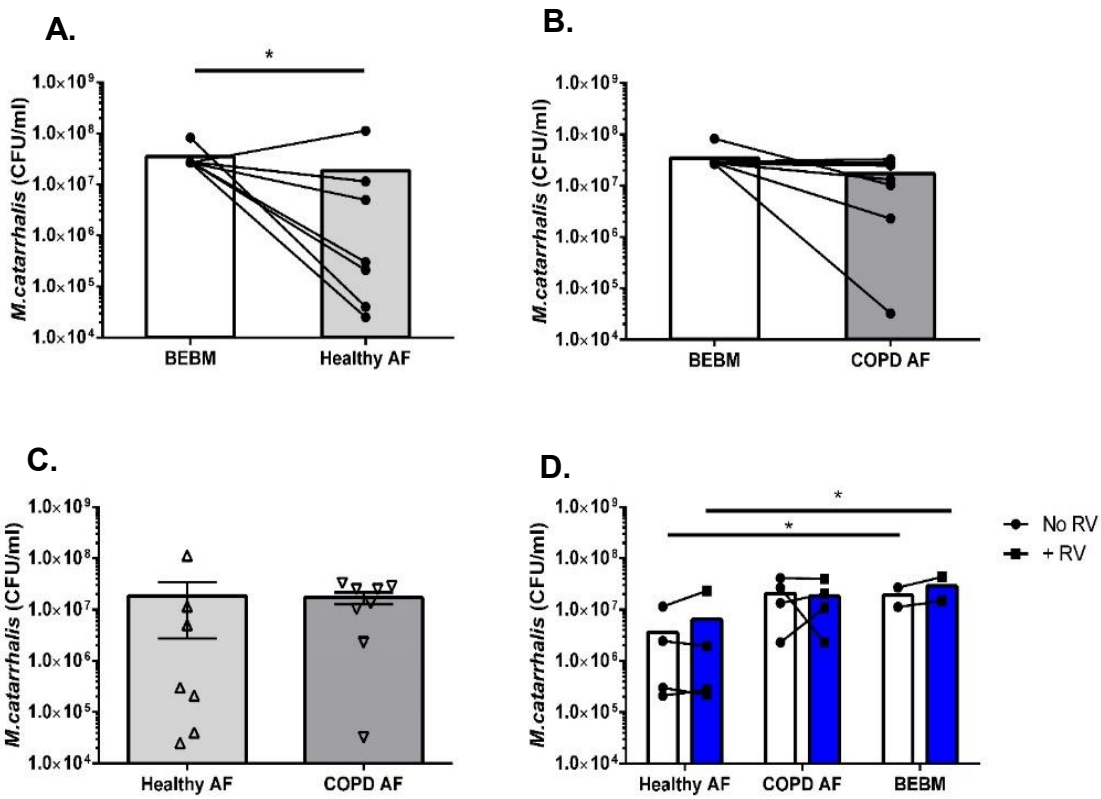

Figure 5-6: *M. catarrhalis* growth at 24h following treatment with apical secretions from ciliated cultures infected or non-infected with rhinovirus.

A) *M. catarrhalis* growth in BEBM and apical fluids of cultures from healthy individuals at 24h, n=7; B) *M. catarrhalis* growth in BEBM and apical fluids of cultures from COPD donors at 24h, n=8; C) Comparison of *M. catarrhalis* growth in apical fluids of cultures from healthy and COPD donors, n=7 Healthy and n=8 COPD, D) *M. catarrhalis* growth in apical fluids of cultures infected with rhinovirus for 24h, n=4 healthy and n=4 COPD. Data points represent average of 2 technical repeats, error bars represent ±SEM, *=p<0.05; AF- apical fluid, RV- rhinovirus

5.2.6 ROS generation in healthy and COPD airway cells following co-infection with rhinovirus and *M. catarrhalis*

ROS contribute to enhanced airway inflammation in chronic respiratory diseases such as asthma and COPD, and several mechanisms are linked to their destructive function (Rahman and Adcock 2006, Barnes 2016). These include ROS signalling via the MAPK and PI3K pathways causing the expression of pro-inflammatory genes, ROS direct reaction with biological proteins and lipids leading to cell dysfunction and injury, dysregulation of protease-anti-protease balances causing loss of lung tissue elasticity, activation of TGF-β promoting lung fibrosis, and stimulation of mucin production (Barnes 2016; Park et al., 2009; Rahman and Adcock 2006). In addition, COPD and asthma patients are characterised as having high ROS production, which increases further during exacerbations (Kirkham and Rahman 2006). More recently, ROS have been implicated in the ciliary dysfunction of bronchial epithelial tissue from asthma patients, which was successfully reversed by antioxidant treatment with an NADPH (Nicotinamide adenine dinucleotide phosphate) inhibitor. NADPH is a source of cellular ROS generation (Wan et al., 2016). My study has already shown that CBF of airway differentiated cultures from COPD donors is severely impaired in the presence of rhinovirus and *M. catarrhalis* (Figure 5-1). It was therefore decided to assess ROS production in epithelial cultures using the rhinovirus- *M. catarrhalis* co-infection model.

NADPH is converted to non-radical hydrogen peroxide by superoxide dismutases (Barnes, 2003). Readily available commercial hydrogen peroxide (H_2O_2) assay kits enabled the evaluation of H_2O_2 levels in epithelial cultures following single rhinovirus infection at 24h and in a following co-infection with *M. catarrhalis*. It was previously suggested that ROS are increased in COPD airways (Barnes, 2015). Although statistical comparisons, that included taking into account corrections for multiple comparisons, did not reach significance, when H_2O_2 production was evaluated some trends appeared. In Figure 5-7 it was shown that COPD airway cells generated more H_2O_2, a 1.25 fold increase (95% CI: 0.88-1.95) in comparison to healthy airway cells ($p=0.69$). Rhinovirus induced higher concentrations of H_2O_2 in ciliated cultures from healthy and COPD donors compared to non-infected controls, though the increases were statistically non-significant ($p=0.17$, healthy and $p=1$, COPD) (Figure 5-7 A). In contrast in terms of ROS generation *M. catarrhalis* infection of ciliated cultures from COPD donors appeared to have the opposite effect, as a lower concentration of H_2O_2 was detected in the COPD cells compared to non-infected cells, the estimated relative change was 0.85 (95% CI: 0.62 – 1.19) (Figure 5-7 B). No difference in H_2O_2

generation was observed between healthy non-infected control and *M. catarrhalis* infection in cultures from healthy donors (Figure 5-7 B). H_2O_2 levels in epithelial cells were detected increased following rhinovirus infection at 24h post co-infection (this equates to 48h of virus infection). In particular, following rhinovirus infection a 1.5 fold (95% CI: 1.08 – 2.1) increase was observed in cultures from healthy donors and a 1.3 fold (95% CI: 0.91 – 1.75) increase was observed in cultures from COPD donors, in comparison to relative to non-infected controls (p=0.15, healthy and p=0.69, COPD) (Figure 5-7 B).

Co-infection with rhinovirus and *M. catarrhalis* in cultures from healthy individuals did not induce higher production of H_2O_2 in comparison to control non-infected cultures (p=1) (Figure 5-7 B). In addition, in cultures from healthy individuals H_2O_2 production was not increased following co-infection compared to rhinovirus infection (relative change 0.7, 95% CI: 0.5 – 0.97, p=0.15) or *M. catarrhalis* infection (relative change 1.1, 95% CI: 0.77 – 1.47). Co-infection with rhinovirus and *M. catarrhalis* in cultures from COPD donors appeared to increase H_2O_2 production in comparison to non-infected controls (relative change 1.2, 95% CI: 0.89 – 1.7, p=0.8) and *M. catarrhalis* infection (relative change 1.4, 95% CI: 1.04 – 1.98, p=0.15). H_2O_2 production in cultures from COPD donors was similar during rhinovirus infection and co-infection at 24h (Figure 5-7 B, p=1). Further, H_2O_2 levels during *M. catarrhalis* infection (p=1) and rhinovirus infection (p=1) were similar between the healthy and COPD groups at 24h post co-infection. However, H_2O_2 production during co-infection with rhinovirus and *M. catarrhalis* of cultures from COPD donors was increased, relative change 1.5 (95% CI: 0.94 - 2.29) compared to cultures from healthy donors (p=0.26).

In the co-infection model, ciliated cultures from COPD donors exhibited higher baseline levels of H_2O_2 compared to ciliated cultures from healthy individuals. Rhinovirus pre-infection increased the H_2O_2 production in both healthy and COPD donors. At 24h of co-infection with rhinovirus and *M. catarrhalis* H_2O_2 levels were higher in cultures from COPD donors than in cultures from healthy donors.

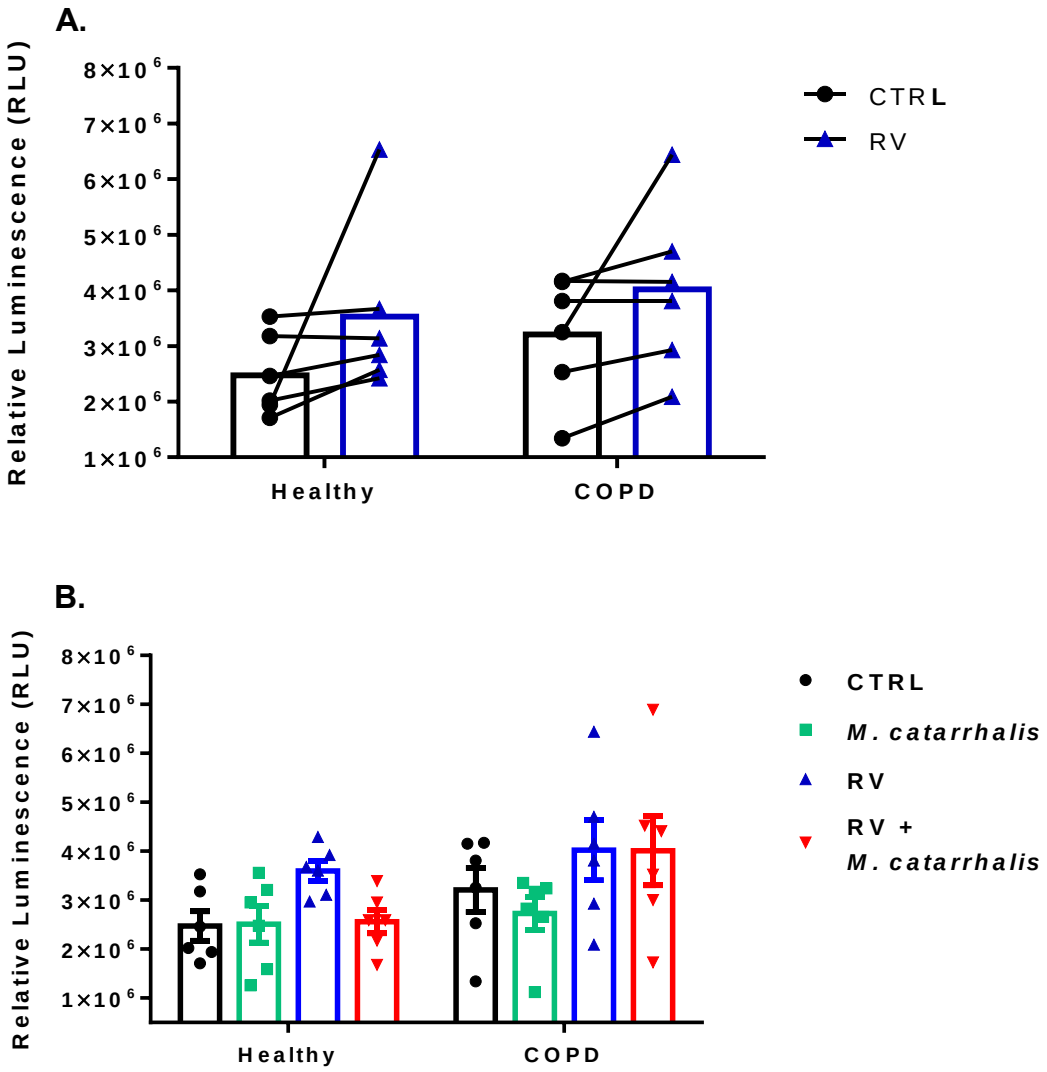

Figure 5-7: H_2O_2 concentration in ciliated cultures infected with *M. catarrhalis* and rhinovirus for 24h.

A) H_2O_2 concentration in ciliated cultures from healthy and COPD donors at 24h of rhinovirus infection; B) H_2O_2 concentration in ciliated cultures from healthy and COPD donors at 24h of co-infection with rhinovirus and *M. catarrhalis*, n=6 healthy and n=6 COPD cultures. Error bars represent ±SEM.

5.2.7 Epithelial inflammation following co-infection with rhinovirus and *M. catarrhalis* in ciliated cultures from healthy and COPD donors

Greater lung function impairment is seen during acute COPD exacerbations in the presence of viral and bacterial pathogens co-infection (Papi et al., 2006). Airway inflammation is a consistent feature of COPD being recognised as a key driver of exacerbations (Brightling and Greening 2019). Previously, in chapter 3 it was shown *M. catarrhalis* stimulated a broad range of inflammatory mediators in differentiated cultures from healthy and COPD donors, of which MIP-3α/ CCL20 and IFN-β were significantly increased. It was also found in chapter 4 that the epithelial response to rhinovirus infection affected the levels of a broad range of cytokines and chemokines including IL-1β, IP-10/ CXCL10, IL-6, IL-8/ CXCL8, TNF-α, RANTES/ CCL5, IL-17c, MIP-3α/ CCL20 and IFNλ2/3, in accordance with previous studies (Papadopoulos et al., 2000; Wark et al., 2009; Mallia et al., 2014; George et al., 2014; Jakiela et al., 2014). Novel findings from our work suggest a significant increase in CSF-3/ GM-CSF and IL-15 in ciliated cultures from COPD donors following rhinovirus infection. To assess whether co-infection with rhinovirus and *M. catarrhalis* was associated with an increased inflammatory response, measurements were made using the cytokine panel that was used in chapters 3 and 4. This allowed analyses of the apical and basolateral fluids of cultures from healthy and COPD donors following co-infection.

Figures 5-8 and 5-9 show cytokine and chemokine measurements following *M. catarrhalis* and rhinovirus co-infection. The results showed markedly increased levels of multiple cytokines and chemokines at 24h in cultures from both healthy and COPD donors. However, the highest levels of IL-6, IP-10/ CXCL10, TNF-α, ENA-78/ CXCL5, MIP-3α/ CCL20 and IL-17c were observed during co-infection with rhinovirus and *M. catarrhalis* of cultures from COPD donors. Figures 5-8 and 5-9 show cytokines and chemokines that were significantly upregulated compared to controls in basolateral and apical fluids respectively. Tables 5-1 and 5-2 show non-significant increase of mediators relative to controls. Two observations from 1 healthy donor for IFN-α and IFN-β were excluded from the analysis as the values were unusually high and produced large value residuals which were in conflict with the model assumptions. Four zero observations from the ENA-78/ CXCL5 and IFN-γ cytokine readings were also excluded from the analysis for the same reason. For discussion purposes direct comparisons of cytokines were grouped into co-infection comparisons, rhinovirus comparisons and *M. catarrhalis* comparisons.

5.2.7.1 Inflammatory mediators secreted in basolateral fluids

Co-infection comparisons were carried out (Figure 5-8). Co-infection with rhinovirus and *M. catarrhalis* led to significantly increased IL-1β and IL-6 levels in cultures from COPD donors in comparison to non-infected control ($p=0.016$ and $p<0.0001$, respectively) and *M. catarrhalis* infection ($p<0.05$ and $p<0.01$, respectively). Significant IL-6 increase was seen also in cultures from healthy individuals in comparison to non-infected control ($p<0.01$) (Figure 5-8 A and C). Significant induction of IP-10/ CXCL10 during co-infection was observed in cultures from healthy and COPD donors in comparison to non-infected control ($p<0.0001$) and *M. catarrhalis* infection ($p<0.0001$) (Figure 5-8 B). Likewise, RANTES/ CCL5 was strongly increased during co-infection in comparison to non-infected control and *M. catarrhalis* infection in healthy ($p<0.0001$ and $p<0.001$ respectively) and COPD donor cultures ($p<0.0001$, both conditions) (Figure 5-8 D). In cultures from COPD donors, significant increase of TNF-α ($p<0.0001$), ENA-78/ CXCL5 ($p<0.0001$), CSF-3/ GM-CSF ($p<0.001$) and IL-17c ($p<0.001$) was observed during co-infection in comparison to non-infected controls (Figures 5-8 E, F, G, H). The mediators were also significantly increased in cultures from healthy individuals in comparison to non-infected controls but to a lower magnitude TNF-α ($p<0.01$), ENA-78/ CXCCL5 ($p<0.001$), CSF-3/ GM-CSF ($p<0.001$), IL-17c ($p<0.001$). CSF-3/ GM-SCF was significantly increased in comparison to *M. catarrhalis* infection in cultures from healthy ($p<0.01$) and COPD ($p<0.05$) donors, while TNF-α was significantly increased in cultures from COPD donors compared to *M. catarrhalis* infection ($p<0.05$). IFNλ2/3 was significantly increased post co-infection in comparison to non-infected control and *M. catarrhalis* infection in cultures from healthy ($p<0.0001$ and $p<0.001$, respectively) and COPD ($p<0.0001$, both conditions) donors (Figure 5-8 J). Of interest, co-infection with rhinovirus and *M. catarrhalis* did not result in many significant changes in comparison to single rhinovirus infection, except for TNF-α in cultures from healthy and COPD donors ($p=0.04$ and $p=0.013$) and CSF-3/ GM-CSF in cultures from healthy donors ($p=0.013$). No statistically significant difference was reported in between cultures from healthy and COPD donors for any of the cytokines compared.

In terms of rhinovirus infection comparisons, significant IP-10/ CXCL10 increase was observed in cultures from healthy and COPD donors in comparison to non-infected control and *M. catarrhalis* infection ($p<0.0001$, both conditions) (Figure 5-8 B). Similarly, RANTES/ CCL5 was significantly increased in comparison to non-infected control and *M. catarrhalis* in cultures from healthy ($p<0.0001$, both conditions) and

COPD ($p<0.0001$, both conditions) donors (Figure 5-8 D). Significant IL-6 and ENA-78/ CCL5 differences were observed between non-infected control and rhinovirus in cultures from COPD donors ($p=0.014$ and $p=0.04$) (Figures 5-8 E and F). IFN-β and IL-17c were significantly increased in cultures from healthy donors during rhinovirus infection in comparison to non-infected controls ($p=0.03$ and $p=0.02$) (Figures 5-8 I and H). Difference of cytokines expression was not observed between the healthy and COPD groups.

In terms of *M. catarrhalis* infection comparisons, significant IP-10/ CXCL10 and ENA-78/ CXCL5 increase was observed in COPD cultures when compared to non-infected controls ($p=0.04$ and $p=0.03$) (Figures 5-8 B and F). No difference between cultures from healthy and COPD donors was observed in the expression of cytokines.

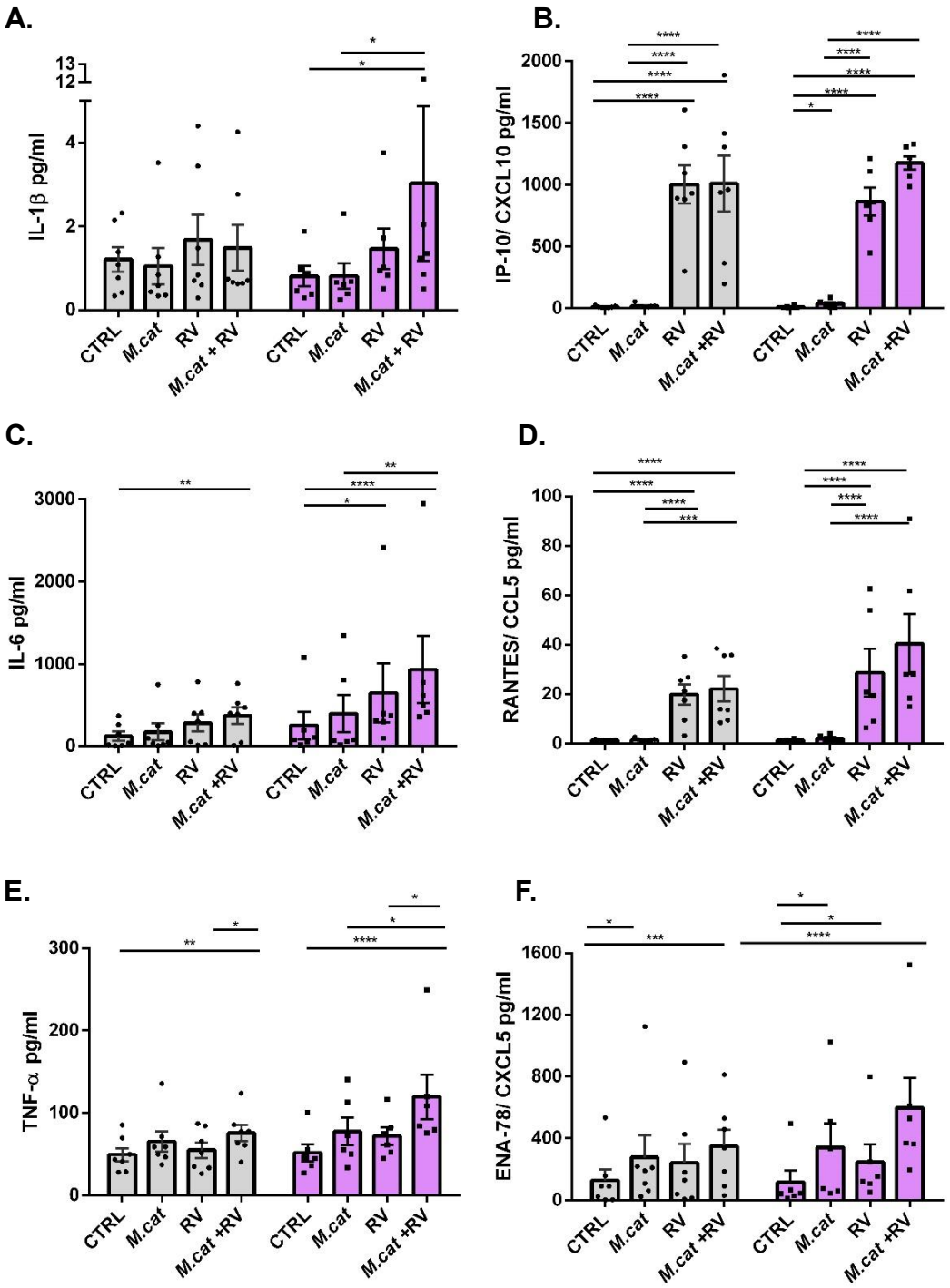
A.
IL-1β pg/ml
13
12
4
2
0
CTRL
M.cat
RV
M.cat + RV
B.
IP-10/ CXCL10 pg/ml
2000
1500
1000
500
0
C.
IL-6 pg/ml
3000
2000
1000
0
D.
RANTES/ CCL5 pg/ml
100
80
60
40
20
0
E.
TNF-α pg/ml
300
200
100
0
F.
ENA-78/ CXCL5 pg/ml
1600
1200
800
400
0
M.cat +RV

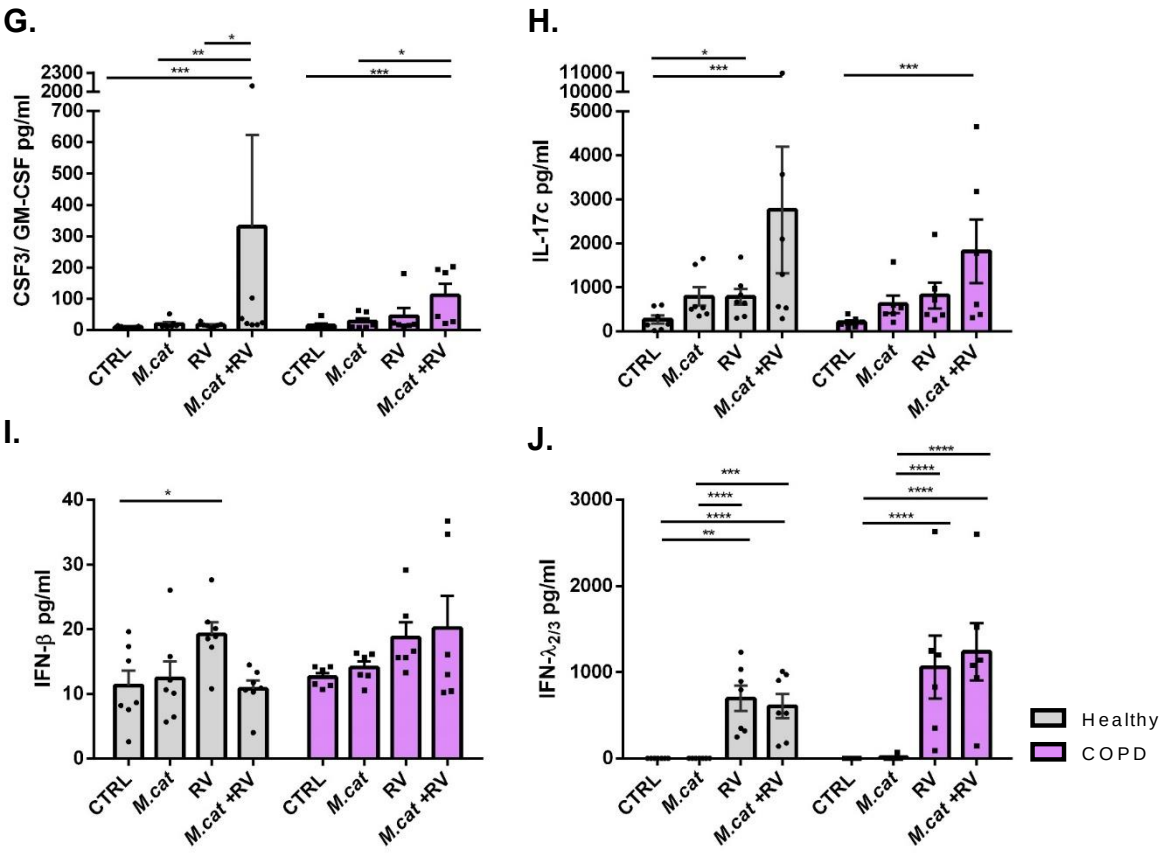

Figure 5-8: Inflammatory mediators following co-infection with rhinovirus and *M. catarrhalis* secreted in the basolateral fluids of ciliated cultures from healthy g and COPD donors for 24h.

A) IL-1β, B) IP-10/ CXCL10, C) IL-6, D) RANTES/ CCL5, E) TNF-α, F) ENA-78/ CXCL5, G) CSF-3/ GM-CSF, H) IL-17c, I) IFN-β, J) IFNλ2/3, grey denotes healthy, purple denotes COPD, n=7 healthy and 7 COPD cultures, error bars represent ±SEM, *=p<0.05, **=p<0.01, ***=p<0.001, ****=p<0.0001.

Table 5-2: Inflammatory mediators secreted in the basolateral fluids of ciliated cultures following co-infection with *M. catarrhalis* and rhinovirus for 24h.

	Healthy				COPD			
pg/ml	**CTRL**	***M. cat***	**RV**	***M. cat + RV***	**CTRL**	***M. cat***	**RV**	***M. cat+ RV***
IL-8/ CXCL8	2129.5± 370.83	2529.6± 494.55	2125.3± 290.02	2854.6± 509.74	1970.0± 243.61	2096.4 ±374.46	1949.7± 374.46	2712.5± 359.69
MCP-1/ CCL2	203.38± 79.08	268.39± 114.06	158.04± 64.56	173.17± 57.87	880.97± 688.24	2098.3± 1696.79	515.93± 286.12	526.35± 261.53
MIP-3α/ CCL20	89.71± 7.50	189.88± 48.73	146.02± 34.96	244.97± 93.78	140.07± 52.66	253.91± 101.94	231.97± 51.02	366.78± 77.98
GRO-α	488.36± 58.26	367.70± 84.88	289.53± 36.93	286.05± 53.73	449.81± 108	302.56± 23.71	267.69± 44.54	332.31± 33.51
IL-15	4.59± 0.38	4.67± 0.24	4.20± 0.22	4.6772± 0.31	4.31± 0.15	4.16± 0.47	4.03± 0.27	5.14± 0.22
IFN-β	2.43± 0.08	2.56± 0.05	3.16± 0.32	2.67± 0.09	2.56± 0.03	2.56± 0.06	3.02± 0.37	2.85± 0.27
IFN-γ	2.47± 0.09	1.75± 0.54	2.19± 0.49	1.59± 0.33	2.06± 0.42	2.22± 0.38	1.44± 0.53	1.22± 0.29
TARC	0.67± 0.15	0.95± 0.27	0.95± 0.21	1.23± 0.36	0.73± 0.15	1.27± 0.39	1.08± 0.23	1.44± 0.42
CXCL14	1248.8± 13.42	1268.0± 11.31	1250.1± 13.08	1258.0± 6.87	1194.7± 34.21	1184.8± 22.43	1179.9± 34.24	1209.7± 27.68
IL-36g	13.56± 1.13	15.20± 1.01	17.51± 2.53	18.90± 2.07	19.17± 1.07	18.56± 1.63	22.23± 3.50	26.44± 6.11

5.2.7.2 Inflammatory mediators secreted in apical fluids

With respect to co-infection comparisons, significant increase of IP-10/ CXCL10, and RANTES/ CCL5, was observed during co-infection in comparison to non-infected control and *M. catarrhalis* single infection in cultures from both healthy and COPD donors ($p<0.0001$, all conditions, groups and cytokines) (Figure 5-9 B, D and G). In addition, co-infection in healthy and COPD significantly increased CSF-3/ GM-CSF in comparison to non-infected control ($p<0.0001$), *M. catarrhalis* infection in COPD ($p=0.048$) and rhinovirus infection in healthy ($p=0.014$). (Figure 5-9 H). IL-6 was also significantly induced in comparison to non-infected control in cultures from healthy ($p<0.0001$) and COPD ($p<0.001$) donors (Figure 5-9 C). Significant increase of TNF-α in comparison to non-infected control was observed in healthy ($p<0.01$) and COPD ($p=0.02$) cultures (Figure 5-9 E). IFN-β was strongly increased in comparison to non-infected control in cultures from healthy ($p<0.0001$) and COPD ($p<0.001$) donors and also in comparison to *M. catarrhalis* infection in healthy ($p=0.03$) (Figure 5-9 J).

Similarly, IFNλ2/3 was strongly increased in cultures from healthy ($p<0.0001$) and COPD ($p<0.0001$) donors in comparison to both non-infected control and *M. catarrhalis* infection (Figure 5-9 K). Interestingly, IL-1β ($p<0.001$), IL-17c ($p=0.01$) and IL-36g ($p<0.01$) were significantly increased in comparison to non-infected controls in cultures from healthy donors only (Figures 5-9 A, H, I). IL-1β was also significantly increased in comparison to *M. catarrhalis* infection ($p=0.04$). No significant differences were observed between the healthy and COPD groups for any of the cytokines compared.

In the analysis of rhinovirus single infection effects on cytokine production, significant increase of IL-1β was observed in cultures from healthy individuals in comparison to non-infected control ($p=0.03$) (Figure 5-9 A). Similar to findings for basolateral fluids, rhinovirus strongly induced IP-10/ CXCL10 and RANTES/ CCL5 in the apical fluids of infected cultures from healthy and COPD donors compared to non-infected controls ($p<0.0001$, both groups and cytokines) (Figures 5-9 B and D). IL-6 was also observed strongly increased in cultures from healthy and COPD donors in comparison to non-infected control ($p<0.01$) (Figure 5-9 C). IFNλ2/3 was significantly induced in cultures from healthy and COPD donors in comparison to non-infected control ($p<0.0001$) (Figure 5-9 J). Statistical significance between cultures from healthy and COPD donors was not observed for any cytokine.

In the analysis of *M. catarrhalis* single infections, in cultures from healthy individuals *M. catarrhalis* significant increased IL-6 ($p=0.03$), TNF-α ($p= 0.03$) and CSF-3/ GM-CSF ($p<0.01$) compared to non-infected controls (Figures 5-9 C, E and G). Interestingly, *M. catarrhalis* infection induced higher MCP-1/ CCL2 secretion than rhinovirus infection ($p=0.02$) in cultures from COPD donors (Figure 5-9 F). No difference between healthy and COPD groups was found for cytokines induction.

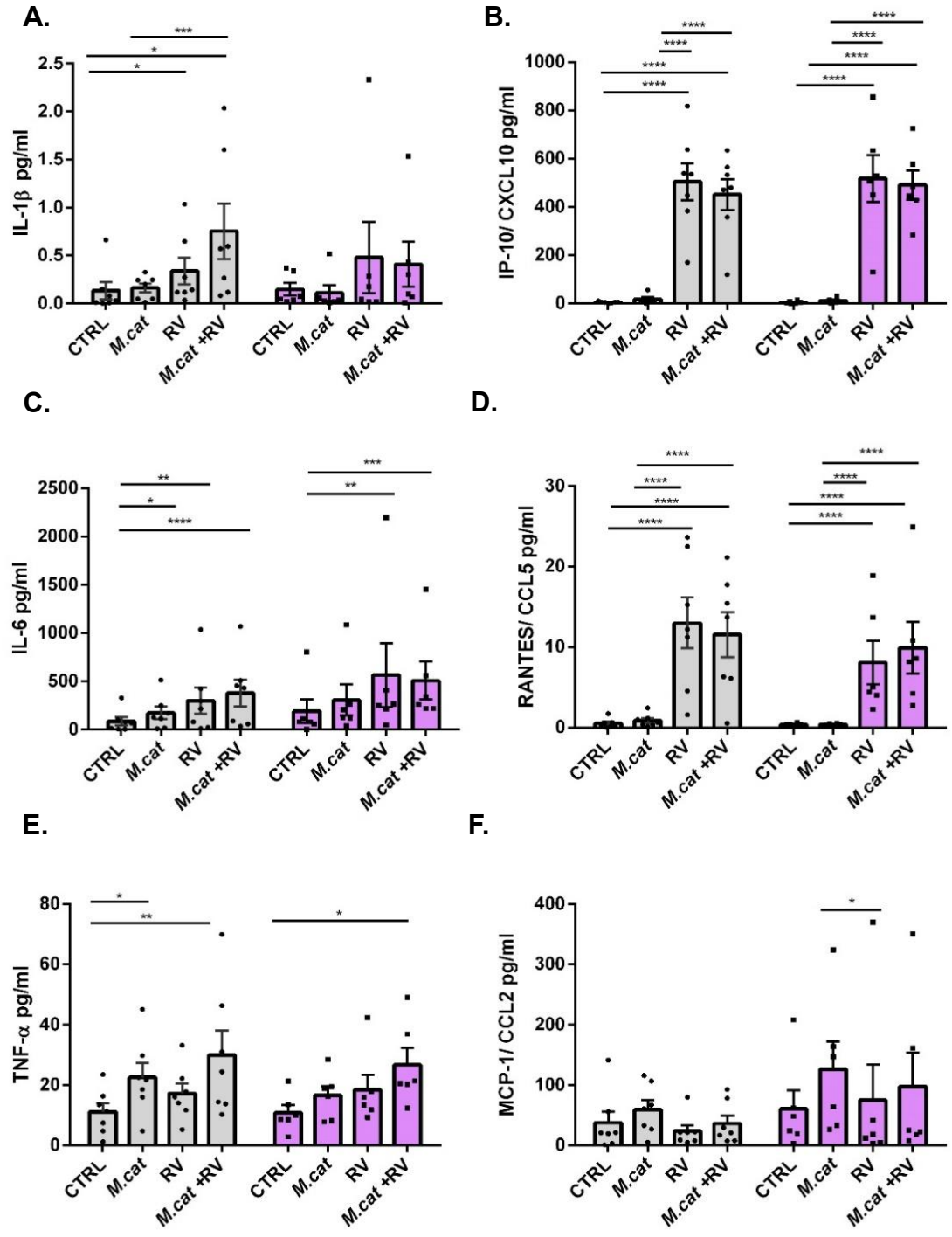
A.
IL-1β pg/ml
B.
IP-10/ CXCL10 pg/ml
C.
IL-6 pg/ml
D.
RANTES/ CCL5 pg/ml
E.
TNF-α pg/ml
F.
MCP-1/ CCL2 pg/ml
CTRL
M.cat
RV
M.cat +RV

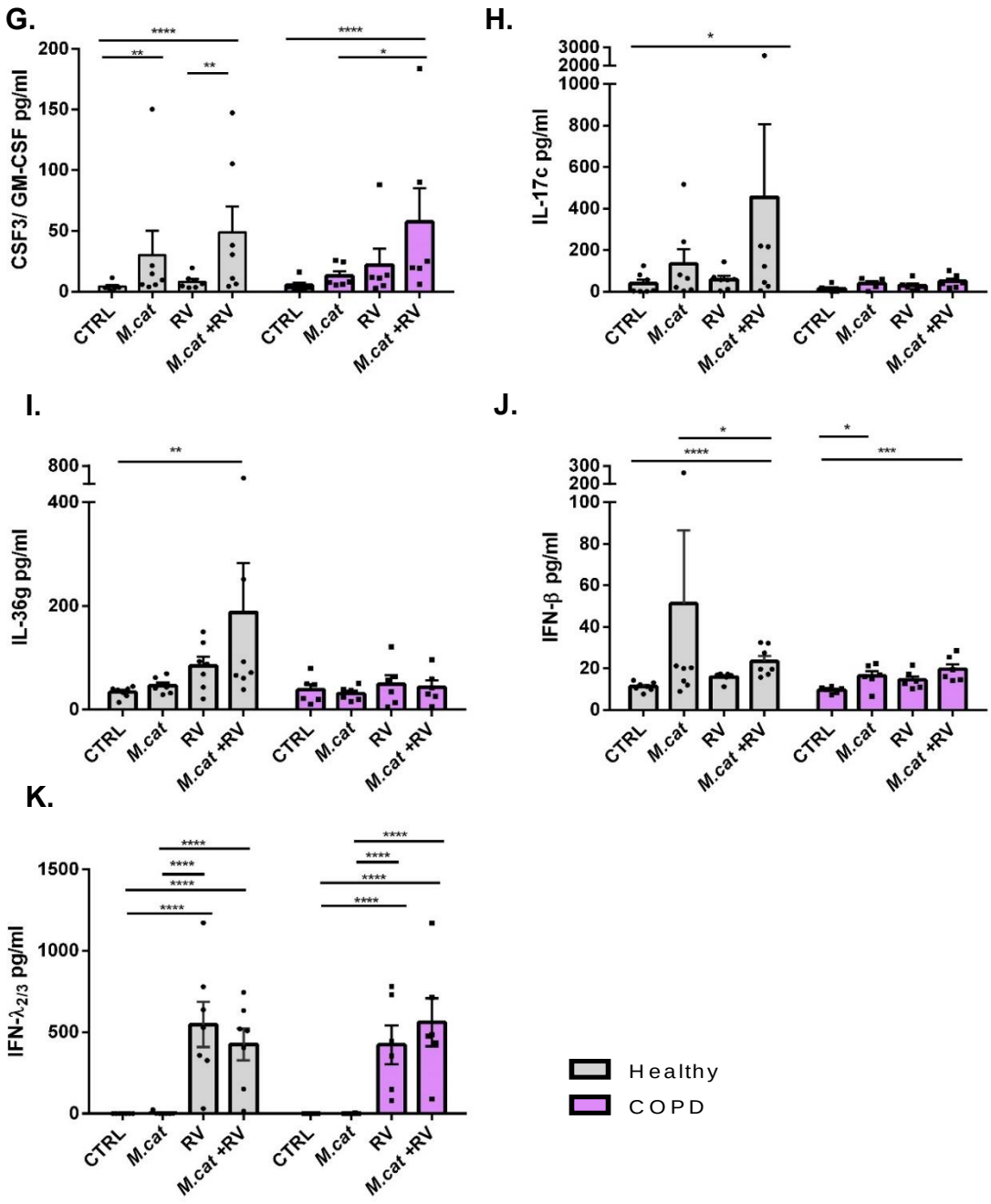

Figure 5-9: Inflammatory mediators following co-infection with rhinovirus and *M. catarrhalis* secreted in the apical fluids of cultures from healthy and COPD donors for 24h.

A) IL-1β, B) IP-10/ CXCL10, C) IL-6, D) RANTES/ CCL5, E) TNF-α, F) MCP-1/ CCL2, G) CSF-3/ GM-CSF, H) IL-17c, I) IL-36g, J) IFN-β, K) IFNλ2/3, grey denotes healthy, purple denotes COPD, n=7 healthy and 7 COPD cultures, error bars represent ±SEM, *=p<0.05, **=p<0.01, ***=p<0.001, ****=p<0.0001.

Table 5-3: Inflammatory mediators secreted in the apical fluids of ciliated cultures following co-infection with *M. catarrhalis* and rhinovirus for 24h.

	Healthy				COPD			
pg/ml	**CTRL**	***M. cat***	**RV**	***M. cat + RV***	**CTRL**	***M. cat***	**RV**	***M. cat+ RV***
IL-8/ CXCL8	743.94 ±156.5	878.22 ±183.88	1097.54 ±187.54	782.96 ±123.91	623.09 ±129.03	698.91 ±120.59	1446.70 ±380.59	1176.1 ±196.92
ENA-78	41.8 ±17.45	188.52 ±75.71	76.46 ±31.31	213.07 ±88.03	36.6 ±21.22	99.2 ±31.96	85.83 ±52.97	134.34 ±45.79
MIP-3α/ CCL20	39.6 ±14.44	144.50 ±82.72	47.96 ±14.68	87.91 ±36.48	36.9 ±13.57	63.9 ±11.77	60.93 ±17.29	62.85 ±14.20
GRO-α	125.7 ±24.77	102.07 ±6.92	166.95 ±39.23	113.98 ±9.80	124.23 ±30.83	103.59 ±16.05	146.9 ±38.41	122.04 ±15.34
IL-15	0.54 ±0.09	0.71 ±0.10	0.71 ±0.07	0.80 ±0.14	0.64 ±0.10	0.53 ±0.06	0.74 ±0.09	0.82 ±0.10
IFN-α	3.30 ±0.06	21.06 ±17.60	3.72 ±0.18	3.52 ±0.09	3.35 ±0.04	3.43 ±0.04	3.61 ±0.13	3.60 ±0.13
IFN-γ	3.35 ±0.82	23.17 ±18.10	4.45 ±0.41	3.711 ±0.59	3.66 ±0.3	5.08 ±0.49	4.21 ±0.49	3.05 ±0.67
TARC	0.39 ±0.11	1.05 ±0.47	0.61 ±0.19	0.65 ±0.12	0.44 ±0.16	0.84 ±0.33	0.50 ±0.12	0.73 ±0.28
CXCL14	471.1 ±81.38	537.47 ±51.63	501.80 ±46.80	544.33 ±62.51	554.26 ±83.76	509.90 ±83.36	551. 2±60.13	481.13 ±74.59

5.2.7.3 Comparison of inflammatory mediators secreted in the basolateral and apical fluids of ciliated cultures

Similar to the single *M. catarrhalis* (chapter 3 section 3.2.11.3) and rhinovirus infection (chapter 4 section 4.2.8.3) studies, a global test was used to combine the co-infection study data from the two groups and the apical and basolateral fluids to investigate if single and combined infection had increased any of the cytokines levels. If the result of the test was $p<0.05$ then apical fluid findings were compared to basolateral fluid findings. The fluid component comparisons were reported as ratios of relative changes to non-infected controls. In this analysis, IL-1β increase in cultures from healthy donors was found significantly higher (7.14 times) in the apical fluids than in the basolateral fluids ($p=0.003$) following rhinovirus and *M. catarrhalis* co-infection. No other significant differences between apical and basolateral fluids were found in terms of cytokines secretion. A larger infection effect following rhinovirus and *M. catarrhalis* on inflammatory mediators' induction was found in the apical fluids of

cultures from healthy individuals for IL-6 (1.69 times higher), RANTES/ CCL5 (1.72 times higher), TNF-α (1.88 times higher), MCP-1/ CCL2 (1.38 times higher), CSF-3/ GM-CSF (1.25 times higher), IL-15 (1.44 times higher), IFN-β (1.92 times higher), TARC (1.35 times higher) and IL-36g (2.5 times higher). In cultures from COPD donors, higher induction of cytokines in the apical fluids was observed for IL-8/ CXCL8 (1.49 times higher), CSF-3/ GM-CSF (1.17 times higher) and IFN-β (1.42 times higher). A greater stimulation of inflammatory mediators was observed in the basolateral fluids of cultures from healthy individuals for ENA-78/ CXCL5 (1.42 times higher) and IFNλ2/3 (3.12 times higher), while in cultures from COPD individuals for IL-1β (1.32 times higher), IL-6 (1.11 times higher), RANTES/ CCL5 (1.17 times higher), ENA-78/ CXCL5 (1.3 times higher), MIP-3α/ CCL20 (1.6 times higher), IFNλ2/3 (3.14 times higher), IL-17c (1.14 times higher) and IL-36g (1.21 times higher).

5.3 Discussion

Previous studies have reported that viral infections predispose to subsequent bacterial infections (Mallia et al., 2011; George et al., 2014; Wilkinson et al., 2017, Hendricks et al., 2016). Human bronchial ciliated cultures infected with rhinovirus have been shown to have increased epithelial susceptibility to *S. pneumoniae* growth (Sajjan et al., 2008) while human nasal ciliated cultures infected with RSV have been found to increase *S. pneumoniae* virulence (Smith et al., 2014) and *P. aeruginosa* growth (Hendricks et al., 2016). In order to investigate if rhinovirus predisposes the respiratory epithelium to a subsequent *M. catarrhalis* infection and if rhinovirus and *M. catarrhalis* co-infection causes greater epithelial damage and inflammatory response, we used air-liquid grown and differentiated primary airway epithelial cells from healthy volunteers and COPD patients. This is the first study which investigated rhinovirus and *M. catarrhalis* co-infection of healthy and COPD ciliated epithelium.

The current study aimed to investigate the initial effects of the *M. catarrhalis* and rhinovirus infections on epithelial barrier function and epithelial inflammatory response, and to assess if there were differences in rhinovirus and *M. catarrhalis* co-

infection between healthy and COPD ciliated epithelium. The complexity of the current study relates not only to the differentiated mucociliary phenotype of the healthy and COPD ALI cultures but also to the differential epithelial response to rhinovirus and *M. catarrhalis* as it was shown in chapters 3 and 4. It was therefore anticipated that this model provided a true representation of an *in vivo* airway co-infection, and would also add knowledge on the potential cellular mechanisms associated with infectious diseases.

5.3.1 Barrier function of epithelial ciliated cultures following co-infection with rhinovirus and *M. catarrhalis*

It has been demonstrated in chapters 3 and 4 that *M. catarrhalis* binds to rapidly beating ciliated cells and that these ciliated cells are also the primary target of rhinovirus, causing epithelial cell shedding. In the co-infection model of infection, it was found that the two pathogens impair further the ciliary function of cultures. The beat frequency of cultures from both healthy and COPD donors was more significantly reduced in the presence of rhinovirus and *M. catarrhalis* at 15min post co-infection compared to the effect of single pathogens (Figure 5-1 A). Likewise, in cultures from healthy individuals the co-infection was associated with a significant reduction of beat frequency at 24h, however no significant reduction was observed in cultures from COPD donors (Figure 5-1 B). Reduction of CBF in cultures from healthy and COPD donors during co-infection was in a parallel with reduced ciliary activity (Figure 5-2 A and B). Ciliary activity was consistently reduced during single rhinovirus infection and co-infection with *M. catarrhalis*. A similar trend was not seen in *M. catarrhalis* single infection. This is the first *in vitro* study to suggest that ciliary function of epithelial cultures is severely disrupted in response to bacterial and viral co-infections in healthy and COPD airway epithelium. Along with directly affected ciliary function, co-infections could be having a general impact on bacterial persistence in patient lungs via reduced mucociliary clearance.

5.3.2 Bacterial interplay with host airway epithelium in the presence of rhinovirus infection

There is a suggestion of interaction between rhinovirus and bacteria in the lower airways of COPD patients during acute exacerbations (Mallia et al., 2012; Mollyneaux et al., 2013; Wilkinson et al., 2006). The current study proposed a mechanism that can contribute to bacterial and viral pathogens dissemination throughout the airways. In particular, detachment of beating ciliated cells with bound bacteria as a result of rhinovirus infection (Figure 5-5) might contribute to the dynamics of respiratory

infections in terms of dissemination of bacteria and in smaller airways contribute to small airway obstruction. Despite the expectations based on published studies that viral respiratory infections lead to a greater bacterial load (Mallia et al., 2011; Wilkinson et al., 2017; Hendricks et al., 2016; Sajjan et al., 2008), the findings from this study suggest that rhinovirus pre-infection of the COPD ciliated epithelium does not upregulate *M. catarrhalis* growth (Figure 5-3). *M. catarrhalis* viability following a 24h rhinovirus infection was consistently decreased, though not statistically significant, in all cultures from COPD patients designated as frequent exacerbators (Table 5-1). The current observation on bacterial load is in an agreement with Wilkinson et al who did not find a positive correlation between *M. catarrhalis* and rhinovirus presence and an increased risk of developing acute exacerbations in COPD patients (Wilkinson et al., 2017). In the same observational cohort study, unlike NTHI which in the presence of rhinovirus infection has been shown to increase the likelihood of an acute exacerbation, *M. catarrhalis* acquisition and the risk of developing COPD exacerbations was the same throughout the whole year and was not associated with seasonal viral infections (Wilkinson et al., 2017).

The current findings that rhinovirus does not increase *M. catarrhalis* growth were investigated further and the effect of apical secretions collected from rhinovirus infected cultures from healthy or COPD donors was tested on bacterial viability. Rhinovirus did not appear to alter antimicrobial effects of the apical airway fluid on *M. catarrhalis* growth as no change in bacterial numbers were observed following treatment with apical secretions from rhinovirus infected cultures (Figure 5-6 D). This is in contrast to previous respiratory *in vivo* and *ex vivo* studies which suggested dysregulation of antimicrobial peptides such as SLPI, elafin, β-defensin, due to a viral infection with RSV, influenza or rhinovirus led to increased susceptibility to *S. aureus* or *H. influenzae* growth (McGillivary et al., 2009; Robinson et al., 2014). In the current study it was found that apical secretions from cultures from healthy individuals did supress *M. catarrhalis* growth, while apical secretions from cultures from COPD donors did not (Figure 5-6 A, B and C), suggesting the apical fluids secreted from cultures from healthy and COPD donors differ in their antimicrobial activity. Of interest, concentration levels of the bactericidal SLPI were found to be low in the sputum of COPD patients at stable state and during exacerbations (Gompertz et al., 2001).

5.3.3 Epithelial cell ROS stimulation by rhinovirus and *M. catarrhalis* infection

Oxidative stress occurs during imbalance between free radicals such as ROS and antioxidants, leading to the destruction of lipids, proteins and tissues in the airways (Barnes, 2003). ROS are mediators of COPD pathogenesis and their main source in the lungs are inflammatory cells such as macrophages and neutrophils, and structural cells such as epithelial and endothelial cells (Barnes et al., 2016; Boukhenouna et al., 2018). Nevertheless, despite that the current study is limited only to findings regarding the epithelial layer, higher baseline concentration of H_2O_2 was found in ciliated cultures from COPD donors than in those from healthy donors (figure 5-7 A). Consistent with previous findings of increased ROS production following rhinovirus infection of bronchial epithelial cells (Comstock et al., 2011), in the current study rhinovirus increased H_2O_2 levels at 24h post infection relative to non-infected cultures, however despite that upregulation was observed in all cultures statistical significance was not reached. A co-infection with rhinovirus and *M. catarrhalis* appeared to increase H_2O_2 concentration at 24h in cultures from COPD donors but not in healthy donors (Figure 5-7 B). H_2O_2 levels were approximately 43% higher during co-infection than *M. catarrhalis* infection alone. It is possible that H_2O_2 studies may have revealed some of *M. catarrhalis* features to deal with exogenous oxidative stress and in particular H_2O_2 through the expression of OxyR and SodA proteins previously shown to regulate *M. catarrhalis* redox sensitivity (Hoofman et al., 2011; Luke et al., 2012). Conversely, high concentrations of ROS have been associated with enhanced induction of inflammatory mediators as oxidation of proteins leads to signalling via MAPK, p38 and NF-kB and ultimately to the transcription of inflammatory genes (Boukhenouna et al., 2018). Future work exploring other ROS such as nitric oxide and superoxide anion generated by epithelial cells following a rhinovirus and *M. catarrhalis* co-infection could explain if free radicals production accounts for the observed decreases in bacterial counts following rhinovirus infection in COPD cultures.

5.3.4 Healthy and COPD airway response to rhinovirus and *M. catarrhalis* co-infection

Inflammatory mediators post co-infection with rhinovirus and *M. catarrhalis* have been shown to be markedly increased in ciliated cultures (Figures 5-8 and 5-9). At a cellular level strong increase was observed of IL-6, IP-10/ CXCL10, TNF-α, RANTES / CLL5, ENA-78/ CXCL5 and IFNλ2/3 in cultures from healthy and COPD donors. This is consistent with clinical data which suggests IL-6 and TNF-α are increased during

acute exacerbations in COPD patients (Barnes, 2003). Further, airway ciliated cells from healthy and COPD donors infected with rhinovirus and *M. catarrhalis* presented with the highest concentration of IL-8/ CXCL8 compared to single pathogens infection (Table 5-1), which is in agreement with high IL-8/ CXCL8 levels found in sputum and BAL collected from COPD patients. IL-8/ CXCL8 is a potent chemoattractant cytokine for neutrophils, which drives phagocytosis of infectious pathogens, however the increased secretion of serine proteases from neutrophils may cause alveolar destruction (Barnes, 2015). Further, migration of neutrophils from COPD patients has been shown as increased but with reduced accuracy, resulting in increased accumulation but defective chemotaxis causing lung tissue damage (Sapey et al., 2011). Other inflammatory mediators which were significantly elevated in healthy and COPD airway cells following rhinovirus infection and co-infection were IP-10/ CXCL10 and RANTES/ CCL5, which are vital for antiviral response and inhibition of viral replication, through the recruitment of cytotoxic T cells which target infected cells (Baines et al., 2013). Bronchial specimens from COPD patients are characterised by greater levels of IP-10/ CXCL10 than smokers or non-smokers, which could lead to infiltration of T cells in the lung parenchyma and obstruction of airflow (Saetta et al., 2002).

IL-17c was significantly induced in healthy and COPD ciliated cells compared to single pathogens infections (Figure 5-8 H), which is consistent with the Jamieson et al study which found IL-17c is synergistically released from bronchial epithelial cells from healthy subjects, healthy smokers and COPD subjects following co-infections with rhinovirus and NTHI (Jamieson et al., 2019). Jamieson found synergistic induction by a virus - bacterial infection to be dependent on rhinovirus active replication and signalling via p38 and NF-kB. In addition, IL-17c was capable to induce GRO-α/ CXCL1, a potent neutrophil chemoattractant, suggesting co-infections important role in driving recruitment of neutrophils in COPD epithelium through the release of IL-17c (Jamieson et al., 2019). An interesting finding from the current co-infection model was that the monocyte recruiter MCP-1/ CCL2 was increased with *M. catarrhalis* infection but not with rhinovirus infection in the basolateral fluid of COPD cells (Figure 5-8 F). Further, in apical secretions MCP-1/ CCL2 was decreased in the presence of rhinovirus and co-infection with *M. catarrhalis* (Table 5-2), suggesting this cytokine as bacteria specific.

Induction of Type I IFN response presented with a significant increase of IFN-β into the basolateral site of ciliated cultures from healthy individuals following rhinovirus

infection (Figure 5-8 I) and a significant induction in the apical site of cultures from healthy and COPD donors (Figure 5-9 J). Consistent with previous studies the current study found IFN-γ response to viral-bacterial infections to be absent (Smith et al., 2014) and the strong induction of IFNλ2/3 was similar to a previous study of co-infection with RSV and *P. aeruginosa* (Hendricks et al., 2016). Recently a strong anti-viral IFN response was associated with enhanced susceptibility to bacterial infections (Hendricks et al., 2016; Kudva et al., 2011; Nakamura et al., 2011). Such an observation was confirmed for IFN-β and IFNλ2/3 which potentiated *P. aeruginosa* growth and biofilm formation on the surface of bronchial epithelial cells (Hendricks et al., 2016). Similarly, influenza infection *in vivo* promoted *S. pneumoniae* growth associated with increased type I IFN response through inadequate macrophage and neutrophil recruitment to the lungs and impaired bacterial clearance mechanisms (Nakamura et al., 2011; Shahangian et al., 2009). Further, *in vivo* co-infection with influenza and *S. aureus* promoted a higher release of type I and III IFNs, mediating defective Th17 signalling pathway, stimulating bacterial pneumonia (Kudva et al., 2011).

A novel feature of the present study was that measurements were carried out for cytokines and chemokines released apically and basolaterally from ciliated cultures from healthy and COPD donors. The broad selection of cytokines analysed enabled a more detailed interpretation of the airway epithelium during viral-bacterial co-infections. It was found that cytokines release was greater in the apical fluids of healthy epithelial cells than the in the basolateral fluids, whereas cytokines secretion in COPD epithelial cells was found greater in the basolateral fluids than in the apical fluids (section 5.2.7.3). The reasons behind this are unclear.

The current study has suggested that co-infections potentiate inflammatory mediators pointing infections' central role in the pathophysiology of COPD. The production of pro-inflammatory cytokines causes the attraction and activation of inflammatory cells in the airways, however infections in COPD patients have been proven to exaggerate inflammatory response causing inflammatory cells accumulation in the lungs, and to increase progression of COPD disease (Baines et al., 2013; Barnes, 2016).

5.4 Summary

Airway epithelial response to rhinovirus and *M. catarrhalis* co-infection was characterised with impaired ciliary function such as decreased ciliary beat frequency and activity and increased inflammatory response than either pathogen alone. The

mechanisms associated with this outcome did not involve outgrowth of bacteria or decreased activity of secreted antimicrobial peptides. Rather, increased production of H_2O_2 is likely to interfere with ciliary function and potentiate the inflammatory response, but only limited data was presented to support this finding.

Chapter 6. Discussion and Future work

Epithelial barrier function and inflammatory response are an important feature of the human airways which provide protection against invading pathogens and pollutants. However, when the physical defence mechanisms and the host immune response are dysregulated, it is thought that airway chronic diseases such as COPD and asthma develop (Barnes, 2016; Tan et al., 2018). Heightened inflammation and recurrent infections are recognised features of COPD which are associated with exacerbations, involving both innate and adaptive immune system activation (Barnes, 2015; Saetta et al., 2002). So far, the impact of bacterial and viral infections has been not completely elucidated in the context of severity and progression of the disease (Wark et al., 2013). It is widely accepted that heightened inflammation and respiratory symptoms account for recruitment and accumulation of inflammatory cells in the lungs, contributing to pathological remodelling of the airways (Barnes, 2016; Wang et al., 2018). Though, the precise cellular mechanisms associated with severe exacerbations are unknown and prior to the start of this study a model of rhinovirus and *M. catarrhalis* co-infection of the COPD ciliated epithelium did not exist.

The primary aim of the present study was to characterise the early initial interaction of healthy and COPD differentiated epithelium with rhinovirus and *M. catarrhalis*, pathogens thought to drive COPD exacerbations (Sethi et al., 2008). To achieve this aim, single bacterial infection, single viral infection and co-infection with the two pathogens were used to characterise respiratory infections in cultured epithelial cells. Experimental *in vitro* infections contributed to the detailed assessment of the underlying mechanisms of exacerbations pathophysiology which can define clinical outcomes. To more accurately recreate an airway infection, the present study used primary airway cells from healthy volunteers and COPD patients which were grown *in vitro* at ALI conditions. The method allowed epithelial cells differentiation into ciliated, goblet and progenitors cells, and development of a mucociliary phenotype. The methodology provided a technical advantage to not only reproduce airway host-pathogens interactions but also to test multiple donors' responses of different disease groups.

6.1 *M. catarrhalis* single infection findings

Several clinical studies suggest the acquisition of a new *M. catarrhalis* strain is often linked to the development of a COPD exacerbation, causing worsening of respiratory symptoms and ultimately progression of the disease (Sethi et al., 2008; Barnes, 2016). Even though COPD patients are treated with antibiotics during exacerbations, polymicrobial biofilm formation of multiple bacteria as discussed in chapter 1 is a common consequence reported to increase antibiotic resistance (Perez and Murphy 2017). Hence, closer analysis of *M. catarrhalis* interaction with the respiratory epithelium, would provide fundamental knowledge for COPD disease management. Previous studies on *M. catarrhalis* infection utilized epithelial cell lines or human bronchial cells from healthy donors, which may not be an accurate representation of the COPD epithelium (Slevogt et al., 2007; Slevogt et al., 2008; N'Guessan et al., 2014, Balder et al., 2009). As *M. catarrhalis* infection is restricted to the human airways, the establishment of an animal *in vivo* infection model is challenging because of its active airway removal (Goldstein et al., 2009; Su et al., 2012). Differentiated healthy and COPD primary epithelial cells are thus an appropriate, comprehensive and representative model of an *M. catarrhalis* infection and its correlation to COPD exacerbations development.

The current findings proposed that *M. catarrhalis* instant adherence to rapidly beating ciliated cells is accompanied by the formation of bacterial aggregates on the apical surface of cultures causing reduction of ciliary beat amplitude and CBF of healthy and COPD epithelial cells. Ciliary function reduction was more profound in COPD cultures. The implications are related to dysregulation of mucociliary clearance, associated with increased mucus build-up and decreased pathogens clearance (Stannard and O'Callaghan 2006). Smoking is the most common risk factor for COPD development, linked to increased mucin production and airway epithelial cell reprogramming leading to abnormally high number of mucus producing cells causing mucus metaplasia (Barnes, 2016, Shaykhiev and Crystal 2014). Reduction of cilia length, loss of ciliated cells and replacement of those with goblet and club cells are just some of the underlining features of the COPD pathophysiology (Shaykhiev and Crystal 2014). One of the mechanisms associated is epithelial EGFR activation identified to drive basal cells switch towards goblet cells differentiation (Shaykhiev and Crystal 2014; Takeyama et al., 2000; Valencia-Gattas et al., 2016). The current study found that *M. catarrhalis* binding to epithelial cells stimulated EGF receptors activation as early as 15min post infection in cultures from COPD donors, which remained on until 24h later.

The consequences of persistent EGFR activation would be structure and function changes of the respiratory epithelium together with inflammation (Ganesan et al., 2013), suggesting *M. catarrhalis* could be having a direct role in the reprogramming of the COPD epithelium. Western blot analysis in the current study revealed that EGFR activation in ciliated cultures from COPD donors occurred with downstream activation of AKT, as previously reported (Ganesan et al., 2013).

A virulence feature of bacteria is their ability to invade host epithelia and stimulate events associated with inflammation (Su et al., 2012). The current study demonstrated *M. catarrhalis* adherence and intracellular uptake was greater in COPD ciliated epithelium by approximately 2 logs compared to healthy ciliated epithelium. Analysis of the mechanisms of how bacteria are internalised in epithelial cells, revealed that macropinocytotic events occur in non-ciliated cells, corresponding with the formation of vacuoles with bacteria visualised by TEM. These findings are in agreement with Slevogt et al who reported *M. catarrhalis* is up-taken in BEAS-2B non-differentiated cells through macropinocytosis (Slevogt et al., 2007). A recent report expanded the knowledge of exosome uptake in a carcinoma cell line and linked macropinocytosis to EGGR activation, membrane ruffling and actin reorganisation (Nakase et al., 2015). Further, the inhibition of active polymerisation of epithelial cells by wortmanin (a PAN PI3K inhibitor) and cytochalasin D reduced *M. catarrhalis* internalisation into BEAS-2B cells (Slevogt et al., 2007). However, in the current study pre-treatment of epithelial ciliated cultures with either Gefitinib (an EGFR inhibitor) or a PAN PI3K inhibitor failed to reduce *M. catarrhalis* invasion, suggesting other than EGFR and AKT activation mechanisms may be associated with bacterial internalisation such as receptor mediated endocytosis. When inflammatory markers were investigated following *M. catarrhalis* infection at 24h, a wide activation of cytokines with chemotactic properties for neutrophils and macrophages was observed. The findings of increased IL-6, TNF-α and MCP-1/ CCL2 in COPD epithelial cells are in agreement with clinical data from COPD patients during exacerbations (Bhowmic et al., 2000; Chung, 2001, Hogg and Timens 2009; Sethi et al., 2007). These findings in combination with observations of severely disrupted ciliary function and increased bacterial invasion in COPD epithelial cells, reveal the differences of epithelial cell response to *M. catarrhalis* infection in cultures from healthy and COPD donors. The findings illustrate the complications of acquisition of an *M. catarrhalis* strain by COPD patients and at least partly the cellular mechanisms associated with exacerbations.

6.2 Rhinovirus single infection findings

Rhinovirus is the most common viral pathogen associated with COPD exacerbations (Jacobs et al., 2013; Barnes, 2016; Wedzicha et al., 2003; Shaykhiev and Crystal 2003; Seemungal et al., 2001). The presentation of a rhinovirus triggered COPD exacerbation involves more severe cold symptoms along with airway obstruction (Mallia et al., 2011). Rhinovirus main mechanisms associated with exacerbations include enhanced stimulation of cytokines and chemokines by airway epithelia initiating the greater recruitment and activation of inflammatory cells in the lungs (Jacobs et al., 2013). In addition, the respiratory epithelium has been identified as the initial rhinovirus target as designated as the main site of replication (Jacobs et al., 2003). In that context, despite that rhinovirus interaction with human monocytes and alveolar macrophages led to cytokines production, no active viral replication was demonstrated (Gern et al., 1996). Gern et al confirmed that rhinovirus can infect efficiently both the lower and upper airways of healthy individuals (Gern et al., 1997). However, the mechanism of infection spread from the upper to the lower airways has never been elucidated. In addition, experimental studies defining rhinovirus effect on epithelial barrier defence mechanisms are missing.

The current study found that rhinovirus preferentially targeted ciliated respiratory cells of airway cultures from healthy and COPD donors, in agreement with previous studies (Griggs et al., 2017; Tan et al., 2018). High speed video microscopy is a powerful tool to trace host-pathogen interactions and to trace the initial pathogen cytotoxic effects on the airway epithelium. Data from high speed video microscopy showed that rhinovirus infection was associated with severe disruption of ciliary activity at 24h, associated with shedding of epithelial cells from the epithelial layer. Annexin V staining established that the underlying mechanism of active epithelial cells shedding and in particular ciliated cells was because of induction by rhinovirus of apoptosis pathways. Using Annexin V staining and various monoclonal antibody staining, Hodge and colleagues reported that bronchial airway cells and T lymphocytes from COPD patients undergo increased apoptosis in comparison to healthy smokers, and the implications encompass weakened host defence through the release of toxic to the cells material and amplified inflammation (Hodge et al., 2005). Therefore, initiation of apoptosis following rhinovirus infection as found in the current study could be of an extended importance to rhinovirus driven progression and pathogenesis of COPD.

The present study failed to determine if there were differences in rhinovirus replication between the healthy and COPD cells as was previously suggested (Schnider et al.,

2013). The reasons however may be due to the different techniques used to quantify viral replication, as titration assays used in the current study determine live virus infectivity whereas Schneider et al used a PCR technique, which also detects dead virus and viral particles that may not be infective. Other reasons could be the increased number of detached ciliated cells, positive for apoptotic and necrotic markers, or the significant induction of anti-viral IFNλ2/3 in both groups.

The expression of the ciliary protein DNAI2 has almost completely disappeared by day 7 of rhinovirus infection in healthy and COPD ciliated epithelium, which was in line with significantly reduced ciliary activity. The finding was consistent with gradually decreasing rhinovirus replication reaching significantly reduced titres at day 7 post infection in cultures from both healthy and COPD donors. Findings from the current study imply that the respiratory epithelium plays an important role in the removal of viral infection, in the absence of active innate or adaptive immune system. Rhinovirus tropism for ciliated cells and shedding is not a full precedent as it has been previously reported for other viruses such as RSV, influenza and coronavirus (Liesman et al., 2014; Zhang et al., 2011; Sims et al., 2005). However, none of these studies appeared to examine further the preferential infection of ciliated cells. The current study has also demonstrated for the first time that the ciliary membrane of ciliated cells is enriched in PI4P lipids. PI4P lipids together with the PI4KIIIβ enzyme have been previously shown to form viral replication platforms of picornaviruses (Hsu et al., 2010; Spickler et al., 2013). It would therefore be of interest to further explore viral tropism for ciliated cells and their preferential shedding, as COPD patients already have impaired airway ciliation (Shaykhiev and Crystal 2014).

The overall lack of effective antiviral compounds against rhinovirus led to our interest in testing a novel PI4KIIIβ inhibitor. High speed video microscopy and virus titration assays revealed a significant downregulation of rhinovirus replication in healthy and COPD cultures when pre-treated with the compound. Further, pre-treatment with the PI4KIIIβ compound preserved healthy cultures ciliary activity, and the same effect was found for COPD cultures, though statistical significance was not reached. Rhinovirus infection of healthy and COPD ciliated cells elicited a significant induction of a wide range of cytokines and chemokines including IL-1β, IP-10/ CXCL10, IL-6, IL-8/ CXCL8, RANTES/ CCL5 and IFNλ2/3 as previously reported (Baines et al., 2013; Schneider et al., 2013).

6.3 Co-infection with rhinovirus and *M. catarrhalis* findings

More severe and prolonged acute exacerbations are reported when viral and bacterial pathogens are detected in the airways of COPD patients (Papi et al., 2006; Wilkinson et al., 2006). Thus far, however, only a few studies analysed the causal relationship between co-infections and acute exacerbations (Gulraiz et al., 2015; Sajjan et al., 2008; Unger et al., 2012; Hendricks et al., 2016; Smith et al., 2014). Therefore, single pathogens infections of human ciliated airway cultures were established in order to later study multiple pathogen effects on the respiratory epithelium. An experimental model of pre-infection with rhinovirus for 24h of healthy and COPD airway cells followed by a *M. catarrhalis* infection was designed to investigate the interplay between bacterial-viral co-infections with the respiratory epithelium *in vitro*. It was hypothesised that a co-infection with rhinovirus and *M. catarrhalis* would lead to a greater ciliary dysfunction and inflammation in ciliated cultures from both healthy and COPD donors than either infection alone.

Investigations into the mechanisms by which the two pathogens were affecting the respiratory epithelium suggested they collectively caused a greater impairment of epithelial barrier defence and a higher induction of inflammatory mediators. From the current experiments it was clear that rhinovirus pre-infection caused a greater CBF reduction when *M. catarrhalis* was added to the primary cultures. Further, in contrast to healthy cultures, co-infection in cultures from COPD donors at 24h presented with a ~2Hz decrease of CBF. Additional decline of ciliary activity was seen in co-infected cultures compared to control non-infected or single *M. catarrhalis* infected cultures. In addition, reduction of ciliary activity was found to be rhinovirus driven by active shedding of ciliated cells. Impaired mucociliary function is a significant factor for COPD pathophysiology (Rogers, 2005). The three essential components of mucociliary clearance are mucus secretion, water and ion transport, and CBF, and epidemiological studies reported that chronic hypersecretion of mucus in COPD patients was associated with increased mortality in the presence of pulmonary infections (Prescott and Vestbo 1995). With the current findings of decreased ciliary function, new consequences of pathogen interactions in relation to co-infection have been revealed in the COPD epithelium.

It was surprising that *M. catarrhalis* viability in cultures from COPD donors was reduced, though non–significantly, following rhinovirus infection. According to previous clinical and *in vitro* findings respiratory viruses increase bacterial outgrowth (Molyneaux et al., 2013; Mallia et al., 2011; George et al., 2014; Hendricks et al.,

2016; Sajjan et al., 2008). With the current results, it is possible that virus pre-infection of COPD cells initiated an inflammatory unfavourable environment for *M. catarrhalis* growth. Nevertheless, upon rhinovirus infection ciliated cells shedding with *M. catarrhalis* attached was observed in the early hours of co-infection. Active shedding caused by viral infections of epithelial cells has been previously demonstrated to lead to distal airway obstruction in the airways *in vivo* (Liesman et al., 2014). Thus, an implication of rhinovirus induced shedding of epithelial cells could exacerbate airway obstruction due to cellular debris, particularly in the small airways, and dissemination of bacteria and viruses throughout the respiratory tract. This may also represent a method of spread from person to person with detached bacteria able to be coughed out of the respiratory tract in aerosolised particles.

It is thought that antioxidant defence in COPD patients is impaired leading to less protection and inability to neutralize oxidative stress, caused by cigarette smoke, inflammatory cells and infections (Kirkham and Barnes 2013; Wang et al., 2009). Pre-infection of the respiratory epithelium with rhinovirus in the current study resulted in an increased H_2O_2 production in cultures from healthy and COPD donors, and interestingly a co-infection with *M. catarrhalis* ciliated cultures from COPD donors generated more H_2O_2 than cultures from healthy donors. The consequences of increased ROS production by bacterial-viral infections imply increased inflammatory response by the airway epithelium, but also reduced responsiveness to corticosteroid therapy due to reduced histone diacetylase expression and activity through PI3K signalling (Barnes, 2013). Further, increased ROS generation in neutrophilic asthma has been recently suggested as a mechanism of reduced ciliary function that was successfully attenuated by an NADPH antioxidant inhibitor (Wan et al., 2016).

At a cellular level rhinovirus and *M. catarrhalis* co-infection triggered a robust inflammatory response, with higher secretion of chemoattractant cytokines in the basolateral and apical fluids of ciliated cultures when compared to single pathogen infections. This is a functional implication which may be associated with increased recruitment of inflammatory cells and a subsequent inflammation. The illustration in Figure 6-1 summarises this study's key findings from rhinovirus – *M. catarrhalis* co-infection of the COPD epithelium.

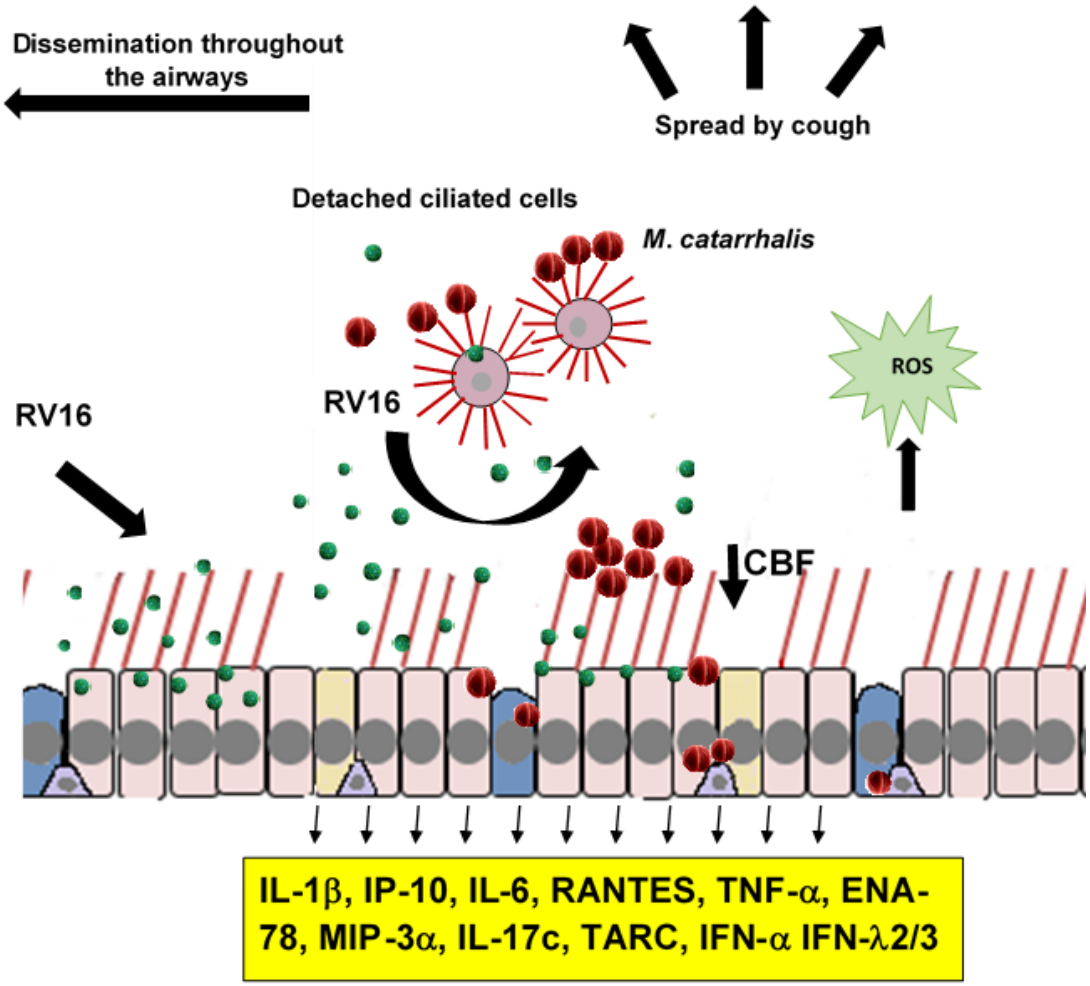

Figure 6-1: Proposed co-infection model of rhinovirus and *M. catarrhalis* interaction with the respiratory epithelium.

Rhinovirus (green circles) preferentially infects ciliated cells, while *M. catarrhalis* (red circles) binds to rapidly beating ciliated cells, severely disrupting CBF. Rhinovirus infection results in the active shedding of ciliated cells with adhered *M. catarrhalis* from the epithelial layer, associated with severe reduction of ciliation. The process is accompanied by enhanced ROS generation by epithelial cells, having an additive effect on inflammatory response. IL-1β, IP-10/ CXCL10, IL-6, RANTES/ CCL5, TNF-α, ENA-78/ CXCL5, MIP-3α/ CCL20, TARC/ CCL17, IFN-β and IFNλ2/3 are secreted following co-infection.

6.4 Differences and similarities of bronchial and nasal epithelial cultures

Tissue for respiratory research can be collected from the upper airways by nasal brushing of the nasal turbinate or from the lower airways by bronchial brushing, bronchial biopsy or resected lung tissue. Collection of nasal airway epithelial cells through nasal brushings has become a widely used method for research purposes (Bai et al., 2015; Hirst et al., 2010; Lopez-Souza et al., 2009; Smith et al., 2014, Tan et al., 2018). Nasal tissue collection is non-invasive and quick, making the procedure easier without the need of anaesthesia or hospitalisation. Thus, providing an easier and alternative to bronchial brushings way to collect airway cells, and increasing the accessibility and possibility to recruit multiple donors for research.

In the current study, human nasal and bronchial epithelial cells were used to investigate healthy volunteers and COPD patients' epithelial response to infection. Nasal and bronchial differentiated cultures presented with similar phenotype *in vitro*. Both types of cultures took an average of 4-5 weeks to fully differentiate at air-fluid interface. They appeared with a similar epithelial morphology and good overall ciliation. Of interest, nasal and bronchial cultures derived from COPD donors exhibited with darker areas of dense material when looked under the microscope, resembling an apical layer of mucus that was difficult to remove by washing. In comparison, nasal and bronchial cultures from healthy volunteers appeared homogenous with minimum indication of mucus production and secretion.

In chapter 3, the use of both types of tissue revealed *M. catarrhalis* ability to adhere instantly to ciliated cells. Live confocal imaging of nasal and bronchial differentiated cultures infected with *M. catarrhalis* showed the bacterium builds aggregates on both types of cultures, resulting in alteration of ciliary activity. Scanning electron microscopy of nasal and bronchial differentiated cultures confirmed these findings and showed *M. catarrhalis* tightly associated with cilia. In nasal differentiated cultures at 12 hours post infection, *M. catarrhalis* appeared mainly in clusters with bacterial strands between aggregates and single bacteria. These findings preceded the observations of formed *M. catarrhalis* biofilm in bronchial cultures at 24 hours.

In chapter 4, nasal and bronchial epithelial cells response to rhinovirus infection was investigated. Reduction of ciliary activity and ciliary beat frequency of nasal and bronchial cultures was seen over 7 days of rhinovirus infection. Further, rhinovirus titre decreased at day 7 compared to day 1 in both nasal and bronchial epithelial cells. Additionally, nasal and bronchial ciliated cultures pre-treated with a PI4KIIIβ inhibitor

prior rhinovirus infection showed a similar marked decrease of rhinovirus replication in comparison to rhinovirus infected cultures. Despite the low number of bronchial epithelial cultures used in this study, similarities between nasal and bronchial epithelial cultures were seen in response to bacterial and viral pathogens.

The choice of tissue becomes important when a comparison between healthy volunteers and patients with chronic lung disorders has to be made. A few published research articles have suggested differences between nasal and bronchial tissue such as immune cells abundance according to anatomical region (Vieira-Braga et al., 2019), inflammatory mediators release from epithelia (McDougall et al., 2008) and magnitude of rhinovirus replication (Lopes-Souza et al., 2009). However, it has also been shown epithelial cell types overlap with different proportions in the upper and lower airways (Vieira-Braga et al., 2019), epithelial cells have similar ciliary beat frequency, cell size, and cell surface receptors expression (McDougall et al., 2008). In COPD, immune cells infiltration, specifically neutrophils and CD8+ T lymphocytes have been found in both airway compartments (Vachier et al., 2004). The studies have suggested similarities but also differences between upper and lower airway epithelial cells, highlighting the importance to interpret results from nasal epithelial cultures used for surrogates of bronchial cultures with caution. To elucidate completely the suitability of nasal epithelial cells instead of bronchial epithelial cells in chronic lung disease research, a comparison between the two airway compartments may be advantageous.

6.5 Strengths and limitations of the ALI models used within the thesis when investigating responses to infection in COPD

The current research aimed to study the effect of *M. catarrhalis* on human ciliated cells at early time-points of infection, the effect of rhinovirus pre-infection on human ciliated cells subsequently infected with *M. catarrhalis* and the effect of single rhinovirus infection. Certain disease states such as COPD and asthma are associated with frequent infections (Barnes, 2011) and thus it is important to determine how infection in such patients varies from healthy individuals. In this study, collection of epithelial cells from nasal and bronchial brushings supplied good populations of epithelial cells, which functionally differentiated into a ciliated epithelium at air-fluid interface. The comparison of viral/bacterial co-infections between healthy and COPD differentiated cells was possible thanks to the constant access to patient cells through the newly developed GOSICH Biobank facility within the respiratory, critical care and anaesthesia department at UCL GOS Institute of Child Health. This enabled for

multiple re-growth of epithelial cells from different donors and increased reproducibility of experiments.

It is thought that ALI cultures closely model the native epithelium and naturally occurring viral and bacterial infections in the human body (Smith et al., 2014; Bae et al., 2015). In this project, the use of human nasal and bronchial differentiated cultures from healthy volunteers and COPD patients helped to understand the onset and progression of an infection with two of the most common COPD exacerbators. The advantage of using differentiated cultures is the formation of tight junctions that contribute to high epithelial integrity and multi-layered organisation of the cells, which resembles the ciliated epithelium lining in the respiratory tract. Airway epithelial cells from COPD donors cultured at air-liquid interface provided a good disease model to study infection mechanisms. In particular, airway cultures from COPD donors characterised with mucus build up in the process of epithelial differentiation, displaying a COPD phenotype of excess mucus production and secretion.

Air-fluid interface enabled to trace the first cytotoxic effects of pathogens on the respiratory epithelium in COPD such as ciliary activity and epithelial permeability. The differentiated epithelium presented with the capacity to release cytokines, essential for regulating innate and adaptive immune responses. The current study pointed at the potential benefits of a basolateral treatment with a PI4KIIIβ inhibitor during rhinovirus infection of ALI cultures. Further, drug compounds can also be aerosolised onto epithelial cultures and closely mimic inhaled powder deposition on the lung epithelium *in vivo* (Lenz et al., 2014). Thus, differentiation of primary epithelial cells at air-liquid interface represents a complex and predictive model for investigating host-pathogen interactions, and efficient drug compound testing in health and disease.

Despite all of the listed strengths of ALI cultures use, the model encompasses some methodological weaknesses. Limitations to use differentiated cells include the high associated cost and the time required to grow and differentiate cultures *in vitro*. Additional limiting factor is the high variability between well inserts seeded with epithelial cells from the same donor as well as the variability between various donors. In the present study, replicates and donor variability was observed in multiple experiments. For instance, bacterial adherence and invasion of epithelial differentiated cells from COPD donors. This illustrated a biological variation, as replicate wells would differ in cell population proportions. To minimise the variability between replicate wells from the same donor, ciliation score quality control sheet was used prior each experiment. Error bars and confidence intervals indicated the

variability between donors throughout the thesis. Quantification of data and statistical analyses showed trends and non-significant differences between healthy controls and disease donors, the findings therefore have to be interpreted with caution as they may have arisen because of a type 2 error. To quantify reliably data, larger sample size with more replicates and donors has to be used. To address this issue pre-study statistical power calculations of sample size may be helpful in future research.

The physiological relevance of ALI cultures for use in respiratory research involves epithelium's function in host defence including the formation of airway surface liquid, secretion of mucus and ciliary movement along with inflammatory and antimicrobial protein secretion. In this study, the respiratory epithelium was implicated in the inflammatory response to pathogens by secreting pro-inflammatory mediators. In cultures from COPD donors, *M. catarrhalis* stimulated elevated levels of IL-6, IP-10/ CXCL10, MIP-3α/ CCL20, ENA-78 /CXCL5, IL-17c while rhinovirus stimulated IL-1β, IL-6, IL-8/ CXCL8, CCL5/RANTES, IP-10/CXCL10 and MCP-1/ CCL5. Previous studies have also confirmed nasal and bronchial inflammation in COPD patients (Vachier et al., 2004; Hirst et al., 2006b). The challenge to accurately represent COPD inflammation driven by pathogens *in vitro* using ALI cultures is primarily due to the absence of immune cells, frequently recruited to the lungs to eradicate an infection. Viruses and bacteria, however, may amplify innate and adaptive immune cell activation, leading to chronic inflammation, infiltration of immune cells from the lungs and tissue remodelling (Barnes, 2016; Wang et al., 2018). Though the current study did not investigate immune and inflammatory associated tissue changes linked to the pathogenesis of COPD, the ciliated epithelium has been suggested to play a central role in early host defence against pathogens.

6.6 Future work

Although the current study provided a good overview of the early initial interaction of rhinovirus and *M. catarrhalis* with the respiratory epithelium along with a 7 day rhinovirus infection, the findings raised a number of questions which could be of clinical interest. Also, because different pathogens provoke variable host response it is important to focus first on a single pathogen infection in order to understand how an ongoing infection could change the epithelial response to a subsequent in this study bacterial infection. Rhinovirus tropism for ciliated cells is an important area to explore further, as reduced ciliation in the airways would have a damaging effect on physical protection in the COPD epithelium, which has already been identified as less ciliated. Future work on PI4P expression in cilia and viral replication in this cell type

during the early hours of infection, would lead to a better understanding of infection mechanisms relevant to COPD and could lead to novel therapeutic targets. Although ciliary function has been comprehensively studied through automated and manual CBF measurement and calculation of active ciliated areas, dyskinesia and ciliary amplitude measurements are other important features and would emphasise more accurately on the beat pattern and ciliary function of epithelial cells during bacterial-viral infections. Besides, it is likely that COPD patients suffer from decreased mucociliary clearance upon bacterial-viral infections which would make the airway epithelium more susceptible to other opportunistic pathogens and lead to prolonged lower airways infections, whose clearance will be reduced. Also, there remains to be determined the level of mucus secretion by the airway epithelium following a co-infection with rhinovirus and *M. catarrhalis* and whether tight junctions disruption affects epithelial integrity. Certainly, it is important to further investigate viral-bacterial induced ROS and their role in reduction of ciliary function and inflammation.

In the light of the current observations that epithelial treatment with an inhibiting PI4KIIIβ compound successfully reduced rhinovirus replication and preserved ciliation in cultures from healthy and COPD donors, it raises questions as to whether it will be as effective in the presence of a subsequent bacterial infection. In addition, a different delivery system and after-treatment instead of pre-treatment followed by rhinovirus exposure might reveal the real potential of the inhibitor in clinical outcomes. To translate clinical observations that secondary bacterial infections peak when viral replication decreases (Mallia et al., 2011), it might be more appropriate to trace long term rhinovirus infection with a follow up *M. catarrhalis* infection. The current study has already shown that by 7 day of rhinovirus infection ciliation and protection of the airway epithelium is irreversibly decreased, which could lead to increased bacterial survival and the formation of biofilm.

It is possible the robustness of the current data was affected by the small numbers of primary epithelial cultures used in some studies. Thus, a bigger population of a certain group would increase the accuracy of findings.

6.7 Conclusion

The current study provided a valid model to study bacterial-viral co-infections of the airway epithelium *in vitro*. The epithelial response to co-infections in terms of inflammation resembled COPD clinical findings during exacerbations, and more specifically elevated IL-6, IL-8/ CXCL8 and IP-10/ CXCL10 levels, providing

supportive information on how these might be triggered. One of the main advantages of the study was the use of primary airway cells from different healthy volunteers and COPD patients who suffer from frequent exacerbations. Collectively, the studies demonstrated that respiratory infections lead to severely impaired ciliary function early on during infection with extra generation of ROS that could have an additive effect on induced pathogen inflammation. The suggested cellular mechanisms are novel and important, as they show the pathogens initial effects on the respiratory epithelium and the multiple consequences they may have. The investigated cellular mechanisms may lead to improvements in the future management and treatment of COPD. Despite the fact that the current *in vitro* model does not involve innate or adaptive host immune responses it points towards to the vital role of the airway epithelium in the resolution and clearance of airway infections.

Chapter 7. References

ABDILLAHI, S. M., BOBER, M., NORDIN, S., HALLGREN, O., BAUMGARTEN, M., ERJEFALT, J., WESTERGREN-THORSSON, G., BJERMER, L., RIESBECK, K., EGESTEN, A. & MORGELIN, M. 2015. Collagen VI Is Upregulated in COPD and Serves Both as an Adhesive Target and a Bactericidal Barrier for Moraxella catarrhalis. J Innate Immun, 7, 506-17.

AKIRA, S., UEMATSU, S. & TAKEUCHI, O. 2006. Pathogen recognition and innate immunity. Cell, 124, 783-801.

ALNAHAS, S., HAGNER, S., RAIFER, H., KILIC, A., GASTEIGER, G., MUTTERS, R., HELLHUND, A., PRINZ, I., PINKENBURG, O., VISEKRUNA, A., GARN, H. & STEINHOFF, U. 2017. IL-17 and TNF-alpha Are Key Mediators of Moraxella catarrhalis Triggered Exacerbation of Allergic Airway Inflammation. Front Immunol, 8, 1562.

ALTAN-BONNET, N. 2017. Lipid Tales of Viral Replication and Transmission. Trends Cell Biol, 27, 201-213.

ALTAN-BONNET, N. & BALLA, T. 2012. Phosphatidylinositol 4-kinases: hostages harnessed to build panviral replication platforms. Trends Biochem Sci, 37, 293-302.

ARITA, M., KOJIMA, H., NAGANO, T., OKABE, T., WAKITA, T. & SHIMIZU, H. 2011. Phosphatidylinositol 4-kinase III beta is a target of enviroxime-like compounds for antipoliovirus activity. J Virol, 85, 2364-72.

ARMBRUSTER, C. E., HONG, W., PANG, B., WEIMER, K. E., JUNEAU, R. A., TURNER, J. & SWORDS, W. E. 2010. Indirect pathogenicity of Haemophilus influenzae and Moraxella catarrhalis in polymicrobial otitis media occurs via interspecies quorum signaling. MBio, 1.

ATHERTON, H. C., JONES, G. & DANAHAY, H. 2003. IL-13-induced changes in the goblet cell density of human bronchial epithelial cell cultures: MAP kinase and phosphatidylinositol 3-kinase regulation. Am J Physiol Lung Cell Mol Physiol, 285, L730-9.

AUGUSTYNIAK, D., SEREDYNSKI, R., MCCLEAN, S., ROSZKOWIAK, J., ROSZNIOWSKI, B., SMITH, D. L., DRULIS-KAWA, Z. & MACKIEWICZ, P. 2018. Virulence factors of Moraxella catarrhalis outer membrane vesicles are major targets for cross-reactive antibodies and have adapted during evolution. Sci Rep, 8, 4955.

BAFADHEL, M., SAHA, S., SIVA, R., MCCORMICK, M., MONTEIRO, W., RUGMAN, P., DODSON, P., PAVORD, I. D., NEWBOLD, P. & BRIGHTLING, C. E. 2009. Sputum IL-5 concentration is associated with a sputum eosinophilia and attenuated by corticosteroid therapy in COPD. Respiration, 78, 256-62.

BAI, J., SMOCK, S. L., JACKSON, G. R., JR., MACISAAC, K. D., HUANG, Y., MANKUS, C., OLDACH, J., ROBERTS, B., MA, Y. L., KLAPPENBACH, J. A., CRACKOWER, M. A., ALVES, S. E. & HAYDEN, P. J. 2015. Phenotypic responses of differentiated asthmatic human airway epithelial cultures to rhinovirus. PLoS One, 10, e0118286.

BAINES, K. J., HSU, A. C., TOOZE, M., GUNAWARDHANA, L. P., GIBSON, P. G. & WARK, P. A. 2013. Novel immune genes associated with excessive inflammatory and antiviral responses to rhinovirus in COPD. Respir Res, 14, 15.

BALDER, R., HASSEL, J., LIPSKI, S. & LAFONTAINE, E. R. 2007. Moraxella catarrhalis strain O35E expresses two filamentous hemagglutinin-like proteins that mediate adherence to human epithelial cells. Infect Immun, 75, 2765-75.

BALDER, R., KRUNKOSKY, T. M., NGUYEN, C. Q., FEEZEL, L. & LAFONTAINE, E. R. 2009. Hag mediates adherence of Moraxella catarrhalis to ciliated human airway cells. Infect Immun, 77, 4597-608.

BARNES, P. J. 2008. Immunology of asthma and chronic obstructive pulmonary disease. Nat Rev Immunol, 8, 183-92.

BARNES, P. J. 2009. The cytokine network in chronic obstructive pulmonary disease. Am J Respir Cell Mol Biol, 41, 631-8.

BARNES, P. J. 2011. Similarities and differences in inflammatory mechanisms of asthma and COPD. Breathe, 7, 229-238.

BARNES, P. J. 2013. New anti-inflammatory targets for chronic obstructive pulmonary disease. Nature Reviews Drug Discovery, 12, 543-559.

BARNES, P. J. 2014. Cellular and molecular mechanisms of chronic obstructive pulmonary disease. Clin Chest Med, 35, 71-86.

BARNES, P. J. 2016. Inflammatory mechanisms in patients with chronic obstructive pulmonary disease. J Allergy Clin Immunol, 138, 16-27.

BARNES, P. J. 2017. Cellular and molecular mechanisms of asthma and COPD. Clin Sci (Lond), 131, 1541-1558.

BARNES, P. J., BURNEY, P. G., SILVERMAN, E. K., CELLI, B. R., VESTBO, J., WEDZICHA, J. A. & WOUTERS, E. F. 2015. Chronic obstructive pulmonary disease. Nat Rev Dis Primers, 1, 15076.

BARNES, P. J. & CELLI, B. R. 2009. Systemic manifestations and comorbidities of COPD. Eur Respir J, 33, 1165-85.

BARNES, P. J., SHAPIRO, S. D. & PAUWELS, R. A. 2003. Chronic obstructive pulmonary disease: molecular and cellular mechanisms. Eur Respir J, 22, 672-88.

BEASLEY, V., JOSHI, P. V., SINGANAYAGAM, A., MOLYNEAUX, P. L., JOHNSTON, S. L. & MALLIA, P. 2012. Lung microbiology and exacerbations in COPD. Int J Chron Obstruct Pulmon Dis, 7, 555-69.

BELLA, J. & ROSSMANN, M. G. 1999. Review: rhinoviruses and their ICAM receptors. J Struct Biol, 128, 69-74.

BENJAMINI, Y, HOCHBERG, Y. 1995. Controlling the false discovery rate: a practical and powerful approach to multiple testing. *J Roy Stat Soc B*. 57, 289–300.

BENTLEY, J. K., NEWCOMB, D. C., GOLDSMITH, A. M., JIA, Y., SAJJAN, U. S. & HERSHENSON, M. B. 2007. Rhinovirus activates interleukin-8 expression via a Src/p110beta phosphatidylinositol 3-kinase/Akt pathway in human airway epithelial cells. J Virol, 81, 1186-94.

BERGER, K. L., KELLY, S. M., JORDAN, T. X., TARTELL, M. A. & RANDALL, G. 2011. Hepatitis C virus stimulates the phosphatidylinositol 4-kinase III alpha-dependent phosphatidylinositol 4-phosphate production that is essential for its replication. J Virol, 85, 8870-83.

BHOWMIK, A., SEEMUNGAL, T. A., SAPSFORD, R. J. & WEDZICHA, J. A. 2000. Relation of sputum inflammatory markers to symptoms and lung function changes in COPD exacerbations. Thorax, 55, 114-20.

BISGROVE, B. W. & YOST, H. J. 2006. The roles of cilia in developmental disorders and disease. Development, 133, 4131-43.

BLAKEWAY, L. V., TAN, A., PEAK, I. R. A. & SEIB, K. L. 2017. Virulence determinants of Moraxella catarrhalis: distribution and considerations for vaccine development. Microbiology, 163, 1371-1384.

BOCHKOV, Y. A. & GERN, J. E. 2012. Clinical and molecular features of human rhinovirus C. Microbes Infect, 14, 485-94.

BOCHKOV, Y. A. & GERN, J. E. 2016. Rhinoviruses and Their Receptors: Implications for Allergic Disease. Curr Allergy Asthma Rep, 16, 30.

BOCHKOV, Y. A., WATTERS, K., ASHRAF, S., GRIGGS, T. F., DEVRIES, M. K., JACKSON, D. J., PALMENBERG, A. C. & GERN, J. E. 2015. Cadherin-related family member 3, a childhood asthma susceptibility gene product, mediates rhinovirus C binding and replication. Proc Natl Acad Sci U S A, 112, 5485-90.

BOERS, J. E., AMBERGEN, A. W. & THUNNISSEN, F. B. 1999. Number and proliferation of clara cells in normal human airway epithelium. Am J Respir Crit Care Med, 159, 1585-91.

BOUCHER, R. C. 2019. Muco-Obstructive Lung Diseases. N Engl J Med, 380, 1941-1953.

BOUDEWIJN, I. M., FAIZ, A., STEILING, K., VAN DER WIEL, E., TELENGA, E. D., HOONHORST, S. J. M., TEN HACKEN, N. H. T., BRANDSMA, C. A., KERSTJENS, H. A. M., TIMENS, W., HEIJINK, I. H., JONKER, M. R., DE BRUIN, H. G., SEBASTIAAN VROEGOP, J., PASMA, H. R., BOERSMA, W. G., WIELDERS, P., VAN DEN ELSHOUT, F., MANSOUR, K., SPIRA, A., LENBURG, M. E., GURYEV, V., POSTMA, D. S. & VAN DEN BERGE, M. 2017. Nasal gene expression differentiates COPD from controls and overlaps bronchial gene expression. Respir Res, 18, 213.

BOUKHENOUNA, S., WILSON, M. A., BAHMED, K. & KOSMIDER, B. 2018. Reactive Oxygen Species in Chronic Obstructive Pulmonary Disease. Oxid Med Cell Longev, 2018, 5730395.

BRIGHTLING, C. & GREENING, N. 2019. Airway inflammation in COPD: progress to precision medicine. Eur Respir J, 54.

British Thoracic Society Bronchoscopy Guidelines Committee, a Subcommittee of Standards of Care Committee of British Thoracic Society. British Thoracic Society guidelines on diagnostic flexible bronchoscopy. Thorax 2011 November vol3: suppl11.guidlines.pdf

BROCKSON, M. E., NOVOTNY, L. A., JURCISEK, J. A., MCGILLIVARY, G., BOWERS, M. R. & BAKALETZ, L. O. 2012. Respiratory syncytial virus promotes Moraxella catarrhalis-induced ascending experimental otitis media. PLoS One, 7, e40088.

BUDHANI, R. K. & STRUTHERS, J. K. 1998. Interaction of Streptococcus pneumoniae and Moraxella catarrhalis: investigation of the indirect pathogenic role of beta-lactamase-producing moraxellae by use of a continuous-culture biofilm system. Antimicrob Agents Chemother, 42, 2521-6.

BUKOWY, Z., ZIETKIEWICZ, E. & WITT, M. 2011. In vitro culturing of ciliary respiratory cells--a model for studies of genetic diseases. J Appl Genet, 52, 39-51.

BULLARD, B., LIPSKI, S. & LAFONTAINE, E. R. 2007. Regions important for the adhesin activity of Moraxella catarrhalis Hag. BMC Microbiol, 7, 65.

BUTLER, C. R., HYNDS, R. E., GOWERS, K. H., LEE DDO, H., BROWN, J. M., CROWLEY, C., TEIXEIRA, V. H., SMITH, C. M., URBANI, L., HAMILTON, N. J., THAKRAR, R. M., BOOTH, H. L., BIRCHALL, M. A., DE COPPI, P., GIANGRECO, A., O'CALLAGHAN, C. & JANES, S. M. 2016. Rapid Expansion of Human Epithelial Stem Cells Suitable for Airway Tissue Engineering. Am J Respir Crit Care Med, 194, 156-68.

BUTTON, B., CAI, L. H., EHRE, C., KESIMER, M., HILL, D. B., SHEEHAN, J. K., BOUCHER, R. C. & RUBINSTEIN, M. 2012. A periciliary brush promotes the lung health by separating the mucus layer from airway epithelia. Science, 337, 937-41.

CAMPAGNARI, A. A., SHANKS, K. L. & DYER, D. W. 1994. Growth of Moraxella catarrhalis with human transferrin and lactoferrin: expression of iron-repressible proteins without siderophore production. Infect Immun, 62, 4909-14.

CASALINO-MATSUDA, S. M., MONZON, M. E. & FORTEZA, R. M. 2006. Epidermal growth factor receptor activation by epidermal growth factor mediates oxidant-induced goblet cell metaplasia in human airway epithelium. Am J Respir Cell Mol Biol, 34, 581-91.

CHEBATH, J., BENECH, P., HOVANESSIAN, A., GALABRU, J. & REVEL, M. 1987. Four different forms of interferon-induced 2',5'-oligo(A) synthetase identified by immunoblotting in human cells. J Biol Chem, 262, 3852-7.

CHEN, Y., HAMATI, E., LEE, P. K., LEE, W. M., WACHI, S., SCHNURR, D., YAGI, S., DOLGANOV, G., BOUSHEY, H., AVILA, P. & WU, R. 2006. Rhinovirus induces airway epithelial gene expression through double-stranded RNA and IFN-dependent pathways. Am J Respir Cell Mol Biol, 34, 192-203.

CHILVERS, M. A., MCKEAN, M., RUTMAN, A., MYINT, B. S., SILVERMAN, M. & O'CALLAGHAN, C. 2001. The effects of coronavirus on human nasal ciliated respiratory epithelium. Eur Respir J, 18, 965-70.

CHILVERS, M. A. & O'CALLAGHAN, C. 2000. Analysis of ciliary beat pattern and beat frequency using digital high speed imaging: comparison with the photomultiplier and photodiode methods. Thorax, 55, 314-7.

CHUNG, K. F. 2001. Cytokines in chronic obstructive pulmonary disease. European Respiratory Journal, 18, 50-59.

COMSTOCK, A. T., GANESAN, S., CHATTORAJ, A., FARIS, A. N., MARGOLIS, B. L., HERSHENSON, M. B. & SAJJAN, U. S. 2011. Rhinovirus-induced barrier dysfunction in polarized airway epithelial cells is mediated by NADPH oxidase 1. J Virol, 85, 6795-808.

CONNERS, R., HILL, D. J., BORODINA, E., AGNEW, C., DANIELL, S. J., BURTON, N. M., SESSIONS, R. B., CLARKE, A. R., CATTO, L. E., LAMMIE, D., WESS, T.,

CORDEY, S., GERLACH, D., JUNIER, T., ZDOBNOV, E. M., KAISER, L. & TAPPAREL, C. 2008. The cis-acting replication elements define human enterovirus and rhinovirus species. RNA, 14, 1568-78.

COSSART, P. & SANSONETTI, P. J. 2004. Bacterial invasion: the paradigms of enteroinvasive pathogens. Science, 304, 242-8.

COX, D. W. & LE SOUEF, P. N. 2014. Rhinovirus and the developing lung. Paediatr Respir Rev, 15, 268-74.

CRYSTAL, R. G. 2014. Airway basal cells. The "smoking gun" of chronic obstructive pulmonary disease. Am J Respir Crit Care Med, 190, 1355-62.

CRYSTAL, R. G., RANDELL, S. H., ENGELHARDT, J. F., VOYNOW, J. & SUNDAY, M. E. 2008. Airway epithelial cells: current concepts and challenges. Proc Am Thorac Soc, 5, 772-7.

CUENDA, A. & ROUSSEAU, S. 2007. p38 MAP-kinases pathway regulation, function and role in human diseases. Biochim Biophys Acta, 1773, 1358-75.

CULPITT, S. V., ROGERS, D. F., TRAVES, S. L., BARNES, P. J. & DONNELLY, L. E. 2005. Sputum matrix metalloproteases: comparison between chronic obstructive pulmonary disease and asthma. Respir Med, 99, 703-10.

CURTIS, J. L. 2005. Cell-mediated adaptive immune defense of the lungs. Proc Am Thorac Soc, 2, 412-6.

CURTIS, M. M. & WAY, S. S. 2009. Interleukin-17 in host defence against bacterial, mycobacterial and fungal pathogens. Immunology, 126, 177-85.

DAVOINE, F. & LACY, P. 2014. Eosinophil cytokines, chemokines, and growth factors: emerging roles in immunity. Front Immunol, 5, 570.

DE BOER, W. I., HAU, C. M., VAN SCHADEWIJK, A., STOLK, J., VAN KRIEKEN, J. H. J. M. & HIEMSTRA, P. S. 2006. Expression of Epidermal Growth Factors and Their Receptors in the Bronchial Epithelium of Subjects With Chronic Obstructive Pulmonary Disease. American Journal of Clinical Pathology, 125, 184-192.

DE ROSE, V., MOLLOY, K., GOHY, S., PILETTE, C. & GREENE, C. M. 2018. Airway Epithelium Dysfunction in Cystic Fibrosis and COPD. Mediators Inflamm, 2018, 1309746.

DE VRIES, S. P., BOOTSMA, H. J., HAYS, J. P. & HERMANS, P. W. 2009. Molecular aspects of Moraxella catarrhalis pathogenesis. Microbiol Mol Biol Rev, 73, 389-406, Table of Contents.

DE VRIES, S. P., ELEVELD, M. J., HERMANS, P. W. & BOOTSMA, H. J. 2013. Characterization of the molecular interplay between Moraxella catarrhalis and human respiratory tract epithelial cells. PLoS One, 8, e72193.

DE VRIES, S. P., VAN HIJUM, S. A., SCHUELER, W., RIESBECK, K., HAYS, J. P., HERMANS, P. W. & BOOTSMA, H. J. 2010. Genome analysis of Moraxella catarrhalis strain BBH18, [corrected] a human respiratory tract pathogen. J Bacteriol, 192, 3574-83.

DEVALIA, J. L., SAPSFORD, R. J., WELLS, C. W., RICHMAN, P. & DAVIES, R. J. 1990. Culture and comparison of human bronchial and nasal epithelial cells in vitro. Respir Med, 84, 303-12.

DI STEFANO, A., CARAMORI, G., OATES, T., CAPELLI, A., LUSUARDI, M., GNEMMI, I., IOLI, F., CHUNG, K. F., DONNER, C. F., BARNES, P. J. & ADCOCK, I. M. 2002. Increased expression of nuclear factor-kappaB in bronchial biopsies from smokers and patients with COPD. Eur Respir J, 20, 556-63.

DIMOPOULOS, G., LERIKOU, M., TSIODRAS, S., CHRANIOTI, A., PERROS, E., ANAGNOSTOPOULOU, U., ARMAGANIDIS, A. & KARAKITSOS, P. 2012. Viral epidemiology of acute exacerbations of chronic obstructive pulmonary disease. Pulm Pharmacol Ther, 25, 12-8.

DONALDSON, G. C., SEEMUNGAL, T. A., BHOWMIK, A. & WEDZICHA, J. A. 2002. Relationship between exacerbation frequency and lung function decline in chronic obstructive pulmonary disease. Thorax, 57, 847-52.

DONALDSON, G. C. & WEDZICHA, J. A. 2006. COPD exacerbations .1: Epidemiology. Thorax, 61, 164-8.

DOUGLAS, R. M., MOORE, B. W., MILES, H. B., DAVIES, L. M., GRAHAM, N. M., RYAN, P., WORSWICK, D. A. & ALBRECHT, J. K. 1986. Prophylactic efficacy of intranasal alpha 2-interferon against rhinovirus infections in the family setting. N Engl J Med, 314, 65-70.

DREES, F., POKUTTA, S., YAMADA, S., NELSON, W. J. & WEIS, W. I. 2005. Alpha-catenin is a molecular switch that binds E-cadherin-beta-catenin and regulates actin-filament assembly. Cell, 123, 903-15.

DU, R. P., WANG, Q., YANG, Y. P., SCHRYVERS, A. B., CHONG, P., KLEIN, M. H. & LOOSMORE, S. M. 1998. Cloning and expression of the Moraxella catarrhalis lactoferrin receptor genes. Infect Immun, 66, 3656-65.

EDWARDS, J. A., GROATHOUSE, N. A. & BOITANO, S. 2005. Bordetella bronchiseptica adherence to cilia is mediated by multiple adhesin factors and blocked by surfactant protein A. Infect Immun, 73, 3618-26.

EDWARDS, M. R., KEBADZE, T., JOHNSON, M. W. & JOHNSTON, S. L. 2006. New treatment regimes for virus-induced exacerbations of asthma. Pulm Pharmacol Ther, 19, 320-34.

ENGELHARDT, J. F., SCHLOSSBERG, H., YANKASKAS, J. R. & DUDUS, L. 1995. Progenitor cells of the adult human airway involved in submucosal gland development. Development, 121, 2031-46.

ERKAN, L., UZUN, O., FINDIK, S., KATAR, D., SANIC, A. & ATICI, A. G. 2008. Role of bacteria in acute exacerbations of chronic obstructive pulmonary disease. Int J Chron Obstruct Pulmon Dis, 3, 463-7.

FADEN, H., HARABUCHI, Y. & HONG, J. J. 1994. Epidemiology of Moraxella catarrhalis in children during the first 2 years of life: relationship to otitis media. J Infect Dis, 169, 1312-7.

FAHY, J. V. & DICKEY, B. F. 2010. Airway mucus function and dysfunction. N Engl J Med, 363, 2233-47.

FARR, B. M., GWALTNEY, J. M., JR., ADAMS, K. F. & HAYDEN, F. G. 1984. Intranasal interferon-alpha 2 for prevention of natural rhinovirus colds. Antimicrob Agents Chemother, 26, 31-4.

GANESAN, S., COMSTOCK, A. T. & SAJJAN, U. S. 2013. Barrier function of airway tract epithelium. Tissue Barriers, 1, e24997.

GANZ, T. 2003. Defensins: antimicrobial peptides of innate immunity. Nat Rev Immunol, 3, 710-20.

GARAY, C., JUDGE, G., LUCARELLI, S., BAUTISTA, S., PANDEY, R., SINGH, T. & ANTONESCU, C. N. 2015. Epidermal growth factor-stimulated Akt phosphorylation requires clathrin or ErbB2 but not receptor endocytosis. Mol Biol Cell, 26, 3504-19.

GARCHA, D. S., THURSTON, S. J., PATEL, A. R., MACKAY, A. J., GOLDRING, J. J., DONALDSON, G. C., MCHUGH, T. D. & WEDZICHA, J. A. 2012. Changes in prevalence and load of airway bacteria using quantitative PCR in stable and exacerbated COPD. Thorax, 67, 1075-80.

GARCIA-GONZALO, F. R., PHUA, S. C., ROBERSON, E. C., GARCIA, G., 3RD, ABEDIN, M., SCHURMANS, S., INOUE, T. & REITER, J. F. 2015. Phosphoinositides Regulate Ciliary Protein Trafficking to Modulate Hedgehog Signaling. Dev Cell, 34, 400-409.

GASTEIGER, G. & RUDENSKY, A. Y. 2014. Interactions between innate and adaptive lymphocytes. Nat Rev Immunol, 14, 631-9.

GEORGE, S. N., GARCHA, D. S., MACKAY, A. J., PATEL, A. R., SINGH, R., SAPSFORD, R. J., DONALDSON, G. C. & WEDZICHA, J. A. 2014. Human rhinovirus infection during naturally occurring COPD exacerbations. Eur Respir J, 44, 87-96.

GERN, J. E. 2010. The ABCs of rhinoviruses, wheezing, and asthma. J Virol, 84, 7418-26.

GERN, J. E., CALHOUN, W., SWENSON, C., SHEN, G. & BUSSE, W. W. 1997. Rhinovirus infection preferentially increases lower airway responsiveness in allergic subjects. Am J Respir Crit Care Med, 155, 1872-6.

GERN, J. E., DICK, E. C., LEE, W. M., MURRAY, S., MEYER, K., HANDZEL, Z. T. & BUSSE, W. W. 1996. Rhinovirus enters but does not replicate inside monocytes and airway macrophages. J Immunol, 156, 621-7.

GJORLOFF WINGREN, A., HADZIC, R., FORSGREN, A. & RIESBECK, K. 2002. The novel IgD binding protein from Moraxella catarrhalis induces human B lymphocyte activation and Ig secretion in the presence of Th2 cytokines. J Immunol, 168, 5582-8.

GOLD REPORT 2018, Global Strategy for the diagnosis, management, and prevention of Chronic Obstructive Pulmonary Disease [WWW document] available from https://goldcopd.org/wp-content/uploads/2017/11/GOLD-2018-v6.0-FINAL-revised-20-Nov_WMS.pdf/ accessed February 2019

GOMI, K., STAUDT, M. R., SALIT, J., KANER, R. J., HELDRICH, J., ROGALSKI, A. M., ARBELAEZ, V., CRYSTAL, R. G. & WALTERS, M. S. 2016. JAG1-Mediated

Notch Signaling Regulates Secretory Cell Differentiation of the Human Airway Epithelium. Stem Cell Rev Rep, 12, 454-63.

GOMPERTZ, S., BAYLEY, D. L., HILL, S. L. & STOCKLEY, R. A. 2001. Relationship between airway inflammation and the frequency of exacerbations in patients with smoking related COPD. Thorax, 56, 36-41.

GONCALVES, R. B., MENDES, Y. S., SOARES, M. R., KATPALLY, U., SMITH, T. J., SILVA, J. L. & OLIVEIRA, A. C. 2007. VP4 protein from human rhinovirus 14 is released by pressure and locked in the capsid by the antiviral compound WIN. J Mol Biol, 366, 295-306.

GONZALEZ-NAVAJAS, J. M., LEE, J., DAVID, M. & RAZ, E. 2012. Immunomodulatory functions of type I interferons. Nat Rev Immunol, 12, 125-35.

GOUBAU, D., DEDDOUCHE, S. & REIS E SOUSA, C. 2013. Cytosolic sensing of viruses. Immunity, 38, 855-69.

GREINER, O., DAY, P. J., ALTWEGG, M. & NADAL, D. 2003. Quantitative detection of Moraxella catarrhalis in nasopharyngeal secretions by real-time PCR. J Clin Microbiol, 41, 1386-90.

GRIGGS, T. F., BOCHKOV, Y. A., BASNET, S., PASIC, T. R., BROCKMAN-SCHNEIDER, R. A., PALMENBERG, A. C. & GERN, J. E. 2017. Rhinovirus C targets ciliated airway epithelial cells. Respir Res, 18, 84.

GRUMELLI, S., CORRY, D. B., SONG, L. Z., SONG, L., GREEN, L., HUH, J., HACKEN, J., ESPADA, R., BAG, R., LEWIS, D. E. & KHERADMAND, F. 2004. An immune basis for lung parenchymal destruction in chronic obstructive pulmonary disease and emphysema. PLoS Med, 1, e8.

GUALDONI, G. A., MAYER, K. A., KAPSCH, A. M., KREUZBERG, K., PUCK, A., KIENZL, P., OBERNDORFER, F., FRUHWIRTH, K., WINKLER, S., BLAAS, D., ZLABINGER, G. J. & STOCKL, J. 2018. Rhinovirus induces an anabolic reprogramming in host cell metabolism essential for viral replication. Proc Natl Acad Sci U S A, 115, E7158-E7165.

GUDIS, D., ZHAO, K. Q. & COHEN, N. A. 2012. Acquired cilia dysfunction in chronic rhinosinusitis. Am J Rhinol Allergy, 26, 1-6.

GULRAIZ, F., BELLINGHAUSEN, C., BRUGGEMAN, C. A. & STASSEN, F. R. 2015. Haemophilus influenzae increases the susceptibility and inflammatory response of airway epithelial cells to viral infections. FASEB J, 29, 849-58.

HACKETT, N. R., HEGUY, A., HARVEY, B. G., O'CONNOR, T. P., LUETTICH, K., FLIEDER, D. B., KAPLAN, R. & CRYSTAL, R. G. 2003. Variability of antioxidant-related gene expression in the airway epithelium of cigarette smokers. Am J Respir Cell Mol Biol, 29, 331-43.

HACKETT, T. L., SHAHEEN, F., JOHNSON, A., WADSWORTH, S., PECHKOVSKY, D. V., JACOBY, D. B., KICIC, A., STICK, S. M. & KNIGHT, D. A. 2008. Characterization of side population cells from human airway epithelium. Stem Cells, 26, 2576-85.

HALL-STOODLEY, L., HU, F. Z., GIESEKE, A., NISTICO, L., NGUYEN, D., HAYES, J., FORBES, M., GREENBERG, D. P., DICE, B., BURROWS, A., WACKYM, P. A., STOODLEY, P., POST, J. C., EHRLICH, G. D. & KERSCHNER, J. E. 2006. Direct detection of bacterial biofilms on the middle-ear mucosa of children with chronic otitis media. JAMA, 296, 202-11.

HARVEY, B. G., HEGUY, A., LEOPOLD, P. L., CAROLAN, B. J., FERRIS, B. & CRYSTAL, R. G. 2007. Modification of gene expression of the small airway epithelium in response to cigarette smoking. J Mol Med (Berl), 85, 39-53.

HASSAN, F., REN, D., ZHANG, W., MERKEL, T. J. & GU, X. X. 2012. Moraxella catarrhalis activates murine macrophages through multiple toll like receptors and has reduced clearance in lungs from TLR4 mutant mice. PLoS One, 7, e37610.

HEINIGER, N., SPANIOL, V., TROLLER, R., VISCHER, M. & AEBI, C. 2007. A reservoir of Moraxella catarrhalis in human pharyngeal lymphoid tissue. J Infect Dis, 196, 1080-7.

HEINIGER, N., TROLLER, R., MEIER, P. S. & AEBI, C. 2005. Cold shock response of the UspA1 outer membrane adhesin of Moraxella catarrhalis. Infect Immun, 73, 8247-55.

HEINRICH, A., HEYL, K. A., KLAILE, E., MULLER, M. M., KLASSERT, T. E., WIESSNER, A., FISCHER, K., SCHUMANN, R. R., SEIFERT, U., RIESBECK, K., MOTER, A., SINGER, B. B., BACHMANN, S. & SLEVOGT, H. 2016. Moraxella

catarrhalis induces CEACAM3-Syk-CARD9-dependent activation of human granulocytes. Cell Microbiol, 18, 1570-1582.

HENDRICKS, M. R., LASHUA, L. P., FISCHER, D. K., FLITTER, B. A., EICHINGER, K. M., DURBIN, J. E., SARKAR, S. N., COYNE, C. B., EMPEY, K. M. & BOMBERGER, J. M. 2016. Respiratory syncytial virus infection enhances Pseudomonas aeruginosa biofilm growth through dysregulation of nutritional immunity. Proc Natl Acad Sci U S A, 113, 1642-7.

HENRICKS, P. A. & NIJKAMP, F. P. 2001. Reactive oxygen species as mediators in asthma. Pulm Pharmacol Ther, 14, 409-20.

HENRIKSEN, L., GRANDAL, M. V., KNUDSEN, S. L., VAN DEURS, B. & GROVDAL, L. M. 2013. Internalization mechanisms of the epidermal growth factor receptor after activation with different ligands. PLoS One, 8, e58148.

HESSEL, J., HELDRICH, J., FULLER, J., STAUDT, M. R., RADISCH, S., HOLLMANN, C., HARVEY, B. G., KANER, R. J., SALIT, J., YEE-LEVIN, J., SRIDHAR, S., PILLAI, S., HILTON, H., WOLFF, G., BITTER, H., VISVANATHAN, S., FINE, J., STEVENSON, C. S., CRYSTAL, R. G. & TILLEY, A. E. 2014. Intraflagellar transport gene expression associated with short cilia in smoking and COPD. PLoS One, 9, e85453.

HEWITT, R., FARNE, H., RITCHIE, A., LUKE, E., JOHNSTON, S. L. & MALLIA, P. 2016. The role of viral infections in exacerbations of chronic obstructive pulmonary disease and asthma. Ther Adv Respir Dis, 10, 158-74.

HEYMANN, P. W., PLATTS-MILLS, T. A. & JOHNSTON, S. L. 2005. Role of viral infections, atopy and antiviral immunity in the etiology of wheezing exacerbations among children and young adults. Pediatr Infect Dis J, 24, S217-22, discussion S220-1.

HIEMSTRA, P. S. 2013. Altered macrophage function in chronic obstructive pulmonary disease. Ann Am Thorac Soc, 10 Suppl, S180-5.

HIEMSTRA, P. S., MCCRAY, P. B., JR. & BALS, R. 2015. The innate immune function of airway epithelial cells in inflammatory lung disease. Eur Respir J, 45, 1150-62.

HILL, D. J., WHITTLES, C. & VIRJI, M. 2012. A novel group of Moraxella catarrhalis UspA proteins mediates cellular adhesion via CEACAMs and vitronectin. PLoS One, 7, e45452.

HIRST, R. A., RUTMAN, A., WILLIAMS, G. & O'CALLAGHAN, C. 2010. Ciliated air-liquid cultures as an aid to diagnostic testing of primary ciliary dyskinesia. Chest, 138, 1441-7.

HODGE, S., HODGE, G., HOLMES, M. & REYNOLDS, P. N. 2005. Increased airway epithelial and T-cell apoptosis in COPD remains despite smoking cessation. Eur Respir J, 25, 447-54.

HOENDERDOS, K. & CONDLIFFE, A. 2013. The neutrophil in chronic obstructive pulmonary disease. Am J Respir Cell Mol Biol, 48, 531-9.

HOGG, J. C., CHU, F., UTOKAPARCH, S., WOODS, R., ELLIOTT, W. M., BUZATU, L., CHERNIACK, R. M., ROGERS, R. M., SCIURBA, F. C., COXSON, H. O. & PARE, P. D. 2004. The nature of small-airway obstruction in chronic obstructive pulmonary disease. N Engl J Med, 350, 2645-53.

HOGG, J. C. & TIMENS, W. 2009. The pathology of chronic obstructive pulmonary disease. Annu Rev Pathol, 4, 435-59.

HOLM, M. M., VANLERBERG, S. L., FOLEY, I. M., SLEDJESKI, D. D. & LAFONTAINE, E. R. 2004. The Moraxella catarrhalis porin-like outer membrane protein CD is an adhesin for human lung cells. Infect Immun, 72, 1906-13.

HOLM, M. M., VANLERBERG, S. L., SLEDJESKI, D. D. & LAFONTAINE, E. R. 2003. The Hag protein of Moraxella catarrhalis strain O35E is associated with adherence to human lung and middle ear cells. Infect Immun, 71, 4977-84.

HOOPMAN, T. C., LIU, W., JOSLIN, S. N., PYBUS, C., BRAUTIGAM, C. A. & HANSEN, E. J. 2011. Identification of gene products involved in the oxidative stress response of Moraxella catarrhalis. Infect Immun, 79, 745-55.

HSU, N. Y., ILNYTSKA, O., BELOV, G., SANTIANA, M., CHEN, Y. H., TAKVORIAN, P. M., PAU, C., VAN DER SCHAAR, H., KAUSHIK-BASU, N., BALLA, T., CAMERON, C. E., EHRENFELD, E., VAN KUPPEVELD, F. J. & ALTAN-BONNET, N. 2010. Viral reorganization of the secretory pathway generates distinct organelles for RNA replication. Cell, 141, 799-811.

HURST, J. R., DONALDSON, G. C., WILKINSON, T. M., PERERA, W. R. & WEDZICHA, J. A. 2005. Epidemiological relationships between the common cold and exacerbation frequency in COPD. Eur Respir J, 26, 846-52.

HURST, J. R., KUCHAI, R., MICHAEL, P., PERERA, W. R., WILKINSON, T. M. & WEDZICHA, J. A. 2006b. Nasal symptoms, airway obstruction and disease severity in chronic obstructive pulmonary disease. Clin Physiol Funct Imaging, 26, 251-6.

URST, J. R., PERERA, W. R., WILKINSON, T. M., DONALDSON, G. C. & WEDZICHA, J. A. 2006a. Systemic and upper and lower airway inflammation at exacerbation of chronic obstructive pulmonary disease. Am J Respir Crit Care Med, 173, 71-8.

HURST, J. R., VESTBO, J., ANZUETO, A., LOCANTORE, N., MULLEROVA, H., TAL-SINGER, R., MILLER, B., LOMAS, D. A., AGUSTI, A., MACNEE, W., CALVERLEY, P., RENNARD, S., WOUTERS, E. F., WEDZICHA, J. A. & EVALUATION OF, C. L. T. I. P. S. E. I. 2010. Susceptibility to exacerbation in chronic obstructive pulmonary disease. N Engl J Med, 363, 1128-38.

HUTCHINSON, A. F., GHIMIRE, A. K., THOMPSON, M. A., BLACK, J. F., BRAND, C. A., LOWE, A. J., SMALLWOOD, D. M., VLAHOS, R., BOZINOVSKI, S., BROWN, G. V., ANDERSON, G. P. & IRVING, L. B. 2007. A community-based, time-matched, case-control study of respiratory viruses and exacerbations of COPD. Respir Med, 101, 2472-81.

ILNYTSKA, O., SANTIANA, M., HSU, N. Y., DU, W. L., CHEN, Y. H., VIKTOROVA, E. G., BELOV, G., BRINKER, A., STORCH, J., MOORE, C., DIXON, J. L. & ALTAN-BONNET, N. 2013. Enteroviruses harness the cellular endocytic machinery to remodel the host cell cholesterol landscape for effective viral replication. Cell Host Microbe, 14, 281-93.

JACKSON, D. J., GANGNON, R. E., EVANS, M. D., ROBERG, K. A., ANDERSON, E. L., PAPPAS, T. E., PRINTZ, M. C., LEE, W. M., SHULT, P. A., REISDORF, E., CARLSON-DAKES, K. T., SALAZAR, L. P., DASILVA, D. F., TISLER, C. J., GERN, J. E. & LEMANSKE, R. F., JR. 2008. Wheezing rhinovirus illnesses in early life predict asthma development in high-risk children. Am J Respir Crit Care Med, 178, 667-72.

JACOBS, S. E., LAMSON, D. M., ST GEORGE, K. & WALSH, T. J. 2013. Human rhinoviruses. Clin Microbiol Rev, 26, 135-62.

JAKIELA, B., BROCKMAN-SCHNEIDER, R., AMINEVA, S., LEE, W. M. & GERN, J. E. 2008. Basal cells of differentiated bronchial epithelium are more susceptible to rhinovirus infection. Am J Respir Cell Mol Biol, 38, 517-23.

JAKIELA, B., GIELICZ, A., PLUTECKA, H., HUBALEWSKA-MAZGAJ, M., MASTALERZ, L., BOCHENEK, G., SOJA, J., JANUSZEK, R., AAB, A., MUSIAL, J., AKDIS, M., AKDIS, C. A. & SANAK, M. 2014. Th2-type cytokine-induced mucus metaplasia decreases susceptibility of human bronchial epithelium to rhinovirus infection. Am J Respir Cell Mol Biol, 51, 229-41.

JAMIESON, K. C., TRAVES, S. L., KOOI, C., WIEHLER, S., DUMONCEAUX, C. J., MACIEJEWSKI, B. A., ARNASON, J. W., MICHI, A. N., LEIGH, R. & PROUD, D. 2019. Rhinovirus and Bacteria Synergistically Induce IL-17C Release from Human Airway Epithelial Cells To Promote Neutrophil Recruitment. J Immunol, 202, 160-170.

JEFFERY, P. K. 2004. Remodeling and inflammation of bronchi in asthma and chronic obstructive pulmonary disease. Proc Am Thorac Soc, 1, 176-83.

JING, Y., GIMENES, J. A., MISHRA, R., PHAM, D., COMSTOCK, A. T., YU, D. & SAJJAN, U. 2019. NOTCH3 contributes to rhinovirus-induced goblet cell hyperplasia in COPD airway epithelial cells. Thorax, 74, 18-32.

JOHNSTON, S. L. 2003. Experimental models of rhinovirus-induced exacerbations of asthma: where to now? Am J Respir Crit Care Med, 168, 1145-6.

JOHNSTON, S. L., BARDIN, P. G. & PATTEMORE, P. K. 1993. Viruses as precipitants of asthma symptoms. III. Rhinoviruses: molecular biology and prospects for future intervention. Clin Exp Allergy, 23, 237-46.

KAKU, Y., IMAOKA, H., MORIMATSU, Y., KOMOHARA, Y., OHNISHI, K., ODA, H., TAKENAKA, S., MATSUOKA, M., KAWAYAMA, T., TAKEYA, M. & HOSHINO, T. 2014. Overexpression of CD163, CD204 and CD206 on alveolar macrophages in the lungs of patients with severe chronic obstructive pulmonary disease. PLoS One, 9, e87400.

KETTERER, M. R., SHAO, J. Q., HORNICK, D. B., BUSCHER, B., BANDI, V. K. & APICELLA, M. A. 1999. Infection of primary human bronchial epithelial cells by Haemophilus influenzae: macropinocytosis as a mechanism of airway epithelial cell entry. Infect Immun, 67, 4161-70.

KHAITOV, M. R., LAZA-STANCA, V., EDWARDS, M. R., WALTON, R. P., ROHDE, G., CONTOLI, M., PAPI, A., STANCIU, L. A., KOTENKO, S. V. & JOHNSTON, S. L. 2009. Respiratory virus induction of alpha-, beta- and lambda-interferons in bronchial epithelial cells and peripheral blood mononuclear cells. Allergy, 64, 375-86.

KIEDROWSKI, M. R. & BOMBERGER, J. M. 2018. Viral-Bacterial Co-infections in the Cystic Fibrosis Respiratory Tract. Front Immunol, 9, 3067.

KIRKHAM, P. A. & BARNES, P. J. 2013. Oxidative stress in COPD. Chest, 144, 266-273.

KOFF, J. L., SHAO, M. X., UEKI, I. F. & NADEL, J. A. 2008. Multiple TLRs activate EGFR via a signaling cascade to produce innate immune responses in airway epithelium. Am J Physiol Lung Cell Mol Physiol, 294, L1068-75.

KOVARIK, P., CASTIGLIA, V., IVIN, M. & EBNER, F. 2016. Type I Interferons in Bacterial Infections: A Balancing Act. Front Immunol, 7, 652.

KRISHNAMURTHY, A., MCGRATH, J., CRIPPS, A. W. & KYD, J. M. 2009. The incidence of Streptococcus pneumoniae otitis media is affected by the polymicrobial environment particularly Moraxella catarrhalis in a mouse nasal colonisation model. Microbes Infect, 11, 545-53.

KRISHNASWAMY, G., MARTIN, R., WALKER, E., LI, C., HOSSLER, F., HALL, K. & CHI, D. S. 2003. Moraxella catarrhalis induces mast cell activation and nuclear factor kappa B-dependent cytokine synthesis. Front Biosci, 8, a40-7.

KUDVA, A., SCHELLER, E. V., ROBINSON, K. M., CROWE, C. R., CHOI, S. M., SLIGHT, S. R., KHADER, S. A., DUBIN, P. J., ENELOW, R. I., KOLLS, J. K. & ALCORN, J. F. 2011. Influenza A inhibits Th17-mediated host defense against bacterial pneumonia in mice. J Immunol, 186, 1666-1674.

LAFONTAINE, E. R., COPE, L. D., AEBI, C., LATIMER, J. L., MCCRACKEN, G. H., JR. & HANSEN, E. J. 2000. The UspA1 protein and a second type of UspA2 protein mediate adherence of Moraxella catarrhalis to human epithelial cells in vitro. J Bacteriol, 182, 1364-73.

LEE, S. L., ADAMS, W. P., LI, B. V., CONNER, D. P., CHOWDHURY, B. A. & YU, L. X. 2009. In vitro considerations to support bioequivalence of locally acting drugs in dry powder inhalers for lung diseases. AAPS J, 11, 414-23.

LEE, J. T., JR. & MCCUBREY, J. A. 2002. The Raf/MEK/ERK signal transduction cascade as a target for chemotherapeutic intervention in leukemia. Leukemia, 16, 486-507.

LENZ, A. G., STOEGER, T., CEI, D., SCHMIDMEIR, M., SEMREN, N., BURGSTALLER, G., LENTNER, B., EICKELBERG, O., MEINERS, S. & SCHMID, O. 2014. Efficient bioactive delivery of aerosolized drugs to human pulmonary epithelial cells cultured in air-liquid interface conditions. Am J Respir Cell Mol Biol, 51, 526-35.

LEMESSURIER, K. S., HACKER, H., CHI, L., TUOMANEN, E. & REDECKE, V. 2013. Type I interferon protects against pneumococcal invasive disease by inhibiting bacterial transmigration across the lung. PLoS Pathog, 9, e1003727.

LEOPOLD, P. L., O'MAHONY, M. J., LIAN, X. J., TILLEY, A. E., HARVEY, B. G. & CRYSTAL, R. G. 2009. Smoking is associated with shortened airway cilia. PLoS One, 4, e8157.

LIESMAN, R. M., BUCHHOLZ, U. J., LUONGO, C. L., YANG, L., PROIA, A. D., DEVINCENZO, J. P., COLLINS, P. L. & PICKLES, R. J. 2014. RSV-encoded NS2 promotes epithelial cell shedding and distal airway obstruction. J Clin Invest, 124, 2219-33.

LINDEN, A. & DAHLEN, B. 2014. Interleukin-17 cytokine signalling in patients with asthma. Eur Respir J, 44, 1319-31.

LIU, G., ERMERT, D., JOHANSSON, M. E., SINGH, B., SU, Y. C., PAULSSON, M., RIESBECK, K. & BLOM, A. M. 2017. PRELP Enhances Host Innate Immunity against the Respiratory Tract Pathogen Moraxella catarrhalis. J Immunol, 198, 2330-2340.

LOOI, K., TROY, N. M., GARRATT, L. W., IOSIFIDIS, T., BOSCO, A., BUCKLEY, A. G., LING, K. M., MARTINOVICH, K. M., KICIC-STARCEVICH, E., SHAW, N. C., SUTANTO, E. N., ZOSKY, G. R., RIGBY, P. J., LARCOMBE, A. N., KNIGHT, D. A., KICIC, A. & STICK, S. M. 2016. Effect of human rhinovirus infection on airway epithelium tight junction protein disassembly and transepithelial permeability. Exp Lung Res, 42, 380-395.

LOPEZ-SOUZA, N., DOLGANOV, G., DUBIN, R., SACHS, L. A., SASSINA, L., SPORER, H., YAGI, S., SCHNURR, D., BOUSHEY, H. A. & WIDDICOMBE, J. H. 2004. Resistance of differentiated human airway epithelium to infection by rhinovirus. Am J Physiol Lung Cell Mol Physiol, 286, L373-81.

LOPEZ-SOUZA, N., FAVORETO, S., WONG, H., WARD, T., YAGI, S., SCHNURR, D., FINKBEINER, W. E., DOLGANOV, G. M., WIDDICOMBE, J. H., BOUSHEY, H. A. & AVILA, P. C. 2009. In vitro susceptibility to rhinovirus infection is greater for bronchial than for nasal airway epithelial cells in human subjects. J Allergy Clin Immunol, 123, 1384-90 e2.

LOTZERICH, M., ROULIN, P. S., BOUCKE, K., WITTE, R., GEORGIEV, O. & GREBER, U. F. 2018. Rhinovirus 3C protease suppresses apoptosis and triggers caspase-independent cell death. Cell Death Dis, 9, 272.

LOVE, K. T., MAHON, K. P., LEVINS, C. G., WHITEHEAD, K. A., QUERBES, W., DORKIN, J. R., QIN, J., CANTLEY, W., QIN, L. L., RACIE, T., FRANK-KAMENETSKY, M., YIP, K. N., ALVAREZ, R., SAH, D. W., DE FOUGEROLLES, A., FITZGERALD, K., KOTELIANSKY, V., AKINC, A., LANGER, R. & ANDERSON, D. G. 2010. Lipid-like materials for low-dose, in vivo gene silencing. Proc Natl Acad Sci U S A, 107, 1864-9.

LUKE, N. R., JURCISEK, J. A., BAKALETZ, L. O. & CAMPAGNARI, A. A. 2007. Contribution of Moraxella catarrhalis type IV pili to nasopharyngeal colonization and biofilm formation. Infect Immun, 75, 5559-64.

LYNCH, T. J. & ENGELHARDT, J. F. 2014. Progenitor cells in proximal airway epithelial development and regeneration. J Cell Biochem, 115, 1637-45.

MACINTYRE RAINA, C., CHUGHTAI, A. A., ZHANG, Y., SEALE, H., YANG, P., CHEN, J., PAN, Y., ZHANG, D. & WANG, Q. 2017. Viral and bacterial upper respiratory tract infection in hospital health care workers over time and association with symptoms. BMC Infect Dis, 17, 553.

MACINTYRE, C. R., CHUGHTAI, A. A., BARNES, M., RIDDA, I., SEALE, H., TOMS, R. & HEYWOOD, A. 2018. The role of pneumonia and secondary bacterial infection in fatal and serious outcomes of pandemic influenza a(H1N1)pdm09. BMC Infect Dis, 18, 637.

MALLIA, P., FOOTITT, J., SOTERO, R., JEPSON, A., CONTOLI, M., TRUJILLO-TORRALBO, M. B., KEBADZE, T., ANISCENKO, J., OLESZKIEWICZ, G., GRAY, K., MESSAGE, S. D., ITO, K., BARNES, P. J., ADCOCK, I. M., PAPI, A., STANCIU, L. A., ELKIN, S. L., KON, O. M., JOHNSON, M. & JOHNSTON, S. L. 2012. Rhinovirus infection induces degradation of antimicrobial peptides and secondary bacterial

infection in chronic obstructive pulmonary disease. Am J Respir Crit Care Med, 186, 1117-24.

MALLIA, P., MESSAGE, S. D., GIELEN, V., CONTOLI, M., GRAY, K., KEBADZE, T., ANISCENKO, J., LAZA-STANCA, V., EDWARDS, M. R., SLATER, L., PAPI, A., STANCIU, L. A., KON, O. M., JOHNSON, M. & JOHNSTON, S. L. 2011. Experimental rhinovirus infection as a human model of chronic obstructive pulmonary disease exacerbation. Am J Respir Crit Care Med, 183, 734-42.

MARTINEZ, F. J., HAN, M. K., ALLINSON, J. P., BARR, R. G., BOUCHER, R. C., CALVERLEY, P. M. A., CELLI, B. R., CHRISTENSON, S. A., CRYSTAL, R. G., FAGERAS, M., FREEMAN, C. M., GROENKE, L., HOFFMAN, E. A., KESIMER, M., KOSTIKAS, K., PAINE, R., 3RD, RAFII, S., RENNARD, S. I., SEGAL, L. N., SHAYKHIEV, R., STEVENSON, C., TAL-SINGER, R., VESTBO, J., WOODRUFF, P. G., CURTIS, J. L. & WEDZICHA, J. A. 2018. At the Root: Defining and Halting Progression of Early Chronic Obstructive Pulmonary Disease. Am J Respir Crit Care Med, 197, 1540-1551.

MCDOUGALL, C. M., BLAYLOCK, M. G., DOUGLAS, J. G., BROOKER, R. J., HELMS, P. J. & WALSH, G. M. 2008. Nasal epithelial cells as surrogates for bronchial epithelial cells in airway inflammation studies. Am J Respir Cell Mol Biol, 39, 560-8.

MCGILLIVARY, G., MASON, K. M., JURCISEK, J. A., PEEPLES, M. E. & BAKALETZ, L. O. 2009. Respiratory syncytial virus-induced dysregulation of expression of a mucosal beta-defensin augments colonization of the upper airway by non-typeable Haemophilus influenzae. Cell Microbiol, 11, 1399-408.

MCNAB, F., MAYER-BARBER, K., SHER, A., WACK, A. & O'GARRA, A. 2015. Type I interferons in infectious disease. Nat Rev Immunol, 15, 87-103.

MICHAEL J. EVANS, L. S. V. W. 2001. Cellular and Molecular Characteristics of Basal Cells in Airway Epithelium. Experimental Lung Research, 27, 401-415.

MICHELSON, P. H., TIGUE, M. & JONES, J. C. 2000. Human bronchial epithelial cells secrete laminin 5, express hemidesmosomal proteins, and assemble hemidesmosomes. J Histochem Cytochem, 48, 535-44.

MILES, A. A., MISRA, S. S. & IRWIN, J. O. 1938. The estimation of the bactericidal power of the blood. J Hyg (Lond), 38, 732-49.

MOLYNEAUX, P. L., MALLIA, P., COX, M. J., FOOTITT, J., WILLIS-OWEN, S. A., HOMOLA, D., TRUJILLO-TORRALBO, M. B., ELKIN, S., KON, O. M., COOKSON, W. O., MOFFATT, M. F. & JOHNSTON, S. L. 2013. Outgrowth of the bacterial airway microbiome after rhinovirus exacerbation of chronic obstructive pulmonary disease. Am J Respir Crit Care Med, 188, 1224-31.

MORALES-NEBREDA, L., MISHARIN, A. V., PERLMAN, H. & BUDINGER, G. R. 2015. The heterogeneity of lung macrophages in the susceptibility to disease. Eur Respir Rev, 24, 505-9.

MOSSER, A. G., BROCKMAN-SCHNEIDER, R., AMINEVA, S., BURCHELL, L., SEDGWICK, J. B., BUSSE, W. W. & GERN, J. E. 2002. Similar frequency of rhinovirus-infectible cells in upper and lower airway epithelium. J Infect Dis, 185, 734-43.

MUNKHOLM, M. & MORTENSEN, J. 2014. Mucociliary clearance: pathophysiological aspects. Clin Physiol Funct Imaging, 34, 171-7.

MURPHY, T. F., BRAUER, A. L., AEBI, C. & SETHI, S. 2005. Identification of surface antigens of Moraxella catarrhalis as targets of human serum antibody responses in chronic obstructive pulmonary disease. Infect Immun, 73, 3471-8.

MURPHY, T. F., BRAUER, A. L., JOHNSON, A., WILDING, G. E., KOSZELAK-ROSENBLUM, M. & MALKOWSKI, M. G. 2017. A Cation-Binding Surface Protein as a Vaccine Antigen To Prevent Moraxella catarrhalis Otitis Media and Infections in Chronic Obstructive Pulmonary Disease. Clin Vaccine Immunol, 24.

MURPHY, T. F., BRAUER, A. L., PETTIGREW, M. M., LAFONTAINE, E. R. & TETTELIN, H. 2019. Persistence of Moraxella catarrhalis in Chronic Obstructive Pulmonary Disease and Regulation of the Hag/MID Adhesin. J Infect Dis, 219, 1448-1455.

NAKAGOME, K., BOCHKOV, Y. A., ASHRAF, S., BROCKMAN-SCHNEIDER, R. A., EVANS, M. D., PASIC, T. R. & GERN, J. E. 2014. Effects of rhinovirus species on viral replication and cytokine production. J Allergy Clin Immunol, 134, 332-41.

NAKAMURA, S., DAVIS, K. M. & WEISER, J. N. 2011. Synergistic stimulation of type I interferons during influenza virus coinfection promotes Streptococcus pneumoniae colonization in mice. J Clin Invest, 121, 3657-65.

NAKASE, I., KOBAYASHI, N. B., TAKATANI-NAKASE, T. & YOSHIDA, T. 2015. Active macropinocytosis induction by stimulation of epidermal growth factor receptor and oncogenic Ras expression potentiates cellular uptake efficacy of exosomes. Sci Rep, 5, 10300.

NEWCOMB, D. C., SAJJAN, U. S., NAGARKAR, D. R., WANG, Q., NANUA, S., ZHOU, Y., MCHENRY, C. L., HENNRICK, K. T., TSAI, W. C., BENTLEY, J. K., LUKACS, N. W., JOHNSTON, S. L. & HERSHENSON, M. B. 2008. Human rhinovirus 1B exposure induces phosphatidylinositol 3-kinase-dependent airway inflammation in mice. Am J Respir Crit Care Med, 177, 1111-21.

N'GUESSAN, P. D., HAARMANN, H., STEINER, T., HEYL, K., SCHREIBER, F., HEINRICH, A. & SLEVOGT, H. 2014. The Moraxella catarrhalis-induced pro-inflammatory immune response is enhanced by the activation of the epidermal growth factor receptor in human pulmonary epithelial cells. Biochem Biophys Res Commun, 450, 1038-44.

NI, L., YANG, S., ZHANG, R., JIN, Z., CHEN, H., CONRAD, J. C. & JIN, F. 2016. Bacteria differently deploy type-IV pili on surfaces to adapt to nutrient availability. NPJ Biofilms Microbiomes, 2, 15029.

NICE Guidelines, National Institute for Health and Care Excellence: Chronic Obstructive Pulmonary disease in over 16s: diagnosis and management [WWW document] available from www.nice.org.uk/ng115 accessed Feb 2019

O'CALLAGHAN, C., CHILVERS, M., HOGG, C., BUSH, A. & LUCAS, J. 2007. Diagnosing primary ciliary dyskinesia. Thorax, 62, 656-7.

OLIVER, B. G., LIM, S., WARK, P., LAZA-STANCA, V., KING, N., BLACK, J. L., BURGESS, J. K., ROTH, M. & JOHNSTON, S. L. 2008. Rhinovirus exposure impairs immune responses to bacterial products in human alveolar macrophages. Thorax, 63, 519-25.

PAPADOPOULOS, N. G., BATES, P. J., BARDIN, P. G., PAPI, A., LEIR, S. H., FRAENKEL, D. J., MEYER, J., LACKIE, P. M., SANDERSON, G., HOLGATE, S. T. & JOHNSTON, S. L. 2000. Rhinoviruses infect the lower airways. J Infect Dis, 181, 1875-84.

PAPI, A., BELLETTATO, C. M., BRACCIONI, F., ROMAGNOLI, M., CASOLARI, P., CARAMORI, G., FABBRI, L. M. & JOHNSTON, S. L. 2006. Infections and airway

inflammation in chronic obstructive pulmonary disease severe exacerbations. Am J Respir Crit Care Med, 173, 1114-21.

PAPI, A. & JOHNSTON, S. L. 1999. Rhinovirus infection induces expression of its own receptor intercellular adhesion molecule 1 (ICAM-1) via increased NF-kappaB-mediated transcription. J Biol Chem, 274, 9707-20.

PARK, H. Y., CHURG, A., WRIGHT, J. L., LI, Y., TAM, S., MAN, S. F., TASHKIN, D., WISE, R. A., CONNETT, J. E. & SIN, D. D. 2013. Club cell protein 16 and disease progression in chronic obstructive pulmonary disease. Am J Respir Crit Care Med, 188, 1413-9.

PARK, K. S., WELLS, J. M., ZORN, A. M., WERT, S. E., LAUBACH, V. E., FERNANDEZ, L. G. & WHITSETT, J. A. 2006. Transdifferentiation of ciliated cells during repair of the respiratory epithelium. Am J Respir Cell Mol Biol, 34, 151-7.

PARKER, D., MARTIN, F. J., SOONG, G., HARFENIST, B. S., AGUILAR, J. L., RATNER, A. J., FITZGERALD, K. A., SCHINDLER, C. & PRINCE, A. 2011. Streptococcus pneumoniae DNA initiates type I interferon signaling in the respiratory tract. MBio, 2, e00016-11.

PARKER, D. & PRINCE, A. 2011. Type I interferon response to extracellular bacteria in the airway epithelium. Trends Immunol, 32, 582-8.

PEARSON, M. M., LAURENCE, C. A., GUINN, S. E. & HANSEN, E. J. 2006. Biofilm formation by Moraxella catarrhalis in vitro: roles of the UspA1 adhesin and the Hag hemagglutinin. Infect Immun, 74, 1588-96.

PENG, D., HONG, W., CHOUDHURY, B. P., CARLSON, R. W. & GU, X. X. 2005. Moraxella catarrhalis bacterium without endotoxin, a potential vaccine candidate. Infect Immun, 73, 7569-77.

PEREZ, A. C. & MURPHY, T. F. 2017. A Moraxella catarrhalis vaccine to protect against otitis media and exacerbations of COPD: An update on current progress and challenges. Hum Vaccin Immunother, 13, 2322-2331.

PEREZ, A. C., PANG, B., KING, L. B., TAN, L., MURRAH, K. A., REIMCHE, J. L., WREN, J. T., RICHARDSON, S. H., GHANDI, U. & SWORDS, W. E. 2014. Residence of Streptococcus pneumoniae and Moraxella catarrhalis within polymicrobial biofilm

promotes antibiotic resistance and bacterial persistence in vivo. Pathog Dis, 70, 280-8.

PEROTIN, J. M., DURY, S., RENOIS, F., DESLEE, G., WOLAK, A., DUVAL, V., DE CHAMPS, C., LEBARGY, F. & ANDREOLETTI, L. 2013. Detection of multiple viral and bacterial infections in acute exacerbation of chronic obstructive pulmonary disease: a pilot prospective study. J Med Virol, 85, 866-73.

PETECCHIA, L., SABATINI, F., VARESIO, L., CAMOIRANO, A., USAI, C., PEZZOLO, A. & ROSSI, G. A. 2009. Bronchial airway epithelial cell damage following exposure to cigarette smoke includes disassembly of tight junction components mediated by the extracellular signal-regulated kinase 1/2 pathway. Chest, 135, 1502-1512.

PETTIGREW, M. M., ALDERSON, M. R., BAKALETZ, L. O., BARENKAMP, S. J., HAKANSSON, A. P., MASON, K. M., NOKSO-KOIVISTO, J., PATEL, J., PELTON, S. I. & MURPHY, T. F. 2017. Panel 6: Vaccines. Otolaryngology–Head and Neck Surgery, 156, S76-S87.

PFEIFER, P., VOSS, M., WONNENBERG, B., HELLBERG, J., SEILER, F., LEPPER, P. M., BISCHOFF, M., LANGER, F., SCHAFERS, H. J., MENGER, M. D., BALS, R. & BEISSWENGER, C. 2013. IL-17C is a mediator of respiratory epithelial innate immune response. Am J Respir Cell Mol Biol, 48, 415-21.

PIATTI, G., AMBROSETTI, U., SANTUS, P. & ALLEGRA, L. 2005. Effects of salmeterol on cilia and mucus in COPD and pneumonia patients. Pharmacol Res, 51, 165-8.

PIERROU, S., BROBERG, P., O'DONNELL, R. A., PAWLOWSKI, K., VIRTALA, R., LINDQVIST, E., RICHTER, A., WILSON, S. J., ANGCO, G., MOLLER, S., BERGSTRAND, H., KOOPMANN, W., WIESLANDER, E., STROMSTEDT, P. E., HOLGATE, S. T., DAVIES, D. E., LUND, J. & DJUKANOVIC, R. 2007. Expression of genes involved in oxidative stress responses in airway epithelial cells of smokers with chronic obstructive pulmonary disease. Am J Respir Crit Care Med, 175, 577-86.

PILETTE, C., GODDING, V., KISS, R., DELOS, M., VERBEKEN, E., DECAESTECKER, C., DE PAEPE, K., VAERMAN, J. P., DECRAMER, M. & SIBILLE, Y. 2001. Reduced epithelial expression of secretory component in small airways

correlates with airflow obstruction in chronic obstructive pulmonary disease. Am J Respir Crit Care Med, 163, 185-94.

PRESCOTT, E., LANGE, P. & VESTBO, J. 1995. Chronic mucus hypersecretion in COPD and death from pulmonary infection. Eur Respir J, 8, 1333-8.

QUINT, J. K., DONALDSON, G. C., GOLDRING, J. J., BAGHAI-RAVARY, R., HURST, J. R. & WEDZICHA, J. A. 2010. Serum IP-10 as a biomarker of human rhinovirus infection at exacerbation of COPD. Chest, 137, 812-22.

RACKLEY, C. R. & STRIPP, B. R. 2012. Building and maintaining the epithelium of the lung. J Clin Invest, 122, 2724-30.

RAHMAN, I. & ADCOCK, I. M. 2006. Oxidative stress and redox regulation of lung inflammation in COPD. Eur Respir J, 28, 219-42.

RAMIREZ-CARROZZI, V., SAMBANDAM, A., LUIS, E., LIN, Z., JEET, S., LESCH, J., HACKNEY, J., KIM, J., ZHOU, M., LAI, J., MODRUSAN, Z., SAI, T., LEE, W., XU, M., CAPLAZI, P., DIEHL, L., DE VOSS, J., BALAZS, M., GONZALEZ, L., JR., SINGH, H., OUYANG, W. & PAPPU, R. 2011. IL-17C regulates the innate immune function of epithelial cells in an autocrine manner. Nat Immunol, 12, 1159-66.

RATLEDGE, C. & DOVER, L. G. 2000. Iron metabolism in pathogenic bacteria. Annu Rev Microbiol, 54, 881-941.

ROBINSON, K. M., MCHUGH, K. J., MANDALAPU, S., CLAY, M. E., LEE, B., SCHELLER, E. V., ENELOW, R. I., CHAN, Y. R., KOLLS, J. K. & ALCORN, J. F. 2014. Influenza A virus exacerbates Staphylococcus aureus pneumonia in mice by attenuating antimicrobial peptide production. J Infect Dis, 209, 865-75.

ROCK, J. R., GAO, X., XUE, Y., RANDELL, S. H., KONG, Y. Y. & HOGAN, B. L. 2011. Notch-dependent differentiation of adult airway basal stem cells. Cell Stem Cell, 8, 639-48.

ROGERS, D. F. 2003. The airway goblet cell. Int J Biochem Cell Biol, 35, 1-6.

ROGERS, D. F. 2005. Mucociliary dysfunction in COPD: effect of current pharmacotherapeutic options. Pulm Pharmacol Ther, 18, 1-8.

ROGERS, D. F. 2007. Physiology of airway mucus secretion and pathophysiology of hypersecretion. Respir Care, 52, 1134-46; discussion 1146-9.

ROHDE, G., BORG, I., WIETHEGE, A., KAUTH, M., JERZINOWSKI, S., AN DUONG DINH, T., BAUER, T. T., BUFE, A. & SCHULTZE-WERNINGHAUS, G. 2008. Inflammatory response in acute viral exacerbations of COPD. Infection, 36, 427-33.

ROHDE, G., WIETHEGE, A., BORG, I., KAUTH, M., BAUER, T. T., GILLISSEN, A., BUFE, A. & SCHULTZE-WERNINGHAUS, G. 2003. Respiratory viruses in exacerbations of chronic obstructive pulmonary disease requiring hospitalisation: a case-control study. Thorax, 58, 37-42.

ROSSEAU, S., WIECHMANN, K., MODERER, S., SELHORST, J., MAYER, K., KRULL, M., HOCKE, A., SLEVOGT, H., SEEGER, W., SUTTORP, N., SEYBOLD, J. & LOHMEYER, J. 2005. Moraxella catarrhalis--infected alveolar epithelium induced monocyte recruitment and oxidative burst. Am J Respir Cell Mol Biol, 32, 157-66.

ROTBART, H. A. 2000. Antiviral therapy for enteroviruses and rhinoviruses. Antivir Chem Chemother, 11, 261-71.

ROULIN, P. S., LOTZERICH, M., TORTA, F., TANNER, L. B., VAN KUPPEVELD, F. J., WENK, M. R. & GREBER, U. F. 2014. Rhinovirus uses a phosphatidylinositol 4-phosphate/cholesterol counter-current for the formation of replication compartments at the ER-Golgi interface. Cell Host Microbe, 16, 677-90.

SAETTA, M., DI STEFANO, A., TURATO, G., FACCHINI, F. M., CORBINO, L., MAPP, C. E., MAESTRELLI, P., CIACCIA, A. & FABBRI, L. M. 1998. CD8+ T-lymphocytes in peripheral airways of smokers with chronic obstructive pulmonary disease. Am J Respir Crit Care Med, 157, 822-6.

SAETTA, M., MARIANI, M., PANINA-BORDIGNON, P., TURATO, G., BUONSANTI, C., BARALDO, S., BELLETTATO, C. M., PAPI, A., CORBETTA, L., ZUIN, R., SINIGAGLIA, F. & FABBRI, L. M. 2002. Increased Expression of the Chemokine Receptor CXCR3 and Its Ligand CXCL10 in Peripheral Airways of Smokers with Chronic Obstructive Pulmonary Disease. American Journal of Respiratory and Critical Care Medicine, 165, 1404-1409.

SAHA, S. & BRIGHTLING, C. E. 2006. Eosinophilic airway inflammation in COPD. Int J Chron Obstruct Pulmon Dis, 1, 39-47.

SAJJAN, U., WANG, Q., ZHAO, Y., GRUENERT, D. C. & HERSHENSON, M. B. 2008. Rhinovirus disrupts the barrier function of polarized airway epithelial cells. Am J Respir Crit Care Med, 178, 1271-81.

SAMUEL, C. E. 2001. Antiviral actions of interferons. Clin Microbiol Rev, 14, 778-809, table of contents.

SAPEY, E., STOCKLEY, J. A., GREENWOOD, H., AHMAD, A., BAYLEY, D., LORD, J. M., INSALL, R. H. & STOCKLEY, R. A. 2011. Behavioral and structural differences in migrating peripheral neutrophils from patients with chronic obstructive pulmonary disease. Am J Respir Crit Care Med, 183, 1176-86.

SCHAIRER, D. O., CHOUAKE, J. S., NOSANCHUK, J. D. & FRIEDMAN, A. J. 2012. The potential of nitric oxide releasing therapies as antimicrobial agents. Virulence, 3, 271-9.

SCHAMBERGER, A. C., STAAB-WEIJNITZ, C. A., MISE-RACEK, N. & EICKELBERG, O. 2015. Cigarette smoke alters primary human bronchial epithelial cell differentiation at the air-liquid interface. Sci Rep, 5, 8163.

SCHMITTER, T., AGERER, F., PETERSON, L., MUNZNER, P. & HAUCK, C. R. 2004. Granulocyte CEACAM3 is a phagocytic receptor of the innate immune system that mediates recognition and elimination of human-specific pathogens. J Exp Med, 199, 35-46.

SCHNEIDER, H., ADAMS, O., WEISS, C., MERZ, U., SCHROTEN, H. & TENENBAUM, T. 2013. Clinical characteristics of children with viral single- and co-infections and a petechial rash. Pediatr Infect Dis J, 32, e186-91.

SCHNEIDER, D., GANESAN, S., COMSTOCK, A. T., MELDRUM, C. A., MAHIDHARA, R., GOLDSMITH, A. M., CURTIS, J. L., MARTINEZ, F. J., HERSHENSON, M. B. & SAJJAN, U. 2010. Increased cytokine response of rhinovirus-infected airway epithelial cells in chronic obstructive pulmonary disease. Am J Respir Crit Care Med, 182, 332-40.

SEEMUNGAL, T., HARPER-OWEN, R., BHOWMIK, A., MORIC, I., SANDERSON, G., MESSAGE, S., MACCALLUM, P., MEADE, T. W., JEFFRIES, D. J., JOHNSTON, S. L. & WEDZICHA, J. A. 2001. Respiratory viruses, symptoms, and inflammatory markers in acute exacerbations and stable chronic obstructive pulmonary disease. Am J Respir Crit Care Med, 164, 1618-23.

SEEMUNGAL, T. A., HARPER-OWEN, R., BHOWMIK, A., JEFFRIES, D. J. & WEDZICHA, J. A. 2000. Detection of rhinovirus in induced sputum at exacerbation of chronic obstructive pulmonary disease. Eur Respir J, 16, 677-83.

SEEMUNGAL, T. A., HURST, J. R. & WEDZICHA, J. A. 2009. Exacerbation rate, health status and mortality in COPD--a review of potential interventions. Int J Chron Obstruct Pulmon Dis, 4, 203-23.

SETHI, S. 2010. Infection as a comorbidity of COPD. Eur Respir J, 35, 1209-15.

SETHI, S. & MURPHY, T. F. 2008. Infection in the pathogenesis and course of chronic obstructive pulmonary disease. N Engl J Med, 359, 2355-65.

SETHI, S. & MURPHY, T. F. 2008. Infection in the pathogenesis and course of chronic obstructive pulmonary disease. N Engl J Med, 359, 2355-65.

SETHI, S., SETHI, R., ESCHBERGER, K., LOBBINS, P., CAI, X., GRANT, B. J. & MURPHY, T. F. 2007. Airway bacterial concentrations and exacerbations of chronic obstructive pulmonary disease. Am J Respir Crit Care Med, 176, 356-61.

SHAHANGIAN, A., CHOW, E. K., TIAN, X., KANG, J. R., GHAFFARI, A., LIU, S. Y., BELPERIO, J. A., CHENG, G. & DENG, J. C. 2009. Type I IFNs mediate development of postinfluenza bacterial pneumonia in mice. J Clin Invest, 119, 1910-20.

SHAYKHIEV, R. 2018. Airway Epithelial Progenitors and the Natural History of Chronic Obstructive Pulmonary Disease. Am J Respir Crit Care Med, 197, 847-849.

SHAYKHIEV, R. & CRYSTAL, R. G. 2013. Innate immunity and chronic obstructive pulmonary disease: a mini-review. Gerontology, 59, 481-9.

SHAYKHIEV, R. & CRYSTAL, R. G. 2014. Basal cell origins of smoking-induced airway epithelial disorders. Cell Cycle, 13, 341-2.

SHAYKHIEV, R. & CRYSTAL, R. G. 2014. Early events in the pathogenesis of chronic obstructive pulmonary disease. Smoking-induced reprogramming of airway epithelial basal progenitor cells. Ann Am Thorac Soc, 11 Suppl 5, S252-8.

SHAYKHIEV, R., KRAUSE, A., SALIT, J., STRULOVICI-BAREL, Y., HARVEY, B. G., O'CONNOR, T. P. & CRYSTAL, R. G. 2009. Smoking-dependent reprogramming of alveolar macrophage polarization: implication for pathogenesis of chronic obstructive pulmonary disease. J Immunol, 183, 2867-83.

SHAYKHIEV, R., ZUO, W. L., CHAO, I., FUKUI, T., WITOVER, B., BREKMAN, A. & CRYSTAL, R. G. 2013. EGF shifts human airway basal cell fate toward a smoking-associated airway epithelial phenotype. Proc Natl Acad Sci U S A, 110, 12102-7.

SHIJUBO, N., ITOH, Y., YAMAGUCHI, T., SHIBUYA, Y., MORITA, Y., HIRASAWA, M., OKUTANI, R., KAWAI, T. & ABE, S. 1997. Serum and BAL Clara cell 10 kDa protein (CC10) levels and CC10-positive bronchiolar cells are decreased in smokers. Eur Respir J, 10, 1108-14.

SHIJUBO, N., ITOH, Y., YAMAGUCHI, T., IMADA, A., HIRASAWA, M., YAMADA, T., KAWAI, T. & ABE, S. 1999. Clara cell protein-positive epithelial cells are reduced in small airways of asthmatics. Am J Respir Crit Care Med, 160, 930-3.

SHIMIZU, K., YOSHII, Y., MOROZUMI, M., CHIBA, N., UBUKATA, K., URUGA, H., HANADA, S., SAITO, N., KADOTA, T., ITO, S., WAKUI, H., TAKASAKA, N., MINAGAWA, S., KOJIMA, J., HARA, H., NUMATA, T., KAWAISHI, M., SAITO, K., ARAYA, J., KANEKO, Y., NAKAYAMA, K., KISHI, K. & KUWANO, K. 2015. Pathogens in COPD exacerbations identified by comprehensive real-time PCR plus older methods. Int J Chron Obstruct Pulmon Dis, 10, 2009-16.

SILVERMAN, R. H. 2007. Viral encounters with 2',5'-oligoadenylate synthetase and RNase L during the interferon antiviral response. J Virol, 81, 12720-9.

SIMS, A. C., BARIC, R. S., YOUNT, B., BURKETT, S. E., COLLINS, P. L. & PICKLES, R. J. 2005. Severe acute respiratory syndrome coronavirus infection of human ciliated airway epithelia: role of ciliated cells in viral spread in the conducting airways of the lungs. J Virol, 79, 15511-24.

SLANINA, H., MUNDLEIN, S., HEBLING, S. & SCHUBERT-UNKMEIR, A. 2014. Role of epidermal growth factor receptor signaling in the interaction of Neisseria meningitidis with endothelial cells. Infect Immun, 82, 1243-55.

SLEVOGT, H., SEYBOLD, J., TIWARI, K. N., HOCKE, A. C., JONATAT, C., DIETEL, S., HIPPENSTIEL, S., SINGER, B. B., BACHMANN, S., SUTTORP, N. & OPITZ, B. 2007. Moraxella catarrhalis is internalized in respiratory epithelial cells by a trigger-like mechanism and initiates a TLR2- and partly NOD1-dependent inflammatory immune response. Cell Microbiol, 9, 694-707.

SLEVOGT, H., TIWARI, K. N., SCHMECK, B., HOCKE, A., OPITZ, B., SUTTORP, N. & SEYBOLD, J. 2006. Adhesion of Moraxella catarrhalis to human bronchial epithelium characterized by a novel fluorescence-based assay. Med Microbiol Immunol, 195, 73-83.

SLEVOGT, H., ZABEL, S., OPITZ, B., HOCKE, A., EITEL, J., N'GUESSAN P, D., LUCKA, L., RIESBECK, K., ZIMMERMANN, W., ZWEIGNER, J., TEMMESFELD-WOLLBRUECK, B., SUTTORP, N. & SINGER, B. B. 2008. CEACAM1 inhibits Toll-like receptor 2-triggered antibacterial responses of human pulmonary epithelial cells. Nat Immunol, 9, 1270-8.

SMITH, C. M., DJAKOW, J., FREE, R. C., DJAKOW, P., LONNEN, R., WILLIAMS, G., POHUNEK, P., HIRST, R. A., EASTON, A. J., ANDREW, P. W. & O'CALLAGHAN, C. 2012. ciliaFA: a research tool for automated, high-throughput measurement of ciliary beat frequency using freely available software. Cilia, 1, 14.

SMITH, C. M., KULKARNI, H., RADHAKRISHNAN, P., RUTMAN, A., BANKART, M. J., WILLIAMS, G., HIRST, R. A., EASTON, A. J., ANDREW, P. W. & O'CALLAGHAN, C. 2014. Ciliary dyskinesia is an early feature of respiratory syncytial virus infection. Eur Respir J, 43, 485-96.

SOLEAS, J. P., PAZ, A., MARCUS, P., MCGUIGAN, A. & WADDELL, T. K. 2012. Engineering airway epithelium. J Biomed Biotechnol, 2012, 982971.

SPANIOL, V., HEINIGER, N., TROLLER, R. & AEBI, C. 2008. Outer membrane protein UspA1 and lipooligosaccharide are involved in invasion of human epithelial cells by Moraxella catarrhalis. Microbes Infect, 10, 3-11.

SPICKLER, C., LIPPENS, J., LABERGE, M. K., DESMEULES, S., BELLAVANCE, E., GARNEAU, M., GUO, T., HUCKE, O., LEYSSEN, P., NEYTS, J., VAILLANCOURT, F. H., DECOR, A., O'MEARA, J., FRANTI, M. & GAUTHIER, A. 2013. Phosphatidylinositol 4-kinase III beta is essential for replication of human rhinovirus and its inhibition causes a lethal phenotype in vivo. Antimicrob Agents Chemother, 57, 3358-68.

STANNARD, W. & O'CALLAGHAN, C. 2006. Ciliary function and the role of cilia in clearance. J Aerosol Med, 19, 110-5.

STOKES, C. A. & CONDLIFFE, A. M. 2018. Phosphoinositide 3-kinase delta (PI3Kdelta) in respiratory disease. Biochem Soc Trans, 46, 361-369.

SU, Y. C., SINGH, B. & RIESBECK, K. 2012. Moraxella catarrhalis: from interactions with the host immune system to vaccine development. Future Microbiol, 7, 1073-100.

SUBAUSTE, M. C., JACOBY, D. B., RICHARDS, S. M. & PROUD, D. 1995. Infection of a human respiratory epithelial cell line with rhinovirus. Induction of cytokine release and modulation of susceptibility to infection by cytokine exposure. J Clin Invest, 96, 549-57.

SUN, Y., HAN, M., KIM, C., CALVERT, J. G. & YOO, D. 2012. Interplay between interferon-mediated innate immunity and porcine reproductive and respiratory syndrome virus. Viruses, 4, 424-46.

SYKES, A., EDWARDS, M. R., MACINTYRE, J., DEL ROSARIO, A., BAKHSOLIANI, E., TRUJILLO-TORRALBO, M. B., KON, O. M., MALLIA, P., MCHALE, M. & JOHNSTON, S. L. 2012. Rhinovirus 16-induced IFN-alpha and IFN-beta are deficient in bronchoalveolar lavage cells in asthmatic patients. J Allergy Clin Immunol, 129, 1506-1514 e6.

SYKES, A., EDWARDS, M. R., MACINTYRE, J., DEL ROSARIO, A., GIELEN, V., HAAS, J., KON, O. M., MCHALE, M. & JOHNSTON, S. L. 2013. TLR3, TLR4 and TLRs7-9 Induced Interferons Are Not Impaired in Airway and Blood Cells in Well Controlled Asthma. PLoS One, 8, e65921.

TAKEUCHI, O. & AKIRA, S. 2010. Pattern recognition receptors and inflammation. Cell, 140, 805-20.

TAKEYAMA, K., DABBAGH, K., JEONG SHIM, J., DAO-PICK, T., UEKI, I. F. & NADEL, J. A. 2000. Oxidative stress causes mucin synthesis via transactivation of epidermal growth factor receptor: role of neutrophils. J Immunol, 164, 1546-52.

TALIKKA, M., MARTIN, F., SEWER, A., VUILLAUME, G., LEROY, P., LUETTICH, K., CHAUDHARY, N., PECK, M. J., PEITSCH, M. C. & HOENG, J. 2017. Mechanistic Evaluation of the Impact of Smoking and Chronic Obstructive Pulmonary Disease on the Nasal Epithelium. Clin Med Insights Circ Respir Pulm Med, 11, 1179548417710928.

TAN, K. S., ONG, H. H., YAN, Y., LIU, J., LI, C., ONG, Y. K., THONG, K. T., CHOI, H. W., WANG, D. Y. & CHOW, V. T. 2018. In Vitro Model of Fully Differentiated Human Nasal Epithelial Cells Infected With Rhinovirus Reveals Epithelium-Initiated Immune Responses. J Infect Dis, 217, 906-915.

TASHKIN, D. P. & WECHSLER, M. E. 2018. Role of eosinophils in airway inflammation of chronic obstructive pulmonary disease. Int J Chron Obstruct Pulmon Dis, 13, 335-349.

THOMAS, B., RUTMAN, A., HIRST, R. A., HALDAR, P., WARDLAW, A. J., BANKART, J., BRIGHTLING, C. E. & O'CALLAGHAN, C. 2010. Ciliary dysfunction and ultrastructural abnormalities are features of severe asthma. J Allergy Clin Immunol, 126, 722-729 e2.

TILLEY, A. E., WALTERS, M. S., SHAYKHIEV, R. & CRYSTAL, R. G. 2015. Cilia dysfunction in lung disease. Annu Rev Physiol, 77, 379-406.

TIMPE, J. M., HOLM, M. M., VANLERBERG, S. L., BASRUR, V. & LAFONTAINE, E. R. 2003. Identification of a Moraxella catarrhalis outer membrane protein exhibiting both adhesin and lipolytic activities. Infect Immun, 71, 4341-50.

TOKUDA, E., ITOH, T., HASEGAWA, J., IJUIN, T., TAKEUCHI, Y., IRINO, Y., FUKUMOTO, M. & TAKENAWA, T. 2014. Phosphatidylinositol 4-phosphate in the Golgi apparatus regulates cell-cell adhesion and invasive cell migration in human breast cancer. Cancer Res, 74, 3054-66.

TRAVES, S. L., SMITH, S. J., BARNES, P. J. & DONNELLY, L. E. 2004. Specific CXC but not CC chemokines cause elevated monocyte migration in COPD: a role for CXCR2. J Leukoc Biol, 76, 441-50.

TURNER, J., ROGER, J., FITAU, J., COMBE, D., GIDDINGS, J., HEEKE, G. V. & JONES, C. E. 2011. Goblet cells are derived from a FOXJ1-expressing progenitor in a human airway epithelium. Am J Respir Cell Mol Biol, 44, 276-84.

TURNER, M. D., NEDJAI, B., HURST, T. & PENNINGTON, D. J. 2014. Cytokines and chemokines: At the crossroads of cell signalling and inflammatory disease. Biochim Biophys Acta, 1843, 2563-2582.

TYNER, J. W., KIM, E. Y., IDE, K., PELLETIER, M. R., ROSWIT, W. T., MORTON, J. D., BATTAILE, J. T., PATEL, A. C., PATTERSON, G. A., CASTRO, M., SPOOR, M. S., YOU, Y., BRODY, S. L. & HOLTZMAN, M. J. 2006. Blocking airway mucous cell metaplasia by inhibiting EGFR antiapoptosis and IL-13 transdifferentiation signals. J Clin Invest, 116, 309-21.

UNGER, B. L., FARIS, A. N., GANESAN, S., COMSTOCK, A. T., HERSHENSON, M. B. & SAJJAN, U. S. 2012. Rhinovirus attenuates non-typeable Hemophilus influenzae-stimulated IL-8 responses via TLR2-dependent degradation of IRAK-1. PLoS Pathog, 8, e1002969.

VACHIER, I., VIGNOLA, A. M., CHIAPPARA, G., BRUNO, A., MEZIANE, H., GODARD, P., BOUSQUET, J. & CHANEZ, P. 2004. Inflammatory features of nasal mucosa in smokers with and without COPD. Thorax, 59, 303-7.

VALENCIA-GATTAS, M., CONNER, G. E. & FREGIEN, N. L. 2016. Gefitinib, an EGFR Tyrosine Kinase inhibitor, Prevents Smoke-Mediated Ciliated Airway Epithelial Cell Loss and Promotes Their Recovery. PLoS One, 11, e0160216.

VAN DER ZALM, M. M., WILBRINK, B., VAN EWIJK, B. E., OVERDUIN, P., WOLFS, T. F. & VAN DER ENT, C. K. 2011. Highly frequent infections with human rhinovirus in healthy young children: a longitudinal cohort study. J Clin Virol, 52, 317-20.

VANEECHOUTTE, M., VERSCHRAEGEN, G., CLAEYS, G., WEISE, B. & VAN DEN ABEELE, A. M. 1990. Respiratory tract carrier rates of Moraxella (Branhamella) catarrhalis in adults and children and interpretation of the isolation of M. catarrhalis from sputum. J Clin Microbiol, 28, 2674-80.

VAREILLE, M., KIENINGER, E., EDWARDS, M. R. & REGAMEY, N. 2011. The airway epithelium: soldier in the fight against respiratory viruses. Clin Microbiol Rev, 24, 210-29.

VEDEL-KROGH, S., NIELSEN, S. F., LANGE, P., VESTBO, J. & NORDESTGAARD, B. G. 2016. Blood Eosinophils and Exacerbations in Chronic Obstructive Pulmonary Disease. The Copenhagen General Population Study. Am J Respir Crit Care Med, 193, 965-74.

VERDUIN, C. M., HOL, C., FLEER, A., VAN DIJK, H. & VAN BELKUM, A. 2002. Moraxella catarrhalis: from emerging to established pathogen. Clin Microbiol Rev, 15, 125-44.

VIEIRA BRAGA, F. A., KAR, G., BERG, M., CARPAIJ, O. A., POLANSKI, K., SIMON, L. M., BROUWER, S., GOMES, T., HESSE, L., JIANG, J., FASOULI, E. S., EFREMOVA, M., VENTO-TORMO, R., TALAVERA-LOPEZ, C., JONKER, M. R., AFFLECK, K., PALIT, S., STRZELECKA, P. M., FIRTH, H. V., MAHBUBANI, K. T., CVEJIC, A., MEYER, K. B., SAEB-PARSY, K., LUINGE, M., BRANDSMA, C. A.,

TIMENS, W., ANGELIDIS, I., STRUNZ, M., KOPPELMAN, G. H., VAN OOSTERHOUT, A. J., SCHILLER, H. B., THEIS, F. J., VAN DEN BERGE, M., NAWIJN, M. C. & TEICHMANN, S. A. 2019. A cellular census of human lungs identifies novel cell states in health and in asthma. Nat Med, 25, 1153-1163.

WALKER, E. J., YOUNESSI, P., FULCHER, A. J., MCCUAIG, R., THOMAS, B. J., BARDIN, P. G., JANS, D. A. & GHILDYAL, R. 2013. Rhinovirus 3C protease facilitates specific nucleoporin cleavage and mislocalisation of nuclear proteins in infected host cells. PLoS One, 8, e71316.

WANG, Z., BAFADHEL, M., HALDAR, K., SPIVAK, A., MAYHEW, D., MILLER, B. E., TAL-SINGER, R., JOHNSTON, S. L., RAMSHEH, M. Y., BARER, M. R., BRIGHTLING, C. E. & BROWN, J. R. 2016. Lung microbiome dynamics in COPD exacerbations. Eur Respir J, 47, 1082-92.

WANG, W., KINKEL, T., MARTENS-HABBENA, W., STAHL, D. A., FANG, F. C. & HANSEN, E. J. 2011. The Moraxella catarrhalis nitric oxide reductase is essential for nitric oxide detoxification. J Bacteriol, 193, 2804-13.

WANG, W., REITZER, L., RASKO, D. A., PEARSON, M. M., BLICK, R. J., LAURENCE, C. & HANSEN, E. J. 2007. Metabolic analysis of Moraxella catarrhalis and the effect of selected in vitro growth conditions on global gene expression. Infect Immun, 75, 4959-71.

WANG, Z., SINGH, R., MILLER, B. E., TAL-SINGER, R., VAN HORN, S., TOMSHO, L., MACKAY, A., ALLINSON, J. P., WEBB, A. J., BROOKES, A. J., GEORGE, L. M., BARKER, B., KOLSUM, U., DONNELLY, L. E., BELCHAMBER, K., BARNES, P. J., SINGH, D., BRIGHTLING, C. E., DONALDSON, G. C., WEDZICHA, J. A., BROWN, J. R. & COPDMAP 2018. Sputum microbiome temporal variability and dysbiosis in chronic obstructive pulmonary disease exacerbations: an analysis of the COPDMAP study. Thorax, 73, 331-338.

WEDZICHA, J. A. & DONALDSON, G. C. 2003. Exacerbations of chronic obstructive pulmonary disease. Respir Care, 48, 1204-13; discussion 1213-5.

WEDZICHA, J. A., SEEMUNGAL, T. A., MACCALLUM, P. K., PAUL, E. A., DONALDSON, G. C., BHOWMIK, A., JEFFRIES, D. J. & MEADE, T. W. 2000. Acute exacerbations of chronic obstructive pulmonary disease are accompanied by elevations of plasma fibrinogen and serum IL-6 levels. Thromb Haemost, 84, 210-5.

WEIGENT, D. A., HUFF, T. L., PETERSON, J. W., STANTON, G. J. & BARON, S. 1986. Role of interferon in streptococcal infection in the mouse. Microb Pathog, 1, 399-407.

WEINER, A., MELLOUK, N., LOPEZ-MONTERO, N., CHANG, Y. Y., SOUQUE, C., SCHMITT, C. & ENNINGA, J. 2016. Macropinosomes are Key Players in Early Shigella Invasion and Vacuolar Escape in Epithelial Cells. PLoS Pathog, 12, e1005602.

WILKINSON, T. M., HURST, J. R., PERERA, W. R., WILKS, M., DONALDSON, G. C. & WEDZICHA, J. A. 2006. Effect of interactions between lower airway bacterial and rhinoviral infection in exacerbations of COPD. Chest, 129, 317-24.

WILKINSON, T. M. A., ARIS, E., BOURNE, S., CLARKE, S. C., PEETERS, M., PASCAL, T. G., SCHOONBROODT, S., TUCK, A. C., KIM, V., OSTRIDGE, K., STAPLES, K. J., WILLIAMS, N., WILLIAMS, A., WOOTTON, S., DEVASTER, J. M. & GROUP, A. S. 2017. A prospective, observational cohort study of the seasonal dynamics of airway pathogens in the aetiology of exacerbations in COPD. Thorax, 72, 919-927.

WINKLER, D. G., FAIA, K. L., DINITTO, J. P., ALI, J. A., WHITE, K. F., BROPHY, E. E., PINK, M. M., PROCTOR, J. L., LUSSIER, J., MARTIN, C. M., HOYT, J. G., TILLOTSON, B., MURPHY, E. L., LIM, A. R., THOMAS, B. D., MACDOUGALL, J. R., REN, P., LIU, Y., LI, L. S., JESSEN, K. A., FRITZ, C. C., DUNBAR, J. L., PORTER, J. R., ROMMEL, C., PALOMBELLA, V. J., CHANGELIAN, P. S. & KUTOK, J. L. 2013. PI3K-delta and PI3K-gamma inhibition by IPI-145 abrogates immune responses and suppresses activity in autoimmune and inflammatory disease models. Chem Biol, 20, 1364-74.

WINTHER, B. 2011. Rhinovirus infections in the upper airway. Proc Am Thorac Soc, 8, 79-89.

WINTHER, B., GREVE, J. M., GWALTNEY, J. M., JR., INNES, D. J., EASTHAM, J. R., MCCLELLAND, A. & HENDLEY, J. O. 1997. Surface expression of intercellular adhesion molecule 1 on epithelial cells in the human adenoid. J Infect Dis, 176, 523-5.

WINTHER, B., GWALTNEY, J. M. & HENDLEY, J. O. 1990. Respiratory virus infection of monolayer cultures of human nasal epithelial cells. Am Rev Respir Dis, 141, 839-45.

WONG, A. P., KEATING, A. & WADDELL, T. K. 2009. Airway regeneration: the role of the Clara cell secretory protein and the cells that express it. Cytotherapy, 11, 676-87.

World Health Organisation 2016, Chronic Obstructive Pulmonary Disease [WWW document] available from https://www.who.int/respiratory/copd/en/ accessed February 2019

XIE, H. & GU, X. X. 2008. Moraxella catarrhalis lipooligosaccharide selectively upregulates ICAM-1 expression on human monocytes and stimulates adjacent naive monocytes to produce TNF-alpha through cellular cross-talk. Cell Microbiol, 10, 1453-67.

YAGHI, A., ZAMAN, A., COX, G. & DOLOVICH, M. B. 2012. Ciliary beating is depressed in nasal cilia from chronic obstructive pulmonary disease subjects. Respir Med, 106, 1139-47.

YANG, M., JOHNSON, A. & MURPHY, T. F. 2011. Characterization and evaluation of the Moraxella catarrhalis oligopeptide permease A as a mucosal vaccine antigen. Infect Immun, 79, 846-57.

ZHANG, J., ZHAN, Z., WU, J., ZHANG, C., YANG, Y., TONG, S., WANG, R., YANG, X., DONG, W. & CHEN, Y. 2013. Relationship between EGF, TGFA, and EGFR Gene Polymorphisms and Traditional Chinese Medicine ZHENG in Gastric Cancer. Evid Based Complement Alternat Med, 2013, 731071.

ZHANG, L., COLLINS, P. L., LAMB, R. A. & PICKLES, R. J. 2011. Comparison of differing cytopathic effects in human airway epithelium of parainfluenza virus 5 (W3A), parainfluenza virus type 3, and respiratory syncytial virus. Virology, 421, 67-77.

ZHANG, X., SEBASTIANI, P., LIU, G., SCHEMBRI, F., ZHANG, X., DUMAS, Y. M., LANGER, E. M., ALEKSEYEV, Y., O'CONNOR, G. T., BROOKS, D. R., LENBURG, M. E. & SPIRA, A. 2010. Similarities and differences between smoking-related gene expression in nasal and bronchial epithelium. Physiol Genomics, 41, 1-8.

Appendix 1

Supplementary Table 1: Details of patients who participated in the current studies

Patient ID	Age	Sex	Current Smoker	Pack years	FEV_1 actual	FEV_1 %	FVC	FVC %	FEV1/FVC	COPD	Exacerbations per years	Allergies/ Hay fever	Asthma
COPD donors													
(1) (36)	57	F	No	39	1.25	49	3.76	118	0.33	Yes	>2	Yes	Yes
(2) (65)	71	F	Yes	30+	1.42	66	2.13	88	0.66	Yes	>2	Yes	Yes
(3) (167)	78	M	yes	52	1.9	22	2.6	64	0.73	Yes	>2	No	No
(4) (168)	76	F	No	20	1.36	40	2.6	70	0.52	Yes	>2	No	No
(5) (171)	77	F	No	50	0.81	45	1.76	81	0.46	Yes	>2	No	No
(6) (172)	69	M	yes	75	0.72	23	1.74	42	0.41	Yes	>2	No	No
(7) (12)	74	M	Yes	30	1.2	52	2.97	97	0.4	Yes	>2	No	No
(8) (190)	81	M	Yes	75						Yes	>2	No	No
(9) (202)	75	M	No	80	1.9	75	3.3	92	0.58	Yes	>2	No	No
(10) (230)	61	M	No	90	1.25	40	2.54	63	0.49	Yes	>2	No	No
(11) (231)	75	F	No	60	0.87	46	1.48	65	0.59	Yes	>2	No	No
(12) (13N)	71	M	No	40	0.99	37	2.77	80	0.35	Yes	1	Yes	Yes
(13) (165N)	68	M	No	44	0.66	24	1.35		0.48	Yes	>2		No
Healthy donors													
(14) (139)	54	M	No							No		Rodents allergy	No
(15) (156)	59	M	No							No		No	No
(16) (161)	56	F	No							No		No	No
(17) (194)	69	F	No							No		No	No
(18) (140)	60	M	No							No		No	No
(19) (141)	57	F	No							No		No	No

(20) (145)	54	F	No							No			
(21) (204)	69	F	No							No		No	No
(22) (240)	54	F	No							No		Yes	No
(23) (160)	64	F	No							No		No	No
(24) (200)	62	F	No							No		No	No
(25) (220)	>50	M	No							No		No	No
(26) (221)	49	M	No							No		No	No
(27) (224)	45	F	No							No		No	No

In the *M. catarrhalis* interaction with the ciliated epithelium study were included the following donors:

Healthy donors: ID156N, ID194N, ID224N, ID161N, ID240N, ID160N, ID200N, ID140N, ID141N, ID145N, ID139N, ID220N, ID221N

COPD donors: ID168N, ID167N, ID171N, ID231N, ID230N, ID202N, ID36N, ID13N, ID65N, ID190N

In the rhinovirus interaction with the ciliated epithelium study were included the following donors:

Healthy donors: ID156N, ID194N, ID161N, ID240N, ID160N, ID200N, ID140N, ID141N, ID145N, ID139N, ID220N, ID221N

COPD donors: ID168N, ID167N, ID171N, ID231N, ID230N, ID202N, ID36N, ID13N, ID65N, ID190N, ID12N

In the rhinovirus and *M. catarrhalis* co-infection of the ciliated epithelium study were included the following donors:

Healthy donors: ID156N, ID194N, ID161N, ID240N, ID160N, ID200N, ID139N, ID204N, ID220N, ID221N, ID224N

COPD donors: ID168N, ID167N, ID171N, ID231N, ID230N, ID202N, ID36N, ID165N, ID190N

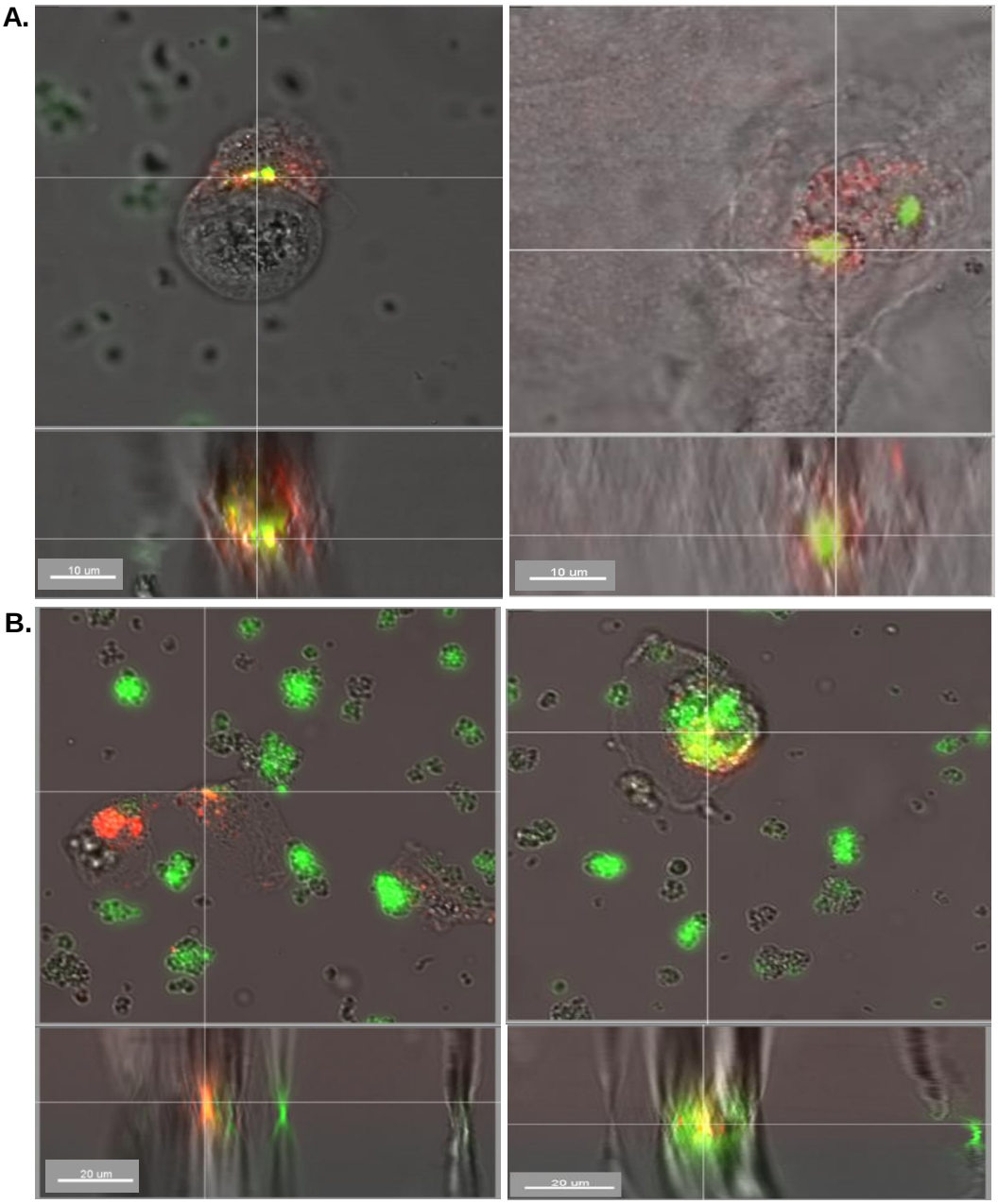

Supplementary Figure 1: Representative live confocal images of internalised *M. catarrhalis* in healthy (A) and COPD (B) epithelial basal cells labelled with dextran

Epithelial basal cells were seeded onto 24 well plastic plates at $1x10^5$ cells/ well and grown until 90% confluency in F-media. *M. catarrhalis* was labelled with Cell Trace™ CFSE 488nm and added to basal cells at $5x10^6$ cfu/ well, dextran red A647 dye MW 10,000 was also added to epithelial cells and incubated for 24h at 37^0C with 5%CO_2. At 24h epithelial cells were scraped and transferred to glass bottom dishes and imaged by live confocal imaging. Co-localisation of green *M. catarrhalis* with red dextran dye was visualised in yellow. (A) scale bars = 10μm, (B) scale bars = 20μm.

A.

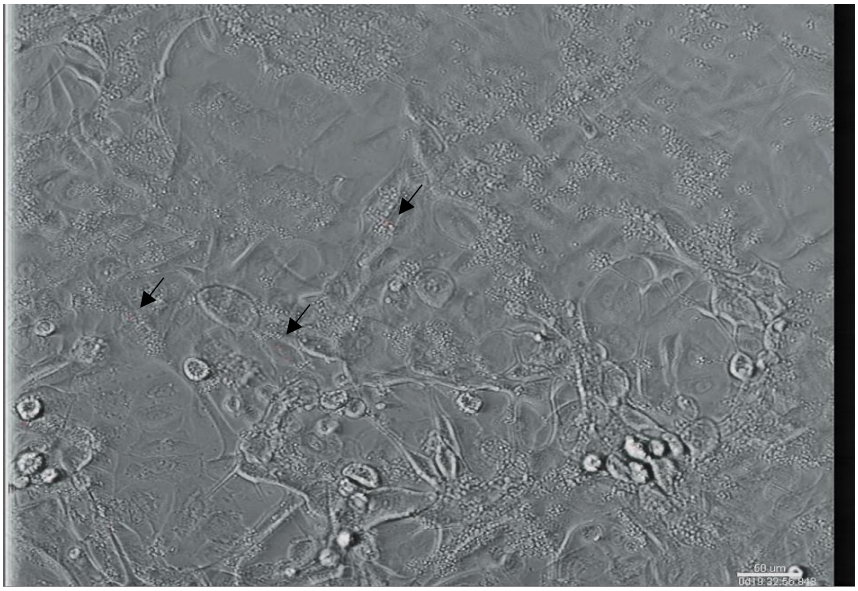

B.

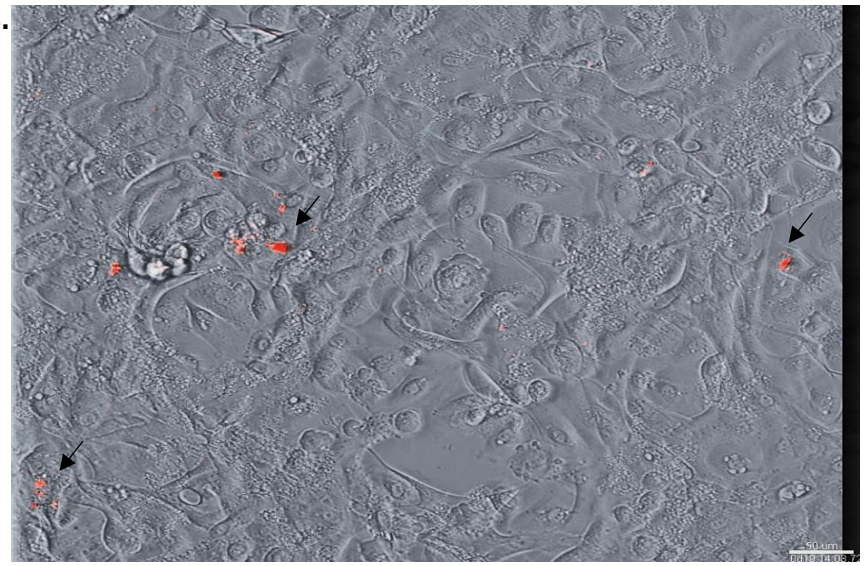

Supplementary Figure 2: Screenshots of time-lapses: *M. catarrhalis* uptake in COPD basal cells at 19h.

Time-lapses are available in Appendix 5 videos 3 & 4, provided on an external drive. Epithelial basal cells were seeded at 1x10^5cells/well concentration in F-media onto 8 well-glass chambers and grown until confluency. Epithelial basal cells were infected with pHrodo™ red labelled *M. catarrhalis* for 20h and imaged every 10min by time-lapse imaging A) No EGF stimulation prior *M. catarrhalis* infection showing little bacterial internalisation; B) stimulation with 100ng/ml EGF for 1h before *M. catarrhalis* infection showing greater bacterial internalisation, scale bars = 50μm.

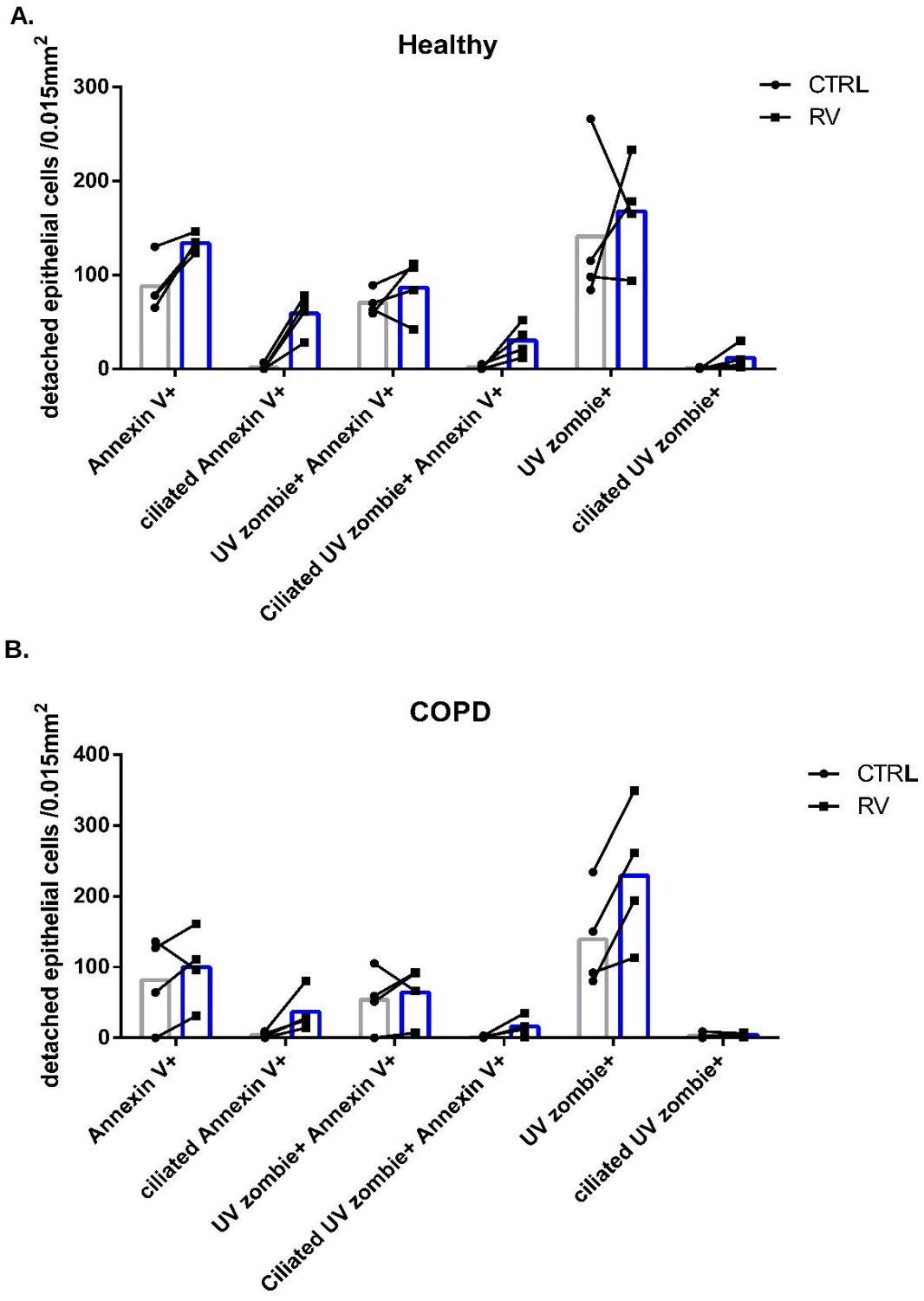

Supplementary Figure 3: Epithelial cells detached from healthy and COPD epithelium infected with rhinovirus for 24h.

A) Number of detached epithelial cells in healthy apical secretions positive for Annexin V, UV zombie dye or Annexin V and UV zombie dye post rhinovirus infection counted per 0.015mm^2 field from 25 random images of each apical secretion; B) Number of

detached epithelial cells in COPD apical secretions positive for Annexin V, UV zombie dye or Annexin V and UV zombie dye post rhinovirus infection counted per 0.015mm^2 field from 25 random images of each apical secretion. Apoptotic cells were indicated by green Annexin V marker, late apoptotic cells were indicated by green Annexin V and blue UV zombie markers, necrotic/ dead cells were indicated by blue UV zombie.

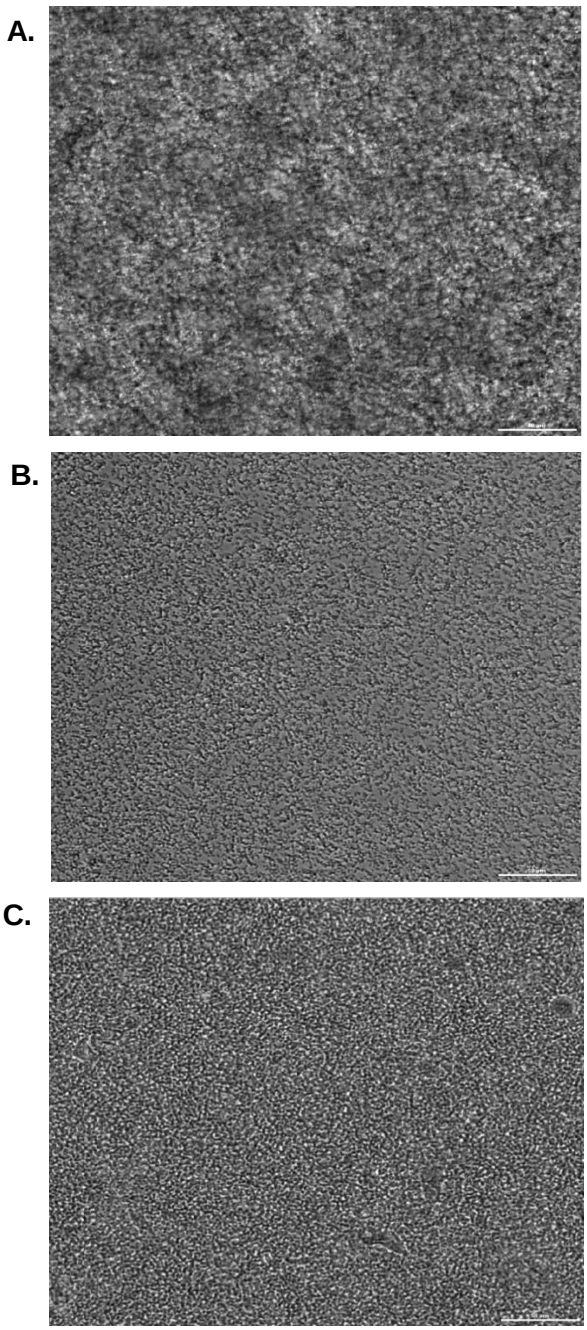

Supplementary Figure 5: **Representative screenshots of *M. catarrhalis* biofilm formation at 24h following treatment with apical fluids imaged every 20min by time-lapse imaging.**

A) *M. catarrhalis* biofilm formation following treatment with plain BEBM media showing dense biofilm formation at 24h, B) *M. catarrhalis* biofilm formation showing marked reduction in biofilm following treatment with apical fluid from a healthy culture (C) *M. catarrhalis* biofilm formation showing reduction in biofilm following treatment with apical fluid from a COPD culture, scale bars = 50μm.

Appendix 2

Data variability of manual CBF and ciliary amplitude measurement

To calculate reproducibility of manual CBF and ciliary beat amplitude measurements, the beat frequency and amplitude of cilia on 20 ciliated cells were measured and compared between 3 assessors, including myself.

Ciliary beat amplitude

The average measurements of beat amplitude obtained from each video by the three assessors were compared and no evidence of difference was found between the assessors with p=0.331. This observation suggested that neither assessor gave higher or lower measurements than the others. The deviation of the average measurements' normal distribution for each video was calculated to be 0.599 and the assessors' variability for amplitude was calculated to lie within 2*0.599 units around their video-specific average.

Ciliary beat frequency

The difference of average CBF measurements was compared between two assessors, including myself (designated as Assessor 2), and the automated software CiliaFa. It was found that the mean measurements of CBF are significantly different between at least two of the assessors determined by p=0.001. The differences of average CBF measurements between assessors are shown in Supplementary Figure 1.

Comparison	Difference in CBF	p-value
Assessor 1 - Software	1.179	0.006
Assessor 2 - Software	-0.225	0.775
Assessor 2 – Assessor 1	-1.403	0.001

Supplementary Figure 1: Average CBF measurements difference between assessors

The results suggested that Assessor 1 was giving significantly higher measurements of CBF than both the software and Assessor 2. No difference was found between Assessor 2 and Software measurements.

The deviation of the average measurements' normal distribution of amplitude for each video was calculated to be 1.025. The variability between Assessor 1 and Assessor 2 was estimates as 1.84 units.

Intra – variability of CBF measurements

To calculate the reproducibility of manual CBF measurements, the beat frequency of 20 ciliated cells from 10 high speed videos (2 ciliated cells/ video) was measured in 3 different days and the obtained results were compared. The standard deviation reported for intra-video, inter-day variability was 1.42 and for intra-video, intra-day variability was 0.52.

Quality control assessment of ALI cultures post 28 days of ciliation

Title of experiment for which this donor is to be used:

Date of experiment:

Donor number and nasal/bronchial										
Passage number										
Co-culture or BEGM										
Disease (healthy/COPD/PCD etc)										
Number of wells in the batch										
Date of seeding										
Date of ALI										
Ciliation Score										
0	No moving cilia observed									
1	A few individual ciliated cells scattered around the transwell (1-20 ciliated cells/well)									
2	Several ciliated cells in small groups but not forming extensive patches.									
3	Extensive patches of cilia (usually around edges). Cilia are usually absent in the centre of the transwell.									
4	A lawn of cilia all around the edges of the transwell. Cilia usually sparse in the middle of the transwell.									
5	Fully ciliated on edges and in the middle. A continuous lawn of cilia covering the entire surface of the transwell.									
Well number	**I**	**II**	**III**	**IV**	**V**	**VI**	**VII**	**VIII**	**IX**	**X**
Ciliation Score										
TEER reading										
Mucus/liquid score										
0=”dry” 1= some liquid/mucus 2= flooded										
Other observations (mucus density, sticky mucus leakage, holes in the epithelium)										

Appendix 3

Preliminary studies

1. Adherence of *M. catarrhalis* to basal epithelial cells to determine bacterial concentration for studies

To determine the optimum concentration of bacteria for single *M. catarrhalis* infections, primary BMI-1 basal epithelial cells were seeded onto collagen coated 8-well glass slide chambers at a density of $5x10^4$ cells/well. Epithelial cells were cultured in basal airway epithelial cell media supplemented with SingleQuots (BEGM, Lonza, UK) for 3-4 days at 37^0C with 5% CO_2 until cells reached 80-90% confluency. Prior infection, epithelial cells were washed with plain BEBM media 2-3 times to remove cell debris. *M. catarrhalis* stock vial was labelled with 10μM CFSE cell tracker dye (Cell Trace, UK) for 30min at 37^0C with 5% CO_2 with gentle agitation. The stained bacteria were washed 3 times with plain BEBM and resuspended in 1ml BEBM. Bacteria were diluted to $2.5x10^6$ CFU/ml and $2.5x10^7$ CFU/ml and epithelial cells were inoculated with $5x10^5$ CFU/well or $5x10^6$ CFU/well in 200μl BEBM plain media. Epithelial cells monolayers infected with *M. catarrhalis* were fixed with 4% PFA for 20min at room temperature at various time-points. To visualise epithelial cells nuclei were stained with Hoechst solution for 30min at room temperature with constant shaking, protected from light. Epithelial cells were washed with PBS, mounted with n-propyl gelate and sealed with cover slips to image on a Nikon TiE fluorescent microscope. Formation of multicellular bacterial structures on the surface of epithelial cells was observed at 4h, 6h and 8h post infection with $5x10^6$ CFU/well *M. catarrhalis.* In contrast, aggregation of bacteria was not observed at 4h or 6h post infection with $5x10^5$ CFU/well. Bacterial aggregation is thought to be a key factor for biofilm formation (De Vries et al., 2009). In addition, interaction with host epithelial cells and formation of aggregates is considered as a feature for pathogenic bacteria, seen *in vivo* (Hall-Stoodley et al., 2006; Heiniger et al., 2007). Aggregation is an important virulence factor for bacteria to colonise the host epithelium and later to become intracellular (Verduin et al., 2002; De Vries et al., 2009). Therefore, to more closely mimic an *in vivo* interaction with host epithelium, a concentration of $5x10^6$ CFU/well *M. catarrhalis* was chosen for all bacterial experiments throughout this project.

A) 5x10^5 CFU/well

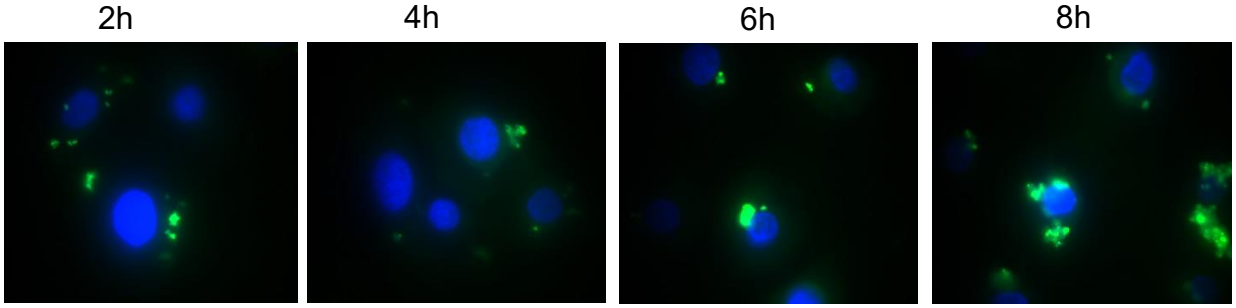

B) 5x10^6 CFU/well

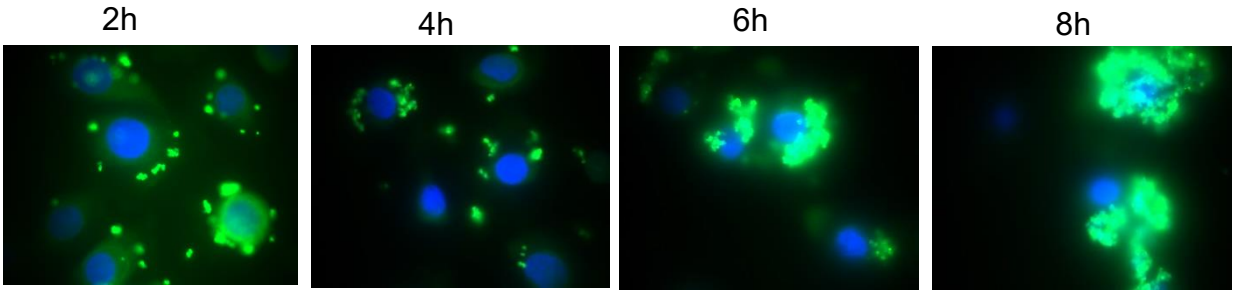

C) Ctrl

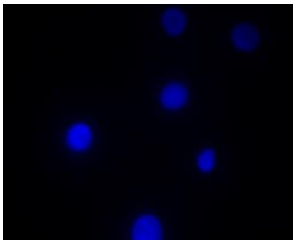

Supplementary Figure 1: Representative immunofluorescent images of adhered *M. catarrhalis* to BMI-1 epithelial basal cells.

A) Infection with 5x10^5 CFU/well *M. catarrhalis*; B) Infection with 5x10^6 CFU/well *M. catarrhalis*; C) Non-infected control epithelial cells. Epithelial basal cells were seeded at 5x10^4 cells/ well in an 8 well glass chamber for 3-4 days in BEGM media at 37^{0}C with 5% CO_2. Confluent epithelial monolayers were infected with different concentrations of *M. catarrhalis* and infection was stopped at 2h, 4h, 6h and 8h post addition of bacteria. *M. catarrhalis* was labelled with Cell Trace™ CFSE 488nm and epithelial cells nuclei with Hoechst solution DAPI 405nm. Infected cells were fixed at various time-points and imaged at 100x objective using a Nikon TiE microscope.

2. Rhinovirus infection of epithelial cells to determine viral concentration for studies

In preparation for the main single rhinovirus infection studies, a stock of rhinovirus 16 was tested on Hela cells. Hela H1 cells were seeded in 96 well flat bottom plates at concentration of $1.5x10^4$ cells/well in 150μl volume of DMEM media supplemented with 2% FCS and 1% Penicillin/Streptomycin. Epithelial cells were cultured at 37^0C with 5%CO_2 for 2 days until they become 80-90% confluent. 10 fold serial dilutions of the rhinovirus stock were prepared to infect three replicate wells of Hela cells with 50μl of each dilution. Control wells of Hela cells with media (no RV) were included for each 96 well plate. Rhinovirus was allowed to attach to epithelial cells for 1h at 37^0C with 5%CO_2 and was then replaced with DMEM media supplemented with 2% FCS and 1% Penicillin/Streptomycin. Infection of epithelial cells was carried out for 24h, when epithelial cells were fixed with 4% PFA for 30min at room temperature. Epithelial cells were permeabilised with 0.1% Triton X for 20min and non-specific binding was blocked by 3% BSA. Rhinovirus infected cells were labelled with anti-VP2 antibody and epithelial cells nuclei with Hoechst solution. Images of rhinovirus infected cells were acquired by a Nikon TiE fluorescent microscope. Infection level was determined according to positive anti-VP2 antibody staining. Compared to control non-infected cells and the lower range of rhinovirus concentrations used, titres of 10^4 $TCID_{50}$/ml, 10^5 $TCID_{50}$/ml, 10^6 $TCID_{50}$/ml, 10^7 $TCID_{50}$/ml indicated infection of epithelial cells (Supplementary Figure 2). The optimal effective concentration for infection with rhinovirus was determined to be 10^6 $TCID_{50}$/ml as a good proportion of rhinovirus positive cells was observed throughout the wells (Supplementary Figure 2 B). For all subsequent experiments with rhinovirus 16 therefore was used 10^6 $TCID_{50}$/ml.

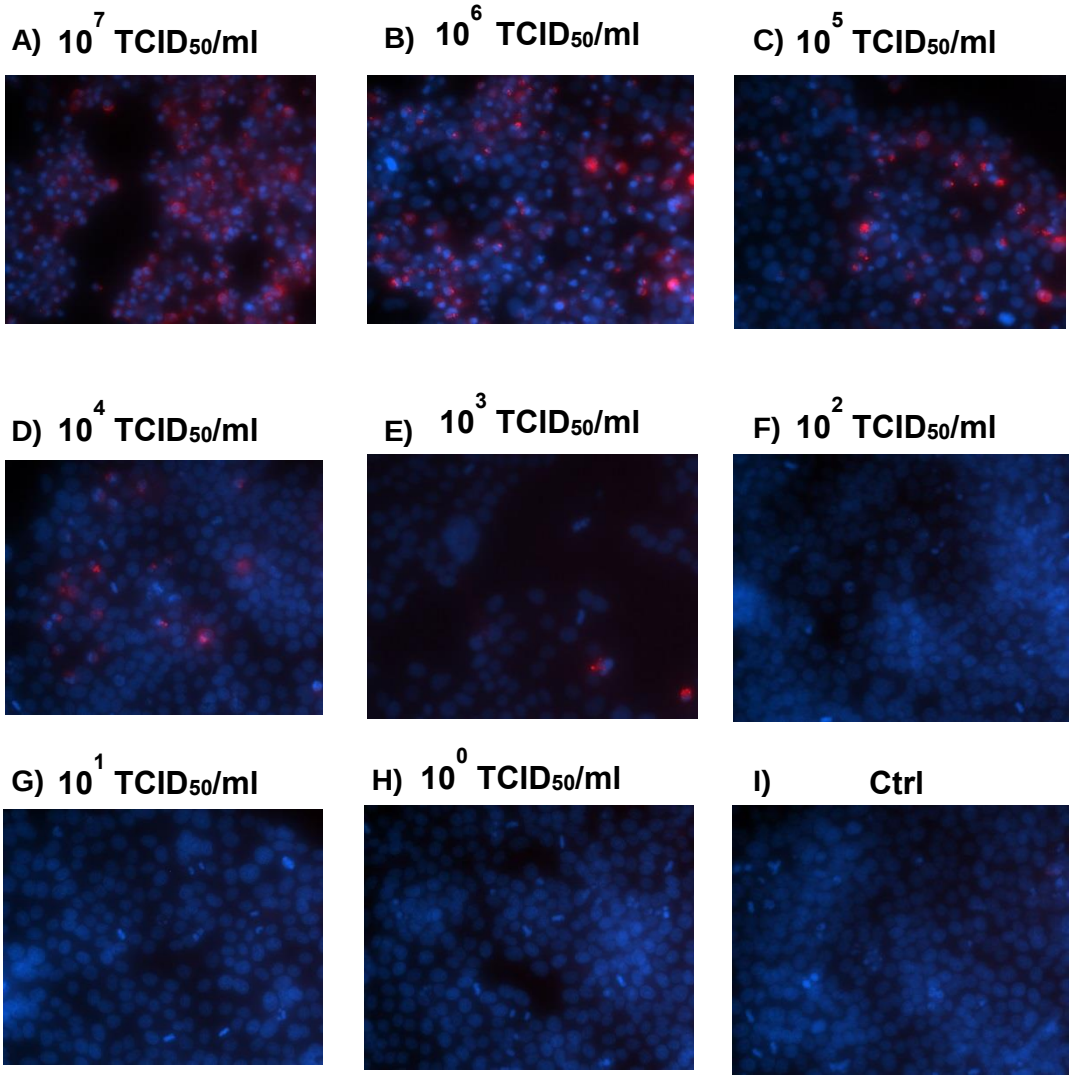

Supplementary Figure 2: Representative immunofluorescent images of infected with rhinovirus 16 Hela epithelial cells.

A) Infection with 10^7 $TCID_{50}$/ml; B) Infection with 10^6 $TCID_{50}$/ml; C) Infection with 10^5 $TCID_{50}$/ml; D) Infection with 10^4 $TCID_{50}$/ml; E) Infection with 10^3 $TCID_{50}$/ml; F) Infection with 10^2 $TCID_{50}$/ml, G) Infection with 10^1 $TCID_{50}$/ml; H) Infection with 10^0 $TCID_{50}$/ml; I) Non-infected control epithelial cells. Hela H1 cells were cultured in 96 well flat bottom plates at $1.5x10^4$ cells/ well density. Once the epithelial cells reached 80-90% confluency, Hela cells were infected with different concentrations of rhinovirus 16 for 24h. Epithelial cells were fixed with 4% PFA, permeabilised with 0.1% Triton X and blocked with 3% BSA. Rhinovirus was stained by anti-VP2 antibody 535nm TRITC and cells nuclei with Hoechst solution 405nm DAPI.

3. Inhibition of EGFR phosphorylation by Gefitinib

To determine the optimum concentration of Gefitinib to inhibit EGFR phosphorylation, primary nasal epithelial cells from 2 COPD donors were differentiated at air-fluid interface for 4 weeks at 37^0C with 5% CO_2 in a humidified incubator. Ciliated cultures were pre-treated with 0.1μM or 1μM Gefitinib or vehicle control (DMSO) basolaterally for 1h. Epithelial cultures were then treated apically with 100nM of recombinant EGF protein (Sigma-Aldrich, UK) for 1h. Epithelial cultures were further incubated for 24h at 37^0C with 5% CO_2 in a humidified incubator. Human primary epithelial cells were harvested by scraping. Protein samples were prepared by lysing for 1h on ice with RIPA buffer (Merck, UK) containing 1% (v/v) cocktail of protease inhibitors (Sigma – Aldrich, UK) and 1% (v/v) phosphatase cocktails inhibitors 2 and 3 (Sigma-Aldrich, UK). Samples were sonicated for 5min with intervals for cooling and then spun down at 10,500 x *g* for 5min to pellet cell debris. Protein amount was determined by using colorimetric BCA assay (Pierce, ThermoFisher, UK) as described in section 2.7.1. For protein separations 8μg of samples were mixed with 5x laemmli buffer containing DTT (Sigma-Aldrich, UK) and boiled for 10min at 95^0C. 10μl of sample/per lane were loaded per well onto 12% polyacrylamide SDS gels (Bio-Rad, UK). SDS-PAGE was carried out in a Mini PROTEAN system (Bio-Rad, UK) in 1x running buffer at 140V using a Bio-Rad power pack (Bio-Rad, UK) until all molecular size proteins were separated. Protein samples were then transferred onto PVDF membranes and blotted with specific antibodies against total EGFR (Cell signalling technologies, UK) and phospho EGFR (Cell signalling technologies, UK) as previously described in sections 2.7.2 and 2.7.4. 1μM concentration of Gefitinib indicated inhibition of EGFR phosphorylation in COPD donor 2. Decreased phosphorylation of EGFR in COPD donor 1 was not seen with any of the Gefitinib doses. Therefore, a concentration of 1μM Gefitinib was used in future experiments with *M. catarrhalis* infection studies.

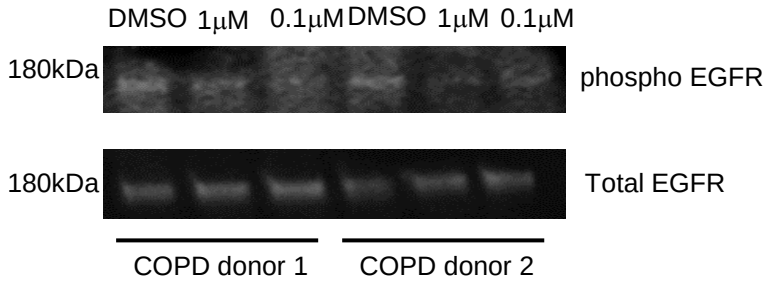

Supplementary Figure 3: Gefitinib inhibits phosphorylation of EGFR in COPD differentiated cells

COPD Differentiated cultures obtained from 2 donors were pre-treated with DMSO, 1μM or 0.1μM Gefitinib basolaterally for 1h before stimulation with 100ng/ml recombinant EGF protein for 1h. Cell lysates were assessed for phosphorylated and total EGFR expression at 24h post treatment.

Appendix 4

Supplementary Table 1: Culture media and supplements.

Product / Media	Composition	Application	Supplier
BEBM™ (bronchial epithelial basal medium) cell media	Serum free basal medium, contains no antimicrobial agents pH 7.4 – 7.6	Culture of primary basal cells; bacteria and virus dilutions	Lonza, UK
BEGM (bronchial epithelium basal medium)	BEBM with added Single Quots supplements (pituitary bovine extract, hydrocortisone, human epidermal growth factor, epinephrine, transferrin, insulin, retinoic acid, triiodothyronine)	ALI media - differentiation of primary basal cells	Lonza, UK
Promocell basal medium	Serum free basal medium, contains no antimicrobial agents pH 7.2 – 7.4	Culture of primary basal cells	Promocell, UK
Promocell airway epithelial cells growth medium	Promocell basal medium with SupplementMix	ALI media - differentiation of primary basal cells	Promocell, UK
Gibco Dulbecco's Modified Eagle Medium (DMEM)	Basal medium with high glucose levels, L-glutamine, phenol red, sodium pyruvate	Expansion of mouse embryonic fibroblasts, primary basal cells and Hela H1 cells	Invitrogen, UK

Ham's F-12 nutrient media	Serum free media supplemented with L-glutamine, phenol red, zinc, putrescine, hypoxanthine, thymidine, sodium pyruvate	Expansion of primary basal cells	Thermofisher, UK
Gibco M199 media	Basal media supplemented with phenol red, HEPES, L-glutamine, adenine, adenosine, hypoxanthine, thymine, vitamins	Nasal/ bronchial brushes sample collection media	Invitrogen, UK
Foetal bovine serum	Heat inactivated serum with haemoglobin ≤ 25mg/ml, endotoxin levels ≤ 10EU/ml	Expansion of mouse embryonic fibroblasts	Gibco, UK
Newborn Calf serum	Sterile – filtered heat inactivated serum with haemoglobin ≤ 20mg/ml, endotoxin levels ≤ 100EU/ml	Expansion of Hela H1 cells	Sigma-Aldrich, UK
Penicillin/ Streptomycin	10,000 units/ml penicillin and 10,000μg/ml streptomycin	Prevention from bacterial contamination during expansion of mouse embryonic fibroblasts and Hela H1 cells	Gibco, UK
Fungizone	250μg Amphotericin B	Prevention of yeast and fungal contamination during expansion of primary airway basal cells and differentiation	Invitrogen, UK
Gentamicin	50mg/ml gentamicin	Prevention of bacterial contamination during expansion of primary airway basal cells	Thermo Fisher, UK

Pro-freeze media	Cryopreservation media with no serum, proteins, insulin, hydrolysate or animal derivatives; Requires the addition of 15% dimethylsulfoxide (DMSO) at the time of use	Freezing media for primary airway cells	Lonza, UK

Supplementary Table 2: List of reagents.

Reagent	Application	Supplier
3,3',5,5, Tetramethylbenzidine (TMB)	ELISA substrate reacts with HRP immobilized antibody	Thermo Fisher, UK
4-(2-hydroxyethyl)-1-piperazinetanesulfonic acid (HEPES)	Virus infection media for extra buffering capacity	Gibco, UK
7.5% Sodium bicarbonate solution	Virus infection media	Sigma-Aldrich, UK
10% Sodium Dodecyl Sulfate Solution (SDS)	SDS-PAGE gel electrophoresis	Fisher Scientific, UK
Annexin V binding buffer 10x	Apoptosis assay of epithelial cells	BD Pharmingen, UK
Assay diluent B and D	ELISA sample and calibrators dilutions	Thermo Fisher, UK
Bovine serum albumin (BSA)	3% and 5% BSA in western blot, immunofluorescence staining	Sigma-Aldrich, UK; Fisher Scientific, UK
Blood agar base (BAB)	Media for preparation of agar plates	Sigma-Aldrich, UK
Brain Heart Infusion (BHI) media	Growth media for *M. catarrhalis*	Sigma-Aldrich, UK

Cell dissociation buffer	Detachment of epithelial cells from transwell inserts	Thermofisher, UK
Cholera toxin	Growth of airway basal cells	Sigma-Aldrich, UK
Clarity ECL western substrate	Staining of HRP-conjugated antibodies in Western Blot	Bio-Rad, UK
Collagen coating solution - PureCol® Bovine Collagen solution 3mg/ml diluted in PBS	Coating plastic plates and transwell inserts	Cellsystems, UK
Diluent 3	MSD buffer for antibody preparation	MSD, USA
Diluent 43	MSD buffer for sample preparation and calibrators	MSD, USA
Dimethylsulfoxide (DMSO)	Freezing cell media	Sigma-Aldrich, UK
Dithiothreitol (DTT)	Loading buffer in samples for gel electrophoresis	Sigma-Aldrich, UK
Glycerol	bacterial stocks prepared in 10% glycerol	Sigma-Aldrich, UK
Glycine	SDS-PAGE electrophoresis	Sigma-Aldrich, UK
Hydrocortisone	Differentiation of basal airway cells	STEMCELL technologies, UK

Insulin-Transferrin	Differentiation of basal airway cells	Fischer Sceintific, UK
Imipenem	Invasion bacterial assays to kill extracellular bacteria	Sigma-Aldrich, UK
Laemmli Sample buffer	Optimal band separation in SDS-PAGE electrophoresis	Bio-Rad, UK
Methanol	Transfer buffer, Western Blot	VWR, UK
MINI-Protean pre-cast gels	SDS-PAGE gel electrophoresis	Bio-Rad, UK
Paraformaldehyde (PFA)	Fixation of epithelial cells prior immunofluorescence	Sigma-Aldrich, UK
Phosphate buffer saline (PBS) tablets	Western blot, Immunofluorescence	MSD, USA
Phosphatase inhibitor II **Phosphatase inhibitor III**	Lysis buffer, gel electrophoresis	Sigma-Aldrich
Protease inhibitors	Lysis buffer, gel electrophoresis	Sigma-Aldrich
Protein ladder 250kDa	SDS-PAGE gel electrophoresis	New England Biolabs, UK
Radioimmunoprecipitation assay buffer (RIPA)	Lysis of epithelial cells	Thermo Fisher, UK
Read buffer	MSD buffer which catalyzes the electro-	MSD, USA

	chemiluminescence reaction	
Recombinant EGF protein	Stimulation of airway epithelial cells; differentiation of airway basal cells	Invitrogen, UK
Retinoic acid	Differentiation of airway epithelial cells	Sigma-Aldrich, UK
ROCK inhibitor (Y-27632)	Proliferation and expansion of airway basal cells	Insight Biotechnology, UK
Saponin	Lysis of epithelial cells	Sigma-Aldrich, UK
Sheep blood	Preparation of blood agar plates for CFU bacterial counts	Sigma-Aldrich, UK
Streptavidin horseradish peroxidase	ELISA reagent	Thermo Fisher, UK
Stop solution, 0.2M sulfuric acid	ELISA reagent to terminate enzyme substrate reaction	Thermo Fisher, UK
Stop solution	MSD biotin containing buffer to stop linker – antibody reaction	MSD, USA
Tris Base	SDS-PAGE gel electrophoresis	Sigma-Aldrich, UK
Triton X solution	Lysis of epithelial cells	Sigma-Aldrich, UK

Trypan blue	Live/dead cell count	Sigma-Aldrich, UK
TrypLe	Dissociation of airway basal cells from flasks	Thermo Fisher, UK
Trypsin / ethylendiaminetetracetic acid EDTA solution	Detachment of epithelial cells from flasks/ plates/ transwell inserts	Sigma-Aldrich, UK
Tween-20 solution	Buffer preparation for western blots	Sigma-Aldrich, UK
Universal Assay buffer	Multiplex Immunoassays	Invitrogen, UK
Universal assay wash buffer	Multiplex Immunoassays	Invitrogen, UK

Supplementary Table 3: Buffers and solutions recipes.

Buffer/ Solution	Composition	Application
Lysis buffer	1xRIPA buffer, 1/50 protease inhibitors, 1/100 phosphatase inhibitors II and III	Lysis of airway epithelial cells
5x Running buffer	15g Tris Base, 94g Glycine, 50ml 10% SDS, top up to 1L with dH_2O	SDS-PAGE electrophoresis
1x Running buffer (1L)	200ml of 5x Running buffer, 800ml dH_2O	SDS-PAGE electrophoresis
10x Transfer Buffer	30g Tris Base, 144g Glycine, filled to 1L with dH_2O	SDS-PAGE electrophoresis
1x Transfer buffer (1L)	100ml of 10x transfer buffer, 700ml dH_2O, 200ml Methanol	SDS-PAGE electrophoresis
Stripping buffer	15g Tris Base, 10ml SDS, 10mL Tween-20, filled to 1L with dH_2O	Western blot, stripping (removing) antibody staining from membranes
10x TBS **(Tris Buffered Saline)**	24g Tris-HCL, 80g NaCl, pH 7.5 (adjusted with HCL or NaOH), filled to 1L with dH_2O	Western blot
1x TBS-T	100ml of 10x TBS, 900ml dH_2O, 1mL Tween-20 (0.1%)	Western blot, wash of membrane between antibody staining
PBS-T	5 tablets PBS in 1L dH_2O, 0.5mL Tween-20 (0.05%)	Western blot, wash of membrane between antibody staining